ISSN 2644-3260 (online)

Artificial Intelligence in *Medical Imaging*

Artif Intell Med Imaging 2021 February 28; 2(1): 1-12

Published by Baishideng Publishing Group Inc

AIMI

Artificial Intelligence in Medical Imaging

Contents

Bimonthly Volume 2 Number 1 February 28, 2021

EDITORIAL

1 New Year's greeting and overview of *Artificial Intelligence in Medical Imaging* in 2021

Wu YXJ, Shen J

MINIREVIEWS

5 Artificial intelligence in ophthalmology: A new era is beginning

Panda BB, Thakur S, Mohapatra S, Parida S

Artificial Intelligence in Medical Imaging

Bimonthly Volume 2 Number 1 February 28, 2021

Contents

ABOUT COVER

Georges Nassar, PhD, Academic Research, Professor, Ultrasonic Division, Institute of Electronic, Microelectronic and Nanotechnology, Lille 59300, Hauts-de-France, France. gnassar@univ-valenciennes.fr

AIMS AND SCOPE

The primary aim of *Artificial Intelligence in Medical Imaging* (*AIMI*, *Artif Intell Med Imaging*) is to provide scholars and readers from various fields of artificial intelligence in medical imaging with a platform to publish high-quality basic and clinical research articles and communicate their research findings online.

AIMI mainly publishes articles reporting research results obtained in the field of artificial intelligence in medical imaging and covering a wide range of topics, including artificial intelligence in radiology, pathology image analysis, endoscopy, molecular imaging, and ultrasonography.

INDEXING/ABSTRACTING

There is currently no indexing.

RESPONSIBLE EDITORS FOR THIS ISSUE

NAME OF JOURNAL
Artificial Intelligence in Medical Imaging

ISSN
ISSN 2644-3260 (online)

LAUNCH DATE
June 28, 2020

FREQUENCY
Bimonthly

PUBLICATION DATE
February 28, 2021

Artificial Intelligence in Medical Imaging

Submit a Manuscript: https://www.f6publishing.com

Artif Intell Med Imaging 2021 February 28; 2(1): 1-4

DOI: 10.35711/aimi.v2.i1.1

ISSN 2644-3260 (online)

EDITORIAL

New Year's greeting and overview of *Artificial Intelligence in Medical Imaging* in 2021

Yun-Xiaojian Wu, Jun Shen

ORCID number: Yun-Xiaojian Wu 0000-0003-1146-7872; Jun Shen 0000-0001-7746-5285.

Author contributions: Wu YXJ drafted this editorial; Shen J revised the manuscript.

Conflict-of-interest statement: The authors declare having no conflicts of interest.

Manuscript source: Invited manuscript

Specialty type: Radiology, nuclear medicine and medical imaging

Country/Territory of origin: United States

Peer-review report's scientific quality classification

Yun-Xiaojian Wu, Production Department, Baishideng Publishing Group Inc, Pleasanton, CA 94566, United States

Jun Shen, Department of Radiology, Sun Yat-Sen Memorial Hospital, Sun Yat-Sen University, Guangzhou 510120, Guangdong Province, China

Corresponding author: Yun-Xiaojian Wu, BSc, Vice Director, Production Department, Baishideng Publishing Group Inc, 7041 Koll Center Parkway, Suite 160, Pleasanton, CA 94566, United States. y.xj.wu@wjgnet.com

Abstract

As editors of *Artificial Intelligence in Medical Imaging* (*AIMI*), it is our great pleasure to take this opportunity to wish all of our authors, subscribers, readers, Editorial Board members, independent expert referees, and staff of the Editorial Office a Very Happy New Year. On behalf of the Editorial Team, we would like to express our gratitude to all of the authors who have contributed their valuable manuscripts, our independent referees, and our subscribers and readers for their continuous support, dedication, and encouragement. Together with an excellent of team effort by our Editorial Board members and staff of the Editorial Office, *AIMI* advanced in 2020 and we look forward to greater achievements in 2021.

Key Words: New Year's greeting; *Artificial Intelligence in Medical Imaging*; Baishideng; Journal development

Core Tip: On behalf of the *Artificial Intelligence in Medical Imaging* (*AIMI*) Editorial Team, we would like to express our gratitude to all authors who have contributed their valuable manuscripts, to our independent referees, and to our subscribers and readers for their continuous support, dedication, and encouragement. Together with an excellent team effort by our Editorial Board members and staff of the Editorial Office, *AIMI* advanced in 2020 and we look forward to greater achievements in 2021.

Citation: Wu YXJ, Shen J. New Year's greeting and overview of *Artificial Intelligence in Medical Imaging* in 2021. *Artif Intell Med Imaging* 2021; 2(1): 1-4

Grade A (Excellent): A
Grade B (Very good): 0
Grade C (Good): 0
Grade D (Fair): 0
Grade E (Poor): 0

Received: January 17, 2021
Peer-review started: January 17, 2021
First decision: January 28, 2021
Revised: February 19, 2021
Accepted: February 22, 2021
Article in press: February 22, 2021
Published online: February 28, 2021

P-Reviewer: Liu G
S-Editor: Wang JL
L-Editor: Filipodia
P-Editor: Xing YX

URL: https://www.wjgnet.com/2644-3260/full/v2/i1/1.htm
DOI: https://dx.doi.org/10.35711/aimi.v2.i1.1

INTRODUCTION

As editors of *Artificial Intelligence in Medical Imaging* (*AIMI*), it is our great pleasure to take this opportunity to wish all of our authors, subscribers, readers, Editorial Board members, independent expert referees, and staff of the Editorial Office a Very Happy New Year. On behalf of the Editorial Team, we would also like to express our gratitude to all authors who have contributed their valuable manuscripts, to independent referees, and to our subscribers and readers for their continuous support, dedication, and encouragement.

AIMI mainly focuses on reporting research results obtained in the field of artificial intelligence (AI) in medical imaging, but covers a wide range of topics within that field. With the joint efforts of Editorial Board members and Editorial Office staff, it is our hope that *AIMI* will achieve further advancement in 2021, establishing a strong foundation upon which we may build to become the top journal in the field of AI.

ACADEMIC INFLUENCE OF *AIMI*

AIMI is a high-quality, bimonthly, online, open-access, and single-blind peer-reviewed journal, featuring research advances in AI involving the emerging fields of medical imaging in each issue. The scope of *AIMI* covers a wide range of topics, including but not limited to coronavirus disease 2019, radiomics, computed tomography, magnetic resonance imaging, machine learning, deep learning, nuclear medicine, positron emission tomography, pathology image analysis, endoscopy, molecular imaging, and ultrasonography.

With the rapid development of AI technology, the combination of deep learning and image-omics will enjoy broader application and more substantive development prospects, ultimately creating new fields of computer-aided diagnosis and personalized medical imaging. As a future research hotspot, they will continue to support even further investigative and clinical focus, advancing the overall use of AI and its benefit to human health. We will invite global experts to contribute original articles that focus on key scientific issues in medical imaging technology, methodology, and applied research, and propose research ideas, key research directions, and future research trends, to lead the development of the field.

As one of the key developing journals of the Baishideng Publishing Group Inc (BPG), *AIMI* was launched in 2020, publishing Volume 1, Issue 1 on June 28[1]. To date, it has published 3 issues with 11 articles (Figure 1). The authors of these manuscripts come from countries across the globe (Figure 2). In 2020, the Editorial Board of *AIMI* consisted of 77 members from 23 countries and regions including 33 from China (42.9%), 9 from the United States (11.7%), 7 from India (9.1%), and 28 from other countries and regions (36.3%) (Figure 3)[2].

To help *AIMI* develop more efficiently, BPG instituted and implemented the following in 2020. (1) In order to provide authors with better services, and supervise and promote BPG's efforts to publish each article more openly and transparently, BPG published the Author Reviews (https://www.f6publishing.com/AuthorReviews) for each publication, so that all can see the authors' evaluation and feedback on the publication process. (2) Throughout 2020, BPG continued systematic efforts to encourage more authors to generate articles that are outstanding for their originality and innovativeness and to strengthen our open-access strategy of publication; these efforts were motivated by our dedication to maximizing readers' access to the latest research results, to promote development of the medical sciences worldwide. In doing so, BPG invited Editorial Board members to conduct Article Quality Tracking-Peer-Review and published the comments (https://www.f6publishing.com/ArticleQualityTrackings) after the publication of the article. (3) To continue to advance BPG's publishing efficiency and quality, we successfully developed an automated manuscript editor system for manuscript revision and submission, as well as an artificially intelligent program to generate a PDF version of the manuscript. (4) To enable more peers to read, share, and cite authors' published research results and to help enhance their global academic influence and reputations, thereby also promoting

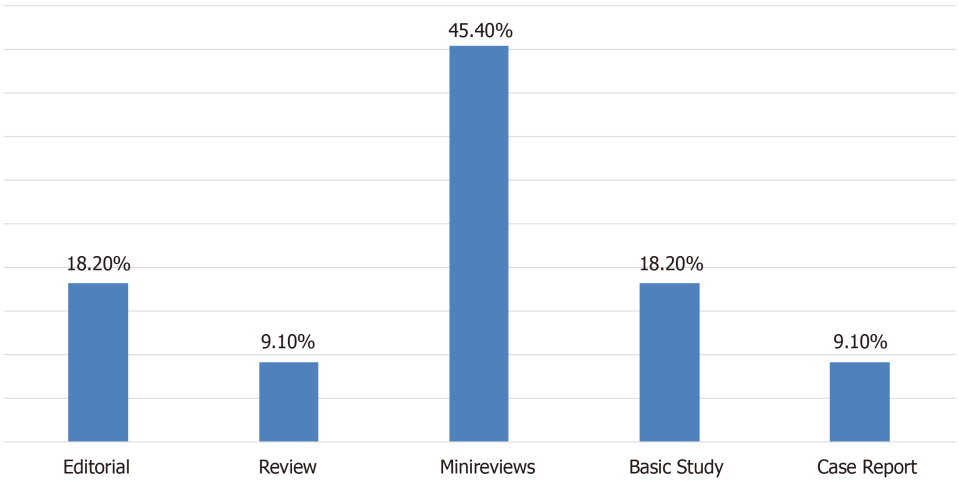

Figure 1 Column type distribution of manuscripts published in *Artificial Intelligence in Medical Imaging* in 2020.

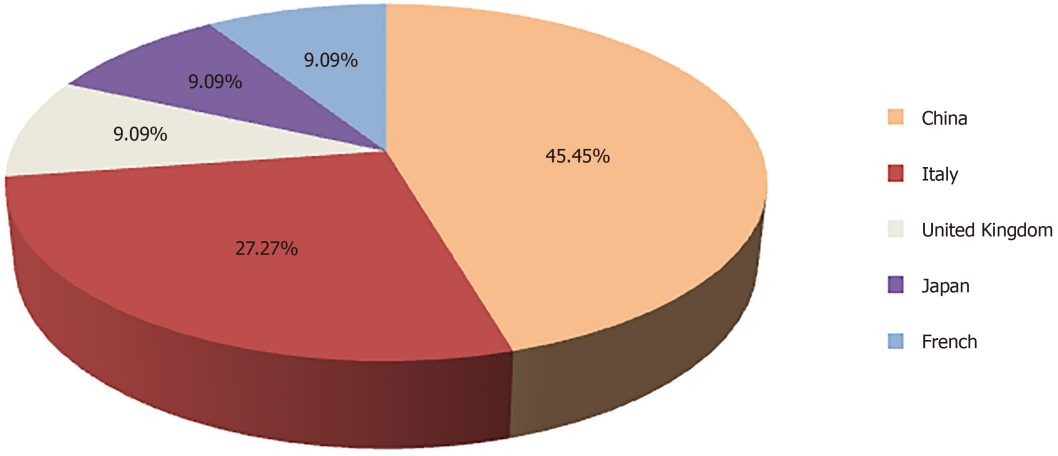

Figure 2 Distribution of authors' countries for the manuscripts published in *Artificial Intelligence in Medical Imaging* in 2020.

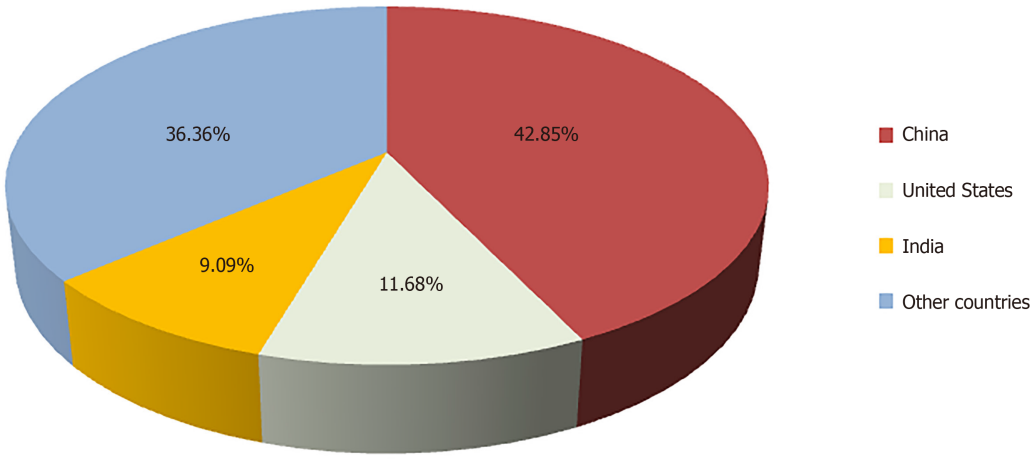

Figure 3 Distribution of Editorial Board members' countries for *Artificial Intelligence in Medical Imaging*.

the overall development of the field, BPG initiated the routine of sending its published articles to 1000-10000 highly influential experts in a topically accurate manner. After completing this outreach activity, BPG formally notifies the paper's authors of the number of experts to whom their manuscript was sent *via* email.

We are pleased to announce that we have now submitted evaluation applications to

the Web of Science, with the expectation that the *AIMI* could be included in Science Citation Index Expanded in 2021.

CONCLUSION

With the collective support of BPG's contributors and staff, we expect to continue the trajectory towards more productive efforts that will raise the academic rank of *AIMI* in 2021. To achieve these goals, we appreciate the need for continuous support and submissions from authors and the dedicated efforts and expertise by our invited reviewers, many of them who also serve on our Editorial Board. As the chief editors of *AIMI*, we strive to work with the journal's Editorial Office staff to make the manuscript submission process as simple as possible and to ensure efficient communication with the authors to provide professional support and answer their questions. We are also open to any suggestions that could improve *AIMI*'s operations and publication. Please feel free to contact us at (editorialoffice@wjgnet.com) with any question on your submission or suggestions.

Once again, on behalf of *AIMI*, we wish you and your families the best for the New Year.

REFERENCES

1 **Baishideng Publishing Group Inc**. All published articles of Artificial Intelligence in Medical Imaging from its launch in 2020 to present. Available from https://www.wjgnet.com/2644-3260/archive.htm

2 **Baishideng Publishing Group Inc**. The Editorial Board of Artificial Intelligence in Medical Imaging. Available from https://www.wjgnet.com/2644-3260/editorialboard.htm

Artificial Intelligence in Medical Imaging

Submit a Manuscript: https://www.f6publishing.com

Artif Intell Med Imaging 2021 February 28; 2(1): 5-12

DOI: 10.35711/aimi.v2.i1.5

ISSN 2644-3260 (online)

MINIREVIEWS

Artificial intelligence in ophthalmology: A new era is beginning

Bijnya Birajita Panda, Subhodeep Thakur, Sumita Mohapatra, Subhabrata Parida

ORCID number: Bijnya Birajita Panda 0000-0002-0887-1690; Subhodeep Thakur 0000-0003-1782-3567; Sumita Mohapatra 0000-0001-7165-9572; Subhabrata Parida 0000-0002-3871-3490.

Author contributions: Panda BB and Thakur S designed the review, collected the data, analyzed the data and prepared the initial draft. Mohapatra S and Parida S revised the manuscript for important intellectual content and prepared the final draft; All authors read the manuscript and approved for the publication.

Conflict-of-interest statement: The authors declare no conflicts of interest.

Manuscript source: Unsolicited manuscript

Bijnya Birajita Panda, Subhodeep Thakur, Sumita Mohapatra, Subhabrata Parida, Department ofOphthalmology, S.C.B Medical College and Hospital, Cuttack 753007, Odisha, India

Corresponding author: Bijnya Birajita Panda, MBBS, MS, Assistant Professor, Ophthalmology, S.C.B Medical College and Hospital, Manglabag, Cuttack 753007, Odisha, India. bigyan_panda@yahoo.co.in

Abstract

The use of artificial intelligence (AI) in ophthalmology is not very new and its use is expanding into various subspecialties of the eye like retina and glaucoma, thereby helping ophthalmologists to diagnose and treat diseases better than before. Incorporating "deep learning" (a subfield of AI) into image-based systems such as optical coherence tomography has dramatically improved the machine's ability to screen and identify stages of diabetic retinopathy accurately. Similar applications have been tried in the field of retinopathy of prematurity and age-related macular degeneration, a silent retinal condition that needs to be diagnosed early to prevent progression. The advent of AI into glaucoma diagnostics in analyzing visual fields and assessing disease progression also holds a promising role. The ability of the software to detect even a subtle defect that the human eye can miss has led to a revolution in the management of certain ocular conditions. However, there are few significant challenges in the AI systems, such as the incorporation of quality images, training sets and the black box dilemma. Nevertheless, despite the existing differences, there is always a chance of improving the machines/software to potentiate their efficacy and standards. This review article shall discuss the current applications of AI in ophthalmology, significant challenges and the prospects as to how both science and medicine can work together.

Key Words: Artificial intelligence; Retina; Diabetic retinopathy; Glaucoma; Retinopathy of prematurity; Image-based learning

Core Tip: Artificial intelligence has improved the diagnostic ability in the ophthalmology field, thereby improving patient care. The in-depth image recognition in diabetic retinopathy, retinopathy of prematurity and age-related macular degeneration has helped in early diagnosis and prevention. The detection of visual filed

Specialty type: Ophthalmology

Country/Territory of origin: India

Peer-review report's scientific quality classification

Grade A (Excellent): 0
Grade B (Very good): 0
Grade C (Good): C
Grade D (Fair): D
Grade E (Poor): 0

Received: November 28, 2020
Peer-review started: November 28, 2020
First decision: December 18, 2020
Revised: December 31, 2020
Accepted: February 12, 2021
Article in press: February 12, 2021
Published online: February 28, 2021

P-Reviewer: Boon CS, Zhang LZ
S-Editor: Wang JL
L-Editor: Filipodia
P-Editor: Xing YX

defect even at its minute stage in glaucoma and other ocular conditions has accurately staged the disease with the prediction of its severity. Still, many challenges need to be addressed, such as image incorporation, training sets and the black box dilemma. Nevertheless, despite the existing differences, there is always a chance of improving machines to potentiate their efficacy and standards.

Citation: Panda BB, Thakur S, Mohapatra S, Parida S. Artificial intelligence in ophthalmology: A new era is beginning. *Artif Intell Med Imaging* 2021; 2(1): 5-12
URL: https://www.wjgnet.com/2644-3260/full/v2/i1/5.htm
DOI: https://dx.doi.org/10.35711/aimi.v2.i1.5

INTRODUCTION

Artificial intelligence (AI) software can perform cognitive functions like problem-solving and learning by processing and analyzing a large amount of data; in other words, the machine can gain experience as humans do. It came into existence in 1956 and in no time spread its roots into many medical fields, including ophthalmology in the late 1990s when colour fundus photography had started gaining importance in diabetic retinopathy (DR) screening[1]. Later on, its use was not limited to but tried extensively in many subspecialties of the eye such as cataract, myopia and glaucoma screening, corneal ectasia, keratoconus, retinopathy of prematurity (ROP) and ocular reconstruction. It can also be used in calculating intraocular lens power and while planning squint surgery and intravitreal injections. AI can even detect cognitive loss, Alzheimer's disease and cerebrovascular stroke risk from fundus photographs and optical coherence tomography (OCT). AI in ophthalmology started with machine learning (ML), which meant automatic behaviour modification after exposure to several inputs. Deep learning (DL) is a subset of ML that uses convolutional neural networks (CNN) to add decision-making capability. When incorporated into OCT, these features can help in the diagnosis of many anterior and posterior segment diseases.

AI AND DR

The disease burden of diabetes mellitus increases day by day, and millions of people are affected. According to published data, the present disease burden is 463 million[2] and likely to rise to 642 million by 2040. DR is a microvascular complication affecting the retina's blood vessels, leading to progressive damage and irreversible blindness. These patients need to be diagnosed early, and prompt treatment should be started regardless of the type of diabetes. Routine dilated fundus screening in these patients with ophthalmoscopy and colour fundus photographs is the need of the hour and, therefore, eases the burden on the retina specialists. AI has shown promising results in the automated grading of DR based on ML and DL models, the CNN and the massive-training artificial neural network. The lesions in DR are recognized by ML as different colours like red (microaneurysms, haemorrhage, venous abnormalities, intraretinal microvascular abnormalities, new vessels, *etc.*), yellow (hard exudates, drusens) and white (cotton wool spots, fibrous proliferation, retinal oedema)[3]. Staging in DR is usually done by the Davis staging practiced worldwide[4]. In 2017, Takahashi *et al*[5] developed a modified Davis staging adopting the DL criterion. The DL approach increases the possibility of identifying neovascularization or other features of proliferative DR (PDR) outside a 45° angle to the posterior pole by detecting non-verbalizable unclear signals. A major breakthrough in this arena was the United States Food and Drug Administration approval of IDx-DR in 2018[6]. A CNN DL algorithm-based AI system to be used along with a Topcon fundus camera has now been proven to be an essential tool in non-ophthalmic healthcare places where it can diagnose DR in just a matter of 20 sec. Lately, the automated DR image accessing system has been applied in conditions affecting the macula such as PDR and clinically significant macular oedema. Another new entity has evolved termed as mtmDR (more than minimal DR), which is defined as the presence of Early Treatment Diabetic Retinopathy Study level 35 or higher, *i.e.* showing microaneurysms, hard exudates,

cotton wool spots and mild retinal haemorrhages and presence of macular oedema in at least one eye[7].

Abràmoff *et al*[8] reported that DL enhanced algorithm for automated detection of DR has better sensitivity than the Iowa Detection Program–without DL components. The sensitivity and specificity of DL-based automated DR detection algorithm was 96.8% [95% confidence interval (CI): 93.3%-98.8%] and 87.0% (95%CI: 84.2%-89.4%) with 6/874 false negatives, resulting in a negative predictive value of 99.0% (95%CI: 97.8%-99.6%). The authors did not miss a single case of severe non-proliferative DR, PDR or macular oedema with DL technology[8]. Gargeya *et al*[9] developed a data-driven DL algorithm where the colour fundus images were classified as healthy (no-retinopathy) or DR. Their model achieved a 0.97 area under the curve with a 94% and 98% sensitivity and specificity, respectively[9].

Several studies came out with different proposals of classifying DR stages, some of which are worth mentioning[10]. A three-layer feed-forward neural network based on identifying microaneurysms and haemorrhages was proposed by Wong *et al*[11] to stage DR. A novel technique known as morphological component analysis was formulated by Imani *et al*[12] to detect oedema and haemorrhages. Yazid *et al*[13] used inverse surface thresholding and Lattice Neural Network with Dendritic Processing or enhancement techniques to identify hard exudates and optic disc pathologies. Akyol *et al*[14] tried using key point detection, texture analysis and visual dictionary techniques to detect automatically the optic disc changes from fundus images. The sensitivity and specificity of these studies ranged from 75% to 94.7%. Few studies have used the Eye Art software smartphone-based fundus photography with a sensitivity of around 95% and specificity of 91.5%. The EyeNuk software using the desktop fundus cameras to evaluate retinal images showed that EyeArt's sensitivity for DR screening was 91.7% and specificity was 91.5%[15-17]. Ting *et al*[18] validated the DL algorithm with retinal images taken with conventional fundus cameras that had high sensitivity and specificity for identifying DR and age-related macular degeneration (AMD). The intelligent retinal imaging system is another milestone achieved in the field of AI. It is a tele-retinal DR screening program that compares non-mydriatic retinal images taken by a fundus camera with a standard set of images from Early Treatment Diabetic Retinopathy Study to recommend referral in selected cases of severe non-proliferative DR or more advanced vision-threatening disease[19].

Wong *et al*[20] pointed out certain limitations of DL technology in AI for the screening of DR. There is no simple, standardized algorithm to follow. The technology can talk about the referral cases but fail to detect severe sight-threatening DR that need urgent attention. The software may fail to detect associated glaucoma and AMD while screening for DR. The most severe problem is the development of the faith of the physicians on the machine. The heterogeneous population, different races and variability in pupil dilatation, cataract severity and media opacities may befool the machine and can be one of the reasons for refusal of the technology by the physicians[20].

AI AND ROP

ROP is one of the leading causes of childhood blindness throughout the world. This vasoproliferative condition affects preterm infants with low gestational age and those with low birth weight. This condition should be diagnosed promptly so that timely intervention can be done. This can be abetted with the help of AI, which provides an automated, quantifiable and highly objective diagnosis in plus disease in ROP[21]. One more area of application of AI in ROP is the utilization of the DL algorithms into medical training to standardize ROP training and education through tele-education. However, there are few clinical and technical challenges in the implementation of AI in the actual scenario.

According to International Classification of Retinopathy of Prematurity, ROP is classified based on the location, extent and severity of disease[22]. However, there is much inter-observer variability in the subjective and qualitative assessment of disease severity (zone, stage and plus-disease) due to wide disparities among the diagnosing abilities of ophthalmologists attending these preterm babies. Therefore, there is a need to add objective methods of diagnosis and record-keeping for future comparisons to improve accuracy. Today, digital fundus photography using telemedicine has already paved the way for screening at-risk preterm babies at any geographical location that can be evaluated by a trained retina specialist sitting at another location.

Earlier systems of computer-based ROP diagnosis as described by Wittenberg *et al*[23]

(2012) include the ROP-Tool, retinal image multiScale analysis, vessel map and computer-assisted image analysis of the retina, which were feature extraction–based systems. These systems could quantify vessel type, dilation and tortuosity into some value that had a variable diagnostic agreement with the clinical diagnosis of ROP.

Newer ML-based systems used a support vector machine that is trained to combine the features (vessel tortuosity) and the field of view (six-disc diameter radius) and then provide the diagnosis, quite similar to what an expert can do. This improved machine efficacy and accuracy to almost 85%-95%[24,25]. However, there were few limitations as they required manual drawings for input. In 2018, Brown *et al*[24] described a fully automated convoluted neural networks-based system known as the i-ROP DL system for the diagnosis of plus-ROP that can diagnose plus disease with a sensitivity and specificity of 93% and 94%, respectively. Taylor *et al*[25] used the i-ROP DL algorithm to create a scoring system related to vascular tortuosity and termed it as continuous ROP vascular severity score (1–9), which could classify ROP as no ROP, mild ROP, type 2 ROP and pre-plus disease or type 1 ROP. This scoring system could help augment treatment regimens by better predicting the preterm infants at risk for treatment failure and disease recurrence. However, few regulatory and medicolegal issues in utilizing the DL systems for ROP diagnosis need to be resolved for proper implication.

AI AND AMD

AMD is considered the leading cause of central vision loss in the elderly age group. The challenges in diagnosing and managing this silent progressive retinal condition have led to the rising prevalence of the disease. AI has evolved to help in the automated detection of drusens in the very early stages and stratify the disease's progression. AMD is clinically characterized by the presence of drusens and retinal pigment epithelium changes progressing into geographic atrophy and neovascularization.

Many of the studies related to incorporating AI in the screening of AMD have used colour fundus images as input materials and then extract features of early, intermediate and late AMD to differentiate from the healthy ones with relatively high accuracy and sensitivity ranging from 87%-100%[26,27]. They found this technique much cheaper than using OCT to stage the disease. Fang *et al*[28] proposed a spectral-domain OCT combined with DL system that could determine the macular fluid quantity of neovascular AMD and the segmentation of the retinal layers of dry AMD and validated the accuracy as 100%. Bogunovic *et al*[29] developed an algorithm to evaluate the response to treatment using OCT images. More recently, Bhuiyan *et al*[30] did pioneer research in creating and validating AI-based models for AMD screening (accuracy 99.2%) and predicting late dry and wet AMD progression within 1 and 2 years (accuracy 66%-83%). They used the DL screening methods on the Age-related Eye Disease Study (AREDS) dataset to classify their colour fundus photos into no, early, intermediate or advanced AMD and further classified them along the AREDS 12 Level severity scale[30]. They combined the AMD scores with sociodemographic, clinical data and other automatically extracted imaging data by a logistic model tree ML technique to predict risk for progression to late AMD.

AI AND GLAUCOMA

Glaucoma is a progressive optic neuropathy caused by high intra-ocular pressure leading to retinal nerve fibre loss and irreversible blindness. Early treatment can retard the progression of the disease. AI can help in identifying the borderline cases and predict the course of the disease. Many studies have tried to apply ML to identify the disease. A comprehensive AI for glaucoma should be able to evaluate all the necessary parameters such as optic disc changes, intraocular pressure (IOP), gonioscopy, retinal nerve fiber layer thickness, visual fields *etc.* However, such a comprehensive package is yet to come to the real-time world. The application of AI in measuring IOP is now limited to the Sensimed Triggerfish, a contact lens-based continuous IOP monitoring device that measures the corneal strain changes induced by IOP fluctuations. Martin *et al*[31] used data from 24 prospective studies of Triggerfish using Random Forest Modelling (a ML method) to identify the parameters associated with glaucoma patients.

Omodaka *et al*[32] developed a ML algorithm based on the segmentation technique where the parameters such as optic disc cupping, neuroretinal rim thickness and

ganglion cell thickness could be quantified with the help of swept-source OCT to the accuracy as high as 87%. Other studies by Christopher *et al*[33], Barella *et al*[34], Bizios *et al*[35] and Larrosa *et al*[36] evaluated unsupervised ML, ML classifiers, artificial neural networks, support vector machines and segmentation methods for glaucoma OCT.

Many studies have evaluated a DL algorithm to detect glaucomatous optic disc changes from colour fundus photographs with high sensitivity and specificity[37,38]. The available AI devices for detecting glaucomatous optic neuropathy from fundus photos are the Pegasus (Orbis Cybersight Consult Platform), NetraAI (Leben Care Technologies Pte Ltd) and the Retinal Image Analysis - Glaucoma (RIA-G). RIA-G is the AI device based on DL made by the Indian startup Kalpah Innovations (Vishakapatnam, India). It is a cloud-based software that uses advanced image processing algorithms to measure the cup disc size and ratio, NeuroRetinal Rim Thickness and Disc Damage Likelihood Score[39].

AI can also augment the interpretation of visual fields in studies showed by Asaoka *et al*[40] and Andersson *et al*[41] using a Feed-Forward Neural Network to identify pre-perimetric visual fields (VF). Goldbaum *et al*[42] used unsupervised ML and variational Bayesian independent component analysis mixture model (vB-ICA-mm) to analyze VF defects. Bowd *et al*[43] used the variational Bayesian independent component analysis-mixture model, which is an unsupervised machine-learning classifier and can be used in the analysis of frequency doubling technology perimetry data[43].

AI AND CATARACT

Studies have described techniques to grade nuclear cataracts by the help of AI using algorithms based on ML or DL systems that work as efficiently as a clinician's grading. Gao *et al*[44] proposed a system that could process slit-lamp images to grade cataracts. Liu *et al*[45] focused on identifying and categorizing pediatric cataracts with excellent accuracy and sensitivity. Wu *et al*[46] developed a universal AI platform and multilevel collaborative pattern that could perform effectively in diagnostic and referral service for pediatric and age-related cataracts. Dong *et al*[47] have proposed the automated detection and grading of cataracts from colour fundus photographs using a combination of a DL system to extract images (Caffe software) followed by a ML algorithm (called as Softmax function) for severity grading. AI has also been tried in residents' cataract surgery training due to recognizing different phases of cataract surgery[48,49]. Some researchers have derived new AI-based calculation formulae for pre-cataract surgery intraocular lens power, *e.g.*, the Hill-Radial basis function method and the Kane formula, which are reported to be able to estimate individual eye's intraocular lens power with promising results with further improvements needed for short axial length eyes[50-52].

CONCLUSION

AI-assisted screening and diagnosis of high incidence diseases will help in better medical care and reduce the limitations to access ophthalmic care at remote areas devoid of ophthalmologists. In doing so, it will also reduce the overburdened healthcare system. However, this project at its infancy is nonetheless riddled with certain limitations. The assessment is highly dependent on image quality. Hence, patient factors such as head and eyeball movement and poor fixation may lead to a substandard image and a wrong assessment. However, this is the basis of ML, and in future, we expect a much more robust system. A certain degree of human supervision is required to find the subtle variations and atypical findings missed by AI. Computational cost and running expenses could be over the roof. AI mainly targets diseases with high incidence and morbidity, but not much effective for rare diseases with fewer incidences.

Future outlook

Not only for screening and diagnosis, AI has also been found to be instrumental in maintaining Electronic Health Record (EHR) data. Given the plethora of diagnostic tests that patients undergo, these collected EHR data could be fed into the AI system and trained through exposure to normal and pathological clinical data. Therefore, it could be used for risk assessment as well as to predict postoperative complications and outcome.

REFERENCES

1 **Ruamviboonsuk P**, Cheung CY, Zhang X, Raman R, Park SJ, Ting DSW. Artificial Intelligence in Ophthalmology: Evolutions in Asia. *Asia Pac J Ophthalmol (Phila)* 2020; **9**: 78-84 [PMID: 32349114 DOI: 10.1097/01.APO.0000656980.41190.bf]

2 **Sinclair A**, Saeedi P, Kaundal A, Karuranga S, Malanda B, Williams R. Diabetes and global ageing among 65-99-year-old adults: Findings from the International Diabetes Federation Diabetes Atlas, 9th edition. *Diabetes Res Clin Pract* 2020; **162**: 108078 [PMID: 32068097 DOI: 10.1016/j.diabres.2020.108078]

3 **Padhy SK**, Takkar B, Chawla R, Kumar A. Artificial intelligence in diabetic retinopathy: A natural step to the future. *Indian J Ophthalmol* 2019; **67**: 1004-1009 [PMID: 31238395 DOI: 10.4103/ijo.IJO_1989_18]

4 **Meyer M**, Wiedorn KH, Hofschneider PH, Koshy R, Caselmann WH. A chromosome 17:7 translocation is associated with a hepatitis B virus DNA integration in human hepatocellular carcinoma DNA. *Hepatology* 1992; **15**: 665-671 [PMID: 1312986]

5 **Takahashi H**, Tampo H, Arai Y, Inoue Y, Kawashima H. Applying artificial intelligence to disease staging: Deep learning for improved staging of diabetic retinopathy. *PLoS One* 2017; **12**: e0179790 [PMID: 28640840 DOI: 10.1371/journal.pone.0179790]

6 **US Food and Drug Administration**. FDA permits marketing of artificial intelligence-based device to detect certain diabetes-related eye problems, 2018. [Cited December 21, 2020]. Available from: https://www.fda.gov/NewsEvents/Newsroom/PressAnnouncements/ucm604357.htm

7 **Optometry Times**. Pros and Cons of Using an AI-Based Diagnosis for Diabetic Retinopathy. [Cited December 21, 2020]. Available from: http://www.optometrytimes.com/article/pros-and-cons-using-ai-based-diagnosis-diabetic-retinopathy

8 **Abràmoff MD**, Lou Y, Erginay A, Clarida W, Amelon R, Folk JC, Niemeijer M. Improved Automated Detection of Diabetic Retinopathy on a Publicly Available Dataset Through Integration of Deep Learning. *Invest Ophthalmol Vis Sci* 2016; **57**: 5200-5206 [PMID: 27701631 DOI: 10.1167/iovs.16-19964]

9 **Gargeya R**, Leng T. Automated Identification of Diabetic Retinopathy Using Deep Learning. *Ophthalmology* 2017; **124**: 962-969 [PMID: 28359545 DOI: 10.1016/j.ophtha.2017.02.008]

10 **Abràmoff MD**, Lavin PT, Birch M, Shah N, Folk JC. Pivotal trial of an autonomous AI-based diagnostic system for detection of diabetic retinopathy in primary care offices. *NPJ Digit Med* 2018; **1**: 39 [PMID: 31304320 DOI: 10.1038/s41746-018-0040-6]

11 **Wong LY**, Acharya R, Venkatesh YV, Chee C, Min LC. Identification of different stages of diabetic retinopathy using retinal optical images. *Inf Sci* 2008; **178**: 106-121

12 **Imani E**, Pourreza HR, Banaee T. Fully automated diabetic retinopathy screening using morphological component analysis. *Comput Med Imaging Graph* 2015; **43**: 78-88 [PMID: 25863517 DOI: 10.1016/j.compmedimag.2015.03.004]

13 **Yazid H**, Arof H, Isa HM. Automated identification of exudates and optic disc based on inverse surface thresholding. *J Med Syst* 2012; **36**: 1997-2004 [PMID: 21318328 DOI: 10.1007/s10916-011-9659-4]

14 **Akyol K**, Şen B, Bayır Ş. Automatic Detection of Optic Disc in Retinal Image by Using Keypoint Detection, Texture Analysis, and Visual Dictionary Techniques. *Comput Math Methods Med* 2016; **2016**: 6814791 [PMID: 27110272 DOI: 10.1155/2016/6814791]

15 **Niemeijer M**, Abràmoff MD, van Ginneken B. Fast detection of the optic disc and fovea in color fundus photographs. *Med Image Anal* 2009; **13**: 859-870 [PMID: 19782633 DOI: 10.1016/j.media.2009.08.003]

16 **Rajalakshmi R**, Subashini R, Anjana RM, Mohan V. Automated diabetic retinopathy detection in smartphone-based fundus photography using artificial intelligence. *Eye (Lond)* 2018; **32**: 1138-1144 [PMID: 29520050 DOI: 10.1038/s41433-018-0064-9]

17 **Bhaskaranand M**, Ramachandra C, Bhat S, Cuadros J, Nittala MG, Sadda S, Solanki K. Automated Diabetic Retinopathy Screening and Monitoring Using Retinal Fundus Image Analysis. *J Diabetes Sci Technol* 2016; **10**: 254-261 [PMID: 26888972 DOI: 10.1177/1932296816628546]

18 **Ting DSW**, Cheung CY, Lim G, Tan GSW, Quang ND, Gan A, Hamzah H, Garcia-Franco R, San Yeo IY, Lee SY, Wong EYM, Sabanayagam C, Baskaran M, Ibrahim F, Tan NC, Finkelstein EA, Lamoureux EL, Wong IY, Bressler NM, Sivaprasad S, Varma R, Jonas JB, He MG, Cheng CY, Cheung GCM, Aung T, Hsu W, Lee ML, Wong TY. Development and Validation of a Deep Learning System for Diabetic Retinopathy and Related Eye Diseases Using Retinal Images From Multiethnic Populations With Diabetes. *JAMA* 2017; **318**: 2211-2223 [PMID: 29234807 DOI: 10.1001/jama.2017.18152]

19 **Huemer J**, Wagner SK, Sim DA. The Evolution of Diabetic Retinopathy Screening Programmes: A Chronology of Retinal Photography from 35 mm Slides to Artificial Intelligence. *Clin Ophthalmol* 2020; **14**: 2021-2035 [PMID: 32764868 DOI: 10.2147/OPTH.S261629]

20 **Wong TY**, Bressler NM. Artificial Intelligence With Deep Learning Technology Looks Into Diabetic Retinopathy Screening. *JAMA* 2016; **316**: 2366-2367 [PMID: 27898977 DOI: 10.1001/jama.2016.17563]

21 **Ataer-Cansizoglu E**, Bolon-Canedo V, Campbell JP, Bozkurt A, Erdogmus D, Kalpathy-Cramer J, Patel S, Jonas K, Chan RV, Ostmo S, Chiang MF; i-ROP Research Consortium. Computer-Based Image Analysis for Plus Disease Diagnosis in Retinopathy of Prematurity: Performance of the "i-

ROP" System and Image Features Associated With Expert Diagnosis. *Transl Vis Sci Technol* 2015; **4**: 5 [PMID: 26644965 DOI: 10.1167/tvst.4.6.5]

22 **International Committee for the Classification of Retinopathy of Prematurity**. The International Classification of Retinopathy of Prematurity revisited. *Arch Ophthalmol* 2005; **123**: 991-999 [PMID: 16009843 DOI: 10.1001/archopht.123.7.991]

23 **Wittenberg LA**, Jonsson NJ, Chan RV, Chiang MF. Computer-based image analysis for plus disease diagnosis in retinopathy of prematurity. *J Pediatr Ophthalmol Strabismus* 2012; **49**: 11-9; quiz 10, 20 [PMID: 21366159 DOI: 10.3928/01913913-20110222-01]

24 **Brown JM**, Campbell JP, Beers A, Chang K, Ostmo S, Chan RVP, Dy J, Erdogmus D, Ioannidis S, Kalpathy-Cramer J, Chiang MF; Imaging and Informatics in Retinopathy of Prematurity (i-ROP) Research Consortium. Automated Diagnosis of Plus Disease in Retinopathy of Prematurity Using Deep Convolutional Neural Networks. *JAMA Ophthalmol* 2018; **136**: 803-810 [PMID: 29801159 DOI: 10.1001/jamaophthalmol.2018.1934]

25 **Taylor S**, Brown JM, Gupta K, Campbell JP, Ostmo S, Chan RVP, Dy J, Erdogmus D, Ioannidis S, Kim SJ, Kalpathy-Cramer J, Chiang MF; Imaging and Informatics in Retinopathy of Prematurity Consortium. Monitoring Disease Progression With a Quantitative Severity Scale for Retinopathy of Prematurity Using Deep Learning. *JAMA Ophthalmol* 2019 [PMID: 31268518 DOI: 10.1001/jamaophthalmol.2019.2433]

26 **Mookiah MR**, Acharya UR, Fujita H, Koh JE, Tan JH, Noronha K, Bhandary SV, Chua CK, Lim CM, Laude A, Tong L. Local configuration pattern features for age-related macular degeneration characterization and classification. *Comput Biol Med* 2015; **63**: 208-218 [PMID: 26093788 DOI: 10.1016/j.compbiomed.2015.05.019]

27 **Burlina P**, Pacheco KD, Joshi N, Freund DE, Bressler NM. Comparing humans and deep learning performance for grading AMD: A study in using universal deep features and transfer learning for automated AMD analysis. *Comput Biol Med* 2017; **82**: 80-86 [PMID: 28167406 DOI: 10.1016/j.compbiomed.2017.01.018]

28 **Fang L**, Cunefare D, Wang C, Guymer RH, Li S, Farsiu S. Automatic segmentation of nine retinal layer boundaries in OCT images of non-exudative AMD patients using deep learning and graph search. *Biomed Opt Express* 2017; **8**: 2732-2744 [PMID: 28663902 DOI: 10.1364/BOE.8.002732]

29 **Bogunovic H**, Waldstein SM, Schlegl T, Langs G, Sadeghipour A, Liu X, Gerendas BS, Osborne A, Schmidt-Erfurth U. Prediction of Anti-VEGF Treatment Requirements in Neovascular AMD Using a Machine Learning Approach. *Invest Ophthalmol Vis Sci* 2017; **58**: 3240-3248 [PMID: 28660277 DOI: 10.1167/iovs.16-21053]

30 **Bhuiyan A**, Wong TY, Ting DSW, Govindaiah A, Souied EH, Smith RT. Artificial Intelligence to Stratify Severity of Age-Related Macular Degeneration (AMD) and Predict Risk of Progression to Late AMD. *Transl Vis Sci Technol* 2020; **9**: 25 [PMID: 32818086 DOI: 10.1167/tvst.9.2.25]

31 **Martin KR**, Mansouri K, Weinreb RN, Wasilewicz R, Gisler C, Hennebert J, Genoud D; Research Consortium. Use of Machine Learning on Contact Lens Sensor-Derived Parameters for the Diagnosis of Primary Open-angle Glaucoma. *Am J Ophthalmol* 2018; **194**: 46-53 [PMID: 30053471 DOI: 10.1016/j.ajo.2018.07.005]

32 **Omodaka K**, An G, Tsuda S, Shiga Y, Takada N, Kikawa T, Takahashi H, Yokota H, Akiba M, Nakazawa T. Classification of optic disc shape in glaucoma using machine learning based on quantified ocular parameters. *PLoS One* 2017; **12**: e0190012 [PMID: 29261773 DOI: 10.1371/journal.pone.0190012]

33 **Christopher M**, Belghith A, Weinreb RN, Bowd C, Goldbaum MH, Saunders LJ, Medeiros FA, Zangwill LM. Retinal Nerve Fiber Layer Features Identified by Unsupervised Machine Learning on Optical Coherence Tomography Scans Predict Glaucoma Progression. *Invest Ophthalmol Vis Sci* 2018; **59**: 2748-2756 [PMID: 29860461 DOI: 10.1167/iovs.17-23387]

34 **Barella KA**, Costa VP, Gonçalves Vidotti V, Silva FR, Dias M, Gomi ES. Glaucoma Diagnostic Accuracy of Machine Learning Classifiers Using Retinal Nerve Fiber Layer and Optic Nerve Data from SD-OCT. *J Ophthalmol* 2013; **2013**: 789129 [PMID: 24369495 DOI: 10.1155/2013/789129]

35 **Bizios D**, Heijl A, Hougaard JL, Bengtsson B. Machine learning classifiers for glaucoma diagnosis based on classification of retinal nerve fibre layer thickness parameters measured by Stratus OCT. *Acta Ophthalmol* 2010; **88**: 44-52 [PMID: 20064122 DOI: 10.1111/j.1755-3768.2009.01784.x]

36 **Larrosa JM**, Polo V, Ferreras A, García-Martín E, Calvo P, Pablo LE. Neural Network Analysis of Different Segmentation Strategies of Nerve Fiber Layer Assessment for Glaucoma Diagnosis. *J Glaucoma* 2015; **24**: 672-678 [PMID: 25055209 DOI: 10.1097/IJG.0000000000000071]

37 **Li Z**, He Y, Keel S, Meng W, Chang RT, He M. Efficacy of a Deep Learning System for Detecting Glaucomatous Optic Neuropathy Based on Color Fundus Photographs. *Ophthalmology* 2018; **125**: 1199-1206 [PMID: 29506863 DOI: 10.1016/j.ophtha.2018.01.023]

38 **Al-Aswad LA**, Kapoor R, Chu CK, Walters S, Gong D, Garg A, Gopal K, Patel V, Sameer T, Rogers TW, Nicolas J, De Moraes GC, Moazami G. Evaluation of a Deep Learning System For Identifying Glaucomatous Optic Neuropathy Based on Color Fundus Photographs. *J Glaucoma* 2019; **28**: 1029-1034 [PMID: 31233461 DOI: 10.1097/IJG.0000000000001319]

39 **Akkara JD**, Kuriakose A. Role of artificial intelligence and machine learning in ophthalmology. *Kerala J Ophthalmol* 2019; **31**: 150-160

40 **Asaoka R**, Murata H, Iwase A, Araie M. Detecting Preperimetric Glaucoma with Standard Automated Perimetry Using a Deep Learning Classifier. *Ophthalmology* 2016; **123**: 1974-1980 [PMID: 27395766 DOI: 10.1016/j.ophtha.2016.05.029]

41 **Andersson S**, Heijl A, Bizios D, Bengtsson B. Comparison of clinicians and an artificial neural network regarding accuracy and certainty in performance of visual field assessment for the diagnosis of glaucoma. *Acta Ophthalmol* 2013; **91**: 413-417 [PMID: 22583841 DOI: 10.1111/j.1755-3768.2012.02435.x]

42 **Goldbaum MH**, Sample PA, Zhang Z, Chan K, Hao J, Lee TW, Boden C, Bowd C, Bourne R, Zangwill L, Sejnowski T, Spinak D, Weinreb RN. Using unsupervised learning with independent component analysis to identify patterns of glaucomatous visual field defects. *Invest Ophthalmol Vis Sci* 2005; **46**: 3676-3683 [PMID: 16186349 DOI: 10.1167/iovs.04-1167]

43 **Bowd C**, Weinreb RN, Balasubramanian M, Lee I, Jang G, Yousefi S, Zangwill LM, Medeiros FA, Girkin CA, Liebmann JM, Goldbaum MH. Glaucomatous patterns in Frequency Doubling Technology (FDT) perimetry data identified by unsupervised machine learning classifiers. *PLoS One* 2014; **9**: e85941 [PMID: 24497932 DOI: 10.1371/journal.pone.0085941]

44 **Gao X**, Lin S, Wong TY. Automatic Feature Learning to Grade Nuclear Cataracts Based on Deep Learning. *IEEE Trans Biomed Eng* 2015; **62**: 2693-2701 [PMID: 26080373 DOI: 10.1109/TBME.2015.2444389]

45 **Liu X**, Jiang J, Zhang K, Long E, Cui J, Zhu M, An Y, Zhang J, Liu Z, Lin Z, Li X, Chen J, Cao Q, Li J, Wu X, Wang D, Lin H. Localization and diagnosis framework for pediatric cataracts based on slit-lamp images using deep features of a convolutional neural network. *PLoS One* 2017; **12**: e0168606 [PMID: 28306716 DOI: 10.1371/journal.pone.0168606]

46 **Wu X**, Huang Y, Liu Z, Lai W, Long E, Zhang K, Jiang J, Lin D, Chen K, Yu T, Wu D, Li C, Chen Y, Zou M, Chen C, Zhu Y, Guo C, Zhang X, Wang R, Yang Y, Xiang Y, Chen L, Liu C, Xiong J, Ge Z, Wang D, Xu G, Du S, Xiao C, Wu J, Zhu K, Nie D, Xu F, Lv J, Chen W, Liu Y, Lin H. Universal artificial intelligence platform for collaborative management of cataracts. *Br J Ophthalmol* 2019; **103**: 1553-1560 [PMID: 31481392 DOI: 10.1136/bjophthalmol-2019-314729]

47 **Dong Y**, Zhang Q, Qiao Z, Yang J. Classification of cataract fundus image based on deep learning. In: 2017 IEEE International Conference on Imaging Systems and Techniques; 2017 Oct 18-20; Beijing, China. IEEE; 2017: 1-5

48 **Yu F**, Silva Croso G, Kim TS, Song Z, Parker F, Hager GD, Reiter A, Vedula SS, Ali H, Sikder S. Assessment of Automated Identification of Phases in Videos of Cataract Surgery Using Machine Learning and Deep Learning Techniques. *JAMA Netw Open* 2019; **2**: e191860 [PMID: 30951163 DOI: 10.1001/jamanetworkopen.2019.1860]

49 **Zisimopoulos O**, Flouty E, Luengo I, Giataganas P, Nehme J, Chow A, Stoyanov D. Deep Phase: surgical phase recognition in CATARACTS videos. In: Frangi A, Schnabel J, Davatzikos C, Alberola-López C, Fichtinger G, editors. Medical Image Computing and Computer Assisted Intervention – MICCAI 2018. Cham: Springer; 2018: 265-272 [DOI: 10.1007/978-3-030-00937-3_31]

50 **Melles RB**, Kane JX, Olsen T, Chang WJ. Update on Intraocular Lens Calculation Formulas. *Ophthalmology* 2019; **126**: 1334-1335 [PMID: 30980854 DOI: 10.1016/j.ophtha.2019.04.011]

51 **Connell BJ**, Kane JX. Comparison of the Kane formula with existing formulas for intraocular lens power selection. *BMJ Open Ophthalmol* 2019; **4**: e000251 [PMID: 31179396 DOI: 10.1136/bmjophth-2018-000251]

52 **Hoffer KJ**. Intraocular lens power calculation after previous laser refractive surgery. *J Cataract Refract Surg* 2009; **35**: 759-765 [PMID: 19304101 DOI: 10.1016/j.jcrs.2009.01.005]

Published by **Baishideng Publishing Group Inc**
7041 Koll Center Parkway, Suite 160, Pleasanton, CA 94566, USA
Telephone: +1-925-3991568
E-mail: bpgoffice@wjgnet.com
Help Desk: https://www.f6publishing.com/helpdesk
https://www.wjgnet.com

ISSN 2644-3260 (online)

Artificial Intelligence in *Medical Imaging*

Artif Intell Med Imaging 2021 April 28; 2(2): 13-55

Published by Baishideng Publishing Group Inc

AIMI

Artificial Intelligence in Medical Imaging

Contents

Bimonthly Volume 2 Number 2 April 28, 2021

MINIREVIEWS

13 Artificial intelligence in radiation oncology

Yakar M, Etiz D

32 Intrathyroidal ectopic thymus: Ultrasonographic features and differential diagnosis

Karavas E, Tokur O, Aydın S, Gokharman D, Uner C

37 Current landscape and potential future applications of artificial intelligence in medical physics and radiotherapy

Ip WY, Yeung FK, Yung SPF, Yu HCJ, So TH, Vardhanabhuti V

Artificial Intelligence in Medical Imaging

Bimonthly Volume 2 Number 2 April 28, 2021

Contents

ABOUT COVER

Editorial Board Member of *Artificial Intelligence in Medical Imaging*, Guo-Lin Ma, MD, PhD, Professor, Department of Radiology, China-Japan Friend Hospital, Beijing 100029, China. maguolin1007@qq.com

AIMS AND SCOPE

The primary aim of *Artificial Intelligence in Medical Imaging* (*AIMI*, *Artif Intell Med Imaging*) is to provide scholars and readers from various fields of artificial intelligence in medical imaging with a platform to publish high-quality basic and clinical research articles and communicate their research findings online.

AIMI mainly publishes articles reporting research results obtained in the field of artificial intelligence in medical imaging and covering a wide range of topics, including artificial intelligence in radiology, pathology image analysis, endoscopy, molecular imaging, and ultrasonography.

INDEXING/ABSTRACTING

There is currently no indexing.

RESPONSIBLE EDITORS FOR THIS ISSUE

NAME OF JOURNAL
Artificial Intelligence in Medical Imaging

ISSN
ISSN 2644-3260 (online)

LAUNCH DATE
June 28, 2020

FREQUENCY
Bimonthly

PUBLICATION DATE
April 28, 2021

INSTRUCTIONS TO AUTHORS
https://www.wjgnet.com/bpg/gerinfo/204

GUIDELINES FOR ETHICS DOCUMENTS
https://www.wjgnet.com/bpg/GerInfo/287

GUIDELINES FOR NON-NATIVE SPEAKERS OF ENGLISH
https://www.wjgnet.com/bpg/gerinfo/240

PUBLICATION ETHICS
https://www.wjgnet.com/bpg/GerInfo/288

PUBLICATION MISCONDUCT
https://www.wjgnet.com/bpg/gerinfo/208

ARTICLE PROCESSING CHARGE
https://www.wjgnet.com/bpg/gerinfo/242

STEPS FOR SUBMITTING MANUSCRIPTS
https://www.wjgnet.com/bpg/GerInfo/239

ONLINE SUBMISSION
https://www.f6publishing.com

Artificial Intelligence in Medical Imaging

Submit a Manuscript: https://www.f6publishing.com

Artif Intell Med Imaging 2021 April 28; 2(2): 13-31

DOI: 10.35711/aimi.v2.i2.13

ISSN 2644-3260 (online)

MINIREVIEWS

Artificial intelligence in radiation oncology

Melek Yakar, Durmus Etiz

ORCID number: Melek Yakar 0000-0002-9042-9489; Durmus Etiz 0000-0002-2225-0364.

Author contributions: Yakar M and Etiz D collected data and wrote the manuscript; Etiz D formatted and revised the article.

Conflict-of-interest statement: The authors declare that they have no conflicts of interest.

Manuscript source: Invited manuscript

Specialty type: Oncology

Country/Territory of origin: Turkey

Peer-review report's scientific quality classification

Grade A (Excellent): 0

Grade B (Very good): B

Melek Yakar, Durmus Etiz, Department of Radiation Oncology, Eskisehir Osmangazi University Faculty of Medicine, Eskisehir 26040, Turkey

Melek Yakar, Durmus Etiz, Center of Research and Application for Computer Aided Diagnosis and Treatment in Health, Eskisehir Osmangazi University, Eskisehir 26040, Turkey

Corresponding author: Melek Yakar, MD, Assistant Professor, Department of Radiation Oncology, Eskisehir Osmangazi University Faculty of Medicine, Büyükdere, Meselik Campus, Eskisehir 26040, Turkey. mcakcay@ogu.edu.tr

Abstract

Artificial intelligence (AI) is a computer science that tries to mimic human-like intelligence in machines that use computer software and algorithms to perform specific tasks without direct human input. Machine learning (ML) is a subunit of AI that uses data-driven algorithms that learn to imitate human behavior based on a previous example or experience. Deep learning is an ML technique that uses deep neural networks to create a model. The growth and sharing of data, increasing computing power, and developments in AI have initiated a transformation in healthcare. Advances in radiation oncology have produced a significant amount of data that must be integrated with computed tomography imaging, dosimetry, and imaging performed before each fraction. Of the many algorithms used in radiation oncology, has advantages and limitations with different computational power requirements. The aim of this review is to summarize the radiotherapy (RT) process in workflow order by identifying specific areas in which quality and efficiency can be improved by ML. The RT stage is divided into seven stages: patient evaluation, simulation, contouring, planning, quality control, treatment application, and patient follow-up. A systematic evaluation of the applicability, limitations, and advantages of AI algorithms has been done for each stage.

Key Words: Radiation oncology; Radiotherapy; Artificial intelligence; Deep learning; Machine learning

Core Tip: Beginning with the initial patient interview, artificial intelligence (AI) can help predict posttreatment disease prognosis and toxicity. Additionally, AI can assist in

Grade C (Good): 0
Grade D (Fair): 0
Grade E (Poor): 0

Received: March 4, 2021
Peer-review started: March 4, 2021
First decision: March 14, 2021
Revised: March 30, 2021
Accepted: April 20, 2021
Article in press: April 20, 2021
Published online: April 28, 2021

P-Reviewer: Lee KS
S-Editor: Wang JL
L-Editor: Filipodia
P-Editor: Xing YX

the automated segmentation of both the organs at risk and target volumes and the treatment planning process with advanced dose optimization. AI can optimize the quality control process and support increased safety, quality, and maintenance efficiency.

Citation: Yakar M, Etiz D. Artificial intelligence in radiation oncology. *Artif Intell Med Imaging* 2021; 2(2): 13-31
URL: https://www.wjgnet.com/2644-3260/full/v2/i2/13.htm
DOI: https://dx.doi.org/10.35711/aimi.v2.i2.13

INTRODUCTION

Artificial intelligence (AI) is a computer science branch that tries to imitate human-like intelligence in machines using computer software and algorithms without direct human input to perform certain tasks[1,2]. Machine learning (ML) is a subunit of AI that uses data-driven algorithms that learn to imitate human behavior based on previous example or experience[3]. Deep learning (DL) is an ML technique that uses deep neural networks to create a model. Increasing computing power and reduction of financial barriers led to the emergence of the domain of DL[4]. The growth and sharing of data, increasing computing power, and developments in AI have initiated a transformation in healthcare services. Advances in radiation oncology, clinical and dosimetric information from increasing cases, and computed tomography (CT) imaging before each fraction have resulted in the accumulation of a significant amount of information in big databases.

Evidence-based medicine is based on randomized controlled trials designed for large patient populations. However, the increasing number of clinical and biological parameters that need to be investigated makes it difficult to design studies[5]. New approaches are required for all patient populations. Clinicians should use all diagnostic tools, such as medical imaging, blood testing, and genetic testing, to decide on the appropriate combination of treatments (*e.g.*, radiotherapy, chemotherapy, targeted therapy, and immunotherapy). There are a number of individual differences that are responsible for each patient's disease or associated with response to treatment and clinical outcome. The concept of personalized treatment is based on determining and using these factors for each patient[6]. Integrating such a large amount of heterogeneous of data and producing accurate models may present difficulties and subjective individual differences for the human brain from time to time.

Beginning with the initial patient interview, AI can help predict posttreatment disease prognosis and toxicity. Additionally, AI can assist in the automated segmentation of both the organs at risk and target volume and the treatment planning process, with advanced dose optimization. AI can optimize the quality control (QA) process and support increased safety, quality, and maintenance efficiency.

The aim of this review is to summarize the radiotherapy (RT) process in workflow order by identifying specific areas where quality and efficiency can be improved with AI. The RT stage is divided into seven stages: patient evaluation, simulation, contouring, planning, QA, treatment application, and patient follow-up, and the flow chart is given in Figure 1. A systematic evaluation of the applicability, limitations, and advantages of AI algorithms has been made to each stage.

CLINICAL EVALUATION

Clinical radiation therapy workflow begins with patient assessment. This step typically includes a series of consultations including reviews of the radiation oncologist on the patient's symptoms, medical history, physical examination, pathological and genomic data, diagnostic studies of prognosis, comorbidities, and risk of toxicity from RT. The radiation oncologist then suggests a treatment plan based on the synthesis of these data. For clinicians involved in this process, the accumulation of big data beyond what people can quickly interpret is the biggest challenge[7]. AI-based methods that can be used in routine functioning may be important decision support tools for clinicians in the future. Such AI-based models have been reported to

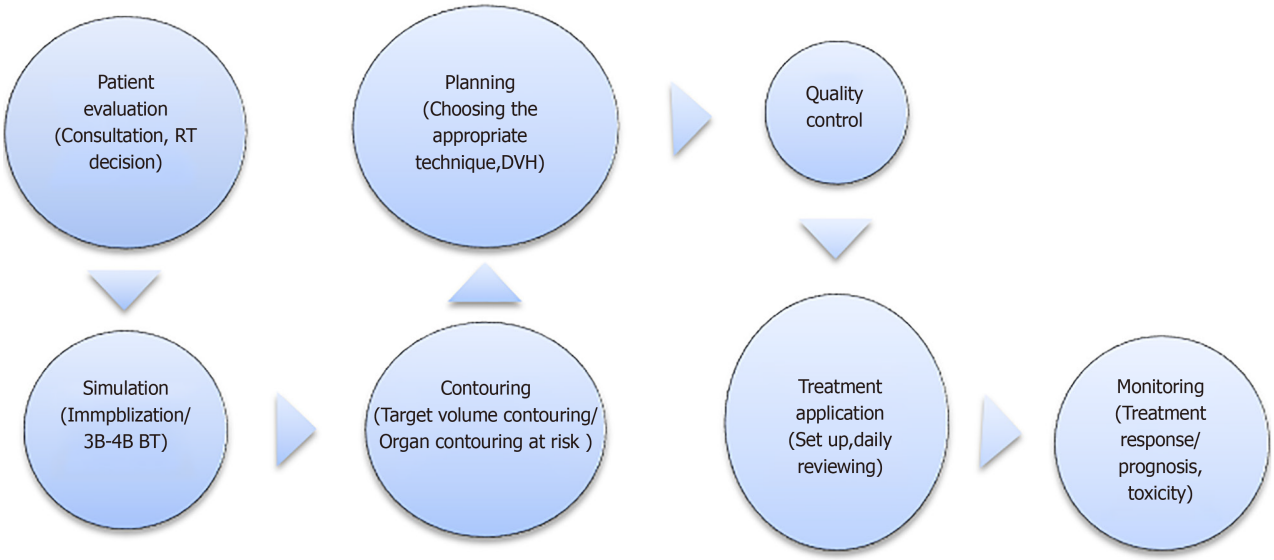

Figure 1 Workflow in radiation oncology. DVH: Dose value histogram; RT: Radiotherapy.

improve prognosis and predict treatment outcomes, but are not yet used in routine clinical practice[8].

The recent implementation of electronic health records has significantly increased the clinical documentation burden of physicians. The notes having constituted 34%-78% of physicians' working days, for each hour a physician spends in direct contact with the patient, he spends an additional 2 h in front of the computer[9]. AI solutions have the potential to automate structured documentation. They can save time requirements that add to the documentation burden, reduce burnout, protect confidentiality, and organize medical data into searchable and available items[10]. In addition, an AI-supported electronic record system may have pre-consultation and disease pre-diagnosis power, by including a timeline and the outcomes of relevant tests, procedures, and treatments from various sources[10]. AI-based systems can record patient-doctor conversations and use speech recognition and natural language processing to create a coherent narrative. Such an AI-based system does not yet exist, significant technical advances for clinical and persuasive speech require the learning of hours of selected recording of patient speech[11]. According to patient demands AI systems can present information to the patient at low, medium, or high complexity levels.

The radiation oncologist should consider many factors during the evaluation of the patient and include consideration of their interactions when making treatment decisions. At this point, data-based forecasting models can guide the doctor and make the decision phase faster and more accurate. For example, when a patient diagnosed with lung cancer is being evaluated for stereotactic RT, the patient's respiratory functions, lung capacity, tumor size, proximity of the tumor to critical organs, comorbid diseases, and performance of the patient will affect both treatment response and toxicity. If modeling is made with these and similar factors, response and toxicity rates can be determined before starting treatment. In a case with a diagnosis of left breast cancer and treatment with breast-conserving surgery, modeling created with the patient and treatment characteristics can be predicted whether she can benefit from a breath-holding technique. Big data are needed to create these estimation models. The transition to the use of AI will also increase collaboration between centers in the data collection phase and make treatments more standardized. In addition, depending on the distribution of technology in the centers in the country, AI can direct patients to appropriate treatment centers. For example, it can direct pediatric cases requiring proton therapy to a specialized center, and cases requiring palliative treatment to a conventional center).

SIMULATION

After the RT decision is made, a good simulation is required to choose the right

treatment. Immobilization technique, scanning range, and the treatment area should be accurately determined. Preliminary preparations such as use of fiducial markers for simulation, full/empty bladder, whether an empty rectum is required, renal function tests, and fasting status should be carefully considered if intravenous contrast is to be applied. Accurate and good simulation is essential to obtain a high-quality, robust treatment plan for the patient. In clinical practice, it is not uncommon to repeat a CT during CT simulation because of deficiencies and inaccuracies such as insufficient scanning range, inadequate/incorrect immobilization technique, an inappropriate level of bladder/rectum content, and hardware-related artifacts[12]. There are many questions that can be answered with AI to improve overall workflow efficiency. For example, will the patient benefit from the use of an intravenous contrast agent? Which immobilization technique should be used? Is 4-dimensional (4D)-CT simulation necessary?

Depending on the location of the disease, this process can be very complex, and optimal patient immobilization is individual, so this process often requires the participation of a radiation oncologist and a medical physicist. For example, special care should be taken to assess potential interference between the immobilization device and treatment beam angles, or patient-specific problems that could cause collisions with the RT device. In simulation, CT is still used in many centers, but brain and prostate tumors can be seen better with magnetic resonance (MR). As a solution, efforts have been made to develop CT scans using MR data, also called synthetic CT (sCT) scans using the atlas-based, sparse coding-based, or learning-based methods. Convolutional neural networks (CNNs), which are less time consuming and more efficient AI-based method with fewer artifacts, increasingly used to convert MR data to sCT[13]. Therefore, in the future, sCT scans with AI-based methods may compensate for the need for CT scanning, as they can be created with electron density data faster and are more reliable for plan generation than MR. Compared with traditional sCT methods, DL methods can be fully automated. Training with MR-CT images has been improved by the use of cycle-consistent generative adversarial networks (GANs)[14]. GANs require a new DL algorithm using two networks, a generator network creates realistic images and a differential mesh distinguishes between real and created images[14]. Studies have reported that images created by sCT and DL are accurate enough for dose calculation[15,16]. The same method can be used for other image syntheses. For example, virtual 4D-MR images can be synthesized from 4D-BT in order to see liver tumors well in image-guided RT (IGRT)[17].

Simulation is one of the most important steps in RT because ant deficiencies or errors that occur are reflected in the entire treatment process. AI techniques can be used to increase the accuracy of the simulation, to personalize it according to the patient characteristics, and to better characterize the tumor, but more studies are needed for its routine clinical use.

IMAGE REGISTRATION - SEGMENTATION

Image registration

Image registration is the process of spatially aligning two or more sets of images of the same region shot in different modalities at different times[17]. Commercially available automated image registration algorithms are typically designed to perform well only with modality-specific registration problems and require additional manual adjustments to achieve a clinically acceptable registration[7]. The two main registration methods used in RT are density based and have rigid registration. In a review of image registration Viergever *et al*[18] examined relevant developments between 1998 and 2016. They stated that DL approaches to registration can be novel game-changers in facilitating the implementation process and doing more, and they advocated the application of DL concepts to make it a routine integral part of the entire clinical imaging spectrum[18]. AI tools are also trained to determine the sequence of motion actions that result in optimal registration. These algorithms can provide better accuracy than various state-of-the-art registration methods and can be generalized to multiple display methods[19]. AI approaches have been shown to mitigate the effects of image artifacts like metal screws, guide wires, prostheses, and motion artifacts, which pose difficulties in both registration and segmentation[7].

Segmentation

In the standard workflow, the target volume and organs at risk (OARs) are manually

contoured by the radiation oncologist in a cross-section. As a result, the process is long and has a high degree of variability as a result of individual differences[20]. Manual segmentation directly affects the quality of the treatment plan and dose distribution for OARs[21]. There have been some attempts at automatic segmentation. It is the most widely available atlas-based segmentation in clinical use. First, the target image is matched with one or more selected reference images. Then, the contours in the reference image are transferred to the target image[22]. Atlas-based methods depend on the choice of atlas and the accuracy of reference images[23]. AI can be used to minimize the differences between physicians and to shorten the duration of this step in RT planning.

Segmentation of at-risk organs: To protect at-risk organs and to correctly evaluate RT toxicity, the segmentation of OARs should be done correctly. To fully benefit from technological developments in RT planning and devices, at-risk organs must be identified correctly. In clinics with high patient density, this step can be rate limiting. In addition, there may be differences among the practitioners, and because of significant anatomical changes (*e.g.*, edema, tumor response, weight loss, and others) during treatment, a new plan with new segmentation may be required. AI, particularly CNN, is a potential tool to reduce physician workload and define a standard segmentation. In recent years, DL methods have been widely used in medical applications such as organ segmentation in CNN, head-neck, lung, brain, and prostate cancers[24-27].

In a head and neck cancer study by Ibragimov *et al*[28] contouring the spinal cord, mandible, parotid glands, submandibular glands, larynx, pharynx, eyes, optic nerves, and optic chiasm was done in 50 patients by DL using CT images. They obtained dice similarity coefficients (DSCs) of between 37.4% (optic chiasm) and 89.5% (mandible). Compared with the contouring algorithm of current commercial software, contouring of the medulla spinalis, mandibular and parotid glands, larynx, pharynx, and eye globes, was better and that of the optic nerve, submandibular gland (SMG), and the optic chiasm was worse with DL. CT images were used in that study, and higher accuracy rates were achieved with MR image support[28]. In a study of head and neck organ segmentation in 200 patients with oropharyngeal squamous cell carcinoma, Chan *et al*[29] used CT for planning, with 160 cases used for training, 20 for internal validation, and 20 for testing. Mandibula, right and left parotid glands, oral cavity, brainstem, larynx, esophagus, right and left SMG, right and left temporomandibular joints were contoured. In a lifelong learning-based CNN (LL-CNN) comparison, manual contouring was used as the gold standard and DSC and root-mean-square error (RMSE) was used for accuracy. LL-CNN was then compared to 2D U-Net, 3D U-Net, single-task CNN (ST-CNN) and multitask CNN. Higher DSC and lower RMSE were obtained with LL-CNN compared with the other algorithms. The study found that LL-CNN had a better prediction accuracy than all alternative algorithms for the head and neck organs at risk[29]. In another study, Rooij *et al*[30] used CT images of 157 head and neck cancer patients, 142 for case training and 15 for testing. The right and left SMGs, right and left parotid glands, larynx, cricopharynx, pharyngeal constrictor muscle, upper esophageal sphincter, brain stem, oral cavity, and esophagus were contoured. With DL, contouring of the 11 OARs was < 10 s per patient. The mean DSC of seven of the 11 contoured organs ranged from 0.78 to 0.83, and the DSC values for the esophagus, brainstem, PMC and cricopharynx were 0.60, 0.64, 0.68 and 0.73, respectively[30]. The study found that for the head and neck OAR, DL-based segmentation was fast and performed well enough for treatment planning purposes for most organs and most patients.

OARs in the thorax area have also contoured for RT with AI[31-34]. Zhu *et al*[25] used CT images of 66 lung cancer cases, 30 cases for training and 36 cases for testing. CNN was used for segmentation, and compared with atlas-based automatic segmentation (ABAS). DSC, the mean surface distance (MSD), and 95% Hausdorff distance (95% HD) were used to evaluate the results. The MSD (mm) values for CNN and ABAS were 2.92 and 3.14 for the heart, 3.21 and 3.83 for the liver, 1.81 and 3.03 for ms, 2.65 and 2.67 for the esophagus, and 1.93 and 1.85 mm for the lungs. The 95% HD (mm) values for CNN and ABAS were 7.98 and 9.53 in the heart, 10.0 and 11.87 in the liver, 8.74 and 11.97 in ms, 9.25 and 9.45 in the esophagus, and 7.96 and 8.07 mm in the lungs[25]. According to the results of that study, CNN can be used in segmentation for RT of lung cancer. Zhang *et al*[33] compared CNN-based segmentation and ABAS and reported that CNN-based segmentation required 1.6 minutes per case and atlas-based contouring required 2.4 min ($P < 0.001$). Accuracy rates were measured by DSC and MSD and found that CNN-based segmentation was better than atlas-based segmentation for left lung and heart RT[33]. A study by Vu *et al*[34] that included

22411 CT images obtained from 168 cases reported training, validation, and test rates of 66%, 17% and 17%, respectively. CNN-based and atlas-based segmentation models were compared with verification by DSC and 95% HD. All differences were found to be statistically significant in favor of CNN-based segmentation[34].

Looking at other studies in the literature, Feng *et al*[32] evaluated 36 cases, with 24 used as training and 12 used as testing. The DSC obtained with 3D U-Net for medulla spinalis, right lung, left lung, heart, and esophagus were 0.89, 0.97, 0.97, 0.92, and 0.72, respectively. The corresponding MSDs were 0.66, 0.93, 0.58, 2.29 and 2.34 mm; and the 95% HDs were 1.89, 3.95, 2.10, 6.57, 8.71[32]. The conclusion was that because of the improved accuracy and low cost of OAR segmentation, DL has the potential to be clinically adopted in RT planning. Loap *et al*[31] performed AI-based heart segmentation with CT images obtained from 20 breast cancer cases. The performance of the model was evaluated by DSC, and this value was found to be 95% for the whole heart and 80% for the heart chambers[31].

Studies on OAR segmentation in the pelvic region have generally been done with cervical and prostate cancer[27,35]. The bladder, bone marrow, left femoral head, right femoral head, rectum, small intestine, and ms were contoured using CT images of 105 locally advanced cervical cancer cases. U-Net was used and the accuracy of the model was evaluated by DSC and 95% HD. The DSC of OARs ranged from 92% to 79%, with the best results in the bladder and the worst in the rectum. 95% HD values ranged between 5.09 and 1.39 mm[35]. Savenije *et al*[27] included 150 prostate cancer cases with MR imaging. DeepMedic and dense V-net were used in modeling. Bladder, rectum and femoral heads are contoured. The duration of DeepMedic, dense V-net, and atlas-based segmentation were 60 s, 4 s and 10-15 min, respectively. The accuracy of the DeepMedic algorithm that had been obtained in a feasibility study was confirmed the clinical setting in that study[27].

Additional evidence is available from a study by Ahn *et al*[36] who used CT images of 70 cases diagnosed with liver cancer, 45 for training, 15 for validation, and 19 for testing. The reference was accepted segmentation by three senior physicians. The model was created with deep CNN (DCNN). The accuracy rate was evaluated with 95% HD, DSC, volume overlap error (VOE), and relative volume difference (RVD). In ABAS, the DSCs were 0.92, 0.93, 0.86, 0.85, and 0.60 for the heart, liver, right kidney, left kidney and stomach. In the DCNN-based model, the values were 0.94, 0.93, 0.88, 0.86, and 0.73. The VOE% values in DCNN and atlas-based segmentation were 10.8 *vs* 15.17, 10.82 *vs* 13.52, 12.19 *vs* 17.51, 16.31 *vs* 25.63 and 37.53 *vs* 62.64. The RVD% values in DCNN and atlas-based segmentation were 5.17 *vs* 12.90, 1.86 *vs* 5.56, 4.53 *vs* 9.75, 2.45 *vs* 10.23 and 21.26 *vs* 50.6[36]. In that study, DL-based segmentation appeared to be more effective and efficient than atlas-based segmentation for most of the OAR in liver cancer RT.

Dolz *et al*[26] performed brainstem segmentation from the MR images of 14 brain cancer cases. A support vector machine (SVM) algorithm was used for the model, DSC, absolute volume difference (AVD) and percentage volume difference (pVD) between automatic and manual contours were used for the performance evaluation of the model. The mean values were, DSC 0.89-0.90, AVD 1.5 cm^3 and pVD 3.99%[26]. The proposed approach has consistently shown similarity to manual segmentation and can be considered promising for adoption in clinical practice. Studies that investigated segmentation of OARs are summarized in Table 1.

Learning algorithms are trained to maximize measures of similarity between outcomes and examples given to them. Therefore, although they are increasingly skilled at imitating human-drawn contours, they are limited by the quality of their training samples. Until more concrete consensus definitions are specified for boundaries, machines cannot be more accurate than the human input taken as their clinically fundamental truth. Machine "accuracy" is only considered to be meaningful in the context of individuals and institutional protocols. More case numbers and multicenter studies are needed for the development and standardization of contouring models.

Target volume contouring: Target volume contouring is a labor-intensive step in the treatment planning flow in RT. Differences in manual contouring result from variability between contours, differences in radiation oncology education, or quality differences in imaging studies. Current automatic contouring methods aim to reduce manual workload and increase contour consistency, but still tend to require significant manual editing[37]. Recent studies have shown that DL-based automatic contouring of target volumes is promising, with greater accuracy and time savings compared with atlas-based methods.

Table 1 Contouring of at-risk organs

Ref.	Tumor site	Artificial intelligence technique	Patient number	Contouring	Results
Ibragimov *et al*[28], 2017	Head-neck	CNN	50	Contoured with CT. OARs: (1) Ms; (2) Mandible; (3) Parotid; (4) SMG; (5) Larynx; (6) Pharynx; (7) Eyes; (8) Optic nerve; and (9) Optic chiasm	DSC: (1) Ms: 87%; (2) Mandible: 89.5%; (3) Right parotid gland: 77.9%; (4) Left parotid gland: 76.6%; (5) Left SMG: 69.7%; (6) Right SMG: 73%; (7) Larynx: 85.6%; (8) Pharynx: 69.3%; (9) Left eye glob: 63.9%; (10) Right eye glob: 64.5%; (11) Left optic nerve: 63.9%; (12) Right optic nerve: 64.5%; and (13) Optical chiasm: 37.4%
Chan *et al*[29], 2019	Orafarenx	LL-CNN, 2D U-Net, 3D U-Net, ST-CNN, MT-CNN	200 (160 training, 20 validation, 20 test)	Contoured with CT. OAR: (1) Mandible; (2) Right and left parotid gland; (3) Oral cavity; (4) Brain stem; (5) Larynx; (6) Esophagus; (7) Right and left SMG; and (8) Right and left TMJ	DSC (mm) for LL-CNN and RMSE: (1) Mandible: 0.91 and 0.66; (2) Right parotid gland: 0.86 and 1.67; (3) Left parotid gland: 0.85 and 1.86; (4) Oral cavity: 0.87 and 0.83; (5) Brain stem: 0.89 *vs* 0.96; (6) Larynx: 0.86 *vs* 1.34; (7) Esophagus: 0.86 *vs* 1.03; (8) Right SMG: 0.85 *vs* 1.24; (9) Left SMG: 0.84 *vs* 1.22; (10) Right TMJ: 0.87 *vs* 0.43; and (11) Left TMJ: 0.84 *vs* 0.47
Rooij *et al*[30], 2019	Head-neck	3D U-Net	157 (142 training, 15 tests)	Contoured with CT. OAR: (1) Right and left SMG; (2) Right and left parotid gland; (3) Larynx; (4) Cricopharynx,; (5) PCM; (6) UES; (7) Brain stem; (8) Oral cavity; and (9) Esophagus	DSC: (1) Right SMG: 0.81; (2) Left SMG: 0.82; (3) Right parotid gland: 0.83; (4) Left parotid gland: 0.83; (5) Larynx: 0.78; (6) Cricopharynx: 0.73; (7) PCM: 0.68; (8) UES: 0.81; (8) Brain stem: 0.64; (9) Oral cavity: 0.78; and (10) Esophagus: 0.60
Zhu *et al*[25], 2017	Lung	CNN	66 (30 training, 36 tests)	Contoured with CT. OAR: (1) Heart; (2) Liver; (3) Ms; (4) Esophagus; and (5) Lung	MSD (mm) (CNN *vs* ABAS): (1) Heart: 2.92 *vs* 3.14; (2) Liver: 3.21 *vs* 3.83; (3) Ms: 1.81 *vs* 3.03; (4) Esophagus: 2.65 *vs* 2.67; and (5) Lung: 193 *vs* 1.85; 95% HD (mm) (CNN *vs* ABAS): (1) Heart: 7.98 *vs* 9.53; (2) Liver: 10.06 *vs* 11.87; (3) Ms: 8.74 *vs* 11.97; (4) Esophagus: 9.25 *vs* 9.45; and (5) Lung: 7.96 *vs* 8.07
Zhang *et al*[33], 2020	Lung	CNN	200: training;50: validation 19: test	Contoured with CT. OAR: (1) Lungs; (2) Esophagus; (3) Heart; (4) Liver; and (5) Ms	DSC (CNN *vs* atlas based): (1) Left lung: 94.8% *vs* 93.2%; (2) Right lung: 94.3% *vs* 94.3%; (3) Heart: 89.3% *vs* 85.8%; (4) Ms: 82.1% *vs* 86.8%; (5) Liver: 93.7% *vs* 93.6%; and (6) Esophagus: 73.2% *vs* -; MSD (mm) (CNN *vs* atlas based): (1) Left lung: 1.10 *vs* 1.73; (2) Right lung: 2.23 *vs* 2.17; (3) Heart: 1.65 *vs* 3.66; (4) Ms: 0.87 *vs* 0.66; (5) Liver: 2.03 *vs* 2.11; and (6) Esophagus: 1.38 *vs* -
Vu *et al*[34], 2020	Lung	2D-CNN	168 (66% training, 17% validation, 17% testing)	Contoured with CT. OAR: (1) Ms; (2) Lungs; (3) Heart; and (4) Esophagus	DSC (CNN *vs* atlas - based model): (1) Ms: 71% *vs* 67%; (2) Right lung: 96% *vs* 94%; (3) Left lung: 96% *vs* 94%; (4) Heart: 91% *vs* 85%; and (5) Esophagus: 63% *vs* 37%; 95% HD (mm) (CNN *vs* atlas - based model): (1) Ms: 9.5 *vs* 25.3; (2) Right lung: 5.1 *vs* 8.1; (3) Left lung: 4.0 *vs* 8.0; (4) Heart: 9.8 *vs* 15.8; and (5) Esophagus: 9.2 *vs* 20
Feng *et al*[32], 2019	Lung	3D U-Net	36 (24 training, 12 tests)	Contoured with CT. OAR: (1) Ms; (2) Right lung; (3) Left lung; (4) Heart; and (5) Esophagus	DSC: (1) Ms: 0.89; (2) Right lung: 0.97; (3) Left lung: 0.97; (4) Heart: 0.92; and (5) Esophagus: 0.72; 95% HD (mm): (1) Ms: 1.89; (2) Right lung: 3.95; (3) Left lung: 2.10; (4) Heart: 6.57; and (5) Esophagus: 8.71; MSD (mm): (1) Ms: 0.66; (2) Right lung: 0.93; (3) Left lung: 0.58; (4) Heart: 2.29; and (5) Esophagus 2.34
Liu *et al*[35], 2019	Cervix	3D U-Net	105 (77 training, 14 validation, 14 tests)	Contoured with CT. OAR: (1) Bladder; (2) Bone Marrow; (3) Left femoral head; (4) Right femoral head; (5) Rectum; (6) Small intestine; and (7) Ms	DSC: (1) Bladder: 0.92; (2) Bone Marrow: 0.86; (3) Left femoral head: 0.89; (4) Right femoral head: 0.89; (5) Rectum: 0.79; (6) Small intestine: 0.83; and (7) Ms: 0.82; 95% HD (mm): (1) Bladder: 5.09; (2) Bone marrow: 1.99; (3) Left femoral head: 1.39; (4) Right femoral head: 1.43; (5) Rectum: 5.94; (6) Small intestine: 5.21; and (7) Ms: 3.26
Savenije *et al*[27], 2020	Prostate	DeepMedic and Dense V-net	48 (36 training, 16 tests) for feasibility study; 150 cases in total (97 train, 53 tests)	Contoured by MR. OAR: (1) Bladder; (2) Rectum; (3) Left femur; and (4) Right femur	DSC/95% HD (mm)/MSD (mm): (DeepMedic and dense V-net (feasibility study): (1) Bladder: 0.95/3.8/1.0; (2) Rectum: 0.85/8.3/2.1; (3) Left femur: 0.96/2.2/0.6; and (4) Right femur: 0.96/1.9/0.6; DSC/95% HD (mm)/MSD (mm): (Clinical application with DeepMedic): (1) Bladder: 0.96/2.5/0.6; (2) Rectum: 0.88/7.4/1.7; (3) Left femur: 0.97/1.6/0.5; and (4) Right femur: 0.97/1.5/0.5
Ahn *et al*[36], 2019	Liver	DCNN	70 (45 training, 15 validation, 10 tests)	Contoured with CT. OAR: (1) Heart; (2) Liver; (3) Kidney; and (4) Stomach	DSC (DCNN *vs* atlas-based contouring): (1) Heart: 0.94 *vs* 0.92; (2) Liver: 0.93 *vs* 0.93; (3) Right kidney: 0.88 *vs* 0.86; (4) Left kidney: 0.86 *vs* 0.85; and (5) Stomach: 0.73 *vs* 0.60

95% HD: 95% Hausdorff distance; ABAS: Atlas-based automatic segmentation; CNN: Convolutional neural network; CT: Computational Tomography; DCNN: Deep convolutional neural network; DSC: Dice similarity coefficient; ms: Medulla spinalis; MSD: Mean surface distance; MSD: The mean surface distance; MT-CNN: Multitask Convolutional neural network, RMSE: Root-mean-square error; OAR: Organ at risk; PCM: Pharyngeal constrictor muscle; SMG: Submandibular gland; ST-CNN: Single-task Convolutional neural network; TMJ: Temporamandibular joint; UES: Upper esophageal sphincter.

The first reason for the necessity of computer-aided delineation is the variation between contours or even between contours of the same person at different times. Chao *et al*[38] reported that differences in defining CTVs from scratch among radiation oncologists is important, and the use of computer-aided methods reduces volumetric variation and improves geometric consistency[38]. The second reason is that it is time consuming. In a study by Chao *et al*[38], computer-assisted contouring provided 36%-29% time savings for experienced physicians and 38%-47% for less experienced physicians[38]. Ikushima *et al*[39] estimated the gross tumor volume (GTV) of 14 lung cancers. Six were solid, six were part-solid, and four had mixed ground-glass opacity (GGO) using AI. Image properties around the GTV contours were taught to the SVM algorithm during training, after which the algorithm was tested to generate GTV for each voxel. Diagnostic CT, planning CT and PET were used for image properties. The final GTV contour was determined using the optimum contour selection method. DSC was used for the performance of the algorithm and was determined to be 0.77 for 14 cases. The DSC values for solid, part-solid and mixed GGO were 0.83, 0.70 and 0.76, respectively[39]. In a study conducted by Cui *et al*[40], 192 cases of lung cancer (118 solid, 53 part-solid, and 21 pure GGO) with stereotactic body radiotherapy (SBRT) were contoured with dense V-networks using planning it. Of those, 147 cases were for training, 26 for validation, and 19 cases were for testing. Evaluation was performed with a DSC and HD 10-fold cross validation test. The 3D-DSC values were 0.838 ± 0.074, 0.822 ± 0.078, and 0.819 ± 0.059 for solid, part-solid, and GGO tumors respectively. The HD value of each inner group was 4.57 ± 2.44 mm[40]. The proposed approach has the potential to assist radiation oncologists in identifying GTVs for planning treatment of lung cancer SBRT.

Zhong *et al*[41] performed segmentation with 3-D DL and fully convolutional networks (DFCN) using both PET and BT images of 60 lung SBRT cases. Delineation was performed by three senior physicians. A simultaneous truth and performance level estimation algorithm was accepted as a reference, and DSC was used to evaluate DFCN performance. The mean DSCs were for 0.861 ± 0.037 for CT and 0.828 ± 0.087 for PET[41]. Kawata *et al*[42] used pixel-based MÖ techniques such as fuzzy-c-means clustering (FCM), artificial neural network (ANN), and SVM to evaluate the GVT of 16 lung cancer tumors (six solid, four GGO, six part-solid) for SBRT by AI using PET/CT. The performance of the algorithms was determined by DSC. The DSC values for FCM, ANN, and SVM were 0.79 ± 0.06, 0.76 ± 0.14 and 0.73 ± 0.14, respectively[42]. FCM had the highest accuracy rates of GTV contouring compared with the other algorithms.

There are also GTV and CTV contouring studies with AI in head and neck cancers[43-47]. In a study by Li *et al*[43], tumor segmentation was performed in nasopharyngeal cancer by using CT images. The U-Net model was used, 302 cases

were used for training, 100 for validation, and 100 for testing. In the U-Net model, DSC was found to be 65.8% for lymph nodes and 74.0% for tumor segmentation. Automatic delineation was calculated as 2.6 h per patient and manual delineation as 3 h[43]. This study found that DL increased the accuracy, consistency, and efficiency of tumor delineation and that additional physician input might be required for lymph node delineation. Multimodality medical images can be very useful for automated tumor segmentation as they provide complementary information that can make the segmentation of tumors more accurate. Ma *et al*[44] used multimodality CNN (M-CNN) based methods to investigate the segmentation of nasopharyngeal cancer using CT and MR images. M-CNN is designed to co-learn the segmentation of matched CT-MR images. Considering that each modality has certain distinctive features, it was planned to create a combined-CNN (C-CNN) using single-modality (S-CNN) and higher-layer features derived from M-CNN. Ninety CT and MR images were used, and positive predictive value (PPV), sensitivity (SE), DSC, and average symmetric surface distance (ASSD) were used to evaluate modalities. The PPV, SE, DSC and ASSD obtained by C-CNN, were 0.797 ± 0.109, 0.718 ± 0.121, 0.752 ± 0.043, and 1.062 ± 0.298 mm respectively. The included two main models, M-CNN and C-CNN, which can integrate complementary information from CT and MR images for tumor identification. The results in the clinical CT-MR dataset show that the proposed M-CNN can learn the correlations of two modalities and tumor segmentation together and perform better than using a single modality[44].

Zhao *et al*[45] used PET-CT and FCN to contour 30 nasopharyngeal cancer tumors. The mean DSC was 87.47% after threefold cross validation. Guo *et al*[46] performed GTV contouring with Dense Net and 3D U-Net using PET/CT and PET-CT in 250 head and neck cancer patients. DSC, MSD, and HD95 were calculated for each of the three imaging methods separately. For Dense Net, the DSC values were 0.73 for PET-CT, 0.67 for PET, and 0.32 for CT. The DSC for 3D-U-Net and PET-CT was 0.71. MSD, HD for Dense Net PET-BT were 2.88, 6.48 and 3.96 mm, respectively. For Dense Net PET, the MSD, and HD95 DC were 3.38, 8.29 and 5.56 mm, respectively. For 3D U-Net, the MSD, HD95, DC were 2.98, 7.57 and 4.40 mm respectively[46]. In a study using a deep deconvolutional neural network (DDNN), the GTV_{tumor}, $GTV_{lymph\ node,}$ and CTV were determined from CT images of 230 nasopharyngeal cancer cases that were randomly allocated to 184 cases for training and 46 cases for testing. The DSC values were 80.9% for GTV_{tumor}, 62.3% for $GTV_{lymph\ node}$, and 82.6% for CTV[47].

AI-based contouring studies have also been performed in primary brain tumors and brain metastases[48-53]. In a study by Jeong *et al*[51], T1-weighted dynamic contrast-enhanced (DCE) perfusion MR images of 21 patients diagnosed with brain tumors were used for tumor segmentation. 3D mask region-based CNN (R-CNN) was used and algorithm performance was evaluated with DSC, HD, MSD, and center of mass distance. The values were 0.90 ± 0.04, 7.16 ± 5.78 mm, 0.45 ± 0.34 mm and 0.86 ± 0.91 mm, respectively[51]. The results support the feasibility of accurate localization and segmentation of brain tumors from DCE perfusion MRIs. Segmentation with 3D mask R-CNN in DCE perfusion imaging holds promise for future clinical use. Tang *et al*[53] described postoperative glioma segmentation of the CTV region using MR image information on CT. A deep feature fusion model (DFFM) guided by multisequence MR was used in CT images for postop glioma segmentation. DFFM is a multisequence MR-guided CNN that simultaneously learns deep features from CT and multisequence MR images and then combines the two deep features. In this study, 59 BT and MR (T1/T2-weighted FLAIR, T1-weighted contrast-enhanced, T2-weighted) data sets were used. The DSCs were 0.836 and 0.836[51]. Given the DSC rate, this algorithm can be used in the presegmentation stage to reduce the workload of the radiation oncologist.

Liver tumor segmentation with CT is difficult because the image contrast between liver tumors and healthy tissues is low, the boundary is blurred, and images of the liver tumor are complex, and vary in size, shape, and location. To solve these problems, Meng *et al*[54] performed liver tumor segmentation with 3D dual-path multiscale CNN (TDP-CNN). In the study, 81 CT images were used for training and 25 were used for the test. Tumor segmentation determined by an experienced radiologist was used as a reference. Performance evaluation was determined as DSC, HD average distance, and the values were 0.689, 7.69, and 1.07mm[54].

There are also studies using AI in pelvic tumor and CTV contouring[55-59]. In a prostate cancer study, MR images and the DeepLabV3 + method were used for with target volume segmentation. Volumetric DSC and surface DSC were used to evaluate performance, and these values were 0.83 ± 0.06 and 0.85 ± 0.11, respectively[56]. According to this model, the planning workflow can be accelerated with MR. Voxel-based ML was evaluated, and MR images of 78 cases were used in a study of tumor

delineation in locally advanced cervical cancer. The model was trained according to the delineation of two radiologists, mean sensitivity was 94% and specificity was 52%[57]. CT images were used for CTV delineation in rectal cancer, and 218 randomly selected cases were used for training and 60 cases for validation. Deep dilated CNN (DDCNN) was used and the DSC for the model was 87.7%[59]. According to that study, the accuracy rate was high and effective in CTV segmentation in the DDCNN rectal cancer. Deep dilated residual network (DD-ResNet) was used in breast cancer CTV contouring, and the model was compared with DDCNN and DDNN. CT images of 800 breast cancer cases were used in the study, and the training/test rate was determined as 80%/20%. Mean DSC was used for segmentation accuracy. For the right and left breast, DD-ResNet was 0.91 and 0.91, 0.85 and 0.85, 0.88 and 0.87 for DDCNN and DDNN, respectively. HD values were 10.5 and 10.7 mm, 15.1 and 15.6 mm, and 13.5 and 14.1 mm, respectively. Mean segmentation times were 4, 21 and 15 s per patient[60]. The method proposed in the study contoured the CTV in a short time and with high accuracy. The studies of target volume segmentation are summarized in Table 2. More cases and multidisciplinary studies are needed to reduce the heterogeneity in tumor response and in GTV and CTV contouring, shorten the contouring step, and create standard delineations.

RADIOTHERAPY PLANNING

RT planning process is quite complex. A mistake during planning can lead to life-threatening situations such as tumor incontinence or high doses of radiation to normal tissue. As technology advances, the margin given to the tumor also decreases, so even with a small margin of error, it is possible to miss the tumor geographically. After target volumes and OARs are defined, the planning process continues with the determination of dosimetric targets for targets and OARs, selection of an appropriate treatment technique [*e.g.*, 3DCRT, intensity-adjusted RT (IMRT), volumetric modulated arc therapy (VMAT), protons], the achievement of planning goals, and evaluation and approval of the plan. Treatment planning, which is an RT design for each case, can be considered as both a science and an art.

Because of the complex mathematics and physics involved, RT planning includes computer-aided systems. During planning, humans interact many times with the computer-aided system, using their experience and skills to ensure the satisfactory quality of each plan. Planning is a very complex process. There are AI studies related to the planning steps of RT, such as dose calculation, dose distribution, dose-volume histogram (DVH), patient-specific dose calculation, IMRT area determination, beam angle determination, real-time tumor tracking, and replanning in adaptive RT[61-71].

The purpose of researching the dose calculation algorithm is to increase calculation accuracy while maximizing computational efficiency. In the study conducted by Zhu *et al*[61], it was aimed to calculate the 3D distribution of total energy release per unit mass and electron density based on CNN. Twelve sets of CT images were used for training, and a random beam configuration was created with a convolution/superposition (CCCS) algorithm. 7500 samples were created for each single-energy photon model training set and 1500 samples for validation. Training included 0.5 MeV, 1 MeV, 2 MeV, 3 MeV, 4 MeV, 5 MeV, and 6 MeV monoenergetic photon models. To evaluate its usability under linear accelerator (Linac) conditions, 12 additional new CT images with different anatomical regions and 1512 samples were used for testing. For all anatomies, the mean value for the criterion of 3%/2mm, 95% lower confidence limit, and 95% upper confidence limit were 99.56%, 99.51%, and 99.61%, respectively. In that study, DL was investigated for CCCS dose calculation[61]. With DL, calculation accuracy can be improved and calculation efficiency can be increased, and the method can speed up dosing algorithms and also has great potential in adaptive RT.

In their study, Zhang *et al*[62] aimed to estimate voxel level doses by integrating the distance information between the planning target volume (PTV) and OAR as well as the image information into the DCNN. First, they created a four-channel feature map consisting of PTV image, OAR image, CT image, and distance image. A neural network was created and trained for dose estimation at the voxel level. Given that the shape and size of OARs are highly variable, dilated convolution was used to capture features from multiple scales. The network was evaluated by five-fold cross validation based on 98 clinically validated treatment plans. The voxel level mean absolute error values of the DCNN for PTV, left lung, right lung, heart, spinal cord and body were 2.1%, 4.6%, 4.0%, 5.1%, 6.0% and 3.4% respectively[62]. This method significantly improved the accuracy of the dose distribution estimated by the DCNN model. In their

Table 2 Target volume segmentation

Ref.	Tumor site	Artificial intelligence technique	Patient number	Contouring	Results
Ikushima *et al*[39], 2017	Lung	SVM	14 (solid: 6, GGO: 4, mixed GGO: 4)	GTV	DSC: (1) 0.777 for 14 cases; and (2) 0.763 for GGO, 0.701 for mixed GGO
Cui *et al*[40], 2021	Lung	DVNs	192 (solid: 118, part-solid:53, pure GGO: 21)	GTV	3D-DSC: (1) Solid: 0.838 ± 0.074; (2) Part-solid: 0.822 ± 0.078; and (3) GGO: 0.819 ± 0.059
Zhong *et al*[41], 2019	Lung	3D-DFCN	60	GTV	DSC: (1) CT: 0.861 ± 0.037; and (2) PET: 0.828 ± 0.087
Kawata *et al*[42], 2017	Lung	FCM, ANN, SVM	16 (solid: 6, GGO:4, part-solid GGO:6)	GTV	DSC: (1) FCM-based framework:0.79 ± 0.06; (2) ANN-based framework: 0.76 ± 0.14; and (3) SVM-based framework: 0.73 ± 0.14
Li *et al*[43], 2019	Nasopharynx	U-Net	502	GTV	DSC: (1) Lymph nodes: 65.86%; (2) Primary tumor: 74.00%; HDs: (1) Lymph nodes: 32.10 mm; and (2) Primary tumor:12.85 mm
Zhao *et al*[45], 2019	Nasopharynx	FCN	30	GTV	DSC: 87.47%
Guo *et al*[46], 2020	Head and neck	Dense Net and 3D U-Net	250	GTV	DSC: (1) Dense Net with PET/CT: 0.73; (2) Dense Net with PET: 0.67; (3) Dense Net with CT: 0.32; and (4) 3D U-Net with PET/CT: 0.71; MSD: (1) Dense Net with PET/CT: 2.88; (2) Dense Net with PET: 3.38; (3) Dense Net with CT: -; and (4) 3D U-Net with PET/CT: 2.98; HD_{95}: (1) Dense Net with PET/CT: 6.48; (2) Dense Net with PET: 8.29; (3) Dense Net with CT: -; and (4) 3D U-Net with PET/CT: 7.57
Jeong *et al*[51], 2020	Brain	3D-R-CNN	21	GTV	DSC: 0.90 ± 0.04; HD: 7.16 ± 5.78 mm; MSD: 0.45 ± 0.34 mm; Center of mass distance: 0.86 ± 0.91 mm
Meng *et al*[54], 2020	Liver	TDP-CNN	106	GTV	DSC: 0.689; HD: 7.69mm; Average distance: 1.07 mm
Elguindi *et al*[56], 2019	Prostate	2D-CNN, DeepLabV3 +	50	Prostate	Volumetric DSCL: 0.83 ± 0.06; Surface DSC: 0.85 ± 0.11
Men *et al*[59], 2017	Rectum	DDCNN	278	CTV	DSC: 87.7%

ANN: Artificial neural network; CT: Computed tomography; CTV: Clinical target volume.; DDCNN: Deep dilated convolutional neural network; DFCN: Fully convolutional network; DSC: Dice similarity coefficient; DVNs: Dense V-network; FCM: Fuzzy-c-means clustering method; GGO: Ground-glass opacity; GTV: Gross tumor volume; HD: Hausdorff distance; MSD: Mean surface distance; PET: Positron emission tomography; R-CNN: Region-based convolutional neural network; SVM: Support vector Machine; SVM: Support vector machine; TDP-CNN: Three-dimensional dual-path multiscale convolutional neural network.

studies, Fan *et al*[64] aimed to develop a 3D dose estimation algorithm based on DL and create a treatment plan based on the dose distribution for IMRT. The DL model was trained to estimate a dose distribution based on patient-specific geometry and prescription dose. A total of 270 head and neck cancer cases, 195 in the training data set, 25 in the validation set, and 50 in the test set, were included in the study. All cases were treated with IMRT. The model input consisted of CT images and contours that

defined the OAR and plot target volumes. The algorithm output was trained to estimate the dose distribution from the CT image slice. The resulting estimation model was used to estimate the patient dose distribution. An optimization target function was then created based on the estimated dose distributions for automatic plan generation. In the study, Differences between the prediction and the actual clinical plan in DVH for all OARs were not significant except for the brainstem, right, and left lens. Differences between PTVs ($PTV_{70.4}$, PTV_{66}, $PTV_{60.8}$, PTV_{60}, PTV_{56}, PTV_{54}, PTV_{51}) in the estimated and the actual plan were significant only for $PTV_{70.4}$[64]. In that study, optimization based on 3D dose distribution and an automatic RT planning system based on 3D dose estimation were developed. The model is a promising approach to realize automatic treatment planning in the future.

Ma *et al*[65] created a DVH prediction model that depended on support vector regression as the backbone of the ML model. A database containing VMAT plans of 63 prostate cancer cases was used, and a PTV plan was created for each patient. A correlative relationship between the OAR DVH (model input) of the PTV plan and the corresponding DVH (model output) of the clinical treatment plan was established with 53 training cases. The predictive model was tested with a validation group of ten cases. In the control of dosimetric endpoints for the training group, 52 of 53 bladder cases (98%) and 45 of 53 rectum cases were found to be within a 10% error limit. In the validation test group, 92% of the bladder cases and 96% of the rectum cases were within the 10% error limit. Eight of the ten validation plans (80%) were found to be within the 10% error margin for both rectum and bladder[65]. In that study, only the PTV plan was used for DVH estimation and an ML model was created based on new dosimetric characteristics. The framework had high accuracy for predicting the DVH for VMAT plans.

In lung cancer, as in other types of cancer, optimum selection of radiation beam directions is required to ensure effective coverage of the target volume by external RT and to prevent unnecessary doses to normal healthy tissues. IMRT planning is a lengthy process that requires the planner to iterate between selecting beam angles, setting dose-volume targets, and conducting IMRT optimization. The beam angle selection is made according to the planner's clinical experience. Mahdavi *et al*[67] planned to create a framework that used ML to automatically select treatment beam angles in thoracic cancers, intended to increase computational efficiency. They created an automatic beam selection model based on learning the relationship between beam angles and anatomical features. The plans of 149 cases who underwent clinically approved thoracic IMRT were used in the study. Twenty-seven cases were randomly selected and used to test the automated plan and the clinical plan. When the estimated and clinically used beam angles were compared, a good mean agreement was observed between the two (angular distance 16.8 ± 10◦, correlation 0.75 ± 0.2). The target volume of automated and clinical plans was found to be equivalent when evaluated in terms of winding and the OAR. The vast majority of plans (93%) were approved as clinically acceptable by three radiation oncologists[69].

Treatment planning is an important step in the RT workflow. It has become more sophisticated in the past few decades with the help of computer science, allowing planners to design highly complex RT plans to minimize damage of normal tissue while maintaining adequate tumor control. A need of individual patient plans has resulted in treatment planning becoming more labor-intensive and time consuming. Many algorithms have been developed to support those involved in RT planning. The algorithms have had a major impact on focusing on automating and/or optimizing the planning process and improving treatment planning efficiency and quality. Studies of treatment planning are summarized in Table 3.

QUALITY ASSURANCE

Quality assurance (QA) is crucial in order to evaluate the RT plan and detect and report errors. Features of RT QA programs such as error detection, and prevention, and treatment device QA are very suitable for AI application[72-75]. Li *et al*[73] developed an application to estimate the performance of medical linear accelerators (Linacs) over time. Daily QA of RT in cancer treatment closely monitors Linac performance and is critical for the continuous improvement of patient safety and quality of care. Cumulative QA measures are valuable for understanding Linac behavior and enabling medical physicists to detect disturbances in output and take preventive action. Li *et al*[73] used a time series estimation model of ANNs and an autoregressive moving average to analyze 5-yr Linac QA data. Verification tests and

Table 3 Radiotherapy planning

Ref.	Aim	Patient number	Artificial intelligence technique	Results
Zhu *et al*[61], 2020	Calculating TERMA and ED	24	CNN	3%/2 mm, 95% LCL, and 95% UCL to 99.56%, 99.51%, 99.61%
Zhang *et al*[62], 2020	Making voxel level dose estimation by integrating the distance information between PTV and OAR	98	DCNN	MAEV: (1) PTV: 2.1%; (2) Left lung: 4.6%; (3) Right lung: 4.0%; (4) Heart: 5.1%; (5) Spinal cord: 6.0%; and (6) Body: 3.4%
Fan *et al*[64], 2019	Developing a 3D dose estimation algorithm	270		Significant difference was found between the estimated and the actual plan in only $PTV_{70.4}$
Ma *et al*[65], 2019	Creating a DVH prediction model	63	SVR	The error limit of 10% for the bladder and rectum was 92% and 96%
Mahdavi *et al*[69], 2015	Selecting treatment beam angles in thoracic cancers	149	ANN	The majority of plans (93%) were approved as clinically acceptable by three radiation oncologists

ANN: Artificial neural networks.; CNN: Convolutional neural network; DCNN: Deep convolutional neural network; DVH: Dose value histogram; ED: Electron density; LCL: Lower confidence limit; MAEV: Voxel level mean absolute error; OAR: Organ at risk; PTV: Planning target volume; SVR: Support vector regression; TERMA: Three-dimensional distribution of total energy release per unit mass; UCL: Upper confidence limit.

other evaluations were made for all models and they reported that the ANN algorithm can be applied correctly and effectively in dosimetry and QA[73]. Valdes *et al*[72] developed AI applications to predict IMRT QA transition rates and automatically detect problems in the Linac imaging system. Carlson *et al*[76] developed an ML approach to predict multileaf collimator (MLC) position errors. Inconsistencies between planned and transmitted motions of multileaf collimators are a major source of error in dose distribution during RT. In their study, factors such as leaf movement parameters, leaf position and speed, leaf movement towards or away from the isocenter of the MLC were calculated from plan files of AI forecasting models. Position differences between synchronized DICOM-RT planning files and DynaLog files reported during QA delivery were used for training the models. To assess the effect on the patient, the DVH in the treated positions and the planned and anticipated DVHs were compared. In all cases, they found that the DVH parameters predicted for the OAR, especially around the treatment area, were closer to the DVHs in the treated position than to the planned DVH parameters[76].

The use of treatment plan features to predict patient-specific QA measurement results facilitate development of automated pretreatment validation workflows or provide a virtual assessment of treatment quality. Granville *et al*[77] trained a linear support vector classifier to classify the results of patient-specific VMAT QA measurements, using the complexity of the treatment plan and characteristics that define the Linac performance criteria. The "targets" in this model are simple classifications that represent the median dose difference between measured and expected dose distributions; median dose deviation was considered "hot" if > 1%, "cold" if < 1%, and "normal" if ± 1%. A total of 1620 patient-specific QA measurements were used for model development and testing' and 75% of the data was used for model development and validation. The remaining 25% was used for the independent evaluation of model performance. Receiver operating characteristic (ROC) curve analysis was used to evaluate model performance. Of the ten variables that are considered important for prediction, half consist of treatment plan characteristics, and half are QA measures that characterize Linac performance. For this model, the micro-averaged area under the ROC curve was 0.93, and the macro-averaged area under the ROC curve was 0.88[77]. The study demonstrates the potential of using both treatment plan features and routine Linac QA results in the development of ML models for patient-specific VMAT QA measurements.

RT APPLICATION, SETUP

During radiation therapy, treatment may need to be adjusted to ensure that the plan is properly implemented. Need of adjustment may result from both online factors such as the patient's pretreatment position, and longer-term factors related to anatomical

changes and response to treatment. Images taken before treatment should be aligned with the images in the planning CT and kept in alignment. Although many modern Linac devices currently have daily "cone-beam" CT (CBCT) using mega-voltage X-rays for treatment confirmation, but that imaging is not sufficient to distinguish soft tissue structures. However, those images are considered suitable for image-guided RT as they are used to adapt the treatment plans to the daily anatomy of the patient and to reduce intra-fractional shifts. When performing daily RT, the CBCT should be reviewed before each treatment. Two, or at least one experienced RT technician, are required for this procedure. When the RT technician sees an anatomical difference between the CBCT and the planning CT, she/he should inform the radiation oncologist and medical physicist. At that stage, it is necessary to decide whether to continue treatment with the difference or to require a new CBCT. Each of the steps delays patient treatment and causes a significant increase in the RT department workload. All this opens a path for the growth of AI in parallel with the training program in radiation oncology. In addition to the ability of existing staff to cope with the growing workload, innovations in modern technology and the ability to benefit from it are limited by access to adequate human resources[78]. In addition, AI replanning has been used to identify candidates for adaptive RT. Based on anatomical and dosimetric variations such as shrinkage of the tumor, weakening of the patient, or edema, classifiers and clustering algorithms have been developed to predict the patients who will benefit most from updated plans during fractionated RT[71,79]. However, it should also be kept in mind that the algorithm will mimic past protocols rather than determine the ideal time for replanning because AI learns from data about previous patients, their plans, and adaptive RT.

PATIENT FOLLOW-UP

AI has the potential to change the way radiation oncologists follow definitive-treated patients. After surgery, the tumor may disappear during imaging, and tumor markers can quickly normalize. In contrast, imaging changes such as loss of contrast-enhancement, PET involvements or diffusion restriction, or size reduction, and the response of tumor markers after RT are gradual. Those characteristics are monitored regularly over time, and response assessments are made according to changes that are complemented by clinical experience and are considered indicative of therapeutic efficacy. Time is required for this assessment. However, if cases that will not respond to treatment can be predicted earlier, additional doses of RT or additional systemic treatments may be introduced earlier, which may improve oncological outcomes. In this context, early work in the field of radiology is promising. In radiology, quantitative features are extracted based on size and shape, image density, texture, relationships between voxels, and some characteristics to typify an image. AI algorithms can be used to correlate image-based features with biological observations or clinical outcomes[80-85]. The use of AI techniques for response and survival prediction in RT patients is a serious opportunity to further improve decision support systems and provide an objective assessment of the relative benefits of various treatment options for patients.

Cancer is the most common cause of death in developed countries, and it is estimated that the number of cases will increase further in aging populations[86,87]. Therefore, cancer research will continue to be the top priority for saving lives in the next decade. Prognosis studies have been conducted with AI on many types of cancer. The use of AI techniques for response and survival prediction in RT patients is a serious opportunity to further improve decision support systems and provide an objective assessment of the relative benefits of various treatment options for patients.

Six different ML algorithms were evaluated in a prognosis study with 72 cases of nasopharyngeal cancer. Age, weight loss, initial neutrophil/lymphocyte ratio, initial lactate dehydrogenase and hemoglobin values, RT time, tumor size, concurrent CT number, and T and N stage were determined as critical variables. The highest performing model among logistic regression, ANN, XGBoost, support-vector clustering, random forest, and Gaussian Naïve Bayes algorithms was determined as Gaussian Naïve Bayes, and the accuracy rate was found to be 88% (CI: 0.68-1)[88]. In a study using radionics obtained from clinical and PET-CT, prognosis was evaluated in 101 lung cancer cases, with 67% used for training and 33% validation and testing. The highest accuracy rate was achieved with an SVM algorithm that had an accuracy rate of 84%, a sensitivity of 86%, and a specificity of 82%[89]. In another study in which prognosis was predicted in prostate cancer, somatic gene mutations were evaluated

and an accuracy rate of 66% was obtained with an SVM algorithm[90]. Post cystectomy bladder cancer prognosis was evaluated in 3503 cases using an SVM algorithm. Recurrence, 1-, 3, and 5-yr survival rates were estimated with sensitivity and specificity above 70%[91]. In a study including 75 gastric cancer patients, the accuracy of survival, distant metastasis, and peritoneal metastasis predictions were 81% for GNB, 86% for XGBoost, and 97% for Random Forest (97%)[92]. Pham *et al*[93] used AI to detect DNp73 expression associated with 5-yr overall survival and prognosis in 143 rectal cancer cases. Ten different CNN algorithms were used, and each immunochemical image was resized. For the algorithm, 90% of the images were used in training and 10% as test data. The accuracy of ten algorithms varied between 90% and 96%[93].

In oncological treatment, forecasting is crucial in the decision-making process because survival prediction is critical in making palliative *vs* curative treatment decisions. In addition, the estimation of remaining life expectancy can be an incentive for patients to live a fuller or more fulfilling life. It is also a question of which answer is sought by health insurance companies. Survival statistics assist oncologists in making treatment decisions. However, these are data from large and heterogeneous groups and are not well suited to predict what will happen to a specific patient. AI algorithms for the prediction of RT and chemotherapy oncological outcomes have attracted considerable attention recently. In cases diagnosed with cancer, predicting survival is critical for improving treatment and providing information to patients and clinicians. Considering the data set of rectal cancer patients with specific demographic, tumor, and treatment information, it is a crucial issue whether patient survival or recurrence can be predicted by any parameter. Today, many hospitals store medical records as digital data. By evaluating these large data sets using AI techniques, it may be possible to predict patient treatment outcomes, plan individualized patient treatment, improve corporate performance, and regulate health insurance premiums.

CONCLUSION

Although AI can take place at every step in radiation oncology, from patient consultation to patient monitoring, and can contribute to the clinician and the society, there are still many challenges and problems to be solved. Initially, Large data sets should be created for AI and then undergo continuing improvement. The development of estimation tools with a wide variety of variables and models limits the comparability of existing studies and the use of standards. Estimation algorithms can be standardized by sharing data between centers, data diversity, and establishing immense databases. In addition, models can be made clinically applicable by updating with entry of new data into the models. Today, the accuracy and quality of data are also of great importance, as no AI algorithm can fix problems in training data.

REFERENCES

1 **Meyer P**, Noblet V, Mazzara C, Lallement A. Survey on deep learning for radiotherapy. *Comput Biol Med* 2018; **98**: 126-146 [PMID: 29787940 DOI: 10.1016/j.compbiomed.2018.05.018]

2 **LeCun Y**, Bengio Y, Hinton G. Deep learning. *Nature* 2015; **521**: 436-444 [PMID: 26017442 DOI: 10.1038/nature14539]

3 **Jarrett D**, Stride E, Vallis K, Gooding MJ. Applications and limitations of machine learning in radiation oncology. *Br J Radiol* 2019; **92**: 20190001 [PMID: 31112393 DOI: 10.1259/bjr.20190001]

4 **Boldrini L**, Bibault JE, Masciocchi C, Shen Y, Bittner MI. Deep Learning: A Review for the Radiation Oncologist. *Front Oncol* 2019; **9**: 977 [PMID: 31632910 DOI: 10.3389/fonc.2019.00977]

5 **Chen C**, He M, Zhu Y, Shi L, Wang X. Five critical elements to ensure the precision medicine. *Cancer Metastasis Rev* 2015; **34**: 313-318 [PMID: 25920354 DOI: 10.1007/s10555-015-9555-3]

6 **Bibault JE**, Giraud P, Burgun A. Big Data and machine learning in radiation oncology: State of the art and future prospects. *Cancer Lett* 2016; **382**: 110-117 [PMID: 27241666 DOI: 10.1016/j.canlet.2016.05.033]

7 **Huynh E**, Hosny A, Guthier C, Bitterman DS, Petit SF, Haas-Kogan DA, Kann B, Aerts HJWL, Mak RH. Artificial intelligence in radiation oncology. *Nat Rev Clin Oncol* 2020; **17**: 771-781 [PMID: 32843739 DOI: 10.1038/s41571-020-0417-8]

8 **Oberije C**, De Ruysscher D, Houben R, van de Heuvel M, Uyterlinde W, Deasy JO, Belderbos J, Dingemans AM, Rimner A, Din S, Lambin P. A Validated Prediction Model for Overall Survival From Stage III Non-Small Cell Lung Cancer: Toward Survival Prediction for Individual Patients. *Int J Radiat Oncol Biol Phys* 2015; **92**: 935-944 [PMID: 25936599 DOI: 10.1016/j.ijrobp.2015.02.048]

9 **Sinsky C**, Colligan L, Li L, Prgomet M, Reynolds S, Goeders L, Westbrook J, Tutty M, Blike G.

Allocation of Physician Time in Ambulatory Practice: A Time and Motion Study in 4 Specialties. *Ann Intern Med* 2016; **165**: 753-760 [PMID: 27595430 DOI: 10.7326/M16-0961]

10 **Lin SY**, Shanafelt TD, Asch SM. Reimagining Clinical Documentation With Artificial Intelligence. *Mayo Clin Proc* 2018; **93**: 563-565 [PMID: 29631808 DOI: 10.1016/j.mayocp.2018.02.016]

11 **Luh JY**, Thompson RF, Lin S. Clinical Documentation and Patient Care Using Artificial Intelligence in Radiation Oncology. *J Am Coll Radiol* 2019; **16**: 1343-1346 [PMID: 31238022 DOI: 10.1016/j.jacr.2019.05.044]

12 **Feng M**, Valdes G, Dixit N, Solberg TD. Machine Learning in Radiation Oncology: Opportunities, Requirements, and Needs. *Front Oncol* 2018; **8**: 110 [PMID: 29719815 DOI: 10.3389/fonc.2018.00110]

13 **Xiang L**, Wang Q, Nie D, Zhang L, Jin X, Qiao Y, Shen D. Deep embedding convolutional neural network for synthesizing CT image from T1-Weighted MR image. *Med Image Anal* 2018; **47**: 31-44 [PMID: 29674235 DOI: 10.1016/j.media.2018.03.011]

14 **Adrian G**, Konradsson E, Lempart M, Bäck S, Ceberg C, Petersson K. The FLASH effect depends on oxygen concentration. *Br J Radiol* 2020; **93**: 20190702 [PMID: 31825653 DOI: 10.1259/bjr.20190702]

15 **Maxim PG**, Tantawi SG, Loo BW Jr. PHASER: A platform for clinical translation of FLASH cancer radiotherapy. *Radiother Oncol* 2019; **139**: 28-33 [PMID: 31178058 DOI: 10.1016/j.radonc.2019.05.005]

16 **Vozenin MC**, De Fornel P, Petersson K, Favaudon V, Jaccard M, Germond JF, Petit B, Burki M, Ferrand G, Patin D, Bouchaab H, Ozsahin M, Bochud F, Bailat C, Devauchelle P, Bourhis J. The Advantage of FLASH Radiotherapy Confirmed in Mini-pig and Cat-cancer Patients. *Clin Cancer Res* 2019; **25**: 35-42 [PMID: 29875213 DOI: 10.1158/1078-0432.CCR-17-3375]

17 **Sheng K**. Artificial intelligence in radiotherapy: a technological review. *Front Med* 2020; **14**: 431-449 [PMID: 32728877 DOI: 10.1007/s11684-020-0761-1]

18 **Viergever MA**, Maintz JBA, Klein S, Murphy K, Staring M, Pluim JPW. A survey of medical image registration - under review. *Med Image Anal* 2016; **33**: 140-144 [PMID: 27427472 DOI: 10.1016/j.media.2016.06.030]

19 **Wu G**, Kim M, Wang Q, Munsell BC, Shen D. Scalable High-Performance Image Registration Framework by Unsupervised Deep Feature Representations Learning. *IEEE Trans Biomed Eng* 2016; **63**: 1505-1516 [PMID: 26552069 DOI: 10.1109/TBME.2015.2496253]

20 **Roques TW**. Patient selection and radiotherapy volume definition - can we improve the weakest links in the treatment chain? *Clin Oncol (R Coll Radiol)* 2014; **26**: 353-355 [PMID: 24667211 DOI: 10.1016/j.clon.2014.02.013]

21 **Weiss E**, Hess CF. The impact of gross tumor volume (GTV) and clinical target volume (CTV) definition on the total accuracy in radiotherapy theoretical aspects and practical experiences. *Strahlenther Onkol* 2003; **179**: 21-30 [PMID: 12540981 DOI: 10.1007/s00066-003-0976-5]

22 **Sharp G**, Fritscher KD, Pekar V, Peroni M, Shusharina N, Veeraraghavan H, Yang J. Vision 20/20: perspectives on automated image segmentation for radiotherapy. *Med Phys* 2014; **41**: 050902 [PMID: 24784366 DOI: 10.1118/1.4871620]

23 **Peressutti D**, Schipaanboord B, van Soest J, Lustberg T, van Elmpt W, Kadir T, Dekker A, Gooding M. TU-AB-202-10: how effective are current atlas selection methods for atlas-based Auto-Contouring in radiotherapy planning? *Medical Physics* 2016; **43**: 3738-3739 [DOI: 10.1118/1.4957432]

24 **Liang S**, Tang F, Huang X, Yang K, Zhong T, Hu R, Liu S, Yuan X, Zhang Y. Deep-learning-based detection and segmentation of organs at risk in nasopharyngeal carcinoma computed tomographic images for radiotherapy planning. *Eur Radiol* 2019; **29**: 1961-1967 [PMID: 30302589 DOI: 10.1007/s00330-018-5748-9]

25 **Zhu J**, Zhang J, Qiu B, Liu Y, Liu X, Chen L. Comparison of the automatic segmentation of multiple organs at risk in CT images of lung cancer between deep convolutional neural network-based and atlas-based techniques. *Acta Oncol* 2019; **58**: 257-264 [PMID: 30398090 DOI: 10.1080/0284186X.2018.1529421]

26 **Dolz J**, Laprie A, Ken S, Leroy HA, Reyns N, Massoptier L, Vermandel M. Supervised machine learning-based classification scheme to segment the brainstem on MRI in multicenter brain tumor treatment context. *Int J Comput Assist Radiol Surg* 2016; **11**: 43-51 [PMID: 26206715 DOI: 10.1007/s11548-015-1266-2]

27 **Savenije MHF**, Maspero M, Sikkes GG, van der Voort van Zyp JRN, T J Kotte AN, Bol GH, T van den Berg CA. Clinical implementation of MRI-based organs-at-risk auto-segmentation with convolutional networks for prostate radiotherapy. *Radiat Oncol* 2020; **15**: 104 [PMID: 32393280 DOI: 10.1186/s13014-020-01528-0]

28 **Ibragimov B**, Xing L. Segmentation of organs-at-risks in head and neck CT images using convolutional neural networks. *Med Phys* 2017; **44**: 547-557 [PMID: 28205307 DOI: 10.1002/mp.12045]

29 **Chan JW**, Kearney V, Haaf S, Wu S, Bogdanov M, Reddick M, Dixit N, Sudhyadhom A, Chen J, Yom SS, Solberg TD. A convolutional neural network algorithm for automatic segmentation of head and neck organs at risk using deep lifelong learning. *Med Phys* 2019; **46**: 2204-2213 [PMID: 30887523 DOI: 10.1002/mp.13495]

30 **van Rooij W**, Dahele M, Ribeiro Brandao H, Delaney AR, Slotman BJ, Verbakel WF. Deep Learning-Based Delineation of Head and Neck Organs at Risk: Geometric and Dosimetric Evaluation. *Int J Radiat Oncol Biol Phys* 2019; **104**: 677-684 [PMID: 30836167 DOI: 10.1016/j.ijrobp.2019.02.040]

31 **Loap P**, Tkatchenko N, Kirova Y. Evaluation of a delineation software for cardiac atlas-based autosegmentation: An example of the use of artificial intelligence in modern radiotherapy. *Cancer Radiother* 2020; **24**: 826-833 [PMID: 33144062 DOI: 10.1016/j.canrad.2020.04.012]

32 **Feng X**, Qing K, Tustison NJ, Meyer CH, Chen Q. Deep convolutional neural network for segmentation of thoracic organs-at-risk using cropped 3D images. *Med Phys* 2019; **46**: 2169-2180 [PMID: 30830685 DOI: 10.1002/mp.13466]

33 **Zhang T**, Yang Y, Wang J, Men K, Wang X, Deng L, Bi N. Comparison between atlas and convolutional neural network based automatic segmentation of multiple organs at risk in non-small cell lung cancer. *Medicine (Baltimore)* 2020; **99**: e21800 [PMID: 32846816 DOI: 10.1097/MD.0000000000021800]

34 **Vu CC**, Siddiqui ZA, Zamdborg L, Thompson AB, Quinn TJ, Castillo E, Guerrero TM. Deep convolutional neural networks for automatic segmentation of thoracic organs-at-risk in radiation oncology - use of non-domain transfer learning. *J Appl Clin Med Phys* 2020; **21**: 108-113 [PMID: 32602187 DOI: 10.1002/acm2.12871]

35 **Liu Z**, Liu X, Xiao B, Wang S, Miao Z, Sun Y, Zhang F. Segmentation of organs-at-risk in cervical cancer CT images with a convolutional neural network. *Phys Med* 2020; **69**: 184-191 [PMID: 31918371 DOI: 10.1016/j.ejmp.2019.12.008]

36 **Ahn SH**, Yeo AU, Kim KH, Kim C, Goh Y, Cho S, Lee SB, Lim YK, Kim H, Shin D, Kim T, Kim TH, Youn SH, Oh ES, Jeong JH. Comparative clinical evaluation of atlas and deep-learning-based auto-segmentation of organ structures in liver cancer. *Radiat Oncol* 2019; **14**: 213 [PMID: 31775825 DOI: 10.1186/s13014-019-1392-z]

37 **La Macchia M**, Fellin F, Amichetti M, Cianchetti M, Gianolini S, Paola V, Lomax AJ, Widesott L. Systematic evaluation of three different commercial software solutions for automatic segmentation for adaptive therapy in head-and-neck, prostate and pleural cancer. *Radiat Oncol* 2012; **7**: 160 [PMID: 22989046 DOI: 10.1186/1748-717X-7-160]

38 **Chao KS**, Bhide S, Chen H, Asper J, Bush S, Franklin G, Kavadi V, Liengswangwong V, Gordon W, Raben A, Strasser J, Koprowski C, Frank S, Chronowski G, Ahamad A, Malyapa R, Zhang L, Dong L. Reduce in variation and improve efficiency of target volume delineation by a computer-assisted system using a deformable image registration approach. *Int J Radiat Oncol Biol Phys* 2007; **68**: 1512-1521 [PMID: 17674982 DOI: 10.1016/j.ijrobp.2007.04.037]

39 **Ikushima K**, Arimura H, Jin Z, Yabu-Uchi H, Kuwazuru J, Shioyama Y, Sasaki T, Honda H, Sasaki M. Computer-assisted framework for machine-learning-based delineation of GTV regions on datasets of planning CT and PET/CT images. *J Radiat Res* 2017; **58**: 123-134 [PMID: 27609193 DOI: 10.1093/jrr/rrw082]

40 **Cui Y**, Arimura H, Nakano R, Yoshitake T, Shioyama Y, Yabuuchi H. Automated approach for segmenting gross tumor volumes for lung cancer stereotactic body radiation therapy using CT-based dense V-networks. *J Radiat Res* 2021; **62**: 346-355 [PMID: 33480438 DOI: 10.1093/jrr/rraa132]

41 **Zhong Z**, Kim Y, Plichta K, Allen BG, Zhou L, Buatti J, Wu X. Simultaneous cosegmentation of tumors in PET-CT images using deep fully convolutional networks. *Med Phys* 2019; **46**: 619-633 [PMID: 30537103 DOI: 10.1002/mp.13331]

42 **Kawata Y**, Arimura H, Ikushima K, Jin Z, Morita K, Tokunaga C, Yabu-Uchi H, Shioyama Y, Sasaki T, Honda H, Sasaki M. Impact of pixel-based machine-learning techniques on automated frameworks for delineation of gross tumor volume regions for stereotactic body radiation therapy. *Phys Med* 2017; **42**: 141-149 [PMID: 29173908 DOI: 10.1016/j.ejmp.2017.08.012]

43 **Li S**, Xiao J, He L, Peng X, Yuan X. The Tumor Target Segmentation of Nasopharyngeal Cancer in CT Images Based on Deep Learning Methods. *Technol Cancer Res Treat* 2019; **18**: 1533033819884561 [PMID: 31736433 DOI: 10.1177/1533033819884561]

44 **Ma Z**, Zhou S, Wu X, Zhang H, Yan W, Sun S, Zhou J. Nasopharyngeal carcinoma segmentation based on enhanced convolutional neural networks using multi-modal metric learning. *Phys Med Biol* 2019; **64**: 025005 [PMID: 30524024 DOI: 10.1088/1361-6560/aaf5da]

45 **Zhao L**, Lu Z, Jiang J, Zhou Y, Wu Y, Feng Q. Automatic Nasopharyngeal Carcinoma Segmentation Using Fully Convolutional Networks with Auxiliary Paths on Dual-Modality PET-CT Images. *J Digit Imaging* 2019; **32**: 462-470 [PMID: 30719587 DOI: 10.1007/s10278-018-00173-0]

46 **Guo Z**, Guo N, Gong K, Zhong S, Li Q. Gross tumor volume segmentation for head and neck cancer radiotherapy using deep dense multi-modality network. *Phys Med Biol* 2019; **64**: 205015 [PMID: 31514173 DOI: 10.1088/1361-6560/ab440d]

47 **Men K**, Chen X, Zhang Y, Zhang T, Dai J, Yi J, Li Y. Deep Deconvolutional Neural Network for Target Segmentation of Nasopharyngeal Cancer in Planning Computed Tomography Images. *Front Oncol* 2017; **7**: 315 [PMID: 29376025 DOI: 10.3389/fonc.2017.00315]

48 **Agn M**, Munck Af Rosenschöld P, Puonti O, Lundemann MJ, Mancini L, Papadaki A, Thust S, Ashburner J, Law I, Van Leemput K. A modality-adaptive method for segmenting brain tumors and organs-at-risk in radiation therapy planning. *Med Image Anal* 2019; **54**: 220-237 [PMID: 30952038 DOI: 10.1016/j.media.2019.03.005]

49 **Estienne T**, Lerousseau M, Vakalopoulou M, Alvarez Andres E, Battistella E, Carré A, Chandra S, Christodoulidis S, Sahasrabudhe M, Sun R, Robert C, Talbot H, Paragios N, Deutsch E. Deep Learning-Based Concurrent Brain Registration and Tumor Segmentation. *Front Comput Neurosci* 2020; **14**: 17 [PMID: 32265680 DOI: 10.3389/fncom.2020.00017]

50 **Liu Y**, Stojadinovic S, Hrycushko B, Wardak Z, Lau S, Lu W, Yan Y, Jiang SB, Zhen X, Timmerman R, Nedzi L, Gu X. A deep convolutional neural network-based automatic delineation strategy for

multiple brain metastases stereotactic radiosurgery. *PLoS One* 2017; **12**: e0185844 [PMID: 28985229 DOI: 10.1371/journal.pone.0185844]

51 **Jeong J**, Lei Y, Kahn S, Liu T, Curran WJ, Shu HK, Mao H, Yang X. Brain tumor segmentation using 3D Mask R-CNN for dynamic susceptibility contrast enhanced perfusion imaging. *Phys Med Biol* 2020; **65**: 185009 [PMID: 32674075 DOI: 10.1088/1361-6560/aba6d4]

52 **Charron O**, Lallement A, Jarnet D, Noblet V, Clavier JB, Meyer P. Automatic detection and segmentation of brain metastases on multimodal MR images with a deep convolutional neural network. *Comput Biol Med* 2018; **95**: 43-54 [PMID: 29455079 DOI: 10.1016/j.compbiomed.2018.02.004]

53 **Tang F**, Liang S, Zhong T, Huang X, Deng X, Zhang Y, Zhou L. Postoperative glioma segmentation in CT image using deep feature fusion model guided by multi-sequence MRIs. *Eur Radiol* 2020; **30**: 823-832 [PMID: 31650265 DOI: 10.1007/s00330-019-06441-z]

54 **Meng L**, Tian Y, Bu S. Liver tumor segmentation based on 3D convolutional neural network with dual scale. *J Appl Clin Med Phys* 2020; **21**: 144-157 [PMID: 31793212 DOI: 10.1002/acm2.12784]

55 **Eppenhof KAJ**, Maspero M, Savenije MHF, de Boer JCJ, van der Voort van Zyp JRN, Raaymakers BW, Raaijmakers AJE, Veta M, van den Berg CAT, Pluim JPW. Fast contour propagation for MR-guided prostate radiotherapy using convolutional neural networks. *Med Phys* 2020; **47**: 1238-1248 [PMID: 31876300 DOI: 10.1002/mp.13994]

56 **Elguindi S**, Zelefsky MJ, Jiang J, Veeraraghavan H, Deasy JO, Hunt MA, Tyagi N. Deep learning-based auto-segmentation of targets and organs-at-risk for magnetic resonance imaging only planning of prostate radiotherapy. *Phys Imaging Radiat Oncol* 2019; **12**: 80-86 [PMID: 32355894 DOI: 10.1016/j.phro.2019.11.006]

57 **Torheim T**, Malinen E, Hole KH, Lund KV, Indahl UG, Lyng H, Kvaal K, Futsaether CM. Autodelineation of cervical cancers using multiparametric magnetic resonance imaging and machine learning. *Acta Oncol* 2017; **56**: 806-812 [PMID: 28464746 DOI: 10.1080/0284186X.2017.1285499]

58 **Karimi D**, Zeng Q, Mathur P, Avinash A, Mahdavi S, Spadinger I, Abolmaesumi P, Salcudean SE. Accurate and robust deep learning-based segmentation of the prostate clinical target volume in ultrasound images. *Med Image Anal* 2019; **57**: 186-196 [PMID: 31325722 DOI: 10.1016/j.media.2019.07.005]

59 **Men K**, Dai J, Li Y. Automatic segmentation of the clinical target volume and organs at risk in the planning CT for rectal cancer using deep dilated convolutional neural networks. *Med Phys* 2017; **44**: 6377-6389 [PMID: 28963779 DOI: 10.1002/mp.12602]

60 **Men K**, Zhang T, Chen X, Chen B, Tang Y, Wang S, Li Y, Dai J. Fully automatic and robust segmentation of the clinical target volume for radiotherapy of breast cancer using big data and deep learning. *Phys Med* 2018; **50**: 13-19 [PMID: 29891089 DOI: 10.1016/j.ejmp.2018.05.006]

61 **Zhu J**, Liu X, Chen L. A preliminary study of a photon dose calculation algorithm using a convolutional neural network. *Phys Med Biol* 2020; **65**: 20NT02 [PMID: 33063695 DOI: 10.1088/1361-6560/abb1d7]

62 **Zhang J**, Liu S, Yan H, Li T, Mao R, Liu J. Predicting voxel-level dose distributions for esophageal radiotherapy using densely connected network with dilated convolutions. *Phys Med Biol* 2020; **65**: 205013 [PMID: 32698170 DOI: 1088/1361-6560/aba87b]

63 **Liu Z**, Fan J, Li M, Yan H, Hu Z, Huang P, Tian Y, Miao J, Dai J. A deep learning method for prediction of three-dimensional dose distribution of helical tomotherapy. *Med Phys* 2019; **46**: 1972-1983 [PMID: 30870586 DOI: 10.1002/mp.13490]

64 **Fan J**, Wang J, Chen Z, Hu C, Zhang Z, Hu W. Automatic treatment planning based on three-dimensional dose distribution predicted from deep learning technique. *Med Phys* 2019; **46**: 370-381 [PMID: 30383300 DOI: 10.1002/mp.13271]

65 **Ma M**, Kovalchuk N, Buyyounouski MK, Xing L, Yang Y. Dosimetric features-driven machine learning model for DVH prediction in VMAT treatment planning. *Med Phys* 2019; **46**: 857-867 [PMID: 30536442 DOI: 10.1002/mp.13334]

66 **Valdes G**, Simone CB 2nd, Chen J, Lin A, Yom SS, Pattison AJ, Carpenter CM, Solberg TD. Clinical decision support of radiotherapy treatment planning: A data-driven machine learning strategy for patient-specific dosimetric decision making. *Radiother Oncol* 2017; **125**: 392-397 [PMID: 29162279 DOI: 10.1016/j.radonc.2017.10.014]

67 **Mahdavi SR**, Tavakol A, Sanei M, Molana SH, Arbabi F, Rostami A, Barimani S. Use of artificial neural network for pretreatment verification of intensity modulation radiation therapy fields. *Br J Radiol* 2019; **92**: 20190355 [PMID: 31317765 DOI: 10.1259/bjr.20190355]

68 **Yan H**, Dai JR. Intelligence-guided beam angle optimization in treatment planning of intensity-modulated radiation therapy. *Phys Med* 2016; **32**: 1292-1301 [PMID: 27344457 DOI: 10.1016/j.ejmp.2016.06.005]

69 **Amit G**, Purdie TG, Levinshtein A, Hope AJ, Lindsay P, Marshall A, Jaffray DA, Pekar V. Automatic learning-based beam angle selection for thoracic IMRT. *Med Phys* 2015; **42**: 1992-2005 [PMID: 25832090 DOI: 10.1118/1.4908000]

70 **Sakata Y**, Hirai R, Kobuna K, Tanizawa A, Mori S. A machine learning-based real-time tumor tracking system for fluoroscopic gating of lung radiotherapy. *Phys Med Biol* 2020; **65**: 085014 [PMID: 32097899 DOI: 10.1088/1361-6560/ab79c5]

71 **Guidi G**, Maffei N, Meduri B, D'Angelo E, Mistretta GM, Ceroni P, Ciarmatori A, Bernabei A, Maggi S, Cardinali M, Morabito VE, Rosica F, Malara S, Savini A, Orlandi G, D'Ugo C, Bunkheila F, Bono M, Lappi S, Blasi C, Lohr F, Costi T. A machine learning tool for re-planning and adaptive RT:

A multicenter cohort investigation. *Phys Med* 2016; **32**: 1659-1666 [PMID: 27765457 DOI: 10.1016/j.ejmp.2016.10.005]

72 **Valdes G**, Morin O, Valenciaga Y, Kirby N, Pouliot J, Chuang C. Use of TrueBeam developer mode for imaging QA. *J Appl Clin Med Phys* 2015; **16**: 322-333 [PMID: 26219002 DOI: 10.1120/jacmp.v16i4.5363]

73 **Li Q**, Chan MF. Predictive time-series modeling using artificial neural networks for Linac beam symmetry: an empirical study. *Ann N Y Acad Sci* 2017; **1387**: 84-94 [PMID: 27627049 DOI: 10.1111/nyas.13215]

74 **Valdes G**, Scheuermann R, Hung CY, Olszanski A, Bellerive M, Solberg TD. A mathematical framework for virtual IMRT QA using machine learning. *Med Phys* 2016; **43**: 4323 [PMID: 27370147 DOI: 10.1118/1.4953835]

75 **Valdes G**, Chan MF, Lim SB, Scheuermann R, Deasy JO, Solberg TD. IMRT QA using machine learning: A multi-institutional validation. *J Appl Clin Med Phys* 2017; **18**: 279-284 [PMID: 28815994 DOI: 10.1002/acm2.12161]

76 **Carlson JN**, Park JM, Park SY, Park JI, Choi Y, Ye SJ. A machine learning approach to the accurate prediction of multi-leaf collimator positional errors. *Phys Med Biol* 2016; **61**: 2514-2531 [PMID: 26948678 DOI: 10.1088/0031-9155/61/6/2514]

77 **Granville DA**, Sutherland JG, Belec JG, La Russa DJ. Predicting VMAT patient-specific QA results using a support vector classifier trained on treatment plan characteristics and linac QC metrics. *Phys Med Biol* 2019; **64**: 095017 [PMID: 30921785 DOI: 10.1088/1361-6560/ab142e]

78 **Boon IS**, Au Yong TPT, Boon CS. Assessing the Role of Artificial Intelligence (AI) in Clinical Oncology: Utility of Machine Learning in Radiotherapy Target Volume Delineation. *Medicines (Basel)* 2018; **5** [PMID: 30544901 DOI: 10.3390/medicines5040131]

79 **Guidi G**, Maffei N, Vecchi C, Gottardi G, Ciarmatori A, Mistretta GM, Mazzeo E, Giacobazzi P, Lohr F, Costi T. Expert system classifier for adaptive radiation therapy in prostate cancer. *Australas Phys Eng Sci Med* 2017; **40**: 337-348 [PMID: 28290067 DOI: 10.1007/s13246-017-0535-5]

80 **Tseng HH**, Luo Y, Cui S, Chien JT, Ten Haken RK, Naqa IE. Deep reinforcement learning for automated radiation adaptation in lung cancer. *Med Phys* 2017; **44**: 6690-6705 [PMID: 29034482 DOI: 10.1002/mp.12625]

81 **Varfalvy N**, Piron O, Cyr MF, Dagnault A, Archambault L. Classification of changes occurring in lung patient during radiotherapy using relative γ analysis and hidden Markov models. *Med Phys* 2017; **44**: 5043-5050 [PMID: 28744863 DOI: 10.1002/mp.12488]

82 **Oakden-Rayner L**, Carneiro G, Bessen T, Nascimento JC, Bradley AP, Palmer LJ. Precision Radiology: Predicting longevity using feature engineering and deep learning methods in a radiomics framework. *Sci Rep* 2017; **7**: 1648 [PMID: 28490744 DOI: 10.1038/s41598-017-01931-w]

83 **Lao J**, Chen Y, Li ZC, Li Q, Zhang J, Liu J, Zhai G. A Deep Learning-Based Radiomics Model for Prediction of Survival in Glioblastoma Multiforme. *Sci Rep* 2017; **7**: 10353 [PMID: 28871110 DOI: 10.1038/s41598-017-10649-8]

84 **Li Z**, Wang Y, Yu J, Guo Y, Cao W. Deep Learning based Radiomics (DLR) and its usage in noninvasive IDH1 prediction for low grade glioma. *Sci Rep* 2017; **7**: 5467 [PMID: 28710497 DOI: 10.1038/s41598-017-05848-2]

85 **Cha KH**, Hadjiiski L, Chan HP, Weizer AZ, Alva A, Cohan RH, Caoili EM, Paramagul C, Samala RK. Bladder Cancer Treatment Response Assessment in CT using Radiomics with Deep-Learning. *Sci Rep* 2017; **7**: 8738 [PMID: 28821822 DOI: 10.1038/s41598-017-09315-w]

86 **Siegel RL**, Miller KD, Jemal A. Cancer statistics, 2019. *CA Cancer J Clin* 2019; **69**: 7-34 [PMID: 30620402 DOI: 10.3322/caac.21551]

87 **DeSantis CE**, Miller KD, Dale W, Mohile SG, Cohen HJ, Leach CR, Goding Sauer A, Jemal A, Siegel RL. Cancer statistics for adults aged 85 years and older, 2019. *CA Cancer J Clin* 2019; **69**: 452-467 [PMID: 31390062 DOI: 10.3322/caac.21577]

88 **Akcay M**, Etiz D, Celik O, Ozen A. Evaluation of Prognosis in Nasopharyngeal Cancer Using Machine Learning. *Technol Cancer Res Treat* 2020; **19**: 1533033820909829 [PMID: 32138606 DOI: 10.1177/1533033820909829]

89 **Sepheri S**, Upadhaya T, Desseroit MC, Visvikis D, Le Rest CC, Hatt M. Comparison of machine learning algorithms for building prognostic models in non-small cell lung cancer using clinical and radiomics features from 18F-FDG PET/CT images. *J Nucl Med* 2018; **59**: 328

90 **Zhang S**, Xu Y, Hui X, Yang F, Hu Y, Shao J, Liang H, Wang Y. Improvement in prediction of prostate cancer prognosis with somatic mutational signatures. *J Cancer* 2017; **8**: 3261-3267 [PMID: 29158798 DOI: 10.7150/jca.21261]

91 **Hasnain Z**, Mason J, Gill K, Miranda G, Gill IS, Kuhn P, Newton PK. Machine learning models for predicting post-cystectomy recurrence and survival in bladder cancer patients. *PLoS One* 2019; **14**: e0210976 [PMID: 30785915 DOI: 10.1371/journal.pone.0210976]

92 **Akcay M**, Etiz D, Celik O. Prediction of Survival and Recurrence Patterns by Machine Learning in Gastric Cancer Cases Undergoing Radiation Therapy and Chemotherapy. *Adv Radiat Oncol* 2020; **5**: 1179-1187 [PMID: 33305079 DOI: 10.1016/j.adro.2020.07.007]

93 **Pham TD**, Fan C, Zhang H, Sun XF. Artificial intelligence-based 5-year survival prediction and prognosis of DNp73 expression in rectal cancer patients. *Clin Transl Med* 2020; **10**: e159 [PMID: 32898334 DOI: 10.1002/ctm2.159]

Artificial Intelligence in Medical Imaging

Submit a Manuscript: https://www.f6publishing.com

Artif Intell Med Imaging 2021 April 28; 2(2): 32-36

DOI: 10.35711/aimi.v2.i2.32

ISSN 2644-3260 (online)

MINIREVIEWS

Intrathyroidal ectopic thymus: Ultrasonographic features and differential diagnosis

Erdal Karavas, Oguzhan Tokur, Sonay Aydın, Dilek Gokharman, Cigdem Uner

ORCID number: Erdal Karavas 0000-0001-6649-3256; Oguzhan Tokur 0000-0003-3319-6663; Sonay Aydın 0000-0002-3812-6333; Dilek Gokharman 0000-0003-1166-0576; Cigdem Uner 0000-0002-4846-7764.

Author contributions: Karavas E, Tokur O, Aydin S, Gokharman D, Uner C contribute to the conceptualization, methodology, supervision, and the manuscript writing, review and editing; Karavas E, Tokur O, Aydin S contribute to the data curation, software; Karavas E, Tokur O, Gokharman D, Uner C contribute to the validation; Karavas E, Tokur O, Uner C contribute to the visualization; Karavas E, Tokur O, Aydin S, Gokharman D contribute to the writing, original draft of the manuscript.

Conflict-of-interest statement: The authors declare no conflict of interest.

Erdal Karavas, Sonay Aydın, Department of Radiology, Erzincan Binali Yildirim University, Erzincan 24100, Turkey

Oguzhan Tokur, Dilek Gokharman, Department of Radiology, Ankara Training and Research Hospital, Ankara 06230, Turkey

Cigdem Uner, Department of Child Radiology, Ankara Sami Ulus Training and Research Hospital, Ankara 06560, Turkey

Corresponding author: Erdal Karavas, MD, MSc, Associate Professor, Department of Radiology, Erzincan Binali Yildirim University, Yalnızbağ Yerleşkesi, Erzincan 24100, Turkey. erdalkaravas@hotmail.com

Abstract

Intrathyroidal ectopic thymus (IET) is defined as an ectopic thymus tissue that is generally found incidentally and rarely in the thyroid gland in the pediatric group. It occurs as a result of disruption of the embryological migration path and the settling of the thymus tissue into the thyroid gland. In the differential diagnosis, it is mostly confused with thyroid nodules. Although thyroid nodules are less common in children than adults, the rate of malignancy is much higher. Therefore, knowing the general ultrasound findings of IET better may prevent unnecessary invasive attempts and surgical procedures. In this article, we tried to compile the key imaging findings of IET.

Key Words: Thymus; Intrathyroidal thymus; Ultrasonography; Diagnosis

Core Tip: The unique ultrasonographic features of intrathyroidal ectopic thymus (IET) can be remembered as; well-circumscribed, hypoechoic eco pattern with linear or punctate echogenic foci resembling thymus, fusiform or oval shape, diameters smaller than 1 cm, location of middle and/or lower 1/3 part of thyroid gland, hypovascularity or avascularity and the same strain ratio values with the surrounding thyroid gland on elastography. Although some studies suggested cytopathological examination for the accurate diagnosis of a suspected IET case, majority of the previous studies stated that IET can be followed without the presence of any atypical findings. So that,

Manuscript source: Invited manuscript

Specialty type: Radiology, nuclear medicine and medical imaging

Country/Territory of origin: Turkey

Peer-review report's scientific quality classification
Grade A (Excellent): 0
Grade B (Very good): B, B, B
Grade C (Good): C
Grade D (Fair): D
Grade E (Poor): 0

Received: March 17, 2021
Peer-review started: March 17, 2021
First decision: March 26, 2021
Revised: March 29, 2021
Accepted: April 20, 2021
Article in press: April 20, 2021
Published online: April 28, 2021

P-Reviewer: Jesus-Silva SG, Madian A, Pekiner FN, Stan F
S-Editor: Wang JL
L-Editor: A
P-Editor: Xing YX

unnecessary surgical or interventional procedures can be avoided.

Citation: Karavas E, Tokur O, Aydın S, Gokharman D, Uner C. Intrathyroidal ectopic thymus: Ultrasonographic features and differential diagnosis. *Artif Intell Med Imaging* 2021; 2(2): 32-36
URL: https://www.wjgnet.com/2644-3260/full/v2/i2/32.htm
DOI: https://dx.doi.org/10.35711/aimi.v2.i2.32

INTRODUCTION

Thyroid lesions in children are mostly in the benign category, but malignant lesions can also be encountered, even rarely. Intrathyroidal ectopic thymus (IET) is a benign lesion that can be encountered in children and does not require treatment. Although it has typical sonographic aspects, it may be misdiagnosed as a thyroid nodule by radiologists who do not have sufficient experience. As a result, a process leading to interventional procedures or even surgery may occur. However, some of its features conflict with thyroid nodules. In these cases, a cytopathological evaluation must be made for the distinction. If IET common ultrasound (US) features are familiarized it can be distinguished from malignant pathologies of the thyroid.

DEVELOPMENT

Thymus tissue develops in the intrauterine 6th week from the 3rd and 4th branchial saccule. Bilaterally developing primordial thymus tissues descend to the anterior mediastinum in the 8th week and combine to form the bilobuled thymus tissue at the 9th week. This descent is from the mandibular angle level to the anterior mediastinum caudally and medially. During migration, the thymic remnant can replace ectopically anywhere along the descent line in the cervical region. Although some articles report that the most ectopic cervical location is intrathyroidal[1], some articles also report it is less common than other ectopic locations in the cervical region[2]. The reason for intrathyroidal localization is thought to be due to the thyroid diverticulum being close to the 3rd branchial sac, although the thyroid tissue basically develops from the 1st and 2nd branchial sac[3].

IET was first described as pathologically by Gilmour in 1937[4]. It does not present with any clinical or physical examination findings in children and is often detected incidentally. Although it is a benign condition, cases showing malignant transformation have been reported in the literature[5]. Its prevalence has been reported between 0.99% and 5.9% in studies[1,4-6]. The mean age of onset varies between 1-10 years in studies[3,5,7,8]. Although not statistically significant, it has been reported slightly more frequently in men[1,3,8].

IET consists of 2 types as abutting and enclosed types, and abutting type is more common than the other. When abutting type is seen, it should be taken into consideration that ectopic thymus tissue may be extending from the anterior mediastinum to the thyroid gland and should be examined carefully[9].

The first diagnostic modality should be US to evaluate the IET and other thyroid lesions[5]. In US, it is observed as a well-circumscribed, hypoechoic lesion containing linear or punctate echogenic foci resembling thymus[1,3,5,7,8,10]. Its contours may be irregular in some cases[8].

Internal punctate echogenicities indicate the Hassall's Corpuscle and their typical histopathological appearance confirms the diagnosis of thymus tissue[10]. Also, because of the similarity of the echo structure and presence of internal echogenic foci, IET can resemble the thymus tissue in the anterior mediastinum[10,11] (Figure 1). When the shape characteristics are examined, IET mostly presents as fusiform or oval[1,3,5,9]. In studies, its dimensions were found to be smaller than 1 cm[3,8,11]. When the location in the thyroid gland is evaluated, it is mostly observed in the middle and lower 1/3 part and more commonly in the posterior parts[1-3,11]. The reason is thought to be that the thymus develops under the pharyngeal sac, where the thyroid develops during embryological development[1]. Only 2 IETs were observed in the upper pole in the study of Erol *et al*[2].

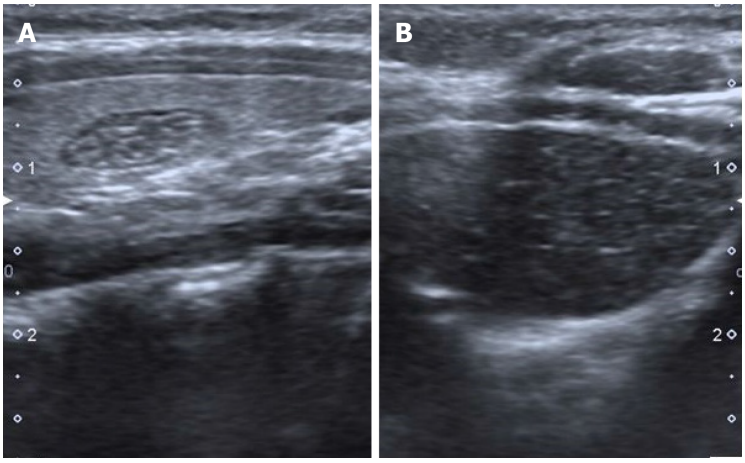

Figure 1 Eight-year-old asymptomatic girl. Longitudinal sonographic images obtained with 7 MHz linear transducer. A: Intrathyroidal ectopic thymus with typical ultrasonographic findings; hypoechoic, fusiform appearance with linear and punctate echogenic focil; B: The resemblance with mediastinal thymic tissue can be seen easily.

In color Doppler examination, IET is hypovascular or avascular compared to surrounding thyroid tissue[1,3,10,11] (Figure 2). Only a few cases have been reported to be isovascular[1,3,11]. Erol *et al*[2] stated that the observation of a vascular structure that passes through the nodule without any compression is a useful hint to differentiate IET and the other nodules.

Elastography was used in two studies, showing that IET had the same stiffness as the surrounding thyroid tissue and the average strain ratio (SR) was defined as 0.99[5,8].

In US follow-up, the dimensions of IET either remain stable or show regression[2,3,12]. Additionally, hormones and enzymes associated with the thyroid gland were also evaluated, and no significant relationship was found with IET[3,5].

In the presence of typical findings of IET described above, absence of palpable thyroid nodule and cervical lymphadenopathy, no prior risk to increased risk of malignancy (radiation exposure to the neck, family history), follow-up will be enough for the management of IET cases[1,2,5,9,10,12]. In the study of Januś *et al*[5], it was underlined that US features of IET can be similar to papillary thyroid cancer (especially diffuse sclerosing variant]. In these cases it can be challenging to differentiate the two entities, and elastography can be helpful[5,8]. Exceptionally, Stasiak *et al*[8] emphasized that cytopathological examination should be performed in cases with suspected IET and the diagnosis could only be reliable in this way[8].

IET is generally confused with thyroid nodules (Figure 3). In pediatric patients, the incidence of thyroid nodules is between 0.2%-1.5%, much less common than adults, but the rate of malignancy is higher[9]. In addition, bilateral lesions in children do not reduce the suspicion of malignancy because thyroid cancer is more common in children when it is multifocal and bilateral[8]. Therefore, further examinations should be made and the distinction between benign and malignant nodules should be revealed. If the ultrasound findings are insufficient for differentiation and the suspicion continues, fine needle aspiration biopsy should be performed first. There are some cases diagnosed by hemi lobectomy in the literature. Although IET is a benign process, it should be known that it may undergo malignant transformation such as thymoma, thymic carcinoma and lymphoblastic lymphoma[5,8]. There are some findings that support the malignant nature of a hypoechoic nodule echo pattern, solid component, ill-defined contour, irregular or round shape, microcalcification, increased vascularity, and pathological lymph node presence[8,9].

Focal thyroiditis is also included in the differential diagnosis. Focal thyroiditis is more hypoechoic and mostly does not contain diffuse echogenic focuses. The contour of focal thyroiditis is ill-defined. Vascularity is also increased (Figure 4)[2].

Intrathyroidal parathyroid gland is similar to IET, but it is differentiated by the absence of echogenic punctate foci. Clinical symptoms and laboratory findings are also useful in differential diagnosis[5].

Intrathyroidal esophageal diverticulum should be considered in differential diagnosis. Its echo pattern is isoechoic or hypoechoic compared to the surrounding thyroid tissue. Internal and peripheral echogenic focuses can be seen. In the differentiation, showing the relationship with the esophagus, changing shape with

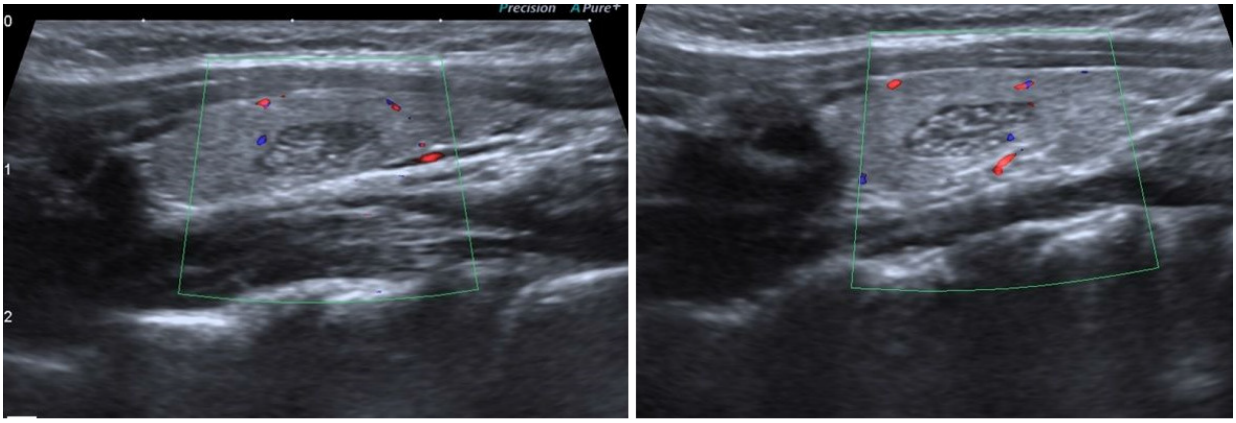

Figure 2 Eight-year-old asymptomatic girl. Longitudinal sonographic images obtained with 7 MHz linear transducer. Both intrathyroidal ectopic thymus cases are hypo vascular in comparison within the surrounding thyroid parenchyma.

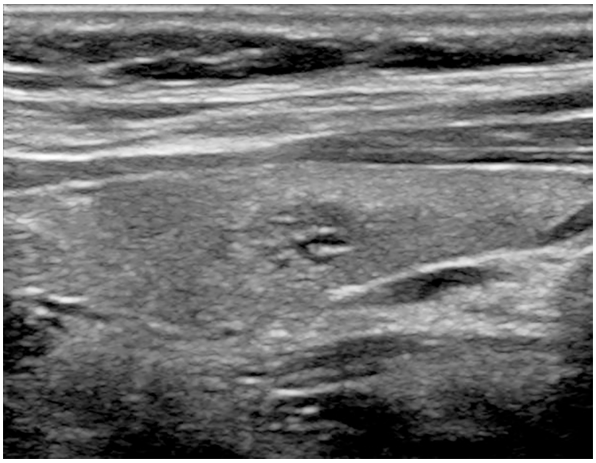

Figure 3 Nine-year-old male with hypothyroidism symptoms. Longitudinal sonographic images obtained with 7 MHz linear transducer. A thyroid nodule presenting with a similar appearance with intrathyroidal ectopic thymus tissue.

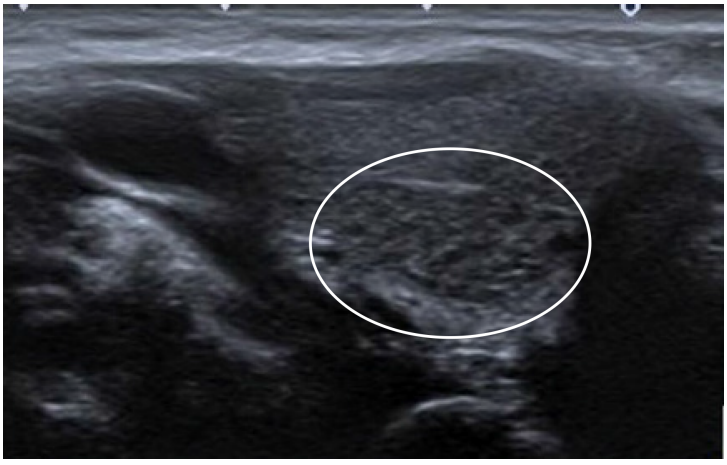

Figure 4 Ten-year-old male with recurrent cough. Longitudinal sonographic images obtained with 7 MHz linear transducer. Abutting type intrathyroidal ectopic thymus. The lesion is located at the lower half of the gland, it has unclear margins. This appearance can be confused with focal thyroiditis.

swallowing and a comet tail artifact due to the inside air can be helpful[1].

Hashimoto thyroiditis nodular form has a solid, hypoechoic echo structure and echogenic punctate focus that can also be observed. It can be well-circumscribed or ill-defined. Laboratory findings may be normal in this type of Hashimoto thyroiditis. Therefore, cytopathological correlation is required[1].

Artificial intelligence (AI) has been playing an increasing role in the diagnosis of thyroidal disease[13], however as far as we know there is not a study concentrating on the use of AI in detecting IET in the English literature.

CONCLUSION

The unique ultrasonographic features of IET can be remembered as well-circumscribed, hypoechoic eco pattern with linear or punctate echogenic foci resembling thymus, fusiform or oval shape, diameters smaller than 1 cm, location of middle and/or lower 1/3 part of thyroid gland, hypovascularity or avascularity and the same SR values with the surrounding thyroid gland on elastography. Although some studies suggested cytopathological examination for the accurate diagnosis of a suspected IET case, most stated that IET can be followed since there is absence of atypical findings. Therefore, unnecessary surgical or interventional procedures can be avoided.

REFERENCES

1 **Yildiz AE**, Elhan AH, Fitoz S. Prevalence and sonographic features of ectopic thyroidal thymus in children: A retrospective analysis. *J Clin Ultrasound* 2018; **46**: 375-379 [PMID: 29575022 DOI: 10.1002/jcu.22590]

2 **Erol OB**, Şahin D, Bayramoğlu Z, Yılmaz R, Akpınar YE, Ünal ÖF, Yekeler E. Ectopic intrathyroidal thymus in children: Prevalence, imaging findings and evolution. *Turk J Pediatr* 2017; **59**: 387-394 [PMID: 29624218 DOI: 10.24953/turkjped.2017.04.004]

3 **Aydin S**, Fatihoglu E, Kacar M. Intrathyroidal ectopic thymus tissue: a diagnostic challenge. *Radiol Med* 2019; **124**: 505-509 [PMID: 30710204 DOI: 10.1007/s11547-019-00987-0]

4 for the Report: "Molecular remission of infant B-ALL after infusion of universal TALEN gene-edited CAR T cells" by W. Qasim, H. Zhan, S. Samarasinghe, S. Adams, P. Amrolia, S. Stafford, K. Butler, C. Rivat, G. Wright, K. Somana, S. Ghorashian, D. Pinner, G. Ahsan, K. Gilmour, G. Lucchini, S. Inglott, W. Mifsud, R. Chiesa, K. S. Peggs, L. Chan, F. Farzeneh, A. J. Thrasher, A. Vora, M. Pule, P. Veys. *Sci Transl Med* 2017; **9** [PMID: 28202780 DOI: 10.1126/scitranslmed.aam9292]

5 **Januś D**, Kalicka-Kasperczyk A, Wójcik M, Drabik G, Starzyk JB. Long-term ultrasound follow-up of intrathyroidal ectopic thymus in children. *J Endocrinol Invest* 2020; **43**: 841-852 [PMID: 31902058 DOI: 10.1007/s40618-019-01172-w]

6 **Fukushima T**, Suzuki S, Ohira T, Shimura H, Midorikawa S, Ohtsuru A, Sakai A, Abe M, Yamashita S, Suzuki S; Thyroid Examination Unit of the Radiation Medical Center for the Fukushima Health Management Survey. Prevalence of ectopic intrathyroidal thymus in Japan: the Fukushima health management survey. *Thyroid* 2015; **25**: 534-537 [PMID: 25778711 DOI: 10.1089/thy.2014.0367]

7 **Bang MH**, Shin J, Lee KS, Kang MJ. Intrathyroidal ectopic thymus in children: A benign lesion. *Medicine (Baltimore)* 2018; **97**: e0282 [PMID: 29620644 DOI: 10.1097/MD.0000000000010282]

8 **Stasiak M**, Adamczewski Z, Stawerska R, Krawczyk T, Tomaszewska M, Lewiński A. Sonographic and Elastographic Features of Extra- and Intrathyroidal Ectopic Thymus Mimicking Malignancy: Differential Diagnosis in Children. *Front Endocrinol (Lausanne)* 2019; **10**: 223 [PMID: 31110490 DOI: 10.3389/fendo.2019.00223]

9 **Yildiz AE**, Ceyhan K, Sıklar Z, Bilir P, Yağmurlu EA, Berberoğlu M, Fitoz S. Intrathyroidal Ectopic Thymus in Children: Retrospective Analysis of Grayscale and Doppler Sonographic Features. *J Ultrasound Med* 2015; **34**: 1651-1656 [PMID: 26269296 DOI: 10.7863/ultra.15.14.10041]

10 **Vlachopapadopoulou EA**, Vakaki M, Karachaliou FE, Kaloumenou I, Kalogerakou K, Gali C, Michalacos S. Ectopic Intrathyroidal Thymus in Childhood: A Sonographic Finding Leading to Misdiagnosis. *Horm Res Paediatr* 2016; **86**: 325-329 [PMID: 27756075 DOI: 10.1159/000450724]

11 **Tritou I**, Raissaki M. Intrathyroidal ectopic thymus tissue: emphasis on details. *Radiol Med* 2019; **124**: 1064-1065 [PMID: 31286340 DOI: 10.1007/s11547-019-01061-5]

12 **Frates MC**, Benson CB, Dorfman DM, Cibas ES, Huang SA. Ectopic Intrathyroidal Thymic Tissue Mimicking Thyroid Nodules in Children. *J Ultrasound Med* 2018; **37**: 783-791 [PMID: 28850707 DOI: 10.1002/jum.14360]

13 **Thomas J**, Haertling T. AIBx, Artificial Intelligence Model to Risk Stratify Thyroid Nodules. *Thyroid* 2020; **30**: 878-884 [PMID: 32013775 DOI: 10.1089/thy.2019.0752]

Artificial Intelligence in Medical Imaging

Submit a Manuscript: https://www.f6publishing.com

Artif Intell Med Imaging 2021 April 28; 2(2): 37-55

DOI: 10.35711/aimi.v2.i2.37

ISSN 2644-3260 (online)

MINIREVIEWS

Current landscape and potential future applications of artificial intelligence in medical physics and radiotherapy

Wing-Yan Ip, Fu-Ki Yeung, Shang-Peng Felix Yung, Hong-Cheung Jeffrey Yu, Tsz-Him So, Varut Vardhanabhuti

ORCID number: Wing-Yan Ip 0000-0002-9118-580X; Fu-Ki Yeung 0000-0003-2721-2356; Shang-Peng Felix Yung 0000-0001-9653-0820; Hong-Cheung Jeffrey Yu 0000-0002-6084-9239; Tsz-Him So 0000-0002-0838-4892; Varut Vardhanabhuti 0000-0001-6677-3194.

Author contributions: Ip WY, Yeung FK, Yung SPF, Yu HCJ, So TH and Vardhanabhuti V contributed to study design, review of literatures, interpretation of data, drafting and revision of the manuscript.

Conflict-of-interest statement: There is no conflict of interest.

Manuscript source: Invited

Wing-Yan Ip, Shang-Peng Felix Yung, Varut Vardhanabhuti, Department of Diagnostic Radiology, Li Ka Shing Faculty of Medicine, The University of Hong Kong, Hong Kong SAR, China

Fu-Ki Yeung, Medical Physics and Research Department, The Hong Kong Sanitorium & Hospital, Hong Kong SAR, China and Department of Diagnostic Radiology, Li Ka Shing Faculty of Medicine, The University of Hong Kong, Hong Kong SAR, China

Hong-Cheung Jeffrey Yu, Li Ka Shing Faculty of Medicine, The University of Hong Kong, Hong Kong SAR, China

Tsz-Him So, Department of Clinical Oncology, Li Ka Shing Faculty of Medicine, The University of Hong Kong, Hong Kong SAR, China

Corresponding author: Varut Vardhanabhuti, BSc, MBBS, PhD, Assistant Professor, Department of Diagnostic Radiology, Li Ka Shing Faculty of Medicine, The University of Hong Kong, Room 406, Block K, Pok Fu Lam Road, Hong Kong SAR, China. varv@hku.hk

Abstract

Artificial intelligence (AI) has seen tremendous growth over the past decade and stands to disrupts the medical industry. In medicine, this has been applied in medical imaging and other digitised medical disciplines, but in more traditional fields like medical physics, the adoption of AI is still at an early stage. Though AI is anticipated to be better than human in certain tasks, with the rapid growth of AI, there is increasing concerns for its usage. The focus of this paper is on the current landscape and potential future applications of artificial intelligence in medical physics and radiotherapy. Topics on AI for image acquisition, image segmentation, treatment delivery, quality assurance and outcome prediction will be explored as well as the interaction between human and AI. This will give insights into how we should approach and use the technology for enhancing the quality of clinical practice.

Key Words: Artificial intelligence; Medical physics; Radiotherapy; Image acquisition; Image segmentation; Treatment planning; Treatment delivery; Quality assurance

manuscript

Specialty type: Oncology

Country/Territory of origin: China

Peer-review report's scientific quality classification

Grade A (Excellent): 0
Grade B (Very good): 0
Grade C (Good): C, C
Grade D (Fair): 0
Grade E (Poor): 0

Received: March 22, 2021
Peer-review started: March 22, 2021
First decision: March 26, 2021
Revised: April 1, 2021
Accepted: April 20, 2021
Article in press: April 20, 2021
Published online: April 28, 2021

P-Reviewer: Jiang Y
S-Editor: Wang JL
L-Editor: A
P-Editor: Xing YX

Core Tip: Artificial intelligence (AI) applications in medical physics and radiotherapy represent an important emerging area in AI applications in medicine. The most notable improvements for the many aspects of radiotherapy are the ability to provide an accurate result with consistency and eliminate inter-and intra-observer variations. Perspectives from physicians and medical physicists about the use of AI are presented, and suggestions of how human can co-exist with AI are made to better equip us for the future.

Citation: Ip WY, Yeung FK, Yung SPF, Yu HCJ, So TH, Vardhanabhuti V. Current landscape and potential future applications of artificial intelligence in medical physics and radiotherapy. *Artif Intell Med Imaging* 2021; 2(2): 37-55
URL: https://www.wjgnet.com/2644-3260/full/v2/i2/37.htm
DOI: https://dx.doi.org/10.35711/aimi.v2.i2.37

INTRODUCTION

Radiotherapy (RT) is an important component of cancer treatment and nearly half of all cancer patients receive RT during their treatment pathways[1]. Increasingly, the use of new technologies such as artificial intelligence (AI) tools plays an important role in RT in various aspects from image acquisition, tumour segmentation, treatment planning, delivery, quality assurance (QA), *etc*. The list will no doubt continue to develop and grow over time as the technology continues to mature. Advancements in computing power and data collection have increased the utilization of AI. The adaptation of a more sophisticated modelling approach has become more widespread creating more accurate predictions. Available datasets from radiation oncology have been generally smaller and more limited than datasets from other medical disciplines such as medical imaging, so the performance of AI is constrained in medical physics disciplines by the available data[2].

According to the data on PubMed search engine performed in Figure 1, which is queried on March 20, 2021, there is a clear increasing trend in AI in the medical literature. Both graphs show an increasing trend but the numbers in medical physics and RT disciplines are several orders of magnitudes lower than in the general medical diagnosis groups. However, the increasing interest in AI applications in medical physics and RT is clear.

In this review article, we will focus on the different aspects of medical physics practice and RT applications and discuss the emerging applications and potentials relating to each area. This is summarised in Figure 2. The structure of this paper is as follows. In section 1, we introduce image synthesis application and benefit in image acquisition. In section 2, we discuss how AI is being used in image segmentation moving from the traditionally manual labour-intensive task to a more automated system. In section 3, we present the function of treatment planning and demonstrate how AI techniques can improve the plan accuracy. In section 4, we describe the benefit in treatment delivery, such as accuracy in position/motion management, organ tracking and dose calculation. In section 5, we explain how AI can be used to improve the performance in the QA process and the advantages of using AI in QA. In section 6, we talk about the prediction of patient outcome and discuss the concerns of patients and clinicians when using AI in the fields that mentioned above. In section 7, we discuss aspects of human-AI interaction. Finally, in section 8, we summarize and evaluate whether AI involved in medical decision making is a benefit or a threat?

IMAGE ACQUISITION

Image synthesis application in RT

RT planning images are used to segment and contour organ at risks (OARs) and target volume (TV), and to plan the treatment. The images require accurate geometric coordinates and excellent image contrast to accurately contour the target in question. A summary, flow chart of image acquisition is shown in Figure 3. The other prerequisites include having a correct electron density of the tissues being imaged to

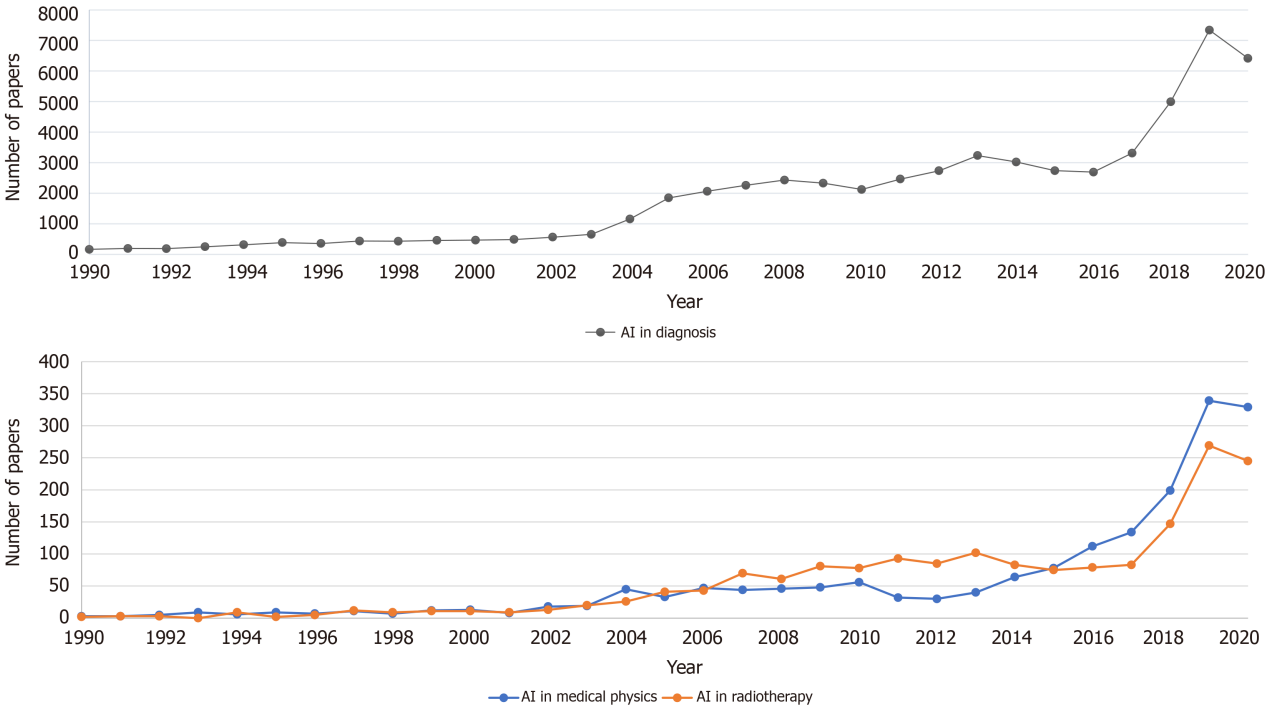

Figure 1 Number of papers in 'Artificial intelligence in diagnosis', 'Artificial intelligence in medical physics', and 'Artificial intelligence in radiotherapy'. AI: Artificial intelligence.

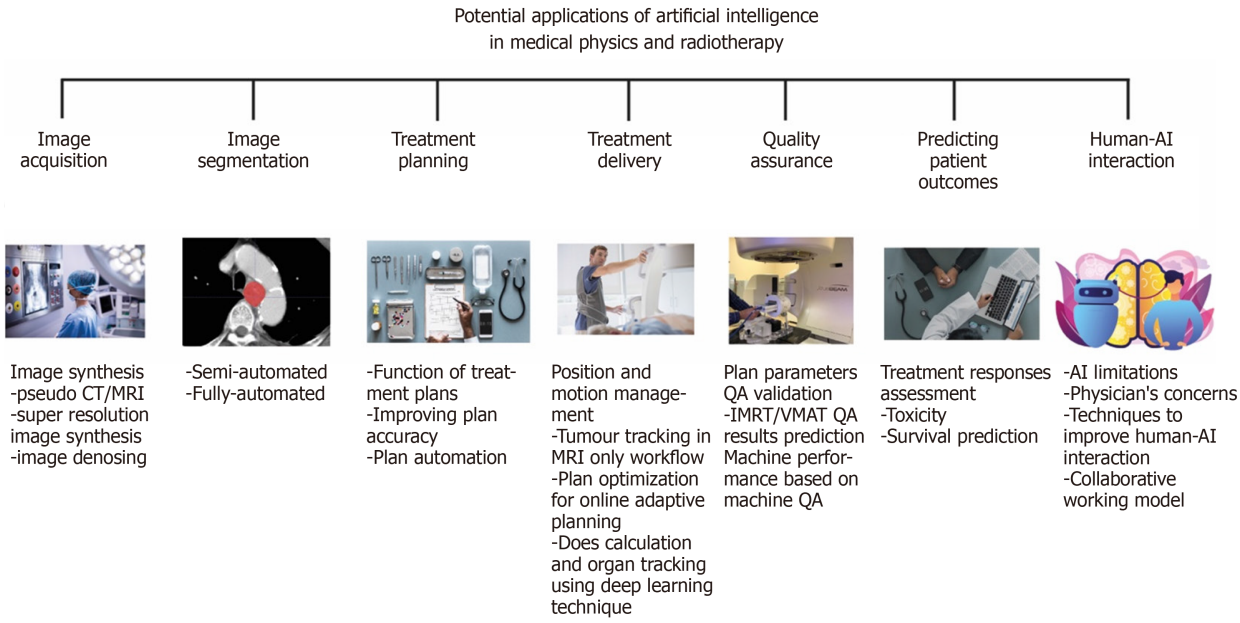

Figure 2 Potential applications of artificial intelligence in medical physics and radiotherapy. AI: Artificial intelligence; QA: Quality assurance; IMRT: Intensity modulated radiotherapy; VMAT: Volumetric-modulated arc therapy; CT: Computed tomography; MRI: Magnetic resonance imaging.

calculate the amount of dose from the treatment beams being attenuated and absorbed by tissues in treatment planning so that an accurate dose can be delivered to the tumour.

Since magnetic resonance imaging (MRI) has advantages in soft tissue contrast for tissues such as brain and prostate (and allows for more accurate lesion localization) but MRI does not have a correlation of electron density in its image. There is a need to fuse the images together with computed tomography (CT) in the current practice. Therefore, when physicians contour on a set of images, the aligned geometric coordinates can ensure a correct contour registration. However, the patient might

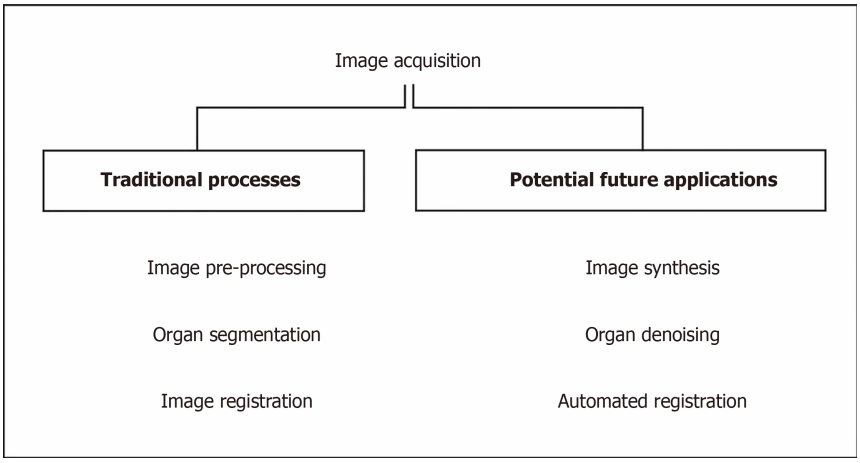

Figure 3 Flow chart of Image processing.

require scanning both MRI and CT image and even the diagnostic PET images beforehand. To reduce the workload or increase the efficiency of those MRI, CT machines, many kinds of image synthesis research have been carrying on based on deep learning technique[3]. The followings are the different applications of image synthesis and advancement using AI as applied to image acquisition. Table 1 summarises the most recent contemporary work.

Pseudo CT/ MRI synthesis

There are several pieces of research on pseudo CT image synthesis from MRI images to help registration of different image modalities or target delineation[4]. Fu *et al*[5] synthesized CT image using cycle consistent generative adversarial network which is an image synthesis network to assist registration of CT-MRI images by directly registering synthetic-CT to original CT images or to have MR-only treatment planning by generating synthetic-CT for treatment planning based on scanned MR image . In addition, Liu *et al*[6,7] researched on generating synthetic-CT from MRI-based treatment planning to derive electron density from routine anatomical MRI so that it can be possible to have MRI-only treatment planning for liver, and prostate cancer.

There is also pseudo MRI synthesis from a CT image for prostate target delineation based on the synthetic MR image from CT image using fully convolution network[8].

Super-resolution image synthesis

To improve the image resolution and quality, Dong *et al*[9] presented a novel super-resolution convolution neural network approach to map between low and high-resolution images in order to synthesize superior-resolution images than other approaches. Bahrami *et al*[10] and Qu *et al*[11] also focus on pseudo synthesis of 7T MRI image from normal 3T MRI using deep learning technique. The high resolution can have a better tissue contrast which can enhance contouring accuracy and on the other hand, will not pose additional dose or scanning time for the patient simulation.

Image denoising

Image denoising is important to improve the signal-to-noise ratio of low-dose CT. Yang *et al*[12] have introduced a CT image denoising method using a generative adversarial network (GAN) with Wasserstein distance and perceptual similarity, so that it can function as conventional CT while keeping a low radiation dose level to the patient. Wang *et al*[13] and Chen *et al*[14] also train the low-dose CT data with a fully convolution neural network with residual blocks and attention gates so to generate a set of data with improved noise, contract-to-noise ratio.

Benefits of using image synthesis technique in RT planning

With the introduction of machine learning and deep learning, various modalities of images can be artificially synthesized for oncologists to take reference, draw different contours on images with superior tissue contrast and fuse together afterwards with the treatment planning software. This can greatly reduce patient scanning time with different modalities. On the other hand, the improvement of images tissue contrast and resolution can help to reduce the margin of the target in order to reduce the

Table 1 Summary of contemporary deep learning methods in image acquisition

Ref.	Architecture	Purpose
Fu *et al*[5], 2020	Cycle consistent generative adversarial network	To enable pseudo CT-aided CT-MRI image registration
Liu *et al*[6], 2019	Cycle generative adversarial network	To derive electron density from routine anatomical MRI for MRI-based SBRT treatment planning
Liu *et al*[7], 2019	3D Cycle-consistent generative adversarial network	To generate pelvic synthetic CT for prostate proton therapy treatment planning
Lei *et al*[8], 2020	Cycle generative adversarial network for synthesis and fully convolution neural network for delineation	To help segment and delineate of prostate target by pseudo MR synthesis from CT
Dong *et al*[9], 2016	Super resolution convolution neural network	To develop novel CNN for high- and low-resolution images mapping
Bahrami *et al*[10], 2016	Convolution neural network	To reconstruct 7T-like super-resolution MRI from 3T MR images
Qu *et al*[11], 2020	Wavelet-based affine transformation layers network	To synthesize superior quality of 7T MRI from its 3T MR images than existing 7T MR images
Yang *et al*[12], 2018	Generative adversarial network with Wasserstein distance and perceptual loss function	To denoise low-dose CT image and improve contrast for lesion detection
Chen *et al*[14], 2017	Deep convolution neural network	To train the mapping between low- and normal-dose images so to efficiently reduce noise in low-dose CT
Wang *et al*[13], 2019	Cycle-consistent adversarial network with residual blocks and attention gates	To improve the contrast-to noise ratio for low-dose CT simulation in brain stereotactic radiosurgery radiation therapy

CNN: Convolutional neural network; CT: Computed tomography; MRI: Magnetic resonance imaging.

uncertainty and improve the dosimetric accuracy of the RT treatment.

IMAGE SEGMENTATION

What is image segmentation?

Image segmentation is an important routine for RT for distinguishing anatomical structures and target[15], as well as comprising sets of pixels[16]. Before the advent of AI, radiation oncologists segment those regions of interest on RT simulation scans (*i.e.*, CT and MRI) manually. They originally used a rigid algorithm and need human interference, professional judgement, and experience. These include thresholding, K-means clustering, histogram-based image segmentation and edge detection[16].

The long duration for manual segmentation is one of the main reasons for the delay in the start of RT treatment, especially in clinics with limited resources. The locoregional control and overall survival rates are lowered because of the inefficiency in the workflow. It also hinders the adaptive RT treatment, because the new images indicating the anatomical changes of the patients have to be segmented for an accurate dose accumulation estimation after each treatment cycle[15].

AI in image segmentation

Accurate segmentation for TV and OARs are necessary for RT plans, but inconsistency such as inter-and intra-observer variability for manual segmentation has been reported. This is because the task is subjective in nature; the decision is made based on an individual's knowledge, judgement and experience. The quantitative and dosimetric analyses are therefore affected, with a varying degree of impact. If an AI tool can be developed with less inherent variability, this would be an invaluable tool for addressing this issue. In order to keep up with modern development, automatic segmentation is needed. It has to overcome image-related problem and provide accurate, efficient and safe RT planning[15].

There are many segmentation types, such as Atlas-based segmentation and Image-based segmentation *etc*. Deep learning in segmentation is a very broad topic, and in broader medical applications, there are several architectures used (Table 1).

The availability of segmented data and computer power were the main reason for manual segmentation in the earlier years. Most segmentation techniques utilised little to no prior knowledge, and these are regarded as low-level segmentation approach.

Examples of these techniques are region growing, heuristic edge detection and intensity thresholding algorithms[15].

Improvement in auto-segmentation

In the past twenty years, a good amount of effort has been poured into the medical imaging field to make use of prior knowledge. Anatomical structures, such as the shape and appearance characteristics are used to compensate for the insufficient soft tissue contrast of CT data, in order to produce an accurate definition of the anatomical boundary[15].

In recent years, deep learning-based software for auto-segmentation has been shown to provide a great leap of improvements over previous approaches. The field of deep learning has become more popular, notably after the seminal paper by Krizhevsky *et al*[17] (2012) which showed a much-improved prediction in image classification and recognition tasks using a deep convolutional neural network (CNN) architecture called AlexNet. More researches followed this approach with the use of a CNN for image segmentation, and the results performed better than prior algorithms, leading to a quick adaptation for deep learning in auto segmentation for medical images[15].

The use of CNNs involves feeding segments of an image as an input, labelling the pixels. The image is scanned by the network, then the network observes the image with a small filter each time until the entire image is mapped[18].

The newest auto-segmentation

Automatic segmentation is usually used in conjunction with manual and semiautomatic segmentation. Manual segmentation requires considerable time and expertise, but often with poor reproducibility. Semiautomatic segmentation relies on human involvement, errors and mistakes can also be expected. Automatic segmentation can provide more accurate results with minimal errors, however, several limitations such as noise existence, partial volume effects, the complexity of three dimensions (3D) spatial multiclass features, spatial and structural variability hinder the effectiveness of automatic segmentation[19].

DeepLab[20], U-Net[21], fully convolutional networks (FCN)[22], dense FCN and residual dense FCN are some of the state-of-the-art neural networks that have been used to tackle this issue. Qayyum *et al*[23] proposed volumetric convolutions for processing 3D input slices as a volume, with no postprocessing steps required. It provided an accurate and robust segmentation that indicated the complete volume of a patient at once.

The test between the proposed model and the current state of the art methods using SegTHOR 2019 dataset was compared. The challenge for this dataset is the position and shape of each organ at each slice has low contrast in CT images as well as the great variation in shape and position. The dataset presented a multiclass problem, and performance metrics are used to evaluate existing deep learning methods and the method proposed by Qayyum *et al*[23] The proposed model provided an improved segmentation performance and produced superior results compared with existing methods.

Limitation in segmentation

The training of deep neural networks (DNNs) for 3D models is challenging, as most deep learning architectures are based on FCN. FCN uses a fixed receptive field and objects with varying size can cause a failure in segmentation. Increasing the field of view and using a sliding window based on complete images can solve the fixed field issue[23].

Several other issues have been reported, such as overfitting, prolonged training time and gradient vanishing. Target organs that do not have a homogeneous appearance and ill-defined borders pose a great challenge to automatic segmentation. In addition, the heterogeneity of appearances even for a single disease entity is a challenge *e.g.*, the appearance of the target could change from patient to patient as well as intra-patient variation between treatment cycles (as if often caused by tumour necrosis). These issues can cause a decrease in performance in 3D deep learning models when handling 3D volumetric datasets. Using an atrous spatial pyramid pooling module with multiscale contextual feature information can assist in handling the issue of changes in sizes, locations and heterogeneous appearances of the target organs and nearby tissues[23].

There is also an issue of paucity of data. A large amount of annotated data is required for training accurate segmentation using deep learning approach.

Increasingly there are several open-source labelled datasets in medical imaging[24-26]. Increasing numbers as well as diversity are needed to increase innovation in this field.

TREATMENT PLANNING

The function of treatment plans

In modern RT, it is crucial to maximize the radiation to the cancer tumour while minimising radiation and potential damage to the surrounding healthy tissues. Intensity modulated RT (IMRT) and volumetric-modulated arc therapy (VMAT) are the two standard treatment techniques for external beam RT treatments that can achieve the tissue-sparing effect while delivering a suitable amount of dose to the planned TV. The treatment plan often involves dose calculations and dose-volume histogram (DVH) which are tools to evaluate the dose to various organs and help the medical staff to determine the quality of the plan. The plans require a lot of time and effort to produce due to the dose constraints and inter-operator variation[27-29].

Methods for improving plan accuracy

Accurate DVH predictions are essential for automated treatment planning, and the predictions keep on improving over the past decade. Concepts such as overlapping volume histogram to describe the geometry of OARs and method for searching similar plans in a clinical database to guide the treatment planning for new patients were proposed. Deep learning methods were used recently to predict the dose distribution in 3D. Because of the nature of DNNs, it relies heavily on the amount and quality of the sample to achieve a high prediction accuracy. The performance could also be affected by parameters such as beam arrangement and voxel spacing in the treatment plan. The robustness of the prediction model can be enhanced with additional pre-processing layers and data augmentation. Through the usage of de-noising auto-encoder for pre-training DNN, more robust feature can be learnt, and less complex neural network can also produce excellent feature fitting capabilities[27].

Benefits provided by automation

Treatment planning is time-consuming, and the method used by each person performing the optimisation can affect the quality of the outcome[30-32]. Automating the treatment planning process can potentially lower the time required for manual labour and reduce the interobserver variations for dose planning. It is generally anticipated that the overall plan quality should improve with the use of AI[32].

The dose objective defined by the dosimetrist determines the dose distribution, usually according to the institution-specific guidelines. However, guidelines cannot provide an optimal dose distribution for specific patients, since the lower achievable dose limit to healthy surrounding tissues for the patient is not known. So, each treatment plan is patient-specific and is produced by trained dosimetrists. Optimisation of the plan is still labour-intensive, it makes it difficult to ensure the clinical treatment plan is properly optimised. All of these concerns lead to the need for automation as a solution to reduce the amount of time spent on the plans and the variations between dosimetrists[32].

The outcome of automated plans

Auto planning software produces comparable or better results for prostate cancer according to Nawa *et al*[28] (2017) and Hazell *et al*[32] (2016). Most OARs receive significant better results with the dose level of the DVHs, and auto planning managed to give clinically acceptable plans for all cases. The results were similar with head and neck cancer treatment. Dosimetrists can potentially have more time to focus on difficult dose planning goals, fine-tuning specific area and spend less time on the mundane tasks of the planning process[32].

TREATMENT DELIVERY

AI in the future will have the ability to accurately identify both normal and TV during treatment and estimates the best modality and beam arrangement from various clinical options. This will lead to an increase in local tumour control and reduces the risk of toxicity to surrounding normal tissue. Integration of clinically relevant data from other

sources in addition will allow AI system to tailor the treatment approach beyond the current state of the art methods. The time burden of human intervention and the time taken for the overall process can be reduced substantially[2].

Position and motion management

Integrated cone-beam CT (CBCT) is commonly used to image the position of the patients. As CBCT has a much lower quality than planning CT images, AI is needed to improve the image quality of CBCT to enable more accurate positioning for treatment[33]. Other imaging techniques such as onboard MRI, ultrasound and infrared surface camera, are used to monitor the motion of the patients as shown in Figure 4. These provide an opportunity for AI to refine and enhance the monitoring during the treatment[34].

The motion of the patient or organ throughout the treatment contributing to inaccuracies in treatment delivery will inevitably increase the radiation dose to surrounding healthy tissues. Motion managements are used for monitoring the extent of the motion from respiration or digestion[35]. There is a potential for the use of AI to predict the diverse variables by creating patient-specific dynamic motion management models[36]. Complex breathing patterns in real-time to accurately track tumour motion are the major task for predictive algorithms[37].

Throughout the treatment, there are changes in the patient's anatomy between the planning appointment and treatment delivery, or even throughout the treatment. Re-planning is necessary when the tumour shrinks or grows, or sometimes with anatomical variations such as the movement of internal organs and gas or liquid filling of the bowels and stomach. Adaptive treatments require a new plan to be created based on up-to-date images of the patient's anatomy. AI tools help predict geometric changes in patient throughout the treatment, thus identify the ideal time point for adaptation[34].

Tumour tracking in MRI only workflow

Apart from conventional cone-beam CT images, AI is involved in the RT treatment for motion tracking using MR images. MRI provides superior soft-tissue contrast compared to conventional CT, and thus target delineation in prostate cancer RT using MRI has become more widespread[38]. However, in RT planning, the combination of MRI and CT image is there is a spatial uncertainty of < 2 mm from the image registration for prostate between MRI and CT[39]. A systematic registration error could lead to an error in treatment, so the dose distribution does not conform to the intended target and results in the tumour control being compromised[40].

As briefly mentioned in section 1, one way to minimize the error is to implement an MRI-only workflow so the plan does not rely on the image from CT scanners. Gold fiducial markers are commonly used in prostate cancer for target positioning, they are detected by using the difference in magnetic susceptibility between the gold markers and the tissue nearby. Multi-echo gradient echo sequence is proposed by Gustafsson *et al*[40] for identifying the fiducial markers. The automatic detection of gold fiducial markers can save time and resources, as well as removing inter-observer differences. From the experiment performed by Gustafsson *et al*[40] and Persson *et al*[41], the true positive detection rates achieved were 97.4% and 99.6% respectively. The results were comparable to manual observer results and they were better than most non deep learning automatic detection methods. A quality control method was also introduced to call upon the attention of the clinical staff when a failure in detection had occurred, which provided a step towards AI automation for MRI-only RT especially for the prostate[40].

Plan optimization for online adaptive planning

Besides monitoring the anatomical changes and motion during treatment, AI is heavily involved in the process of delivery of the treatment beam. VMAT delivery is one of the current standard RT technique. Currently, the treatment plan for VMAT is time-consuming[42]. Machine parameter optimization (MPO) is used to determine the sequence of linac parameters such as multileaf collimators (MLCs) movements, the planning usually involves a manual trial and error approach to determine the best optimizer inputs to obtain an acceptable plan, and execution time for the optimizer is escalated further due to it being run multiple times. There is a need for a fast VMAT MPO algorithm, so while the patient is in the treatment position, the MPO can be executed multiple times for online adaptive planning[43-45].

Reinforcement learning (RL) is a form of machine learning approach, trained to estimate the best sequence of actions to reduce a cost as low as possible in a simulated

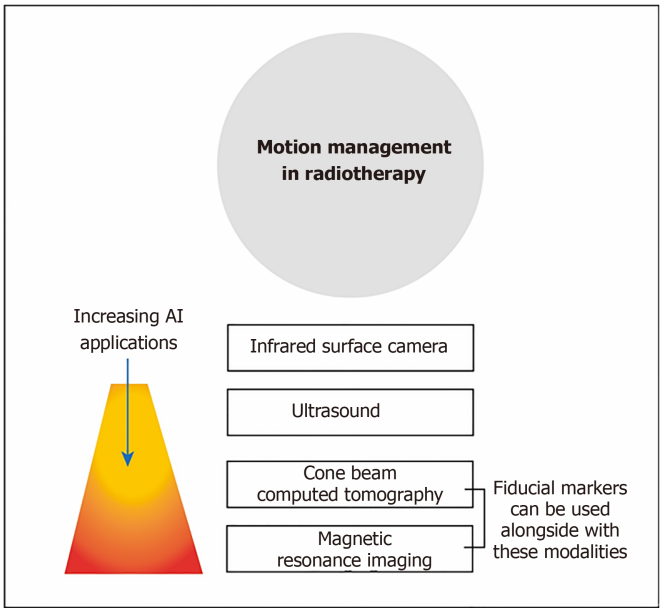

Figure 4 Different strategies used in motion management in radiotherapy. AI: Artificial intelligence.

environment through trial and error. It can be applied to new cases to quickly optimise treatment plans, machine parameters and corresponding dose distributions. The result shows RL VMAT approach produces a rapid and consistent result in both training and test cohort, showing a generalisable machine control policy without notable overfitting in the training cohort despite the small number of patients. The total execution time for plan optimisation was 30 s, with the potential to decrease the time even further because the algorithm can be implemented in parallel across different slices within the plan[45].

Dose calculation and organ tracking using a deep learning technique

Dose calculation of RT treatment using Monte Carlo (MC) simulation is very time consuming[1]. Kernel-based algorithm using DNN proposed by Debus *et al*[46] manages to calculate the peak dose and valley dose in a few minutes with little difference to MC simulation.

Besides the fast calculation speed for dose, kernel-based algorithm is used for identifying the irradiation angle to optimized beam angle for intensity-modulated RT plan. The optimized beam angle spares the organs at risk better in pancreatic and intracranial cancer[47]. It also gives a low-cost computational solution to markerless tracking of tumour motion, such as in kilovoltage fluoroscopy image sequence in image-guided RT (IGRT). The kernel-based algorithm provides a better tracking performance than the conventional template matching method, and it is comparable to the fluoroscopic image sequence[48]. DNN is used to interpret projection X-ray images for markerless prostate localization. The experimental result shows the accuracy is high and can be used for real-time tracking of the prostate and patient positioning[1,49].

QUALITY ASSURANCE

QA is a way to figure out and eliminate errors in radiation planning and delivery but more importantly to ensure consistent quality of the treatment plans. It is an important tool in evaluating the dosimetric and geometric accuracy of the machine and treatment plans. There are a lot of QA researches based on deep learning and machine learning technique[50,51] for improving the accuracy and efficiency of QA procedures. Most adopt a 'human creates while machine verifies' approach. The followings are different sorts of applications of applying AI onto QA in RT. A summary is presented in Table 2.

Plan parameters QA validation

Machine learning can be applied to automated RT plan verification. It aims to verify

Table 2 Summary of contemporary deep learning methods in quality assurance

Ref.	Architecture	Purpose
Chang *et al*[52], 2017	Bayesian network model	To verify and detect external beam radiotherapy physician prescription errors
Kalet *et al*[53], 2015	Bayesian network model	To detect any unusual outliners from treatment plan parameters
Tomori *et al*[54], 2018	Convolutional neural network	To predict gamma evaluation of patient-specific QA in prostate treatment planning
Nyflot *et al*[55], 2019	Convolutional neural network	To detect the presence of introduced RT delivery errors from patient-specific IMRT QA gamma images
Granville *et al*[56], 2019	Support vector classifier	To predict VMAT patient-specific QA results
Li *et al*[57], 2017	ANNs and ARMA time-series prediction modelling	To evaluate the prediction ability of Linac's dosimetry trends from routine machine data for two methods (ANNs and ARMA)

QA: Quality assurance; RT: Radiotherapy; IMRT: Intensity modulated radiotherapy; VMAT: Volumetric-modulated arc therapy; ANNs: Artificial neural networks; ARMA: Autoregressive moving average.

the human-created treatment plan to eliminate any outliners in plan parameters, error-containing contours. Chang *et al*[52] developed a Bayesian network model to detect external beam RT physician order errors ranging from total prescription dose, modality, patient setup options so that these errors can be figured out and rectified as soon as possible without undergoing re-simulation and re-planning. Kalet *et al*[53] further investigated around 5000 prescription treatment plans within 5 years and construct a Bayesian learning model for estimating the probability of different RT parameters from given clinical information. It can act as a database to cross-reference with existing physicians' prescription, for example, to safeguard against human errors, *e.g.*, new doctors. However, such QA checking does not mean to override some exceptional case/physicians' decisions but acts as supporting information as a safety net.

IMRT/VMAT QA results prediction

Patient-specific QA is time-consuming, but this is the most direct and comprehensive way to validate an IMRT or VMAT plan that uses sophisticated MLC patterns. Tomori *et al*[54] made use of a CNN network to predict and estimate the gamma passing rate of these planning plans for prostate cancer based on input training data (volume of planning TV and rectum, monitor unit values of individual field). In the future, patient-specific QA can hopefully be fully automated. Nyflot *et al*[55] also use a CNN with triplet learning to extract the features from IMRT QA gamma comparison results and train the model to distinguish any introduced RT treatment delivery errors like MLC mispositioning error just based on QA gamma results.

Granville *et al*[56] also trained a linear support vector classifier to predict the VMAT QA measurements results based on training measured dose distribution using biplanar diode arrays.

Machine performance prediction based on machine QA

To ensure the accuracy and stability of the treatment machine and plans, sufficient QA tests ought to be performed. Kalet *et al*[50] highlighted that by using machine performance and regular QA measurement logs as input, it can train the model to predict machine performance so as to trigger any preventive maintenance from the service engineers or save time spent to perform additional routine machine QAs.

Li *et al*[57] have used longitudinal daily Linear accelerator (Linac) QA results over 5 years to build and train the model using artificial neural networks or autoregressive moving average time-series prediction modelling techniques so to help understand Linac's behaviour over time and predict the trends in the output[57]. In the future, timely preventive maintenance can be scheduled if necessary after prediction.

The benefit of AI in QA

Chan *et al*[51] highlighted currently many research applications of AI in RT QA focused on predicting the machine performance and patient-specific QA passing rate results. These QA prediction tools based on deep and machine learning can be

incorporated into the treatment planning optimiser so that has a timely prediction of QA gamma rate before finalizing the plan. It minimises time spent on repeating measurement/replanning in case of failing QA tests. By monitoring the machine output performance, it can also help to give feedback to the treatment planning system to improve the accuracy of planning.

PREDICTING PATIENT OUTCOMES

AI also has a role in following outcomes of patients being treated with RT. Many prediction models have been developed, which can be organised by the outcomes predicted as well as the methods used. For RT, the main outcomes that have been investigated are treatment response (*e.g.*, local tumour control and survival) and toxicity. However, the methods used to make these predictions vary widely based on the available data. As studies often acquire these data points retrospectively, the availability of 'ground truth' data may vary according to the clinical setting. To reflect the heterogeneity of data used in some studies, for example, Xu *et al*[58] predicted the chemoRT response of NSCLC patients using 2 datasets. The first set did not have surgery, whereas the second set required surgery and thereby providing data for the pathologic response.

Studies also required data in varying quantity. Various combinations of clinical, imaging, dosimetry, pathological, genomic data have been used to generate the models. Longitudinal data is also important, as shown by Shi *et al*[59] using both a pre-treatment and mid radiation MRI to predict chemoradiation therapy response in rectal cancer . To overcome, difficulties of acquiring large amounts of medical data, techniques such as transfer learning has been used to allow algorithms to train on separate large data sets[60].

The outcome predicted: Treatment response assessment

Tumor control occurs when the appropriate dose is delivered to the tumor, leading to a reduction in the growth of the tumor. It can be assessed grossly by the degree to which the tumor's size changes. Increasingly, changes have been assessed at a more microscopic level based on imaging characteristics (*e.g.*, functional imaging and quantitative analysis such as radiomics). It can also be conceptualized over multiple time points, ranging from the initial treatment response to recurrence, and to the overall survival.

For example, Mizutani *et al*[61] used clinical variables and dosimetry to predict the overall survival of malignant glioma patients after RT using SVM. Oikonomou *et al*[62] analyzed radiomics of PET/CT to predict recurrence and survival after SBRT for lung cancer. Regarding treatment failure, Aneja *et al*[63] used a DNN to predict the local failure over 2 years after SBRT for NSCLC, while Zhou *et al*[64] predicted the distant failure after SBRT for NSCLC using SVM . In shorter time frames, Wang *et al*[65] predicted the anatomic evolution of lung tumors halfway through the 6-wk course of RT using a CNN. Furthermore, Tseng *et al*[66] used RL to allow 'adaptation' of RT to the tumor response. Several studies have also examined treatment response in terms of prediction of pathological response following neoadjuvant chemotherapy using pre-treatment CT scans using radiomics with machine learning classification[67,68].

There are several studies utilising machine learning and AI in the task of prognostication. For example, a multi-centre study using a radiomics approach was utilised in predicting recurrence-free survival in nasopharyngeal carcinoma using MRI data[69]. In this study, an attempt was also made to explain the model using SHAP analysis which could help derive feature importance used in the predictive model.

The outcome predicted: Toxicity

Radiation toxicity is the other outcome that has been used for prediction. Whereas tumor control is the desired outcome from radiation targeting tumorous tissue, toxicity is the unwanted effects of radiation inevitably affecting surrounding normal tissue. Various applications have been applied to different sites of cancer. For example, Zhen *et al*[60] predicted rectum toxicity in cervical cancer using CNN, Ibragimov *et al*[70] predicted hepatobiliary toxicity after liver SBRT using CNN, and Valdes *et al*[71] predicted radiation pneumonitis after SBRT for stage I NSCLC using RUSBoost algorithm with regularization.

There have also been works that combine the outcomes of both the toxicity and the tumor response to RT. For example, Qi *et al*[72], applied a DNN to predict the patient reported quality of life in urinary and bowel symptoms, after SBRT for prostate cancer.

The model was trained on the dosimetry data alone. The urinary symptoms were predicted by the volume of the tumor, while the bowel symptoms represent the toxicity to the rectum.

HUMAN AI INTERACTION

As the use of AI technology progress, we need to examine the role of AI in conjunction with human. In the short term, this is likely to be in a collaborative/hybrid manner, rather AI operating autonomously, although this will depend on the tasks at hand. The impact of AI in the radiation oncology field is increasing rapidly, but at the same time the concern surrounding the use of AI is rising. One of the main concerns is the replacement of many jobs in the field of medical physics and radiation oncology, which can lead to a change in how patients are being treated. It is important to understand the perception of radiation oncology staff about the progression of AI and increase the awareness of the using of AI as a cooperative tool instead of job replacements. With the integration of AI in the profession, there is a huge potential in improving radiation oncology treatments and decision-making processes[73].

Limitations of AI

The efficiency and accuracy will be revolutionized by AI, but the future role of AI is not as clear, and the responsibility of the AI algorithm and clinicians using the AI needs to be addressed. In RT treatment planning, most plans are generated based on ground truth with low variability, but the optimization requires insights from clinicians to provide a creative solution for the patient. With the heavy reliance on technology, the innovative aspect may be reduced with the lack of human inputs. Safety risks such as AI being reluctant to highlight its own limitations are possible, with the potential of suboptimal plans being passed for treatment[74]. There is likely to be ongoing need of human/clinical oversight, not least due to regulatory requirements.

The concerns of using AI stem from the key issues surrounding the lack of empathy and intuition, unlike human practitioners. The development of empathy, which leads to the clinician focusing on the patients' well-being could play a subconscious role in providing a creative, innovative and safe RT treatment. This philosophical issue relates to human consciousness, and it contributes to how health practitioners should approach, use and interact with AI. The term preconceptual understanding, can be referred to as common sense for human in general. Since AI is perceived to not possess human common sense, it may affect its ability to perform certain tasks that require incorporation of these kinds of thinking[74].

Human cognition has two main attributes, which are concept and intuition. Human relies on these attributes to relate to the world and people around us. The concept of being affected by other people has an impact on how we behave towards them. Affectivity between individuals makes us take responsibility for other people, altering our behaviours either consciously or unconsciously. The intended consequence is generally thought to be that humans will behave in an ethical manner. In RT practice, clinical guidance exists for clinicians to follow and failure to act ethically would have serious consequences[74].

With the lack of intuition, AI may not behave with identical traits as human. The focus of the AI will be based on preprogrammed objectives, instead of patient outcomes and may even display a lack of creative input. Patient care and communication should be performed by human professionals because human needs to be involved in the RT routines, so the safety, creativity and innovation can be maintained. In the short term, the use of AI may assist treatment planning, potentially saving time. Clinicians will be required to integrate the technology into their practice, being aware of limitations, and how it can assist decision making. The unintended consequence may be that there are less opportunities or experience in training, and the training the future generation of medical staff for providing competent oversight may need to be addressed[74].

Karches[75] proposed that AI should not replace physician judgement. Technology should help us to extract things from their context, but when technological advancement leads us to reduce qualitative into quantitative information, eventually interactions between people could become mere data and information, driven to the point where only the quantifiable entities matter. Karches[75] mentioned two examples, which are stethoscopes and electronic health record (HER), to explain technologies can both help or hinder primary care. A stethoscope allows the

physicians to pay attention to the sounds of the patients' body functions. The physicians merely utilize a tool to increase their ability to extract information, the tool acts as an extension of the physician which still allows the physicians to conform their judgement to the patients' reality. However, EHR tends to distance the physician from the patient. A collection of fact is presented to the physicians before meeting the patient can surely make the examination process to be more efficient, but the lack of interaction between physician and patient can lead the physician to be less adapted to handle aspects of patient care that is not quantifiable by technology[75]. Limiting patient interaction also leads to less empathy and rapport, potentially leading to less trust in medical professionals.

They are unlikely to devote more time to uncompensated activities such as educating students[75]. These examples are an important reminder of how clinicians should interact with AI, where AI needs to be a tool to assist the clinicians to gain a better understanding of the patient and situation, but not something to distract themselves which compromise primary care. The more optimistic model of AI usage may be that AI frees the physicians or medical practitioners from repetitive or mundane, enabling them to spend more time with patients.

AI perception

Wong *et al* have surveyed the Canadian radiation oncology staff in 2020 regarding their views towards the impact of AI. Even though more than 90% of the respondents were interested in learning more about AI, only 12% of them felt they were knowledgeable about AI. For the forecast of AI, the majority of the respondents felt optimistic, and it would save time and benefit the patients. Common concerns among the staff were the economic implications and the lack of patient interaction. The precision of AI in identifying organs at risk is the top priority, and most concurred that AI system could produce better than average performance, but human oversight is still necessary for providing the best quality of patient care. Many respondents, especially radiation trainees, had concerns about AI could replace their professional responsibilities[73].

Medical practitioners have expressed frustration at the technologies because the relationship between the patient and medical staff are undermined. The AI produces a medical judgement, often disregarding the particular circumstances of each patient. This is because any extra consideration for the patient may lead to an increase in cost, lowering efficiency. Many experienced clinicians would not rely solely on the patients' verbal description because patients could be untruthful about their purpose of visit, or they might understate the burden of their symptoms. AI would tend to take the history of patients at face value, and depending on the technology used, it may never have the ability to interpret subtle non-verbal cues. The ability to understand the patients' needs remain questionable, as the best patient outcome does not always have a binary result which computers are good at producing[75].

The reduction of time-consuming tasks due to the AI integration may cause a reduction in job opportunities. On the other hand, the decrease in a more time-consuming task can lead to better inter-professional collaboration and an increase in interaction time with the patient. According to the survey from Wong *et al*[73], the cost benefits of AI was unclear for the respondents and it can be one of the reasons for the limitation on AI advancement. There could be a need for incorporating the knowledge of AI in the early stages of education, this is because the trainees which will be the future generation of practitioners, showed the least positivity towards AI. The fear of the unknown is part of human nature, and therefore, the investment of educating professionals to raise the knowledge and importance of AI is essential[73].

Techniques to improve human-AI interaction

Although AI has the potential to expand or extend beyond the cognitive abilities of humans, it still has its limitations in its current form that only humans can demonstrate such as generalisability and empathy. These limitations are especially pronounced in fields where data is limited and social context is paramount, such as in medicine and RT. There is an idea to create systems that combine humans and AI in symbiosis, with the intention that the whole is greater than the sum of its parts[76]. The ideal hybridized system would allow the two parties to combine the strengths yet hide the weaknesses of each other. However, the key to optimizing these systems is to have an efficient Human-AI interaction process. The interaction process has been subject to recent research. Design principles have been set forth, though applications within RT may be in its infancy.

To conceptualise the process of human-AI interaction, some groups have written guidelines and taxonomies for the design of such processes. Amershi *et al*[77] have created design guidelines for human-AI interaction, based on the feedback and experience of design practitioners. The focus is on a human-centric system with AI as an assistant. Key features can be divided over different time points of the interaction: (1) Before interaction (initiation): How does AI set expectations on its strengths and limitations? (2) On interaction: How does AI present information to a human? How does human provide feedback to AI? and (3) After interaction (over time): How does AI learn and adapt to human preferences?

The initiation phase occurs before any interaction occurs when expectations are set out for each other. Cai *et al*[78] have investigated what medical practitioners desired to know about the AI before using it. The requirements were akin to what the users desired to know about their human colleagues when consulting or cooperating with them. The properties of the AI can be described along these lines including its known strengths and limitations (*e.g.*, bias of training data), its functionality (*e.g.*, the task it was trained to perform), its objective (*e.g.*, was it designed to be sensitive or specific) and socioeconomic implications. With appropriate expectations set, the user may be motivated to adopt the system in various modes of collaboration. For example, the human-AI system can divide labour according to their strengths, or they can perform the same task as a second opinion to each other.

During the interaction, the AI and human communicate to share information. Firstly, there is a consideration of what information is to be shared. With current AI systems using deep learning, a decision or prediction is made based on given inputs. However, there is a common concern of interpretability of such decisions of AI systems because of the lack of explicit steps of reasoning between input and output. In order to gain trust in AI decision, interpretability or explanability has been a growing area in AI research in general. To this end, Luo *et al*[79] reviewed different AI algorithms with improved interpretability for RT outcome prediction. Some examples include using handcrafted features or activation maps. However, there is a trade-off between the algorithm's interpretability and its accuracy. Other methods include using SHAP analysis which is used to explain feature importance in tree-based models[80]. Secondly, there is a consideration of how to present the information in the workflow so that this integrates well in clinical practice. Ramkumar *et al*[81] explored the user interaction in semi-automatic segmentation of organs at risk. It was shown that the physicians' subjective preferences of different workflows play an important role, suggesting flexibility in system design needs to be bourne in mind. The experience and/or personal preference of an individual practitioner may also play a role. A recent study demonstrated that humans are susceptible to bias when given advice and this is particularly more pronounced with doctors with less experience on the task of chest radiograph interpretation[82]. Figure 5 shows the likely future direction of the development of AI and human-AI interaction. The incorporation of AI under human supervision will likely become mainstream in clinical practice in the future, until the AI has sufficient or near-human consciousness to perform tasks autonomously. In between, there may also be a hybrid mode of operation, whereby a direct interface with human may be used. For example, there are developments to implant chips in human brain so that we can directly interface with a computer system. This mode of operation could be used for example, for real-time adjustment in treatment plan during treatment delivery.

CONCLUSION

The examples of applications and potential of AI provide insights on how and why health care professionals such as medical physicists and radiation oncologists should use AI. The pros and cons with AI usage needs to be understood fully in order to both strengthen our ability to provide primary care and reduce the amount of weaknesses that human and AI possess.

The role of medical physicists will likely migrate away from QA of equipment, towards the QA of the patient treatments and overall treatment environment and processes. The decision-making capacity is expected to be improved and the knowledge gaps between experts and non-experts of a specific domain may be lowered. Clinicians are going to interact with computers more often and the efficiency of the human-computer interface will play a larger role in reducing duplicative and manual efforts. With the advancement of AI in the near future, the performance may, if not already, have surpassed human in specific tasks. It is crucial to re-think the

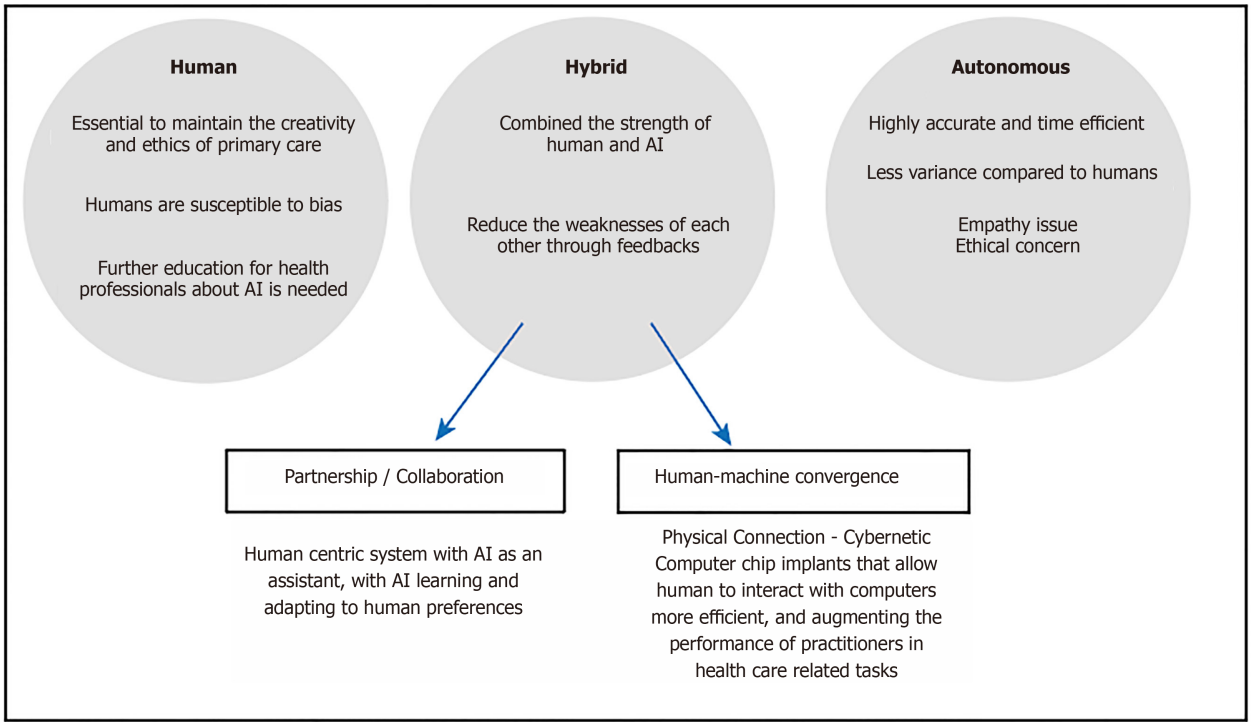

Figure 5 Future direction of human and artificial Intelligence. AI: Artificial intelligence.

ethical clinical practice, when do we decide to let a human make a "correction" to the output provided by an AI[2], or when can we allow AI system to operate autonomously.

The growth of AI also poses security challenges as the data are shared more often across governance structures and stakeholders. Implications of unintended third-party data reuse may be more common. As a consequent, already there are some efforts such as the increased requirements of European Union's General Data Protection Regulation to reduce the concern of the breach in privacy. Early AI that is clinically adopted might have flaws that result in patient harm just as some early IMRT systems. Nevertheless, AI will one day become widespread and effective technology[2].

Despite the potential drawbacks, the enormous benefit provided by AI will allow medical practitioners to provide a better healthcare service to patients. In the previous sections of this review, many techniques are currently in research. The clinical practice will be adopting the use of AI more in the future, and the examples listed above will likely become available and applied within the next decade.

While we are still a long way from having fully autonomous AI to determine the best treatment options, steps were taken in this direction such as improving AI algorithms through trainings and feedbacks. In the short term, there are likely to be some changes in the working environment. It would be foolhardy to expect that we maintain the status quo. Although medical practitioners are unlikely to be replaced any time soon, we expect the profession to evolve. Displacement of practitioner's roles rather than replacement may be the impact in the foreseeable future.

REFERENCES

1 **Siddique S**, Chow JCL. Artificial intelligence in radiotherapy. *Rep Pract Oncol Radiother* 2020; **25**: 656-666 [PMID: 32617080 DOI: 10.1016/j.rpor.2020.03.015]

2 **Thompson RF**, Valdes G, Fuller CD, Carpenter CM, Morin O, Aneja S, Lindsay WD, Aerts HJWL, Agrimson B, Deville C Jr, Rosenthal SA, Yu JB, Thomas CR Jr. Artificial intelligence in radiation oncology: A specialty-wide disruptive transformation? *Radiother Oncol* 2018; **129**: 421-426 [PMID: 29907338 DOI: 10.1016/j.radonc.2018.05.030]

3 **Meyer P**, Noblet V, Mazzara C, Lallement A. Survey on deep learning for radiotherapy. *Comput Biol Med* 2018; **98**: 126-146 [PMID: 29787940 DOI: 10.1016/j.compbiomed.2018.05.018]

4 **Wang T**, Lei Y, Fu Y, Wynne JF, Curran WJ, Liu T, Yang X. A review on medical imaging synthesis using deep learning and its clinical applications. *J Appl Clin Med Phys* 2021; **22**: 11-36 [PMID: 33305538 DOI: 10.1002/acm2.13121]

5 **Fu Y**, Lei Y, Zhou J, Wang T, Yu DS, Beitler JJ, Curran WJ; Liu T, Yang, X. Synthetic CT-aided MRI-CT image registration for head and neck radiotherapy. In: Gimi BS, Krol A. Medical Imaging 2020: Biomedical Applications in Molecular, Structural, and Functional Imaging. SPIE, 2020: 77 [DOI: 10.1117/12.2549092]

6 **Liu Y**, Lei Y, Wang T, Kayode O, Tian S, Liu T, Patel P, Curran WJ, Ren L, Yang X. MRI-based treatment planning for liver stereotactic body radiotherapy: validation of a deep learning-based synthetic CT generation method. *Br J Radiol* 2019; **92**: 20190067 [PMID: 31192695 DOI: 10.1259/bjr.20190067]

7 **Liu Y**, Lei Y, Wang Y, Shafai-Erfani G, Wang T, Tian S, Patel P, Jani AB, McDonald M, Curran WJ, Liu T, Zhou J, Yang X. Evaluation of a deep learning-based pelvic synthetic CT generation technique for MRI-based prostate proton treatment planning. *Phys Med Biol* 2019; **64**: 205022 [PMID: 31487698 DOI: 10.1088/1361-6560/ab41af]

8 **Lei Y**, Dong X, Tian Z, Liu Y, Tian S, Wang T, Jiang X, Patel P, Jani AB, Mao H, Curran WJ, Liu T, Yang X. CT prostate segmentation based on synthetic MRI-aided deep attention fully convolution network. *Med Phys* 2020; **47**: 530-540 [PMID: 31745995 DOI: 10.1002/mp.13933]

9 **Dong C**, Loy CC, He K, Tang X. Image Super-Resolution Using Deep Convolutional Networks. *IEEE Trans Pattern Anal Mach Intell* 2016; **38**: 295-307 [PMID: 26761735 DOI: 10.1109/TPAMI.2015.2439281]

10 **Bahrami K**, Shi F, Rekik I, Shen D. Convolutional neural network for reconstruction of 7T-like images from 3T MRI using appearance and anatomical features. In: Carneiro G, Mateus D, Peter L, Bradley A, Tavares JMRS, Belagiannis V, Papa JP, Nascimento JC, Loog M, Lu Z, Cardoso JS, Cornebise J. Deep Learning and Data Labeling for Medical Applications. DLMIA 2016, LABELS 2016. Lecture Notes in Computer Science, vol 10008. Cham: Springer, 2016: 39-47 [DOI: 10.1007/978-3-319-46976-8_5]

11 **Qu L**, Zhang Y, Wang S, Yap PT, Shen D. Synthesized 7T MRI from 3T MRI *via* deep learning in spatial and wavelet domains. *Med Image Anal* 2020; **62**: 101663 [PMID: 32120269 DOI: 10.1016/j.media.2020.101663]

12 **Yang Q**, Yan P, Zhang Y, Yu H, Shi Y, Mou X, Kalra MK, Sun L, Wang G. Low-Dose CT Image Denoising Using a Generative Adversarial Network With Wasserstein Distance and Perceptual Loss. *IEEE Trans Med Imaging* 2018; **37**: 1348-1357 [PMID: 29870364 DOI: 10.1109/TMI.2018.2827462]

13 **Wang T**, Lei Y, Tian Z, Dong X, Liu Y, Jiang X, Curran WJ, Liu T, Shu HK, Yang X. Deep learning-based image quality improvement for low-dose computed tomography simulation in radiation therapy. *J Med Imaging (Bellingham)* 2019; **6**: 043504 [PMID: 31673567 DOI: 10.1117/1.JMI.6.4.043504]

14 **Chen H**, Zhang Y, Zhang W, Liao P, Li K, Zhou J, Wang G. Low-dose CT *via* convolutional neural network. *Biomed Opt Express* 2017; **8**: 679-694 [PMID: 28270976 DOI: 10.1364/BOE.8.000679]

15 **Cardenas CE**, Yang J, Anderson BM, Court LE, Brock KB. Advances in Auto-Segmentation. *Semin Radiat Oncol* 2019; **29**: 185-197 [PMID: 31027636 DOI: 10.1016/j.semradonc.2019.02.001]

16 **Zhou SK**, Greenspan H, Shen D. Deep Learning for Medical Image Analysis. 1st ed. San Diego: Elsevier, 2017

17 **Krizhevsky A**, Sutskever I, Hinton GE. ImageNet classification with deep convolutional neural networks. In: Bartlett P, Pereira PCN, Burges CJC, Bottou L, Weinberger KQ. Advances in Neural Information Processing Systems 25. Curran Associates, 2012

18 **Ibragimov B**, Toesca D, Chang D, Koong A, Xing L. Combining deep learning with anatomical analysis for segmentation of the portal vein for liver SBRT planning. *Phys Med Biol* 2017; **62**: 8943-8958 [PMID: 28994665 DOI: 10.1088/1361-6560/aa9262]

19 **Li W**, Jia F, Hu Q. Automatic Segmentation of Liver Tumor in CT Images with Deep Convolutional Neural Networks. *J Comput Commun* 2015; **3**: 146-151 [DOI: 10.4236/jcc.2015.311023]

20 **Chen LC**, Papandreou G, Schroff F, Adam H. Rethinking atrous convolution for semantic image segmentation. 2017 Preprint. Available from: arXiv:1706.05587

21 **Ronneberger O**, Fischer P, Brox T. U-net: Convolutional networks for biomedical image segmentation. In: Navab N, Hornegger J, Wells W, Frangi A. Medical Image Computing and Computer-Assisted Intervention – MICCAI 2015. MICCAI 2015. Lecture Notes in Computer Science, vol 9351. Cham: Springer, 2015: 234-241 [DOI: 10.1007/978-3-319-24574-4_28]

22 **Shelhamer E**, Long J, Darrell T. Fully Convolutional Networks for Semantic Segmentation. *IEEE Trans Pattern Anal Mach Intell* 2017; **39**: 640-651 [PMID: 27244717 DOI: 10.1109/TPAMI.2016.2572683]

23 **Qayyum A**, Ahmad I, Mumtaz W, Alassafi MO, Alghamdi R, Mazher M. Automatic Segmentation Using a Hybrid Dense Network Integrated With an 3D-Atrous Spatial Pyramid Pooling Module for Computed Tomography (CT) Imaging. *IEEE Access* 2020; **8**: 169794-169803 [DOI: 10.1109/access.2020.3024277]

24 **Clark K**, Vendt B, Smith K, Freymann J, Kirby J, Koppel P, Moore S, Phillips S, Maffitt D, Pringle M, Tarbox L, Prior F. Browse Data Collections. The Cancer Imaging Archive (TCIA), 2021

25 **Freimuth M**. NIH Clinical Center releases dataset of 32,000 CT images. National Institutes of Health, US. Available from: https://www.nih.gov/news-events/news-releases/nih-clinical-center-releases-dataset-32000-ct-images

26 **University of Southern California**. Medical imaging data archived in the IDA. Available from: https://ida.loni.usc.edu/services/Menu/IdaData.jsp?project=

27 **Jiang D**, Yan H, Chang N, Li T, Mao R, Du C, Guo B, Liu J. Convolutional neural network-based dosimetry evaluation of esophageal radiation treatment planning. *Med Phys* 2020; **47**: 4735-4742 [PMID: 32767840 DOI: 10.1002/mp.14434]

28 **Nawa K**, Haga A, Nomoto A, Sarmiento RA, Shiraishi K, Yamashita H, Nakagawa K. Evaluation of a commercial automatic treatment planning system for prostate cancers. *Med Dosim* 2017; **42**: 203-209 [PMID: 28549556 DOI: 10.1016/j.meddos.2017.03.004]

29 **Krayenbuehl J**, Zamburlini M, Ghandour S, Pachoud M, Tanadini-Lang S, Tol J, Guckenberger M, Verbakel WFAR. Planning comparison of five automated treatment planning solutions for locally advanced head and neck cancer. *Radiat Oncol* 2018; **13**: 170 [PMID: 30201017 DOI: 10.1186/s13014-018-1113-z]

30 **Nelms BE**, Robinson G, Markham J, Velasco K, Boyd S, Narayan S, Wheeler J, Sobczak ML. Variation in external beam treatment plan quality: An inter-institutional study of planners and planning systems. *Pract Radiat Oncol* 2012; **2**: 296-305 [PMID: 24674168 DOI: 10.1016/j.prro.2011.11.012]

31 **Batumalai V**, Jameson MG, Forstner DF, Vial P, Holloway LC. How important is dosimetrist experience for intensity modulated radiation therapy? *Pract Radiat Oncol* 2013; **3**: e99-e106 [PMID: 24674377 DOI: 10.1016/j.prro.2012.06.009]

32 **Hazell I**, Bzdusek K, Kumar P, Hansen CR, Bertelsen A, Eriksen JG, Johansen J, Brink C. Automatic planning of head and neck treatment plans. *J Appl Clin Med Phys* 2016; **17**: 272-282 [PMID: 26894364 DOI: 10.1120/jacmp.v17i1.5901]

33 **Kida S**, Nakamoto T, Nakano M, Nawa K, Haga A, Kotoku J, Yamashita H, Nakagawa K. Cone Beam Computed Tomography Image Quality Improvement Using a Deep Convolutional Neural Network. *Cureus* 2018; **10**: e2548 [PMID: 29963342 DOI: 10.7759/cureus.2548]

34 **Huynh E**, Hosny A, Guthier C, Bitterman DS, Petit SF, Haas-Kogan DA, Kann B, Aerts HJWL, Mak RH. Artificial intelligence in radiation oncology. *Nat Rev Clin Oncol* 2020; **17**: 771-781 [PMID: 32843739 DOI: 10.1038/s41571-020-0417-8]

35 **Langen KM**, Jones DT. Organ motion and its management. *Int J Radiat Oncol Biol Phys* 2001; **50**: 265-278 [PMID: 11316572 DOI: 10.1016/S0360-3016(01)01453-5]

36 **Murphy MJ**, Pokhrel D. Optimization of an adaptive neural network to predict breathing. *Med Phys* 2009; **36**: 40-47 [PMID: 19235372 DOI: 10.1118/1.3026608]

37 **Isaksson M**, Jalden J, Murphy MJ. On using an adaptive neural network to predict lung tumor motion during respiration for radiotherapy applications. *Med Phys* 2005; **32**: 3801-3809 [PMID: 16475780 DOI: 10.1118/1.2134958]

38 **Ménard C**, Paulson E, Nyholm T, McLaughlin P, Liney G, Dirix P, van der Heide UA. Role of Prostate MR Imaging in Radiation Oncology. *Radiol Clin North Am* 2018; **56**: 319-325 [PMID: 29420985 DOI: 10.1016/j.rcl.2017.10.012]

39 **Wegener D**, Zips D, Thorwarth D, Weiß J, Othman AE, Grosse U, Notohamiprodjo M, Nikolaou K, Müller AC. Precision of T2 TSE MRI-CT-image fusions based on gold fiducials and repetitive T2 TSE MRI-MRI-fusions for adaptive IGRT of prostate cancer by using phantom and patient data. *Acta Oncol* 2019; **58**: 88-94 [PMID: 30264629 DOI: 10.1080/0284186X.2018.1518594]

40 **Gustafsson CJ**, Swärd J, Adalbjörnsson SI, Jakobsson A, Olsson LE. Development and evaluation of a deep learning based artificial intelligence for automatic identification of gold fiducial markers in an MRI-only prostate radiotherapy workflow. *Phys Med Biol* 2020; **65**: 225011 [PMID: 33179610 DOI: 10.1088/1361-6560/abb0f9]

41 **Persson E**, Jamtheim Gustafsson C, Ambolt P, Engelholm S, Ceberg S, Bäck S, Olsson LE, Gunnlaugsson A. MR-PROTECT: Clinical feasibility of a prostate MRI-only radiotherapy treatment workflow and investigation of acceptance criteria. *Radiat Oncol* 2020; **15**: 77 [PMID: 32272943 DOI: 10.1186/s13014-020-01513-7]

42 **Unkelbach J**, Bortfeld T, Craft D, Alber M, Bangert M, Bokrantz R, Chen D, Li R, Xing L, Men C, Nill S, Papp D, Romeijn E, Salari E. Optimization approaches to volumetric modulated arc therapy planning. *Med Phys* 2015; **42**: 1367-1377 [PMID: 25735291 DOI: 10.1118/1.4908224]

43 **Bohoudi O**, Bruynzeel AME, Senan S, Cuijpers JP, Slotman BJ, Lagerwaard FJ, Palacios MA. Fast and robust online adaptive planning in stereotactic MR-guided adaptive radiation therapy (SMART) for pancreatic cancer. *Radiother Oncol* 2017; **125**: 439-444 [PMID: 28811038 DOI: 10.1016/j.radonc.2017.07.028]

44 **Lamb J**, Cao M, Kishan A, Agazaryan N, Thomas DH, Shaverdian N, Yang Y, Ray S, Low DA, Raldow A, Steinberg ML, Lee P. Online Adaptive Radiation Therapy: Implementation of a New Process of Care. *Cureus* 2017; **9**: e1618 [PMID: 29104835 DOI: 10.7759/cureus.1618]

45 **Hrinivich WT**, Lee J. Artificial intelligence-based radiotherapy machine parameter optimization using reinforcement learning. *Med Phys* 2020; **47**: 6140-6150 [PMID: 33070336 DOI: 10.1002/mp.14544]

46 **Debus C**, Oelfke U, Bartzsch S. A point kernel algorithm for microbeam radiation therapy. *Phys Med Biol* 2017; **62**: 8341-8359 [PMID: 28922140 DOI: 10.1088/1361-6560/aa8d63]

47 **Bangert M**, Oelfke U. Spherical cluster analysis for beam angle optimization in intensity-modulated radiation therapy treatment planning. *Phys Med Biol* 2010; **55**: 6023-6037 [PMID: 20858916 DOI: 10.1088/0031-9155/55/19/025]

48 **Zhang X**, Homma N, Ichiji K, Abe M, Sugita N, Takai Y, Narita Y, Yoshizawa M. A kernel-based method for markerless tumor tracking in kV fluoroscopic images. *Phys Med Biol* 2014; **59**: 4897-4911 [PMID: 25098382 DOI: 10.1088/0031-9155/59/17/4897]

49 **Zhao W**, Han B, Yang Y, Buyyounouski M, Hancock SL, Bagshaw H, Xing L. Incorporating imaging information from deep neural network layers into image guided radiation therapy (IGRT). *Radiother Oncol* 2019; **140**: 167-174 [PMID: 31302347 DOI: 10.1016/j.radonc.2019.06.027]

50 **Kalet AM**, Luk SMH, Phillips MH. Radiation Therapy Quality Assurance Tasks and Tools: The Many Roles of Machine Learning. *Med Phys* 2020; **47**: e168-e177 [PMID: 30768796 DOI: 10.1002/mp.13445]

51 **Vandewinckele L**, Claessens M, Dinkla A, Brouwer C, Crijns W, Verellen D, van Elmpt W. Overview of artificial intelligence-based applications in radiotherapy: Recommendations for implementation and quality assurance. *Radiother Oncol* 2020; **153**: 55-66 [PMID: 32920005 DOI: 10.1016/j.radonc.2020.09.008]

52 **Chang X**, Li H, Kalet A, Yang D. Detecting External Beam Radiation Therapy Physician Order Errors Using Machine Learning. *Int J Radiat Oncol* 2017; **99**: S71 [DOI: 10.1016/j.ijrobp.2017.06.174]

53 **Kalet AM**, Gennari JH, Ford EC, Phillips MH. Bayesian network models for error detection in radiotherapy plans. *Phys Med Biol* 2015; **60**: 2735-2749 [PMID: 25768885 DOI: 10.1088/0031-9155/60/7/2735]

54 **Tomori S**, Kadoya N, Takayama Y, Kajikawa T, Shima K, Narazaki K, Jingu K. A deep learning-based prediction model for gamma evaluation in patient-specific quality assurance. *Med Phys* 2018 [PMID: 30066388 DOI: 10.1002/mp.13112]

55 **Nyflot MJ**, Thammasorn P, Wootton LS, Ford EC, Chaovalitwongse WA. Deep learning for patient-specific quality assurance: Identifying errors in radiotherapy delivery by radiomic analysis of gamma images with convolutional neural networks. *Med Phys* 2019; **46**: 456-464 [PMID: 30548601 DOI: 10.1002/mp.13338]

56 **Granville DA**, Sutherland JG, Belec JG, La Russa DJ. Predicting VMAT patient-specific QA results using a support vector classifier trained on treatment plan characteristics and linac QC metrics. *Phys Med Biol* 2019; **64**: 095017 [PMID: 30921785 DOI: 10.1088/1361-6560/ab142e]

57 **Li Q**, Chan MF. Predictive time-series modeling using artificial neural networks for Linac beam symmetry: an empirical study. *Ann N Y Acad Sci* 2017; **1387**: 84-94 [PMID: 27627049 DOI: 10.1111/nyas.13215]

58 **Xu Y**, Hosny A, Zeleznik R, Parmar C, Coroller T, Franco I, Mak RH, Aerts HJWL. Deep Learning Predicts Lung Cancer Treatment Response from Serial Medical Imaging. *Clin Cancer Res* 2019; **25**: 3266-3275 [PMID: 31010833 DOI: 10.1158/1078-0432.CCR-18-2495]

59 **Shi L**, Zhang Y, Nie K, Sun X, Niu T, Yue N, Kwong T, Chang P, Chow D, Chen JH, Su MY. Machine learning for prediction of chemoradiation therapy response in rectal cancer using pre-treatment and mid-radiation multi-parametric MRI. *Magn Reson Imaging* 2019; **61**: 33-40 [PMID: 31059768 DOI: 10.1016/j.mri.2019.05.003]

60 **Zhen X**, Chen J, Zhong Z, Hrycushko B, Zhou L, Jiang S, Albuquerque K, Gu X. Deep convolutional neural network with transfer learning for rectum toxicity prediction in cervical cancer radiotherapy: a feasibility study. *Phys Med Biol* 2017; **62**: 8246-8263 [PMID: 28914611 DOI: 10.1088/1361-6560/aa8d09]

61 **Mizutani T**, Magome T, Igaki H, Haga A, Nawa K, Sekiya N, Nakagawa K. Optimization of treatment strategy by using a machine learning model to predict survival time of patients with malignant glioma after radiotherapy. *J Radiat Res* 2019; **60**: 818-824 [PMID: 31665445 DOI: 10.1093/jrr/rrz066]

62 **Oikonomou A**, Khalvati F, Tyrrell PN, Haider MA, Tarique U, Jimenez-Juan L, Tjong MC, Poon I, Eilaghi A, Ehrlich L, Cheung P. Radiomics analysis at PET/CT contributes to prognosis of recurrence and survival in lung cancer treated with stereotactic body radiotherapy. *Sci Rep* 2018; **8**: 4003 [PMID: 29507399 DOI: 10.1038/s41598-018-22357-y]

63 **Aneja S**, Shaham U, Kumar RJ, Pirakitikulr N, Nath SK, Yu JB, Carlson DJ, Decker RH. Deep Neural Network to Predict Local Failure Following Stereotactic Body Radiation Therapy: Integrating Imaging and Clinical Data to Predict Outcomes. *Int J Radiat Oncol* 2017; **99**: S47 [DOI: 10.1016/j.ijrobp.2017.06.120]

64 **Zhou Z**, Folkert M, Cannon N, Iyengar P, Westover K, Zhang Y, Choy H, Timmerman R, Yan J, Xie XJ, Jiang S, Wang J. Predicting distant failure in early stage NSCLC treated with SBRT using clinical parameters. *Radiother Oncol* 2016; **119**: 501-504 [PMID: 27156652 DOI: 10.1016/j.radonc.2016.04.029]

65 **Wang C**, Rimner A, Hu YC, Tyagi N, Jiang J, Yorke E, Riyahi S, Mageras G, Deasy JO, Zhang P. Toward predicting the evolution of lung tumors during radiotherapy observed on a longitudinal MR imaging study *via* a deep learning algorithm. *Med Phys* 2019; **46**: 4699-4707 [PMID: 31410855 DOI: 10.1002/mp.13765]

66 **Tseng HH**, Luo Y, Cui S, Chien JT, Ten Haken RK, Naqa IE. Deep reinforcement learning for automated radiation adaptation in lung cancer. *Med Phys* 2017; **44**: 6690-6705 [PMID: 29034482 DOI: 10.1002/mp.12625]

67 **Hu Y**, Xie C, Yang H, Ho JWK, Wen J, Han L, Lam KO, Wong IYH, Law SYK, Chiu KWH, Vardhanabhuti V, Fu J. Computed tomography-based deep-learning prediction of neoadjuvant chemoradiotherapy treatment response in esophageal squamous cell carcinoma. *Radiother Oncol* 2021; **154**: 6-13 [PMID: 32941954 DOI: 10.1016/j.radonc.2020.09.014]

68 **Hu Y**, Xie C, Yang H, Ho JWK, Wen J, Han L, Chiu KWH, Fu J, Vardhanabhuti V. Assessment of Intratumoral and Peritumoral Computed Tomography Radiomics for Predicting Pathological Complete Response to Neoadjuvant Chemoradiation in Patients With Esophageal Squamous Cell

Carcinoma. *JAMA Netw Open* 2020; **3**: e2015927 [PMID: 32910196 DOI: 10.1001/jamanetworkopen.2020.15927]

69 **Du R**, Lee VH, Yuan H, Lam KO, Pang HH, Chen Y, Lam EY, Khong PL, Lee AW, Kwong DL, Vardhanabhuti V. Radiomics Model to Predict Early Progression of Nonmetastatic Nasopharyngeal Carcinoma after Intensity Modulation Radiation Therapy: A Multicenter Study. *Radiol Artif Intell* 2019; **1**: e180075 [DOI: 10.1148/ryai.2019180075]

70 **Ibragimov B**, Toesca D, Chang D, Yuan Y, Koong A, Xing L. Development of deep neural network for individualized hepatobiliary toxicity prediction after liver SBRT. *Med Phys* 2018; **45**: 4763-4774 [PMID: 30098025 DOI: 10.1002/mp.13122]

71 **Valdes G**, Solberg TD, Heskel M, Ungar L, Simone CB 2nd. Using machine learning to predict radiation pneumonitis in patients with stage I non-small cell lung cancer treated with stereotactic body radiation therapy. *Phys Med Biol* 2016; **61**: 6105-6120 [PMID: 27461154 DOI: 10.1088/0031-9155/61/16/6105]

72 **Qi X**, Neylon J, Santhanam A. Dosimetric Predictors for Quality of Life After Prostate Stereotactic Body Radiation Therapy *via* Deep Learning Network. *Int J Radiat Oncol* 2017; **99**: S167 [DOI: 10.1016/j.ijrobp.2017.06.384]

73 **Wong K**, Gallant F, Szumacher E. Perceptions of Canadian radiation oncologists, radiation physicists, radiation therapists and radiation trainees about the impact of artificial intelligence in radiation oncology - national survey. *J Med Imaging Radiat Sci* 2021; **52**: 44-48 [PMID: 33323332 DOI: 10.1016/j.jmir.2020.11.013]

74 **Bridge P**, Bridge R. Artificial Intelligence in Radiotherapy: A Philosophical Perspective. *J Med Imaging Radiat Sci* 2019; **50**: S27-S31 [PMID: 31591033 DOI: 10.1016/j.jmir.2019.09.003]

75 **Karches KE**. Against the iDoctor: why artificial intelligence should not replace physician judgment. *Theor Med Bioeth* 2018; **39**: 91-110 [PMID: 29992371 DOI: 10.1007/s11017-018-9442-3]

76 **Jarrahi MH**. Artificial intelligence and the future of work: Human-AI symbiosis in organizational decision making. *Bus Horiz* 2018; **61**: 577-586 [DOI: 10.1016/j.bushor.2018.03.007]

77 **Amershi S**, Weld D, Vorvoreanu M, Fourney A, Nushi B, Collisson P, Suh J, Iqbal S, Bennett PN, Inkpen K, Teevan J, Kikin-Gil R, Horvitz E. Guidelines for human-AI interaction. In: CHI '19: Proceedings of the 2019 CHI Conference on Human Factors in Computing Systems; 2019 May 4-9; Glasgow Scotland; UK. New York: Association for Computing Machinery, 2019: 1-13 [DOI: 10.1145/3290605.3300233]

78 **Cai CJ**, Winter S, Steiner D, Wilcox L, Terry M. "Hello AI": Uncovering the onboarding needs of medical practitioners for human–AI collaborative decision-making. *Proc ACM Hum Comput Interact* 2019; **3**: 104 [DOI: 10.1145/3359206]

79 **Luo Y**, Tseng HH, Cui S, Wei L, Ten Haken RK, El Naqa I. Balancing accuracy and interpretability of machine learning approaches for radiation treatment outcomes modeling. *BJR Open* 2019; **1**: 20190021 [PMID: 33178948 DOI: 10.1259/bjro.20190021]

80 **Lundberg SM**, Lee SI. A unified approach to interpreting model predictions. In: Guyon I, Luxburg UV, Bengio S, Wallach H, Fergus R, Vishwanathan S, Garnett R, editors. Advances in Neural Information Processing Systems 30. Curran Associates, 2017

81 **Ramkumar A**, Dolz J, Kirisli HA, Adebahr S, Schimek-Jasch T, Nestle U, Massoptier L, Varga E, Stappers PJ, Niessen WJ, Song Y. User Interaction in Semi-Automatic Segmentation of Organs at Risk: a Case Study in Radiotherapy. *J Digit Imaging* 2016; **29**: 264-277 [PMID: 26553109 DOI: 10.1007/s10278-015-9839-8]

82 **Gaube S**, Suresh H, Raue M, Merritt A, Berkowitz SJ, Lermer E, Coughlin JF, Guttag JV, Colak E, Ghassemi M. Do as AI say: susceptibility in deployment of clinical decision-aids. *NPJ Digit Med* 2021; **4**: 31 [PMID: 33608629 DOI: 10.1038/s41746-021-00385-9]

Published by **Baishideng Publishing Group Inc**
7041 Koll Center Parkway, Suite 160, Pleasanton, CA 94566, USA
Telephone: +1-925-3991568
E-mail: bpgoffice@wjgnet.com
Help Desk: https://www.f6publishing.com/helpdesk
https://www.wjgnet.com

ISSN 2644-3260 (online)

Artificial Intelligence in *Medical Imaging*

Artif Intell Med Imaging 2021 June 28; 2(3): 56-85

Published by Baishideng Publishing Group Inc

AIMI

Artificial Intelligence in Medical Imaging

Contents

Bimonthly Volume 2 Number 3 June 28, 2021

OPINION REVIEW

56 Implementation of lung ultrasound in the triage of pregnant women during the SARS-CoV-2 pandemics

Tekin AB, Yassa M

MINIREVIEWS

64 Application of radiomics in hepatocellular carcinoma: A review

Jin ZC, Zhong BY

73 Artificial intelligence in coronary computed tomography angiography

Zhang ZZ, Guo Y, Hou Y

Artificial Intelligence in Medical Imaging

Bimonthly Volume 2 Number 3 June 28, 2021

Contents

ABOUT COVER

Editorial board member of *Artificial Intelligence in Medical Imaging*, Quan Zhou, MD, Professor, Department of Medical Imaging, The Third Affiliated Hospital of Southern Medical University, Guangzhou 510630, Guangdong Province, China

AIMS AND SCOPE

The primary aim of *Artificial Intelligence in Medical Imaging* (*AIMI*, *Artif Intell Med Imaging*) is to provide scholars and readers from various fields of artificial intelligence in medical imaging with a platform to publish high-quality basic and clinical research articles and communicate their research findings online.

AIMI mainly publishes articles reporting research results obtained in the field of artificial intelligence in medical imaging and covering a wide range of topics, including artificial intelligence in radiology, pathology image analysis, endoscopy, molecular imaging, and ultrasonography.

INDEXING/ABSTRACTING

There is currently no indexing.

RESPONSIBLE EDITORS FOR THIS ISSUE

NAME OF JOURNAL
Artificial Intelligence in Medical Imaging

ISSN
ISSN 2644-3260 (online)

LAUNCH DATE
June 28, 2020

FREQUENCY
Bimonthly

EDITORS-IN-CHIEF
Xue-Li Chen, Caroline Chung, Jun Shen

EDITORIAL BOARD MEMBERS
https://www.wjgnet.com/2644-3260/editorialboard.htm

PUBLICATION DATE
June 28, 2021

INSTRUCTIONS TO AUTHORS
https://www.wjgnet.com/bpg/gerinfo/204

GUIDELINES FOR ETHICS DOCUMENTS
https://www.wjgnet.com/bpg/GerInfo/287

GUIDELINES FOR NON-NATIVE SPEAKERS OF ENGLISH
https://www.wjgnet.com/bpg/gerinfo/240

PUBLICATION ETHICS
https://www.wjgnet.com/bpg/GerInfo/288

PUBLICATION MISCONDUCT
https://www.wjgnet.com/bpg/gerinfo/208

ARTICLE PROCESSING CHARGE
https://www.wjgnet.com/bpg/gerinfo/242

STEPS FOR SUBMITTING MANUSCRIPTS
https://www.wjgnet.com/bpg/GerInfo/239

ONLINE SUBMISSION
https://www.f6publishing.com

E-mail: bpgoffice@wjgnet.com https://www.wjgnet.com

Artificial Intelligence in Medical Imaging

Submit a Manuscript: https://www.f6publishing.com

Artif Intell Med Imaging 2021 June 28; 2(3): 56-63

DOI: 10.35711/aimi.v2.i3.56

ISSN 2644-3260 (online)

OPINION REVIEW

Implementation of lung ultrasound in the triage of pregnant women during the SARS-CoV-2 pandemics

Arzu Bilge Tekin, Murat Yassa

ORCID number: Arzu Bilge Tekin 0000-0001-8054-2624; Murat Yassa 0000-0001-8661-1192.

Author contributions: Tekin AB and Yassa M contributed equally to this work; Tekin AB and Yassa M performed the research, analyzed the data and wrote the manuscript; all authors have read and approved the final manuscript.

Conflict-of-interest statement: The authors report no conflict of interest.

Manuscript source: Invited manuscript

Specialty type: Obstetrics and gynecology

Arzu Bilge Tekin, Murat Yassa, Department of Obstetrics and Gynecology, Sancaktepe Sehit Prof. Dr. Ilhan Varank Training and Research Hospital, Istanbul 34785, Sancaktepe, Turkey

Corresponding author: Arzu Bilge Tekin, MD, Associate Specialist, Department of Obstetrics and Gynecology, Sancaktepe Sehit Prof. Dr. Ilhan Varank Training and Research Hospital, Emek Mahallesi, Namık Kemal Caddesi No. 54, Istanbul 34785, Sancaktepe, Turkey. arzubilgetekin@gmail.com

Abstract

Lung ultrasound (US) has been shown that it is able to detect interstitial lung disease, subpleural consolidations and acute respiratory distress syndrome in clinical and physical studies that assess its role in upper respiratory infections. It is used worldwide in the coronavirus disease 2019 (COVID-19) outbreak and the effectiveness has been assessed in several studies. Fast diagnosis of COVID-19 is essential in deciding for patient isolation, clinical care and reducing transmission. Imaging the lung and pleura by ultrasound is efficient, cost-effective, and safe and it is recognized as rapid, repeatable, and reliable. Obstetricians are already using the US and are quite proficient in doing so. During the pandemic, performing lung US (LUS) right after the fetal assessment until reverse transcription polymerase chain reaction results are obtained, particularly in settings that have a centralized testing center, was found feasible for the prediction of the severe acute respiratory syndrome coronavirus 2 (SARS-CoV-2) infection. The use of LUS is efficient in the triage and monitoring of pregnant women. Clinicians dealing with pregnant women should consider LUS as the first-line diagnostic tool in pregnant women during the SARS-CoV-2 pandemic.

Key Words: COVID-19 pandemics; Lung; Ultrasound imaging; Pregnancy; SARS-CoV-2; Triage

Core Tip: Lung ultrasound (US) is based on specific pattern recognition and does not require complex measurements, therefore obstetricians can easily learn and use lung ultrasound (LUS) in the pandemic. LUS examination can be a routine after a routine obstetric US examination. Fast diagnosis of coronavirus disease 2019 is essential in

Country/Territory of origin: Turkey

Peer-review report's scientific quality classification
Grade A (Excellent): 0
Grade B (Very good): B
Grade C (Good): 0
Grade D (Fair): D
Grade E (Poor): 0

Received: April 10, 2021
Peer-review started: April 10, 2021
First decision: April 28, 2021
Revised: May 6, 2021
Accepted: June 4, 2021
Article in press: June 4, 2021
Published online: June 28, 2021

P-Reviewer: Samadder S, Thandassery RB
S-Editor: Fan JR
L-Editor: Filipodia
P-Editor: Xing YX

deciding for patient isolation, clinical care, and reducing transmission. Clinicians dealing with pregnant women should consider LUS as the first-line diagnostic tool in pregnant women during the severe acute respiratory syndrome coronavirus 2 pandemic.

Citation: Tekin AB, Yassa M. Implementation of lung ultrasound in the triage of pregnant women during the SARS-CoV-2 pandemics. *Artif Intell Med Imaging* 2021; 2(3): 56-63
URL: https://www.wjgnet.com/2644-3260/full/v2/i3/56.htm
DOI: https://dx.doi.org/10.35711/aimi.v2.i3.56

INTRODUCTION

Lung ultrasound (US) use has been discussed for years in emergency medicine, intensive care units, and cardiovascular diseases. The use of lung US (LUS) has increased in the last 15-20 years upon advancements in the visualization of pleural effusions, lung masses, and afterward evolved to be able to evaluate lung parenchyma mainly as a point-of-care technique[1]. Pulmonologists, emergency medicine physicians, thoracic and cardiac surgeons often benefit from LUS in the management of traumatic conditions and intraoperative situations[2]. Coronavirus disease 2019 (COVID-19) pneumonia mainly involves the lung periphery and causes interstitial pneumonia. Therefore, LUS is highly suitable for the management of this disease[3]. The obstetricians are already familiar with the US and they are at the frontline in the fight against the severe acute respiratory syndrome coronavirus 2 (SARS-CoV-2) pandemic for infected pregnant women treatment[4]. LUS is based on specific pattern recognition and does not require complex measurements, therefore the obstetricians can easily learn and use LUS in the pandemic[1,5].

SCORING SYSTEM FOR LUS

LUS has been shown that it is able to detect interstitial lung disease, subpleural consolidations and acute respiratory distress syndrome in clinical and physical studies that assess its role in upper respiratory infections[6-8]. It is widely used worldwide in the COVID-19 outbreak and the effectiveness has been assessed in several studies[9-14]. LUS evaluation covers 14 anatomical regions, 3 posterior, 2 lateral, 2 anterior, in both hemithorax and intercostal spaces in supine, right lateral, left lateral positions during at least 10 s[6]. In different scoring systems, the target regions were varied between 4 to 7 regions for each hemithorax[15]. Pleural thickness, pleural continuity, pleural drift (with inspiration and expiration), presence of subpleural consolidated areas, parenchymal artifacts (vertical, horizontal), and the presence of a white lung pattern should be focused in every region. The results of 14 anatomical regions are scored between 0 and 3; LUS 0 is defined as normal LUS findings, LUS score of 1 is defined as mild involvement, LUS score of 2 is defined as moderate involvement and LUS score of 3 is defined as severe lung involvement[6]. Normal US findings (LUS 0) represent thin, continuous, and regular pleural lines, presence of respiratory pleural shift and parenchymal horizontal artifacts due to normally aerated lung surface reflectivity (A lines) in LUS. Mild involvement (LUS 1) is defined with an indented pleural line (irregularities in the pleural line, continuity is not broken), the sporadic vertical white area under the pleura (B line). Moderate involvement (LUS 2) is defined with broken pleura (continuity disorder in the pleural line), small to the large white area of consolidation under pleura, and multiple white vertical lines (B lines) that progress to the end of the viewed area. Severe lung involvement (LUS 3) is defined as a severe broken pleura pattern in addition to a dense and wide "white lung" pattern with or without consolidated area in LUS[6]. B lines, small consolidated areas and broken pleural lines are suggestive of COVID-19[16]. Bacterial pneumonia is mainly represented with isolated large lobar consolidation with or without pleural effusion and dynamic air bronchograms[17].

ADVANTAGES OF LUS

Fast diagnosis of COVID-19 is essential in deciding for patient isolation, clinical care and reducing transmission. For diagnosis of COVID-19, symptoms are leading us and mainly reverse transcription polymerase chain reaction (RT-PCR) testing is the first choice for definitive diagnosis. However, the sensitivity of the SARS-CoV-2 RT-PCR which is the gold standard for diagnosis is estimated as 75%[18]. Furthermore, RT-PCR results may need several days and cannot be sufficient in places with high patient density[18]. Concerning radiologic diagnosis of COVID-19 is based on chest computed tomography (CT) with typical ground-glass opacities and patchy infiltrates in chest radiography, or both[10]. The main advantage of LUS is not only reducing the exposure to ionizing radiation but also reducing the risk of contamination and decrease the burden on the health system. Moreover, it enables monitoring (repetitive measurements)[4,9-11]. However, CT has disadvantages of ionizing radiation exposure, the need for extensive decontamination and is unobtainable in resource-limited situations. Owing to these facts, CT is not an optimal screening tool and not feasible in monitoring the patient's clinical situation[18]. Especially when we think of a special population such as pregnant women or pediatric patients, CT is not an attractive choice for the diagnosis of lung involvement. A low level of ionizing radiation exposure by chest imaging during pregnancy is considered relatively safe, but this can cause anxiety for many pregnant women and health care providers[10]. More than half of the pregnant women refused to have the chest CT in our center (unpublished data).

Imaging the lung and pleura by the US is efficient, cost-effective, and safe, and it is recognized as rapid, repeatable, and reliable[8]. LUS is convenient for bedside evaluation of patients and suitable for vulnerable populations such as pregnant women and children[11,19]. It is already well-known that LUS has the advantages of being a non-ionizer, rapid and easy to perform, and provides dynamic imaging. In addition, LUS has a value and an advantage of applicability to a variety of practice environments, when the other diagnostic tools are unavailable[18].

Obstetricians are already using the US and quite proficient in the use of it. During the pandemic, it was proposed that LUS may be performed by obstetricians and therefore, LUS examination can be a routine after a routine obstetric US examination [4]. This approach might have an impact on reducing the workload of radiologists and the need for chest CT, thereby minimizing the risk of transmission. Pregnant and non-pregnant women have previously been reported to be similar with regard to radiologic findings of COVID-19[10,20]. Performing LUS right after the fetal assessment until RT-PCR results are obtained, particularly in settings that have a centralized testing center, was found feasible for the prediction of the SARS-CoV-2 infection. This approach is successful in reducing the use of chest CT or X-rays for pregnant women.

TRIAGE WITH LUS

Despite the extensive use of LUS in clinical studies, the use of LUS in the triage of pregnant women during the COVID-19 pandemic is still scarce in the literature.

One of the main problems in the management of the population during the SARS-CoV-2 pandemic is to determine the asymptomatic carriers[21]. This issue becomes prominent in pregnant women due to the mixed symptoms that can naturally be interpreted as common complaints of pregnancy. In a recent study by Sutton *et al*[21], the asymptomatic carrier rate in the labor ward was found as 13.7%. Another milestone study from Vintzileos *et al*[22] showed that two-thirds of all pregnant women infected with SARS-CoV-2 were asymptomatic during admission to the labor ward unit. Those results have raised concerns about the high rate of asymptomatic carriers during intensely progressing pandemic.

In our clinic, patients with symptoms are isolated in the hospital until SARS-CoV-2 RT-PCR results are obtained. Asymptomatic pregnant women are initially triaged using LUS and their clinic management is adjusted according to the obtained LUS score. Asymptomatic patients with mild lung involvement were closely followed up until RT-PCR results with home isolation and further close monitoring with LUS is planned. Pregnant women with moderate or severe lung involvement in US receive medical treatment regardless of being symptomatic or asymptomatic. Possible false-negative cases, that are symptomatic with initial normal LUS findings are scheduled for a repeat US in 3 d and offered for Chest CT. This algorithm is schematized in Figure 1.

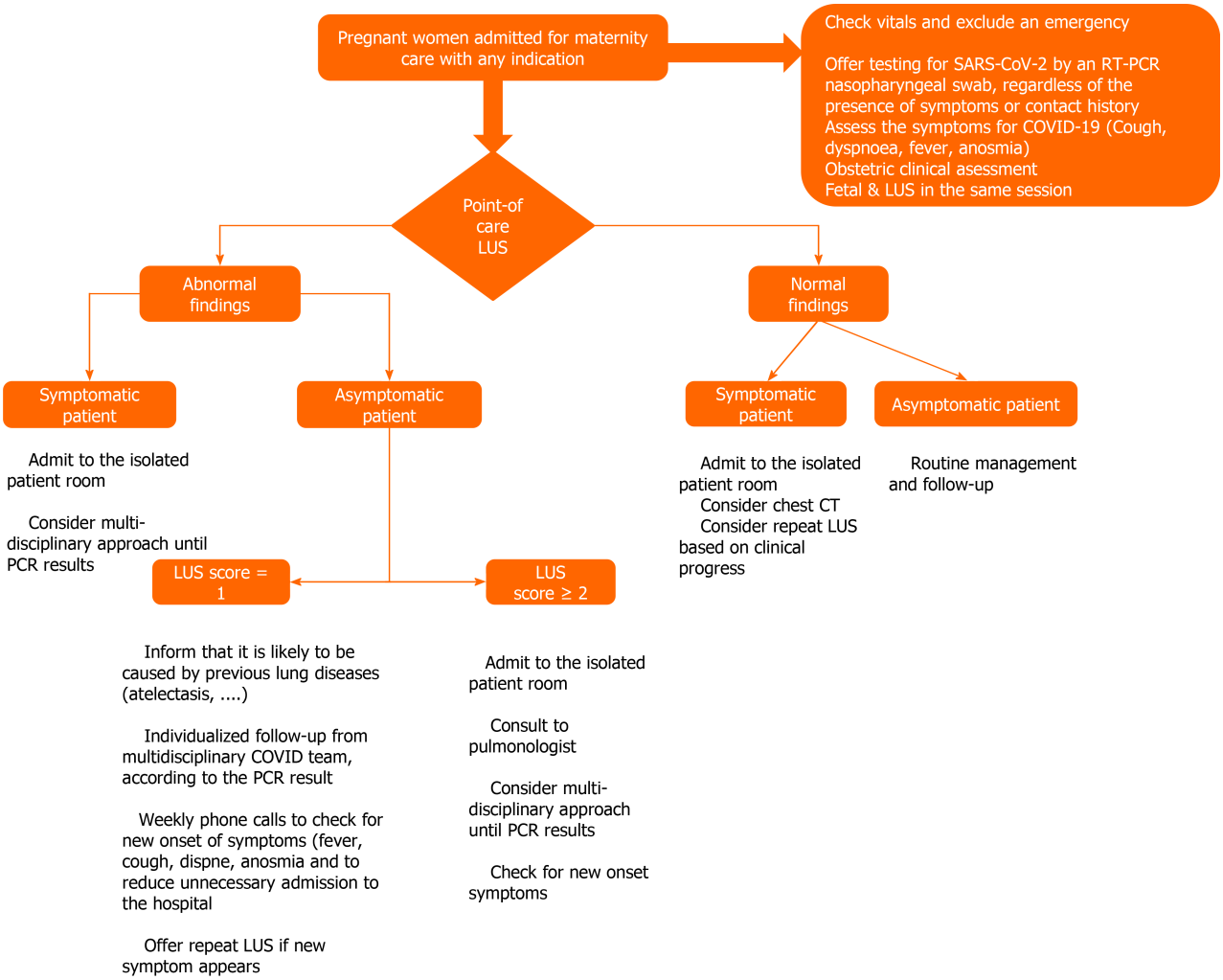

Figure 1 Main triage algorithm of pregnant women based on lung ultrasound. COVID: Coronavirus disease; COVID-19: Coronavirus disease 2019; CT: Computed tomography; LUS: Lung ultrasound; PCR: Polymerase chain reaction; SARS-CoV-2: Severe acute respiratory syndrome coronavirus 2.

Pregnant women are vulnerable population that possess medical and social burdens. In the COVID-19 pandemic, they require several encounters with the healthcare staff, and most of them are hospitalized for birth[23]. The common physiological changes of pregnancy may coincide with the symptoms of COVID-19 infection and undetected cases of COVID-19 were 4-9 cases to 1 detected case in a study in the labor ward[24]. The undetected infection has been thought to contribute to the transmission of the virus[25]. Due to the excess of undetected cases and transmission of infection from asymptomatic carriers, the need for universal screening of pregnant women is emphasized[21,22]. All pregnant women should be offered RT-PCR testing for SARS-CoV-2 infection regardless of the maternal symptoms on admission to the hospital according to the Royal College of Obstetricians & Gynecologists statement[26]. Our study investigating the universal testing strategy for SARS-CoV-2 infection with RT-PCR in pregnant women who were admitted to the hospital showed an overall and asymptomatic infection diagnosis rate of 7.77% and 4.05%, respectively[27]. The false positivity of LUS was due to previous benign lung diseases where the main maternal symptom status comes forward in the interpretation of LUS findings[27]. In our routine approach, LUS comes prior to the maternal symptomatology because mild COVID-19 symptoms can interfere with the natural pregnancy-related symptoms, moreover, we observed that LUS signs can alert the clinician before bothersome symptoms occur. In our algorithm for the interpretation of LUS findings that combines the lung imaging and the maternal symptomatology; a LUS score of 1 was accepted as a normal finding in asymptomatic pregnant women with aiming to reduce the false positivity of LUS imaging. LUS scores of 2 and 3 were adopted as abnormal regardless of the symptom status. In addition, using LUS in the triage of pregnant women was found more predictive in detecting the infection than the use of symptomatology solely with a positive predictive value and sensitivity of

82.3% and 60.9%, respectively[27].

MONITORING WITH LUS AND OTHER AREAS OF USE

In monitoring the clinical progress of pregnant women, LUS is a harmless choice and valuable in terms of deciding either delivery or upgrade the medical treatment[10]. LUS is a very practical alternative in the respiratory system propaedeutic as it allows for repetition of exams, can be portable and performed at the patient's bedside[15]. The recent study suggested the integration of LUS into the routine clinical management of COVID-19[28]. In addition, this recent study emphasized in the emergency department that LUS may correctly triage patients according to their degree of lung involvement[28]. Abnormal LUS findings were reported as relevant with early admission into emergency units or intensive care units[27]. It is reasonable to offer LUS for the triage and monitoring of the clinical progress of patients with leaving the indication of chest CT scan as reserved only for the more complex cases, such as unexpected deterioration in clinical progress and patients with previous lung diseases[28]. Moreover, the detection power for the presence of consolidations there was found in a good agreement between the chest CT and LUS[29]. The studies regarding LUS usage in pregnant women are summarized in Table 1[10,27,30-36].

Considering the patients who are receiving respiratory support is recommended that they should be monitored closely for clinical deterioration[37]. In this regard, serial LUS is suitable for efficient monitoring[37]. The decision to proceed with invasive mechanical ventilation and intubation can be a challenging choice and LUS might be an accurate indicator of the ideal moment of intubation[37]. In intubated patients, LUS could evaluate the pulmonary aeration loss and ventilation condition dynamically thus, enabling the prediction of the healing process[37]. In intensive care units, chest CT scan is risky for transporting critically unwell patients, and decontamination is a time-consuming process[37]. The use of portable chest radiographs is not suitable due to the poor correlation with clinical picture[37].

LIMITATIONS OF LUS

Despite the several advantages of LUS in the COVID-19 pandemic setting, the diagnostic accuracy of LUS may be affected by the patient's characteristics and co-morbidities including elevated body-mass index and pre-existing interstitial lung diseases[38,39]. The findings of preexisting interstitial inflammation, scarring, and pleural thickening can mimic the initial COVID-19 imaging. In addition, heart failure causing pulmonary edema or end-stage renal disease may lead to diagnostic confusion with the interstitial inflammation caused by COVID-19. Approximately 70% of the lung surface can be visualized with a systematic LUS examination, however, lesions located in the blind area of the US can be missed[31].

The studies investigating the use of LUS in the COVID-19 pandemic have included small sample sizes and much effort is needed to increase the quality of those studies to promote the LUS scanning in the triage of COVID-19[15]. The specific protocols for triage should be formed and the effects of the clinicians' experience and the inter-operator agreement should be further studied[40-42].

User-related limitations can be challenging in the management of the patient that depends on the LUS scores. It is postulated that less-experienced users are tended to label the mild abnormalities in a single lung field as compatible with COVID-19. The US settings of the LUS can affect the interpretation of LUS images such as undergained or overgained images may lead to false-negative or positive assessments[18].

CONCLUSION

LUS is promising in the management of pregnant women with COVID-19 with considering the advantages of being non-ionizer, dynamic, rapid, reliable, and reproducible. The use of LUS seems efficient in the triage and monitoring of pregnant women. LUS scanning can be combined with initial maternal symptom status in order to reduce the false positivity of LUS. Clinicians dealing with pregnant women may consider LUS as the first-line diagnostic tool in pregnant women during the SARS-CoV-2 pandemic.

Table 1 Studies reported the use of lung ultrasound in pregnant women with coronavirus disease 2019

Ref.	Country	Type of study	Cohort	Diagnosis	LUS technic	Conclusion
Buonsenso *et al*[30], 2020	Italy	Case report	4 pregnant women at 24, 38, 17, and 35 wk gestational age	LUS was carried out before the positive RT-PCR result. Nasopharyngeal swab RT-PCR confirmation	14 regions evaluation with the convex probe.	LUS was correlated with CT findings, this tool should be considered in clinical deterioration to check the lung status for COVID-19 pneumonia and LUS might be preferred to chest X-ray in pregnant women
Deng *et al* [31], 2021	China	Retrospective study	27 of pregnant women at the third trimester, 8 of them at the second trimester, and 4 of them at the first trimester	29 of them with pharynx RT-PCR testing and 10 with epidemiologic history, symptoms, and imaging results	12 zones: 2 anterior zones, 2 lateral zones, and 2 posterior zones *per* side. Each zone was scored 0 to 3 and total LUS scores were used in the clinical assessment of patients	Quantitative LUS can be considered a reliable follow-up tool for dynamic lung monitoring in pregnant women with COVID-19 and can reduce the use of chest CT
Gil-Rodrigo *et al*[32], 2021	Spain	Letter to the editor	4 women at gestational weeks 6, 9, 19 and 25, 2 of them confirmed as COVID-19	Symptoms and LUS were used as initial assessment and nasopharyngeal swab RTPCR was used for confirmation	With convex transducer, 8 posterior lung areas	With regard to potential disease transmission during a pandemic, LUS in pregnant women enables safe diagnosis and early treatment. One of the limitations is the absence of standardized training, the learning curve is relatively
Inchingolo *et al*[33], 2020	Italy	Case report	1 pregnant woman at 23 wk gestational age	Oropharyngeal swab RT-PCR	14 regions with Convex wireless transducer (3.5 MHz)	Point-of-care LUS examination could play a key role in the assessment of pregnant women with suspected COVID-19
Kalafat E *et al* [34], 2020	Turkey	Case report	32-yr-old woman at 35 + 3 wk gestational age	Symptoms and lung ultrasound findings first and confirmed by nasopharyngeal RT-PCR after	Thick and bilateral B-lines in the basal posterior lungs area (during the first assessment), diffuse B-lines (2 d later)	Report of positive lung ultrasound findings consistent with COVID-19 in a pregnant woman with an initially negative RT-PCR result
Porpora *et al* [35], 2021	Italy	Prospective observational study	30 pregnant women at 36 wk of median gestational age (range between 28-38 wk)	Nasopharyngeal swab RT-PCR	Linear or convex probes, the LUS investigation was carried out with the 12-zone method, both in the supine and lateral positions	LUS is proven to be safe, reliable, sensitive, easily repeatable, and could be a guide to define the most appropriate strategy for improving clinical and pregnancy outcomes
Yassa *et al* [10], 2021	Turkey	Case series	8 Pregnant women (9-38 wk) who underwent LUS examinations after obstetric US examinations	Symptoms and LUS first and confirmed by nasopharyngeal RT-PCR testing later	Fourteen areas (3 posterior, 2 lateral, and 2 anterior) were scanned *per* patient for 10 seconds along the indicated lines	After an obstetric US assessment, the routine use of LUS can substantially influence the clinical treatment of pregnant women with COVID-19
Yassa *et al* [27], 2020	Turkey	Prospective Cohort	296 pregnant women (23 with a positive result for COVID-19) at 5 to 42 wk gestational ages (mean = 35.18 wk)	LUS first and confirmed by nasopharyngeal RT-PCR later	12 areas, with the posterior ones in the posterior axillary line	Using lung ultrasound was found more predictive in detecting the infection than the use of symptomatology solely
Youssef *et al* [36], 2020	Italy	Case report	1 pregnant woman, 33 yr old at 26 wk of gestational age	LUS findings were former, positive nasopharyngeal swab RTPCR confirmation later	6 regions in each hemithorax (2 anterior, 2 lateral, and 2 posterior). Linear or convex probes	We believe that extensive training of physicians may be considerably helpful in terms of the ongoing pandemic of COVID-19

COVID-19: Coronavirus disease 2019; CT: Computed tomography; LUS: Lung ultrasound; RT-PCR: Reverse transcription polymerase chain reaction; US: Ultrasound.

REFERENCES

1 **Gargani L**, Volpicelli G. How I do it: lung ultrasound. *Cardiovasc Ultrasound* 2014; **12**: 25 [PMID: 24993976 DOI: 10.1186/1476-7120-12-25]

2 **Francisco Neto MJ**, Rahal Junior A, Vieira FAC, Silva PSDd, Funari MBdG. Advances in lung ultrasound. *Einstein (Sao Paulo)* 2016; **14**: 443-448 [DOI: 10.1590/S1679-45082016MD3557]

3 **Kuzan TY**, Murzoğlu Altıntoprak K, Çiftçi HÖ, Kuzan BN, Yassa M, Tuğ N, Çimşit NÇ. Clinical and radiologic characteristics of symptomatic pregnant women with COVID-19 pneumonia. *J Turk Ger Gynecol Assoc* 2021 [PMID: 33631874 DOI: 10.4274/jtgga.galenos.2021.2020.0215]

4 **Moro F**, Buonsenso D, Moruzzi MC, Inchingolo R, Smargiassi A, Demi L, Larici AR, Scambia G, Lanzone A, Testa AC. How to perform lung ultrasound in pregnant women with suspected COVID-19. *Ultrasound Obstet Gynecol* 2020; **55**: 593-598 [PMID: 32207208 DOI: 10.1002/uog.22028]

5 **Yassa M**, Mutlu MA, Kalafat E, Birol P, Yirmibeş C, Tekin AB, Sandal K, Ayanoğlu E, Yassa M, Kılınç C, Tug N. How to perform and interpret the lung ultrasound by the obstetricians in pregnant women during the SARS-CoV-2 pandemic. *Turk J Obstet Gynecol* 2020; **17**: 225-232 [PMID: 33072428 DOI: 10.4274/tjod.galenos.2020.93902]

6 **Soldati G**, Smargiassi A, Inchingolo R, Buonsenso D, Perrone T, Briganti DF, Perlini S, Torri E, Mariani A, Mossolani EE, Tursi F, Mento F, Demi L. Proposal for International Standardization of the Use of Lung Ultrasound for Patients With COVID-19: A Simple, Quantitative, Reproducible Method. *J Ultrasound Med* 2020; **39**: 1413-1419 [PMID: 32227492 DOI: 10.1002/jum.15285]

7 **Soldati G**, Demi M, Smargiassi A, Inchingolo R, Demi L. The role of ultrasound lung artifacts in the diagnosis of respiratory diseases. *Expert Rev Respir Med* 2019; **13**: 163-172 [PMID: 30616416 DOI: 10.1080/17476348.2019.1565997]

8 **Mayo PH**, Copetti R, Feller-Kopman D, Mathis G, Maury E, Mongodi S, Mojoli F, Volpicelli G, Zanobetti M. Thoracic ultrasonography: a narrative review. *Intensive Care Med* 2019; **45**: 1200-1211 [PMID: 31418060 DOI: 10.1007/s00134-019-05725-8]

9 **Soldati G**, Smargiassi A, Inchingolo R, Buonsenso D, Perrone T, Briganti DF, Perlini S, Torri E, Mariani A, Mossolani EE, Tursi F, Mento F, Demi L. Is There a Role for Lung Ultrasound During the COVID-19 Pandemic? *J Ultrasound Med* 2020; **39**: 1459-1462 [PMID: 32198775 DOI: 10.1002/jum.15284]

10 **Yassa M**, Birol P, Mutlu AM, Tekin AB, Sandal K, Tug N. Lung Ultrasound Can Influence the Clinical Treatment of Pregnant Women With COVID-19. *J Ultrasound Med* 2021; **40**: 191-203 [PMID: 32478445 DOI: 10.1002/jum.15367]

11 **Inchingolo R**, Smargiassi A, Mormile F, Marra R, De Carolis S, Lanzone A, Valente S, Corbo GM. Look at the lung: can chest ultrasonography be useful in pregnancy? *Multidiscip Respir Med* 2014; **9**: 32 [PMID: 24936303 DOI: 10.1186/2049-6958-9-32]

12 **Sultan LR**, Sehgal CM. A Review of Early Experience in Lung Ultrasound in the Diagnosis and Management of COVID-19. *Ultrasound Med Biol* 2020; **46**: 2530-2545 [PMID: 32591166 DOI: 10.1016/j.ultrasmedbio.2020.05.012]

13 **Kulkarni S**, Down B, Jha S. Point-of-care lung ultrasound in intensive care during the COVID-19 pandemic. *Clin Radiol* 2020; **75**: 710.e1-710. e4 [PMID: 32405081 DOI: 10.1016/j.crad.2020.05.001]

14 **Buonsenso D**, Pata D, Chiaretti A. COVID-19 outbreak: less stethoscope, more ultrasound. *Lancet Respir Med* 2020; **8**: e27 [PMID: 32203708 DOI: 10.1016/S2213-2600(20)30120-X]

15 **Peixoto AO**, Costa RM, Uzun R. , Fraga AMA, Ribeiro JD, Marson FAL. Applicability of lung ultrasound in COVID-19 diagnosis and evaluation of the disease progression: A systematic review. *Pulmonology* 2021; Online ahead of print [PMID: 33931378 DOI: 10.1016/j.pulmoe.2021.02.004]

16 **Tan G**, Lian X, Zhu Z, Wang Z, Huang F, Zhang Y, Zhao Y, He S, Wang X, Shen H, Lyu G. Use of Lung Ultrasound to Differentiate Coronavirus Disease 2019 (COVID-19) Pneumonia From Community-Acquired Pneumonia. *Ultrasound Med Biol* 2020; **46**: 2651-2658 [PMID: 32622684 DOI: 10.1016/j.ultrasmedbio.2020.05.006]

17 **Volpicelli G**, Gargani L. Sonographic signs and patterns of COVID-19 pneumonia. *Ultrasound J* 2020; **12**: 22 [PMID: 32318891 DOI: 10.1186/s13089-020-00171-w]

18 **Brenner DS**, Liu GY, Omron R, Tang O, Garibaldi BT, Fong TC. Diagnostic accuracy of lung ultrasound for SARS-CoV-2: a retrospective cohort study. *Ultrasound J* 2021; **13**: 12 [PMID: 33644829 DOI: 10.1186/s13089-021-00217-7]

19 **Denina M**, Scolfaro C, Silvestro E, Pruccoli G, Mignone F, Zoppo M, Ramenghi U, Garazzino S. Lung Ultrasound in Children With COVID-19. *Pediatrics* 2020; **146** [PMID: 32317309 DOI: 10.1542/peds.2020-1157]

20 **Wu X**, Sun R, Chen J, Xie Y, Zhang S, Wang X. Radiological findings and clinical characteristics of pregnant women with COVID-19 pneumonia. *Int J Gynaecol Obstet* 2020; **150**: 58-63 [PMID: 32270479 DOI: 10.1002/ijgo.13165]

21 **Sutton D**, Fuchs K, D'Alton M, Goffman D. Universal Screening for SARS-CoV-2 in Women Admitted for Delivery. *N Engl J Med* 2020; **382**: 2163-2164 [PMID: 32283004 DOI: 10.1056/NEJMc2009316]

22 **Vintzileos WS**, Muscat J, Hoffmann E, John NS, Vertichio R, Vintzileos AM, Vo D. Screening all pregnant women admitted to labor and delivery for the virus responsible for coronavirus disease 2019. *Am J Obstet Gynecol* 2020; **223**: 284-286 [PMID: 32348743 DOI: 10.1016/j.ajog.2020.04.024]

23 **Khalil A**, Hill R, Ladhani S, Pattisson K, O'Brien P. Severe acute respiratory syndrome coronavirus 2 in pregnancy: symptomatic pregnant women are only the tip of the iceberg. *Am J Obstet Gynecol* 2020; **223**: 296-297 [PMID: 32387327 DOI: 10.1016/j.ajog.2020.05.005]

24 **Gagliardi L**, Danieli R, Suriano G, Vaccaro A, Tripodi G, Rusconi F, Ramenghi LA. Universal severe acute respiratory syndrome coronavirus 2 testing of pregnant women admitted for delivery in 2 Italian regions. *Am J Obstet Gynecol* 2020; **223**: 291-292 [PMID: 32407787 DOI: 10.1016/j.ajog.2020.05.017]

25 **Li R**, Pei S, Chen B, Song Y, Zhang T, Yang W, Shaman J. Substantial undocumented infection

facilitates the rapid dissemination of novel coronavirus (SARS-CoV-2). *Science* 2020; **368**: 489-493 [PMID: 32179701 DOI: 10.1126/science.abb3221]

26 **Royal College of Obstetrics and Gynaecology**. Principles for the Testing and Triage of Women Seeking Maternity Care in Hospital Settings, During the COVID-19 Pandemic. 2nd ed. [cited 25 January 2021]. Available from: https://www.rcog.org.uk/globalassets/ documents/guidelines/2020-08-10-principles-for-the-testingand-triage-of-women-seeking-maternity-care-in-hospitalsettings-during-the-covid-19-pandemic.pdf

27 **Yassa M**, Yirmibes C, Cavusoglu G, Eksi H, Dogu C, Usta C, Mutlu M, Birol P, Gulumser C, Tug N. Outcomes of universal SARS-CoV-2 testing program in pregnant women admitted to hospital and the adjuvant role of lung ultrasound in screening: a prospective cohort study. *J Matern Fetal Neonatal Med* 2020; **33**: 3820-3826 [PMID: 32691641 DOI: 10.1080/14767058.2020.1798398]

28 **Secco G**, Delorenzo M, Salinaro F, Zattera C, Barcella B, Resta F, Sabena A, Vezzoni G, Bonzano M, Briganti F, Cappa G, Zugnoni F, Demitry L, Mojoli F, Baldanti F, Bruno R, Perlini S; GERICO (Gruppo Esteso RIcerca COronarovirus) Lung US Pavia Study Group. Lung ultrasound presentation of COVID-19 patients: phenotypes and correlations. *Intern Emerg Med* 2021 [PMID: 33646508 DOI: 10.1007/s11739-020-02620-9]

29 **Dargent A**, Chatelain E, Kreitmann L, Quenot JP, Cour M, Argaud L; COVID-LUS study group. Lung ultrasound score to monitor COVID-19 pneumonia progression in patients with ARDS. *PLoS One* 2020; **15**: e0236312 [PMID: 32692769 DOI: 10.1371/journal.pone.0236312]

30 **Buonsenso D**, Raffaelli F, Tamburrini E, Biasucci DG, Salvi S, Smargiassi A, Inchingolo R, Scambia G, Lanzone A, Testa AC, Moro F. Clinical role of lung ultrasound for diagnosis and monitoring of COVID-19 pneumonia in pregnant women. *Ultrasound Obstet Gynecol* 2020; **56**: 106-109 [PMID: 32337795 DOI: 10.1002/uog.22055]

31 **Deng Q**, Cao S, Wang H, Zhang Y, Chen L, Yang Z, Peng Z, Zhou Q. Application of quantitative lung ultrasound instead of CT for monitoring COVID-19 pneumonia in pregnant women: a single-center retrospective study. *BMC Pregnancy Childbirth* 2021; **21**: 259 [PMID: 33771120 DOI: 10.1186/s12884-021-03728-2]

32 **Gil-Rodrigo A**, Llorens-Soriano P, Ramos-Rincón JM. Ultrasound in Pregnant Women With Suspected COVID-19 Infection. *J Ultrasound Med* 2021; **40**: 645-647 [PMID: 32776592 DOI: 10.1002/jum.15419]

33 **Inchingolo R**, Smargiassi A, Moro F, Buonsenso D, Salvi S, Del Giacomo P, Scoppettuolo G, Demi L, Soldati G, Testa AC. The diagnosis of pneumonia in a pregnant woman with coronavirus disease 2019 using maternal lung ultrasound. *Am J Obstet Gynecol* 2020; **223**: 9-11 [PMID: 32360111 DOI: 10.1016/j.ajog.2020.04.020]

34 **Kalafat E**, Yaprak E, Cinar G, Varli B, Ozisik S, Uzun C, Azap A, Koc A. Lung ultrasound and computed tomographic findings in pregnant woman with COVID-19. *Ultrasound Obstet Gynecol* 2020; **55**: 835-837 [PMID: 32249471 DOI: 10.1002/uog.22034]

35 **Porpora MG**, Merlino L, Masciullo L, D'Alisa R, Brandolino G, Galli C, De Luca C, Pecorini F, Fonsi GB, Mingoli A, Franchi C, Oliva A, Manganaro L, Mastroianni CM, Piccioni MG. Does Lung Ultrasound Have a Role in the Clinical Management of Pregnant Women with SARS COV2 Infection? *Int J Environ Res Public Health* 2021; **18** [PMID: 33803223 DOI: 10.3390/ijerph18052762]

36 **Youssef A**, Serra C, Pilu G. Lung ultrasound in the coronavirus disease 2019 pandemic: a practical guide for obstetricians and gynecologists. *Am J Obstet Gynecol* 2020; **223**: 128-131 [PMID: 32437667 DOI: 10.1016/j.ajog.2020.05.014]

37 **Smith MJ**, Hayward SA, Innes SM, Miller ASC. Point-of-care lung ultrasound in patients with COVID-19 - a narrative review. *Anaesthesia* 2020; **75**: 1096-1104 [PMID: 32275766 DOI: 10.1111/anae.15082]

38 **Brainin P**, Claggett B, Lewis EF, Dwyer KH, Merz AA, Silverman MB, Swamy V, Biering-Sørensen T, Rivero J, Cheng S, McMurray JJV, Solomon SD, Platz E. Body mass index and B-lines on lung ultrasonography in chronic and acute heart failure. *ESC Heart Fail* 2020; **7**: 1201-1209 [PMID: 32077268 DOI: 10.1002/ehf2.12640]

39 **Maw AM**, Hassanin A, Ho PM, McInnes MDF, Moss A, Juarez-Colunga E, Soni NJ, Miglioranza MH, Platz E, DeSanto K, Sertich AP, Salame G, Daugherty SL. Diagnostic Accuracy of Point-of-Care Lung Ultrasonography and Chest Radiography in Adults With Symptoms Suggestive of Acute Decompensated Heart Failure: A Systematic Review and Meta-analysis. *JAMA Netw Open* 2019; **2**: e190703 [PMID: 30874784 DOI: 10.1001/jamanetworkopen.2019.0703]

40 **Fox S**, Dugar S. Point-of-care ultrasound and COVID-19. *Cleve Clin J Med* 2020 [PMID: 32409431 DOI: 10.3949/ccjm.87a.ccc019]

41 **Piliego C**, Strumia A, Stone MB, Pascarella G. The Ultrasound-Guided Triage: A New Tool for Prehospital Management of COVID-19 Pandemic. *Anesth Analg* 2020; **131**: e93-e94 [PMID: 32345853 DOI: 10.1213/ANE.0000000000004920]

42 **Dudea SM**. Ultrasonography and SARS-CoV 2 infection: a review of what we know and do not yet know. *Med Ultrason* 2020; **22**: 129-132 [PMID: 32399522 DOI: 10.11152/mu-2612]

Artificial Intelligence in Medical Imaging

Submit a Manuscript: https://www.f6publishing.com

Artif Intell Med Imaging 2021 June 28; 2(3): 64-72

DOI: 10.35711/aimi.v2.i3.64

ISSN 2644-3260 (online)

MINIREVIEWS

Application of radiomics in hepatocellular carcinoma: A review

Zhi-Cheng Jin, Bin-Yan Zhong

ORCID number: Zhi-Cheng Jin 0000-0002-6114-154X; Bin-Yan Zhong 0000-0001-9716-1211.

Author contributions: Jin ZC and Zhong BY contributed to study design, review of literature, interpretation of data, and drafting and revision of the manuscript.

Conflict-of-interest statement: The authors declare that the research was conducted in the absence of any commercial or financial relationships that could be construed as a potential conflict of interest.

Manuscript source: Invited manuscript

Specialty type: Oncology

Country/Territory of origin: China

Zhi-Cheng Jin, Center of Interventional Radiology and Vascular Surgery, Department of Radiology, Zhongda Hospital, Medical School, Southeast University, Nanjing 210009, Jiangsu Province, China

Bin-Yan Zhong, Department of Interventional Radiology, The First Affiliated Hospital of Soochow University, Suzhou 215006, Jiangsu Province, China

Corresponding author: Bin-Yan Zhong, MD, PhD, Doctor, Department of Interventional Radiology, The First Affiliated Hospital of Soochow University, No. 188 Shizi Street, Suzhou 215006, Jiangsu Province, China. byzhongir@sina.com

Abstract

Hepatocellular carcinoma (HCC) is the most common form of primary liver cancer with low 5-year survival rate. The high molecular heterogeneity in HCC poses huge challenges for clinical practice or trial design and has become a major barrier to improving the management of HCC. However, current clinical practice based on single bioptic or archived tumor tissue has been deficient in identifying useful biomarkers. The concept of radiomics was first proposed in 2012 and is different from the traditional imaging analysis based on the qualitative or semi-quantitative analysis by radiologists. Radiomics refers to high-throughput extraction of large amounts number of high-dimensional quantitative features from medical images through machine learning or deep learning algorithms. Using the radiomics method could quantify tumoral phenotypes and heterogeneity, which may provide benefits in clinical decision-making at a lower cost. Here, we review the workflow and application of radiomics in HCC.

Key Words: Hepatocellular carcinoma; Radiomics; Machine learning; Deep learning; Radiogenomics

Core Tip: The high molecular heterogeneity in hepatocellular carcinoma poses huge challenges for clinical practice or trial design and has become a major barrier to improving the management of hepatocellular carcinoma. Radiomics could quantify tumoral phenotypes and heterogeneity, which may provide benefits in clinical decision-making at a lower cost. Here, we review the workflow and application of radiomics in hepatocellular carcinoma.

Peer-review report's scientific quality classification
Grade A (Excellent): 0
Grade B (Very good): 0
Grade C (Good): C
Grade D (Fair): 0
Grade E (Poor): 0

Received: May 13, 2021
Peer-review started: May 13, 2021
First decision: June 2, 2021
Revised: June 19, 2021
Accepted: June 30, 2021
Article in press: June 30, 2021
Published online: June 28, 2021

P-Reviewer: Calabro F
S-Editor: Liu M
L-Editor: Filipodia
P-Editor: Xing YX

Citation: Jin ZC, Zhong BY. Application of radiomics in hepatocellular carcinoma: A review. *Artif Intell Med Imaging* 2021; 2(3): 64-72
URL: https://www.wjgnet.com/2644-3260/full/v2/i3/64.htm
DOI: https://dx.doi.org/10.35711/aimi.v2.i3.64

INTRODUCTION

Liver cancer is one of the most common malignant tumors worldwide. There are approximately 906000 new cases and 830000 deaths every year, ranking as the sixth most commonly diagnosed cancer and the third mortality[1]. Hepatocellular carcinoma (HCC) comprises 75%-85% of cases of primary liver cancer. There is high molecular heterogeneity in HCC at three levels, including the heterogeneity between tumor nodules within the same individual (intertumoral heterogeneity), between different regions of the same tumor nodule (intratumor heterogeneity), and between patients (interpatient heterogeneity)[2]. HCC has one of the fewest somatic mutations in solid tumors that can be targeted by molecular therapies and of which treatment response could not be predicted by mutations in clinical practice[3]. These characteristics of HCC pose huge challenges for clinical practice or trial design and have become a major barrier to improving the management of HCC[4,5]. However, current clinical practice based on single bioptic or archived tumor tissue has been deficient in identifying useful biomarkers[5].

Radiomics was first proposed in 2012 and is different from the traditional imaging analysis based on the qualitative or semi-quantitative analysis by radiologists[6]. This method refers to high-throughput extraction of large amounts of high-dimensional quantitative features from medical images through machine learning (ML) or deep learning (DL) algorithms[7,8]. These features that have been transformed into minable data could be used for diagnosis, treatment evaluation, and prognosis prediction[9]. Using the radiomics method could quantify tumoral phenotypes and heterogeneity, which may provide benefits in clinical decision-making at a lower cost[10,11]. Here, we review the workflow and application of radiomics in HCC.

WORKFLOW OF RADIOMICS

The workflow of radiomics mainly includes: image data acquisition and preprocessing, the volume of interest (VOI) segmentation, feature extraction, model establishment, and performance validation (Figure 1)[9].

Data acquisition

Although radiomics was first and widely utilized in computed tomography (CT) and magnetic resonance imaging (MRI) images, there were more and more studies using ultrasound (US) as well as positron emission tomography images. Most studies were conducted based on retrospective image data sets, even different hospitals and different scanning equipment. The standardized imaging protocols could reduce the unnecessary confounding variability, or it will affect the quality and stability of the extracted imaging features. A previous study found that the feature variability caused by different CT scanners was even comparable to the feature variability found in the tumor[12]. The disclosed imaging protocols were suggested to increase the reproducibility and comparability in future radiomics studies[9].

Segmentation

The three-dimensional VOI segmentation that captures the tumor comprehensive panorama could be delineated by using manual, semi-automatic, and automatic segmentation methods. However, the variability in the segmentation process inevitably introduces bias. Meanwhile, the partial volume effect makes the segmentation challenge that could lead to the blurring of the edge and morphological variation of the lesion. Multiple segmentation is an effective method that can limit bias and help to select robust features, including the evaluation by multiple clinicians and the combination of different segmentation algorithms. However, the commonly used segmentation method in radiomics is manual segmentation and relies on an experienced clinician, which is quite boring and time-consuming. Several semi-automatic or automatic segmentation methods have been reported[13,14]. These

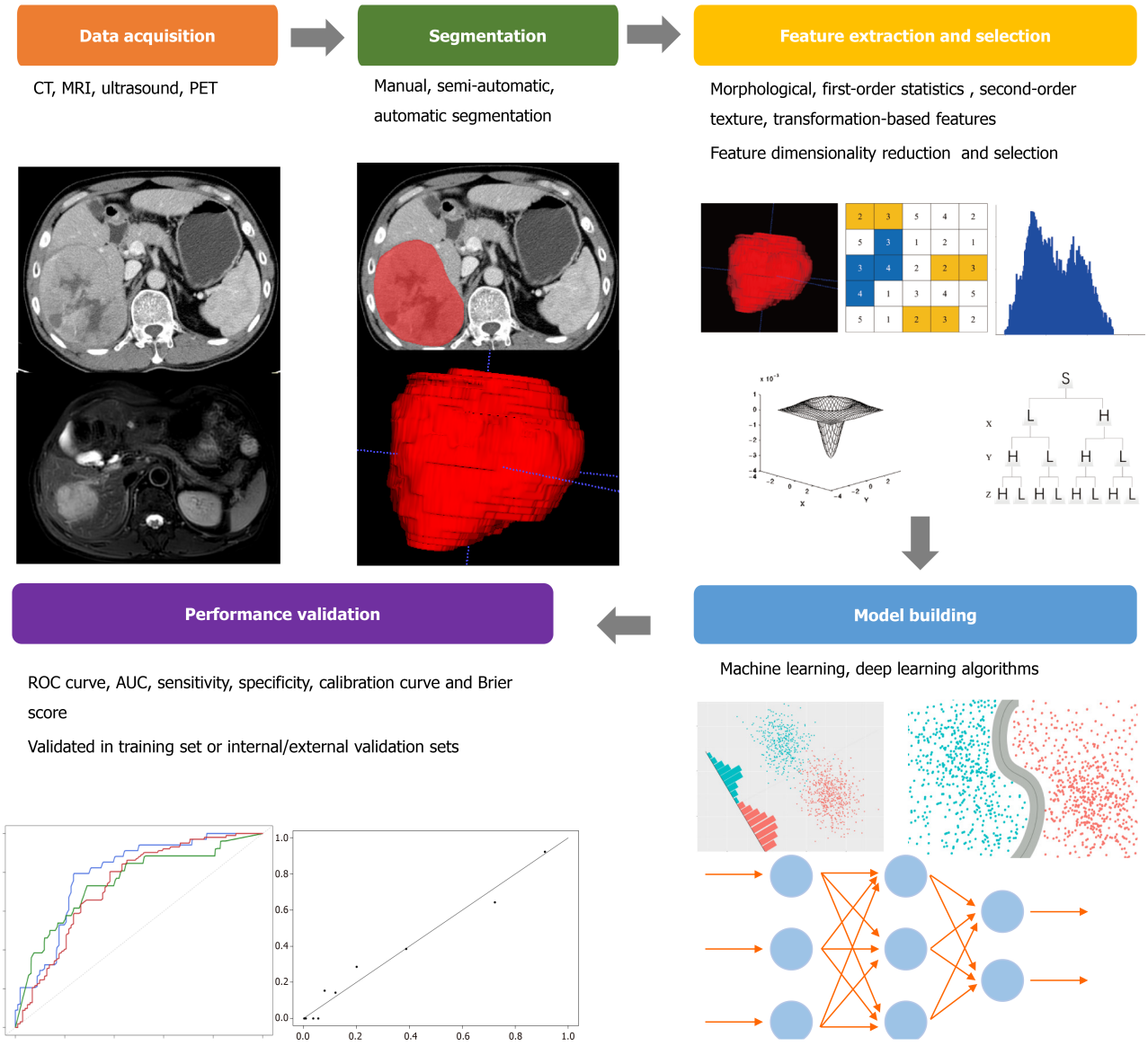

Figure 1 The workflow of radiomics. AUC: Area under the curve; CT: Computed tomography; MRI: Magnetic resonance imaging; PET: Positron emission tomography; ROC: Operating curve.

methods could minimize labor costs and improve the repeatability and reliability of studies but are not widely recognized and applied.

Feature extraction and selection

The high-throughput extraction of quantitative features from VOI is the key process in radiomics analysis after appropriate image preprocessing. The imaging features that are empirically defined by radiologists are named semantic features. These features cannot be described by specific mathematical expressions nor can they be specifically extracted from images, but they are still meaningful in imaging interpretation and clinical application. These non-semantic features quantitatively described by mathematical expressions can usually be divided into four categories: morphological features, first-order statistics features, second-order texture features, and transformation-based features. Morphological features describe the three-dimensional and two- dimensional size and shape of VOI, such as diameter, perimeter, sphericity, and flatness. First-order statistics features (also called histogram features) evaluate the gray-level frequency distribution in VOI, including maximum, median, minimum, and entropy, while second-order texture features are often derived from the gray-level matrix and describe the statistical relationship between voxel gray levels, including gray-level co-occurrence matrix and gray level run length matrix. The voxel gray-level patterns in different spatial frequencies are analyzed by transformation-based features, including Fourier, Gabor, and wavelet features.

According to the number of filters, feature categories, and other parameters, the number of features extracted from the images can be infinite. The inclusion of all relevant features in a predictive model inevitably leads to overfitting, which negatively impacts the efficacy of its prediction performance. It is necessary to introduce a feature selection method to eliminate unsuitable features, that is, feature dimensionality reduction methods (such as principal component analysis or clustering). By reducing redundant and interference items by dimensionality reduction, the features for further analysis contain useful and repeatable information to a large extent.

Model building and performance validation

The prediction model composed of selected features was constructed by an ML algorithm, including support vector machine, random forest, linear discriminant analysis, and so on. The specific method was chosen according to the preference and experience of the researchers. However, different modeling methods have been proved to affect the prediction performance of imaging models and have inherent limitations, such as the independence assumption in logistic regression, feature discretization in Bayesian networks, or network structure dependence in DL. Therefore, a variety of ways could be considered to build the model in the study.

The predictive performance evaluation of the model requires an internal or external validation set to determine whether the model has good generalization performance or only predictability for the specific samples analyzed. This process is often measured by the receiver operating characteristic curve with area under the curve (AUC), sensitivity, and specificity. In addition, the consistency between the observed results and the model prediction was also evaluated necessarily, which can be evaluated by the calibration curve and Brier score. An effective model shows consistency in both training and validation sets. The models validated by an independent external set are more reliable than those validated by an internal set, and of course, the models that could be prospectively verified are more persuasive.

THE APPLICATION OF RADIOMICS IN HCC

Diagnosis

Imaging is a crucial part of the HCC diagnosis. Multiphasic contrast-enhanced CT or contrast-enhanced MRI should be used first with high sensitivity recommended by the European Association for the Study of the Liver[15]. Li *et al*[16] extracted the texture features from the SPAIR T2WI sequence in MRI and used four different classifiers to identify single intrahepatic lesions (hepatic hemangioma, hepatic metastases, and HCC). The error rates were 11.7% (hepatic hemangioma *vs* hepatic metastases), 9.6% (hepatic metastases *vs* HCC), and 9.7% (hepatic hemangioma *vs* HCC). The combination of quantitative apparent diffusion coefficient histogram parameters and the Liver Imaging Reporting And Data System could distinguish HCC from other subtypes of primary liver cancer, such as intrahepatic cholangiocarcinoma and mixed HCC-intrahepatic cholangiocarcinoma[17]. A total of 63 patients confirmed by pathology were included, and it was found that the model combined with gender, Liver Imaging Reporting And Data System, and the fifth percentile apparent diffusion coefficient could achieve a good prediction efficiency. The AUCs could reach 0.90/0.89 with the accuracy of 81.5%/80.0%, the sensitivity of 79.3%/86.2%, and the specificity of 88.9%/77.8% for two independent observers. Huang *et al*[18] managed to distinguish dual phenotypic HCC by different classifiers based on Gd-EOB-DTPA-enhanced MRI and showed good predictive performance.

For the new HCC nodules in patients with a liver cirrhosis background, radiomics features extracted from multiphasic contrast-enhanced CT combined with the ML algorithm could bring benefits. Mokrane *et al*[19] retrospectively included 178 patients from 27 centers and divided them into a training set (142 patients) and validation set (36 patients). All the patients had nodules that were classified as indeterminate liver nodules by the European Association for the Study of the Liver guidelines, and the histological classification was finally confirmed by liver biopsy. A total of 13920 quantitative radiomics features were extracted from the plain, arterial, venous, and dual-phase (delta) phases. Three supervised ML classification algorithms: K nearest neighbor, support vector machine, and random forest algorithm were used to establish the models. A single feature was finally obtained, which represented the characteristics of changes in nodule phenotype between arterial and portal venous phases (corresponds to the "washout" pattern during the contrast agent clearance). Finally,

the radiomics signature used reached an AUC value of 0.66 with a sensitivity of 0.70 and specificity of 0.59 in the external validation set.

US is one of the important methods in the diagnostic algorithm and recall policy by the European Association for the Study of the Liver guidelines[15]. However, US images are more heterogeneous because of the images acquired by different clinicians with multiple examination parameters. There was a study that reported that the features extracted from US images could be classified by using neural network classifiers to distinguish focal liver lesions, including typical and atypical cysts, hepatic hemangiomas, liver metastases, and HCC lesions, with an accuracy of up to 95%[20]. A multitask DL algorithm was constructed that detects and characterizes focal liver lesions in a public dataset[21]. The model simultaneously yielded AUCs of 0.935 for lesion detection and 0.916 for focal liver lesions characterization (benign *vs* malignant).

Radiomics could effectively diagnose and distinguish the HCC lesion from the different intrahepatic lesions, new nodules, and even the subtypes of primary liver cancer. Although the above studies are based on different imaging modalities and ML/DL methods, this method is expected to further assist doctors in clinical diagnosis and decision-making in the future.

Treatment evaluation

Surgical resection is the first choice for HCC patients with good performance status and liver function reserve. But the postoperative 5-year recurrence rate could be as high as 70%. To solve this problem, a multicenter retrospective study was carried out from three independent centers. The study included 295 early-stage HCC patients within Milan criteria who have received preoperative contrast-enhanced CT examination. Recurrence-free survival was selected as the primary endpoint of this study. Based on 177 patients from one center (training set), two prediction models have been constructed that incorporated preoperative variables or postoperative variables. The results showed that the prediction efficiency of the two radiomics-based models was higher than that of previous clinical models and staging systems and can well stratify patients with a low, moderate, and high risk of recurrence.

The application of radiomics in predicting postoperative recurrence has also been verified in other studies. In addition, some studies have found that the radiomics model based on preoperative MRI images can better predict the 5-year survival of patients after hepatectomy. Cai *et al*[22] retrospectively included 112 patients who underwent hepatectomy to predict postoperative liver failure by a radiomics-based nomogram. The AUC value of the training set was 0.822 (95% confidence interval: 0.753-0.917), and the AUC value of the validation set was 0.762 (95% confidence interval: 0.576-0.948). When it was compared with MELD, Child-Pugh, and ALBI score, the radiomics model showed a significant advantage. The researchers conducted a prospective validation analysis of 13 patients who underwent hepatectomy with an AUC of 0.833 (95% confidence interval: 0.591-1.000). Decision curve analysis showed that the model could bring clinical benefits. Radiomic features could identify the tumor invasion and predict recurrence after liver transplantation[23].

Ablation is recommended for HCC patients with Barcelona Clinic Liver Cancer 0 or A stage who are not suitable for surgery. Radiomic features extracted from perioperative CT images could predict early recurrence after curative ablation[24,25]. Among them, the features based on portal vein phase CT images performed best in the validation set. When the clinicopathological factors were added to the model, the portal vein phase-based combined model showed good prediction performance in the training/validation set and significantly better than that of the simple clinical model. Microwave ablation was performed in pigs under CT guidance for improving the visualization of post ablational coagulation necrosis in a proof of concept study[26]. The results showed that radiomic profiles of the fully necrotic areas seemed to be different from those areas with vital tissue. The subregion radiomics analysis could identify these differences with classification algorithms.

Transarterial chemoembolization (TACE) is the most widely used treatment for unresectable HCC in clinical practice. Radiomics plays a role in the prediction of treatment response to TACE[27-29]. Chen *et al*[27] analyzed the radiomic features extracted from tumoral VOI and peritumoral VOI, drawn at the hepatic arterial and non-contrast phases, respectively. The radiomic signature extracted from the peritumoral VOI with expanded 10 mm rim away from the main tumor part achieved excellent performance in predicting the first TACE response. Several studies established a radiomic model based on the preoperative images to predict long-term outcomes of patients who underwent TACE with good performance[30,31]. However, there were various confounding factors during multiple TACE sessions that may weaken the actual predictive performance. Fu *et al*[32] included 520 patients from five

independent centers (divided into a training set and validation set). A comprehensive model including treatment (liver resection or TACE), age, sex, modified Barcelona Clinic Liver Cancer stage, fusion focus, tumor capsule, and three radiomic features was established with good differentiation and calibration. The AUC value of the predicted 3-year recurrence-free survival was 0.80 in the training set and 0.75 in the test set.

Sorafenib is the first oral multikinase inhibitor recommended in patients with advanced HCC. Various clinical trials tried to explore the possibility of combining sorafenib and TACE that may inhibit revascularization and tumor proliferation after TACE. Most of these trials failed, except the TACTICS trial conducted recently. It is important to identify HCC patients who may benefit from the combination of TACE plus sorafenib. A DL-based radiomic model provided a significant prediction value with an AUC value of 0.717 in the training set and 0.714 in the validation set[33].

Radiopathologic evaluation

Microvascular invasion (MVI) of HCC mainly refers to the presence of cancer cells in the endothelial-lined vascular lumen under the microscope, which is a powerful validated, important independent risk factor for early recurrence and poor survival after surgical resection of HCC. Radiomic features extracted from preoperative enhanced MRI multi-phase images could predict the occurrence of MVI favorably[34, 35]. By using the least absolute shrinkage and selection operator method to select appropriate radiomic features, the predictive performance of the combined model incorporating clinicoradiological predictors and radiomic features was better than the clinicoradiological model (AUC 0.943 *vs* 0.850 in the training set, and 0.861 *vs* 0.759 in the validation set). The sensitivity, specificity, and accuracy of the combined model were 88.2%/89.5%, 87.5%/81.4%, and 87.7%/83.9% in two sets, respectively. Several studies reported that using contrast-enhanced CT images to develop and validate radiomics nomogram was a clinically useful tool to identify patients[36,37]. However, a retrospective study that included 495 patients with postoperative MVI status confirmed by histology (MVI- group, n = 346, and MVI + group, n = 149)[38] found that radiomics analysis with current CT imaging protocols does not provide significant additional value to the conventional semantic features.

Pathological grading of HCC is one of the factors that influence prognosis. Most patients with high-grade tumors have a higher rate of intrahepatic recurrence than those without low-grade tumors. The radiomics signatures based on MRI T1WI or T2WI images could be helpful for the preoperative prediction of the pathological grade of HCC[39]. The combination of the radiomic signatures and clinical factors achieved the best predictive performance over the other simple model and distinguished between high-grade and low-grade HCC (AUC = 0.800). In addition, cytokeratin 19 status of HCC that is associated with clinical aggressiveness could be identified by a radiomic-based model with satisfactory prediction performance[40]. Ye *et al*[41] managed to use the texture feature analysis on gadoxetic acid-enhanced MRI images preoperatively to predict Ki-67 status of HCC. However, the optimal cut-off value of the Ki-67 level was defined by the researcher, which weakened the generalization of the study.

Radiogenomics

Gene expression patterns of cancer tissues could reflect the underlying cellular pathophysiology and enrich the understanding of cellular pathways and numerous pathological conditions. Imaging traits have the potential to be a surrogate marker of the clinically relevant genomic/molecular signature of HCC[42-45]. One study found that the dynamic imaging traits from CT systematically correlated with the global gene expression programs of HCC[42]. The combination of 28 imaging traits was sufficient to reconstruct the variation of 116 gene expression profiles, revealing cell proliferation, liver synthetic function, and patient prognosis. Moreover, they developed a two-imaging-trait decision tree, including internal arteries and hypodense halos in HCC that is associated with a gene expression signature of venous invasion and could predict histologic venous invasion and survival of patients. Based on that result, a similar team defined a contrast-enhanced CT imaging biomarker for predicting MVI named radiogenomic venous invasion[43]. In a multicenter retrospective study, the radiogenomic venous invasion biomarker was a robust predictor of MVI with a diagnostic accuracy of 89%, sensitivity of 76%, and specificity of 94% and was associated with a poor overall survival that could have broad clinical use. They considered that radiogenomic venous invasion derived from a gene expression signature of venous invasion may reflect a more fundamental phenotype of the tumor.

Qualitative and quantitative MRI radiomic features could serve as the noninvasive biomarker to predict HCC immuno-oncological characteristics and tumor recurrence [46]. One study analyzed the correlation between radiomics, immunoprofiling (CD3, CD68, CD31), and genomic (PD-1 at the protein level, *PD-L1* and *CTLA4* at the mRNA expression level) features with statistical significance[46]. Radiomic features, including tumor size, showed good prediction performance for early HCC recurrence after resection, while immunoprofiling and genomic features did not.

CONCLUSION

Systemic therapy in advanced HCC has developed rapidly in recent years, with the most prominent success of the combination of atezolizumab (anti-PD-L1 antibody) and bevacizumab (anti-VEGF antibody). However, due to the huge tumor heterogeneity in HCC, several promising trials (such as keynote-240 and checkmate-459) have failed, and the best objective response rates of successful systemic therapies are only around 30%. In addition, there are more and more ongoing trials in the adjuvant or combination therapies setting of HCC that are explored and practiced currently. Personalized treatment and more precise patient stratification may be required under such circumstances. Radiomics technology based on ML/DL algorithms is expected to become a bridge that connects the clinical personalized precision treatment of HCC patients and its tumor phenotype. Further radiomics research with multicenter and prospective validation is still needed for improving its interpretability and reproducibility.

REFERENCES

1 **Sung H**, Ferlay J, Siegel RL, Laversanne M, Soerjomataram I, Jemal A, Bray F. Global Cancer Statistics 2020: GLOBOCAN Estimates of Incidence and Mortality Worldwide for 36 Cancers in 185 Countries. *CA Cancer J Clin* 2021; **71**: 209-249 [PMID: 33538338 DOI: 10.3322/caac.21660]

2 **Craig AJ**, von Felden J, Garcia-Lezana T, Sarcognato S, Villanueva A. Tumour evolution in hepatocellular carcinoma. *Nat Rev Gastroenterol Hepatol* 2020; **17**: 139-152 [PMID: 31792430 DOI: 10.1038/s41575-019-0229-4]

3 **Villanueva A**. Hepatocellular Carcinoma. *N Engl J Med* 2019; **380**: 1450-1462 [PMID: 30970190 DOI: 10.1056/NEJMra1713263]

4 **Lin DC**, Mayakonda A, Dinh HQ, Huang P, Lin L, Liu X, Ding LW, Wang J, Berman BP, Song EW, Yin D, Koeffler HP. Genomic and Epigenomic Heterogeneity of Hepatocellular Carcinoma. *Cancer Res* 2017; **77**: 2255-2265 [PMID: 28302680 DOI: 10.1158/0008-5472.CAN-16-2822]

5 **Lu LC**, Hsu CH, Hsu C, Cheng AL. Tumor Heterogeneity in Hepatocellular Carcinoma: Facing the Challenges. *Liver Cancer* 2016; **5**: 128-138 [PMID: 27386431 DOI: 10.1159/000367754]

6 **Lambin P**, Rios-Velazquez E, Leijenaar R, Carvalho S, van Stiphout RG, Granton P, Zegers CM, Gillies R, Boellard R, Dekker A, Aerts HJ. Radiomics: extracting more information from medical images using advanced feature analysis. *Eur J Cancer* 2012; **48**: 441-446 [PMID: 22257792 DOI: 10.1016/j.ejca.2011.11.036]

7 **Piccialli F**, Calabrò F, Crisci D, Cuomo S, Prezioso E, Mandile R, Troncone R, Greco L, Auricchio R. Precision medicine and machine learning towards the prediction of the outcome of potential celiac disease. *Sci Rep* 2021; **11**: 5683 [PMID: 33707543 DOI: 10.1038/s41598-021-84951-x]

8 **Piccialli F**, Somma VD, Giampaolo F, Cuomo S, Fortino G. A survey on deep learning in medicine: Why, how and when? *Information Fusion* 2021; **66**: 111-137 [DOI: 10.1016/j.inffus.2020.09.006]

9 **Lambin P**, Leijenaar RTH, Deist TM, Peerlings J, de Jong EEC, van Timmeren J, Sanduleanu S, Larue RTHM, Even AJG, Jochems A, van Wijk Y, Woodruff H, van Soest J, Lustberg T, Roelofs E, van Elmpt W, Dekker A, Mottaghy FM, Wildberger JE, Walsh S. Radiomics: the bridge between medical imaging and personalized medicine. *Nat Rev Clin Oncol* 2017; **14**: 749-762 [PMID: 28975929 DOI: 10.1038/nrclinonc.2017.141]

10 **Aerts HJ**, Velazquez ER, Leijenaar RT, Parmar C, Grossmann P, Carvalho S, Bussink J, Monshouwer R, Haibe-Kains B, Rietveld D, Hoebers F, Rietbergen MM, Leemans CR, Dekker A, Quackenbush J, Gillies RJ, Lambin P. Decoding tumour phenotype by noninvasive imaging using a quantitative radiomics approach. *Nat Commun* 2014; **5**: 4006 [PMID: 24892406 DOI: 10.1038/ncomms5006]

11 **O'Connor JP**, Rose CJ, Waterton JC, Carano RA, Parker GJ, Jackson A. Imaging intratumor heterogeneity: role in therapy response, resistance, and clinical outcome. *Clin Cancer Res* 2015; **21**: 249-257 [PMID: 25421725 DOI: 10.1158/1078-0432.CCR-14-0990]

12 **Mackin D**, Fave X, Zhang LF, Fried D, Yang JZ, Taylor B, Rodriguez-Rivera E, Dodge C, Jones AK, Court L. Measuring Computed Tomography Scanner Variability of Radiomics Features. *Invest Radiol* 2015; **50**: 757-765 [PMID: 26115366 DOI: 10.1097/rli.0000000000000180]

13 **Heye T**, Merkle EM, Reiner CS, Davenport MS, Horvath JJ, Feuerlein S, Breault SR, Gall P, Bashir MR, Dale BM, Kiraly AP, Boll DT. Reproducibility of dynamic contrast-enhanced MR imaging. Part II. Comparison of intra- and interobserver variability with manual region of interest placement versus semiautomatic lesion segmentation and histogram analysis. *Radiology* 2013; **266**: 812-821 [PMID: 23220891 DOI: 10.1148/radiol.12120255]

14 **Parmar C**, Rios Velazquez E, Leijenaar R, Jermoumi M, Carvalho S, Mak RH, Mitra S, Shankar BU, Kikinis R, Haibe-Kains B, Lambin P, Aerts HJ. Robust Radiomics feature quantification using semiautomatic volumetric segmentation. *PLoS One* 2014; **9**: e102107 [PMID: 25025374 DOI: 10.1371/journal.pone.0102107]

15 **European Association for the Study of the Liver**. EASL Clinical Practice Guidelines: Management of hepatocellular carcinoma. *J Hepatol* 2018; **69**: 182-236 [PMID: 29628281 DOI: 10.1016/j.jhep.2018.03.019]

16 **Li Z**, Mao Y, Huang W, Li H, Zhu J, Li W, Li B. Texture-based classification of different single liver lesion based on SPAIR T2W MRI images. *BMC Med Imaging* 2017; **17**: 42 [PMID: 28705145 DOI: 10.1186/s12880-017-0212-x]

17 **Lewis S**, Peti S, Hectors SJ, King M, Rosen A, Kamath A, Putra J, Thung S, Taouli B. Volumetric quantitative histogram analysis using diffusion-weighted magnetic resonance imaging to differentiate HCC from other primary liver cancers. *Abdom Radiol (NY)* 2019; **44**: 912-922 [PMID: 30712136 DOI: 10.1007/s00261-019-01906-7]

18 **Huang X**, Long L, Wei J, Li Y, Xia Y, Zuo P, Chai X. Radiomics for diagnosis of dual-phenotype hepatocellular carcinoma using Gd-EOB-DTPA-enhanced MRI and patient prognosis. *J Cancer Res Clin Oncol* 2019; **145**: 2995-3003 [PMID: 31664520 DOI: 10.1007/s00432-019-03062-3]

19 **Mokrane FZ**, Lu L, Vavasseur A, Otal P, Peron JM, Luk L, Yang H, Ammari S, Saenger Y, Rousseau H, Zhao B, Schwartz LH, Dercle L. Radiomics machine-learning signature for diagnosis of hepatocellular carcinoma in cirrhotic patients with indeterminate liver nodules. *Eur Radiol* 2020; **30**: 558-570 [PMID: 31444598 DOI: 10.1007/s00330-019-06347-w]

20 **Virmani J**, Kumar V, Kalra N, Khandelwal N. Neural network ensemble based CAD system for focal liver lesions from B-mode ultrasound. *J Digit Imaging* 2014; **27**: 520-537 [PMID: 24687642 DOI: 10.1007/s10278-014-9685-0]

21 **Schmauch B**, Herent P, Jehanno P, Dehaene O, Saillard C, Aubé C, Luciani A, Lassau N, Jégou S. Diagnosis of focal liver lesions from ultrasound using deep learning. *Diagn Interv Imaging* 2019; **100**: 227-233 [PMID: 30926443 DOI: 10.1016/j.diii.2019.02.009]

22 **Cai W**, He B, Hu M, Zhang W, Xiao D, Yu H, Song Q, Xiang N, Yang J, He S, Huang Y, Huang W, Jia F, Fang C. A radiomics-based nomogram for the preoperative prediction of posthepatectomy liver failure in patients with hepatocellular carcinoma. *Surg Oncol* 2019; **28**: 78-85 [PMID: 30851917 DOI: 10.1016/j.suronc.2018.11.013]

23 **Guo D**, Gu D, Wang H, Wei J, Wang Z, Hao X, Ji Q, Cao S, Song Z, Jiang J, Shen Z, Tian J, Zheng H. Radiomics analysis enables recurrence prediction for hepatocellular carcinoma after liver transplantation. *Eur J Radiol* 2019; **117**: 33-40 [PMID: 31307650 DOI: 10.1016/j.ejrad.2019.05.010]

24 **Yuan C**, Wang Z, Gu D, Tian J, Zhao P, Wei J, Yang X, Hao X, Dong D, He N, Sun Y, Gao W, Feng J. Prediction early recurrence of hepatocellular carcinoma eligible for curative ablation using a Radiomics nomogram. *Cancer Imaging* 2019; **19**: 21 [PMID: 31027510 DOI: 10.1186/s40644-019-0207-7]

25 **Shan QY**, Hu HT, Feng ST, Peng ZP, Chen SL, Zhou Q, Li X, Xie XY, Lu MD, Wang W, Kuang M. CT-based peritumoral radiomics signatures to predict early recurrence in hepatocellular carcinoma after curative tumor resection or ablation. *Cancer Imaging* 2019; **19**: 11 [PMID: 30813956 DOI: 10.1186/s40644-019-0197-5]

26 **Bressem KK**, Adams LC, Vahldiek JL, Erxleben C, Poch F, Lehmann KS, Hamm B, Niehues SM. Subregion Radiomics Analysis to Display Necrosis After Hepatic Microwave Ablation-A Proof of Concept Study. *Invest Radiol* 2020; **55**: 422-429 [PMID: 32028297 DOI: 10.1097/RLI.0000000000000653]

27 **Chen M**, Cao J, Hu J, Topatana W, Li S, Juengpanich S, Lin J, Tong C, Shen J, Zhang B, Wu J, Pocha C, Kudo M, Amedei A, Trevisani F, Sung PS, Zaydfudim VM, Kanda T, Cai X. Clinical-Radiomic Analysis for Pretreatment Prediction of Objective Response to First Transarterial Chemoembolization in Hepatocellular Carcinoma. *Liver Cancer* 2021; **10**: 38-51 [PMID: 33708638 DOI: 10.1159/000512028]

28 **Park HJ**, Kim JH, Choi SY, Lee ES, Park SJ, Byun JY, Choi BI. Prediction of Therapeutic Response of Hepatocellular Carcinoma to Transcatheter Arterial Chemoembolization Based on Pretherapeutic Dynamic CT and Textural Findings. *AJR Am J Roentgenol* 2017; **209**: W211-W220 [PMID: 28813195 DOI: 10.2214/AJR.16.17398]

29 **Jin Z**, Chen L, Zhong B, Zhou H, Zhu H, Song J, Guo J, Zhu X, Ji J, Ni C, Teng G. Machine-learning analysis of contrast-enhanced computed tomography radiomics predicts patients with hepatocellular carcinoma who are unsuitable for initial transarterial chemoembolization monotherapy: A multicenter study. *Transl Oncol* 2021; **14**: 101034 [PMID: 33567388 DOI: 10.1016/j.tranon.2021.101034]

30 **Kong C**, Zhao Z, Chen W, Lv X, Shu G, Ye M, Song J, Ying X, Weng Q, Weng W, Fang S, Chen M, Tu J, Ji J. Prediction of tumor response *via* a pretreatment MRI radiomics-based nomogram in HCC treated with TACE. *Eur Radiol*2021 epub ahead of print [PMID: 33860832 DOI: 10.1007/s00330-021-07910-0]

31 **Zhao Y**, Wang N, Wu J, Zhang Q, Lin T, Yao Y, Chen Z, Wang M, Sheng L, Liu J, Song Q, Wang F,

An X, Guo Y, Li X, Wu T, Liu AL. Radiomics Analysis Based on Contrast-Enhanced MRI for Prediction of Therapeutic Response to Transarterial Chemoembolization in Hepatocellular Carcinoma. *Front Oncol* 2021; **11**: 582788 [PMID: 33868988 DOI: 10.3389/fonc.2021.582788]

32 **Fu S**, Wei J, Zhang J, Dong D, Song J, Li Y, Duan C, Zhang S, Li X, Gu D, Chen X, Hao X, He X, Yan J, Liu Z, Tian J, Lu L. Selection Between Liver Resection Versus Transarterial Chemoembolization in Hepatocellular Carcinoma: A Multicenter Study. *Clin Transl Gastroenterol* 2019; **10**: e00070 [PMID: 31373932 DOI: 10.14309/ctg.0000000000000070]

33 **Zhang L**, Xia W, Yan ZP, Sun JH, Zhong BY, Hou ZH, Yang MJ, Zhou GH, Wang WS, Zhao XY, Jian JM, Huang P, Zhang R, Zhang S, Zhang JY, Li Z, Zhu XL, Gao X, Ni CF. Deep Learning Predicts Overall Survival of Patients With Unresectable Hepatocellular Carcinoma Treated by Transarterial Chemoembolization Plus Sorafenib. *Front Oncol* 2020; **10**: 593292 [PMID: 33102242 DOI: 10.3389/fonc.2020.593292]

34 **Yang L**, Gu D, Wei J, Yang C, Rao S, Wang W, Chen C, Ding Y, Tian J, Zeng M. A Radiomics Nomogram for Preoperative Prediction of Microvascular Invasion in Hepatocellular Carcinoma. *Liver Cancer* 2019; **8**: 373-386 [PMID: 31768346 DOI: 10.1159/000494099]

35 **Song D**, Wang Y, Wang W, Cai J, Zhu K, Lv M, Gao Q, Zhou J, Fan J, Rao S, Wang M, Wang X. Using deep learning to predict microvascular invasion in hepatocellular carcinoma based on dynamic contrast-enhanced MRI combined with clinical parameters. *J Cancer Res Clin Oncol*2021 epub ahead of print [PMID: 33839938 DOI: 10.1007/s00432-021-03617-3]

36 **Ma X**, Wei J, Gu D, Zhu Y, Feng B, Liang M, Wang S, Zhao X, Tian J. Preoperative radiomics nomogram for microvascular invasion prediction in hepatocellular carcinoma using contrast-enhanced CT. *Eur Radiol* 2019; **29**: 3595-3605 [PMID: 30770969 DOI: 10.1007/s00330-018-5985-y]

37 **Ni M**, Zhou X, Lv Q, Li Z, Gao Y, Tan Y, Liu J, Liu F, Yu H, Jiao L, Wang G. Radiomics models for diagnosing microvascular invasion in hepatocellular carcinoma: which model is the best model? *Cancer Imaging* 2019; **19**: 60 [PMID: 31455432 DOI: 10.1186/s40644-019-0249-x]

38 **Xu X**, Zhang HL, Liu QP, Sun SW, Zhang J, Zhu FP, Yang G, Yan X, Zhang YD, Liu XS. Radiomic analysis of contrast-enhanced CT predicts microvascular invasion and outcome in hepatocellular carcinoma. *J Hepatol* 2019; **70**: 1133-1144 [PMID: 30876945 DOI: 10.1016/j.jhep.2019.02.023]

39 **Wu M**, Tan H, Gao F, Hai J, Ning P, Chen J, Zhu S, Wang M, Dou S, Shi D. Predicting the grade of hepatocellular carcinoma based on non-contrast-enhanced MRI radiomics signature. *Eur Radiol* 2019; **29**: 2802-2811 [PMID: 30406313 DOI: 10.1007/s00330-018-5787-2]

40 **Wang W**, Gu D, Wei J, Ding Y, Yang L, Zhu K, Luo R, Rao SX, Tian J, Zeng M. A radiomics-based biomarker for cytokeratin 19 status of hepatocellular carcinoma with gadoxetic acid-enhanced MRI. *Eur Radiol* 2020; **30**: 3004-3014 [PMID: 32002645 DOI: 10.1007/s00330-019-06585-y]

41 **Ye Z**, Jiang H, Chen J, Liu X, Wei Y, Xia C, Duan T, Cao L, Zhang Z, Song B. Texture analysis on gadoxetic acid enhanced-MRI for predicting Ki-67 status in hepatocellular carcinoma: A prospective study. *Chin J Cancer Res* 2019; **31**: 806-817 [PMID: 31814684 DOI: 10.21147/j.issn.1000-9604.2019.05.10]

42 **Segal E**, Sirlin CB, Ooi C, Adler AS, Gollub J, Chen X, Chan BK, Matcuk GR, Barry CT, Chang HY, Kuo MD. Decoding global gene expression programs in liver cancer by noninvasive imaging. *Nat Biotechnol* 2007; **25**: 675-680 [PMID: 17515910 DOI: 10.1038/nbt1306]

43 **Banerjee S**, Wang DS, Kim HJ, Sirlin CB, Chan MG, Korn RL, Rutman AM, Siripongsakun S, Lu D, Imanbayev G, Kuo MD. A computed tomography radiogenomic biomarker predicts microvascular invasion and clinical outcomes in hepatocellular carcinoma. *Hepatology* 2015; **62**: 792-800 [PMID: 25930992 DOI: 10.1002/hep.27877]

44 **Taouli B**, Hoshida Y, Kakite S, Chen X, Tan PS, Sun X, Kihira S, Kojima K, Toffanin S, Fiel MI, Hirschfield H, Wagner M, Llovet JM. Imaging-based surrogate markers of transcriptome subclasses and signatures in hepatocellular carcinoma: preliminary results. *Eur Radiol* 2017; **27**: 4472-4481 [PMID: 28439654 DOI: 10.1007/s00330-017-4844-6]

45 **Xia W**, Chen Y, Zhang R, Yan Z, Zhou X, Zhang B, Gao X. Radiogenomics of hepatocellular carcinoma: multiregion analysis-based identification of prognostic imaging biomarkers by integrating gene data-a preliminary study. *Phys Med Biol* 2018; **63**: 035044 [PMID: 29311419 DOI: 10.1088/1361-6560/aaa609]

46 **Hectors SJ**, Lewis S, Besa C, King MJ, Said D, Putra J, Ward S, Higashi T, Thung S, Yao S, Laface I, Schwartz M, Gnjatic S, Merad M, Hoshida Y, Taouli B. MRI radiomics features predict immuno-oncological characteristics of hepatocellular carcinoma. *Eur Radiol* 2020; **30**: 3759-3769 [PMID: 32086577 DOI: 10.1007/s00330-020-06675-2]

Artificial Intelligence in Medical Imaging

Submit a Manuscript: https://www.f6publishing.com

Artif Intell Med Imaging 2021 June 28; 2(3): 73-85

DOI: 10.35711/aimi.v2.i3.73

ISSN 2644-3260 (online)

MINIREVIEWS

Artificial intelligence in coronary computed tomography angiography

Zhe-Zhe Zhang, Yan Guo, Yang Hou

ORCID number: Zhe-Zhe Zhang 0000-0002-4947-8270; Yan Guo 0000-0002-0565-640X; Yang Hou 0000-0002-9184-5441.

Author contributions: Zhang ZZ performed the majority of literature search and manuscript revision, and prepared the figures and tables; Guo Y performed data acquisition and coordinated the writing; Hou Y read and approved the final manuscript.

Supported by the National Natural Science Foundation of China, No. 82071920 and No. 81901741; and the Key Research & Development Plan of Liaoning Province, No. 2020JH2/10300037.

Conflict-of-interest statement: There is no conflict of interest associated with any of the senior author or other coauthors who contributed their efforts in this manuscript.

Zhe-Zhe Zhang, Yang Hou, Department of Radiology, Shengjing Hospital of China Medical University, Shenyang 110004, Liaoning Province, China

Yan Guo, GE Healthcare, Beijing 100176, China

Corresponding author: Yang Hou, PhD, Professor, Department of Radiology, Shengjing Hospital of China Medical University, No. 36 Sanhao Street, Heping District, Shenyang 110004, Liaoning Province, China. houyang1973@163.com

Abstract

Coronary computed tomography angiography (CCTA) is recommended as a frontline diagnostic tool in the non-invasive assessment of patients with suspected coronary artery disease (CAD) and cardiovascular risk stratification. To date, artificial intelligence (AI) techniques have brought major changes in the way that we make individualized decisions for patients with CAD. Applications of AI in CCTA have produced improvements in many aspects, including assessment of stenosis degree, determination of plaque type, identification of high-risk plaque, quantification of coronary artery calcium score, diagnosis of myocardial infarction, estimation of computed tomography-derived fractional flow reserve, left ventricular myocardium analysis, perivascular adipose tissue analysis, prognosis of CAD, and so on. The purpose of this review is to provide a comprehensive overview of current status of AI in CCTA.

Key Words: Coronary computed tomography angiography; Coronary artery disease; Artificial intelligence; Deep learning; Machine learning; Prognosis

Core Tip: The application of artificial intelligence in coronary computed tomography angiography mainly focuses on the following aspects: (1) Studies based on the coronary arteries and plaques for determination of stenosis degree, identification of plaque types, quantification of coronary artery calcium score, prediction of myocardial infarction, and prognosis evaluation; (2) Studies around the perivascular adipose tissue, which were mainly conducted using radiomics analysis and machine learning algorithm, for improvement of risk stratification; and (3) Studies based on the texture analysis of the left ventricular myocardium for assessment of functionally significant stenosis or for prognosis evaluation.

Manuscript source: Invited manuscript

Specialty type: Medical laboratory technology

Country/Territory of origin: China

Peer-review report's scientific quality classification

Grade A (Excellent): 0
Grade B (Very good): B
Grade C (Good): C
Grade D (Fair): 0
Grade E (Poor): 0

Received: May 22, 2021
Peer-review started: May 22, 2021
First decision: June 16, 2021
Revised: June 20, 2021
Accepted: July 2, 2021
Article in press: July 2, 2021
Published online: June 28, 2021

P-Reviewer: Kosuga T, Tanabe S
S-Editor: Liu M
L-Editor: Wang TQ
P-Editor: Xing YX

Citation: Zhang ZZ, Guo Y, Hou Y. Artificial intelligence in coronary computed tomography angiography. *Artif Intell Med Imaging* 2021; 2(3): 73-85
URL: https://www.wjgnet.com/2644-3260/full/v2/i3/73.htm
DOI: https://dx.doi.org/10.35711/aimi.v2.i3.73

INTRODUCTION

Coronary computed tomography angiography (CCTA) has merged as a first-line diagnostic tool in the non-invasive evaluation of patients with suspected coronary artery disease (CAD), as recommended in the international guidelines[1,2]. With rich information provided in the luminal stenosis, the morphology and composition of plaques, and the overall circulation, CCTA can safely rule out the obstructive CAD and improve prognosis.

However, the information derived from CCTA images is recognized and interpreted by human readers, and varies among different scanning protocols, scanners, contrast medium injection protocols, and readers. The arrival of artificial intelligence (AI) brought hope that it can be applied for intelligent decision-making with autonomous acquired knowledge by identifying and extracting patterns among a group of observations[3,4].

With the frontline role of CCTA in the diagnostic strategies for CAD, "big data" is available and offers an optimal platform to bridge AI with CCTA. Recently, AI techniques in CCTA have gained much attention and have been widely applied in clinical care ranging from diagnosis to prognostic stratification. We seek to summarize the recent application of AI techniques in CCTA images, so as to investigate and identify the most important and promising research topics, the problems that have been resolved and remain to be resolved, and the future directions with many challenges and opportunities.

CURRENT APPLICATION OF AI IN CCTA

The application of AI in CCTA images mainly focuses on the following aspects: (1) Studies based on the coronary arteries and plaques for determination of stenosis degree, identification of plaque types, quantification of coronary artery calcium (CAC) score, prediction of myocardial infarction (MI), and prognosis evaluation; (2) studies around the perivascular adipose tissue (PVAT), which were mainly conducted using radiomics analysis and machine learning (ML) algorithm, for improvement of risk stratification; and (3) studies based on the texture analysis of the left ventricular myocardium (LVM) for assessment of functionally significant stenosis or for prognosis evaluation, as shown in Figure 1.

AUTOMATIC DETECTION AND CLASSIFICATION OF CORONARY ARTERY PLAQUE AND STENOSIS

Since different grades of coronary artery stenosis and varying types of plaque would lead to different patient management strategies, it is therefore crucial to: (1) Detect and determine the stenosis; (2) Detailedly characterize plaques (*i.e.*, non-calcified, calcified, mixed plaques); and (3) Identify the so-called "high-risk" plaque features. Recently, there are already applications of AI techniques in related CCTA fields, including stenosis evaluation and plaque characterization. Commonly, the anatomical evaluation of coronary stenosis and quantification of plaques rely on a relative accurate segmentation and successful automatic lesion localization in CCTA images. Several vendors are developing AI-based platform for stenosis evaluation. However, the identification of "high-risk" plaques remains challenging, and only a few studies have been proposed but are of great promise with prognostic value.

Kang *et al*[5] proposed a structured learning technique for automatic detection of obstructive and non-obstructive CAD on CCTA. Taking the visual identification of lesions with stenosis ≥ 25% by three expert readers, using consensus reading, as the reference standard, the method achieved a high sensitivity (93%), specificity (95%), and diagnostic accuracy (94%), with an area under the curve (AUC) of 0.94. Zreik *et al*

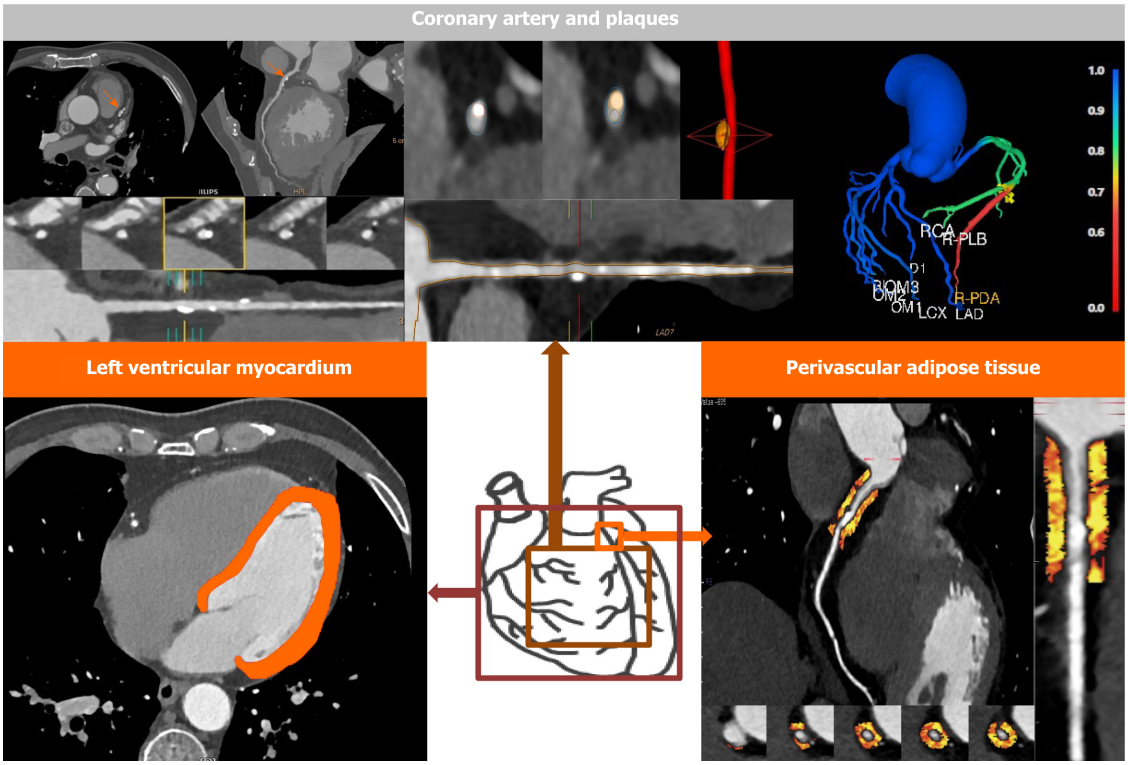

Figure 1 The application of artificial intelligence in coronary computed tomography angiography.

[6] employed a multi-task recurrent convolutional neural network to determine the stenosis severity based on the MPR view of a coronary artery extracted from the CCTA scan, as well as to automatically detect and characterize the coronary plaques. The approach achieved an accuracy of 0.80 for the determination of the anatomical significance of the coronary artery stenosis, and 0.77 for the detection and characterization of coronary plaques. Wei *et al*[7] developed a topological soft-gradient (TSG) detection method to prescreen for noncalcified plaque (NCP) candidates, which achieved AUCs of 0.87 ± 0.01 and 0.85 ± 0.01 in the training and validation sets, respectively. Jawaid *et al*[8] utilized support vector machine algorithms for automated detection of NCPs, and their approach achieved a detection accuracy of 88.4% with respect to the manual expert and a dice similarity coefficient of 83.2%.

In 2017, Kolossváry *et al*[9] investigated whether radiomics analysis improves the identification of coronary plaques with or without Napkin-ring sign (NRS). NRS is characterized as a so-called "high-risk" plaque features, which is defined as a plaque core with low CT attenuation apparently in contact with the lumen that is surrounded by a ring-shaped higher attenuation as napkin ring like in CCTA images[10,11]. However, the identification of the NRS remains challenging because it is assessed by a qualitative read of CCTA images which is affected by clinical experience and intra-/inter-reader variability[12]. Based on the segmented CCTA datasets, 8 conventional quantitative metrics and 4440 radiomic features were extracted. They found that none of the conventional quantitative parameters but 20.6% (916/4440) of radiomics features were significantly different between NRS and non-NRS plaques (Bonferroni-corrected $P < 0.0012$). In addition, almost half of the features (418/916) reached an AUC > 0.80, of which three features, including short- and long-run low gray-level emphasis and surface ratio of high attenuation voxels to total surface, exhibited excellent discriminatory value with AUCs of 0.918, 0.894, and 0.890, respectively. In 2019, the same research group validated the radiomics features extracted from CCTA in an *ex-vivo* histological study. One ML algorithm incorporating 13 parameters was superior compared with visual assessment (AUC = 0.73 *vs* 0.65) in the identification of advanced lesions[13].

DEEP LEARNING FOR AUTOMATIC CAC SCORING

CAC scoring plays a key role in risk stratification of CAD. Non-contrast-enhanced

cardiac CT, which is routinely acquired as a stand-alone test or an adjunct study prior to CCTA, is considered as the reference for quantification of CAC. CAC is defined as a high-attenuation area with > 130 HU in at least three contiguous pixels in non-contrast-enhanced cardiac CT. Recently, it has been shown that CAC can be also detected in CCTA images, which could reduce the radiation dose of a typical cardiac CT examination by 40%-50%[14]. Besides, the increased visibility of the coronary arteries in CCTA compared to non-contrast-enhanced cardiac CT could improve the identification of CAC. However, manual quantification of CAC requires substantial clinical experience to identify and make of every calcified lesion in each image slice, which is a time-consuming process. Consequently, a series of automatic methods have been proposed for CAC scoring in CCTA. Many investigations have shown promising results for clinical application in this field.

Some researchers[15,16] developed the automatic methods using two stages, including: (1) Segmentation of the coronary arteries; and (2) Identification of the CAC with the deviation from a trend line through the lumen intensity, or the voxels above a specific HU threshold, or the deviation from a model of non-calcified artery segments.

Wolterink *et al*[17,18] proposed an automatic CAC quantification method without a need for segmentation of the coronary artery tree in CCTA images using a combination of a convolutional neural network (CNN) and a Random Forest classifier. Thereafter, the same working group further extended and optimized their framework using a pair of CNNs in five ways[18], and the automatic CAC scoring in CCTA using a pair of CNNs yielded a high correlation (Pearson P = 0.950) and high consistency (intraclass correlation coefficient of 0.944) with the reference CAC scoring in non-contrast-enhanced CT.

In 2020, Fischer *et al*[19] proposed a novel fully automated algorithm using recurrent neural network with long short-term memory to detect CAC from CCTA data in a total of 565 vessels. An accuracy of 90.3% [95% confidence interval (CI): 88.0%-90.0%] was achieved on a per-vessel basis.

In summary, the CAC scoring performed on routine CCTA images without additional radiation exposure is highly desirable and the application of AI has provided considerable progress in the field and would become more influential in the clinical setting. In the near future, with the widespread application of AI techniques, CAC scoring using CCTA may eliminate the need for separate dedicated coronary calcium-scoring non-contrast enhanced CT scans.

IDENTIFICATION OF MYOCARDIAL ISCHEMIA

ML-based fractional flow reserve-CT for detection of functionally significant stenosis

It has been demonstrated that the anatomically significant appearance of a coronary stenosis is insufficient to detect hemodynamic significance and does not always equate with functional significance, which is particularly true for intermediate type coronary lesions[20,21]. Fractional flow reserve (FFR) performed during cardiac catheterization has been the reference standard in the detection of lesion-specific ischemia and is recommended for therapeutic decision-making[22]. However, the invasive measurement with a pressure wire and the relatively high cost restrict the clinical applica-tion of FFR.

Recently, novel non-invasive approaches utilizing ML algorithms for determination of FFR based on conventional CCTA images (FFR-CT) were developed and validated with a considerable diagnostic accuracy. The most popular algorithm is FFR-CT_{ML} (Figure 2). FFR-CT_{ML} was developed by Itu *et al*[23] in 2016 and provided by only one vendor (Siemens Healthineers, Germany) for research purpose. With the rapid development of AI, some FFR-CT platforms were provided for commercial use, such as the DEEPVESSE-FFR Platform provided by Keya Medical (Beijing, China). The DEEPVESSE-FFR Platform was developed by Wang *et al*[24] using MLNN + BRNN and has been commercially available since 2020.

So far, ML-based FFR-CT has been evaluated in several multi-center and single-center studies[23-35] using a threshold of ≤ 0.80 acquired from invasive FFR to detect lesion-specific ischemia. It has been demonstrated that ML-based FFR-CT performed equally in detecting flow-limiting stenosis compared with the computer fluid dynamics (CFD) based FFR-CT (FFR-CT_{CFD})[26], while the FFR-CT_{CFD} algorithm is time-consuming and heavily affected by the image quality[25,27,36]. The performance of ML-based FFR-CT in the related literature is summarized in Table 1.

Table 1 Summary of the current literature on machine learning-based fractional flow reserve-computed tomography

Ref.	Journal	Prospective	Multi- or single center	Platform	No. of patients	No. of vessels	Compared with CT-FFR_{CFD}	Accuracy	AUC
Itu *et al*[23], 2016	*Journal Application Physiology*	No	Single center	-	87	125	Yes	Per-lesion: 83%	Per-lesion: 0.90
Coenen *et al* [25], 2018	*Circulation: Cardiovascular Imaging*	Yes	The MACHINE registry	cFFR, version 2.1, Siemens	351	525	Yes	Per-lesion: 78%Per-patient: 85%	Per-lesion: 0.84
Tesche *et al* [26], 2018	*Radiology*	No	Single Center	cFFR, version 1.4, Siemens	85	104	Yes	Per-lesion: 88%; Per-patient: 92%	Per-lesion: 0.89; Per-patient: 0.91
Mastrodicasa *et al*[34], 2019	*Journal of Cardiovascular Computed Tomograph*	No	Single center	cFFR, version 3.0, Siemens	10/40	160	No	IRIS: 82%; FBP: 82%	-
Baumann *et al* [32], 2019	*European Journal of Radiology*	No	The MACHINE registry	cFFR, version 2.1, Siemens	351	525	No	-	Per-patient: Women:0.83; Men: 0.83
Doeberitz *et al* [27], 2019	*European Radiology*	No	Single center	cFFR, version 2.1, Siemens	48	103	No	-	Per-lesion: 0.93
Wang *et al* [24], 2019	*Journal of Geriatric Cardiology*	Yes	Single center	DEEPVESSE-FFR Platform	63	71	No	Per-lesion: 89%; Per-patient: 87%	Per-lesion: 0.93; Per-patient: 0.93
Tesche *et al* [30], 2020	*Journals of the American College of Cardiology: Cardiovascular Imaging*	Yes	The MACHINE registry	cFFR, version 2.1, Siemens	314	482	No	Per-lesion: 78%; CAC ≥ 400: 76%CAC 0-100: 79%; CAC 100-400: 76%	Total: 0.84 CAC ≥ 400: 0.71; CAC 0-400: 0.85
De Geer *et al* [31], 2019	*American Journal of Roentgenology*	No	The MACHINE registry	cFFR, version 2.1, Siemens	351	525	No	Total: 78%; 80 kv: 86%; 100 kv: 77%; 120 kv: 78%	Total: 0.84; 80 kv: 0.90; 100 kv: 0.82; 120 kv: 0.84
Xu *et al*[33], 2020	*European Radiology*	No	10 individual centers across China	cFFR, version 3.2.0, Siemens	437	570	No	Total: 89%; High quality: 94%; Low quality: 83%	Total: 0.89; High quality: 0.93; Low quality: 0.80
Kumamaru *et al*[28], 2020	*European Heart Journal - Cardiovascular Imaging*	No	Multi-center	Python 3.6	131	-	No	Per-patient: 76%	Per-patient: 0.78
Li *et al*[29], 2021	*Acta Radiologica*	No	Single center	DEEPVESSE-FFR Platform	73	85	No	Per-lesion: 92%; Per-patient: 91%	Per-lesion: 0.96
Xu *et al*[35], 2020	*European Radiology*	No	A Chinese multicenter study	cFFR, version 3.1.0, Siemens	442	544	No	Per lesion: 90%	-

IRIS: Iterative reconstruction in image space; FBP: Filtered back projection; CAC: Coronary artery calcium; FFR: Fractional flow reserve; AUC: Area under the curve; CT: Computed tomography.

In addition, the influences of CT reconstruction algorithms, image quality, tube voltage, coronary calcium, and gender on the diagnostic performance of FFR-CT_{ML} were investigated in several studies. In a sub-study of MACHINE Registry, Tesche *et al* [30] examined the impact of calcification on CT-FFR_{ML} determination and concluded that CT-FFR_{ML} revealed a statistically significant different (P = 0.04) performance as Agatston calcium score increased: The AUC in high Agatston scores (CAC ≥ 400) was 0.71 (95%CI: 0.57-0.85) and in low-to-intermediate Agatston scores (CAC > 0 to < 400) was 0.85 (95%CI: 0.82-0.89). In another sub-study of MACHINE Registry, De Geer *et al* [31] examined the impact of different tube voltages on CT-FFRML determination and concluded that performance does not vary significantly between tube voltages of 100 kVp (AUC: 0.82) and 120 kVp (AUC: 0.84), while the AUC was 0.90 in examination with a tube voltage of 80 kVp. Based on data of the MACHINE Registry, Baumann *et al*

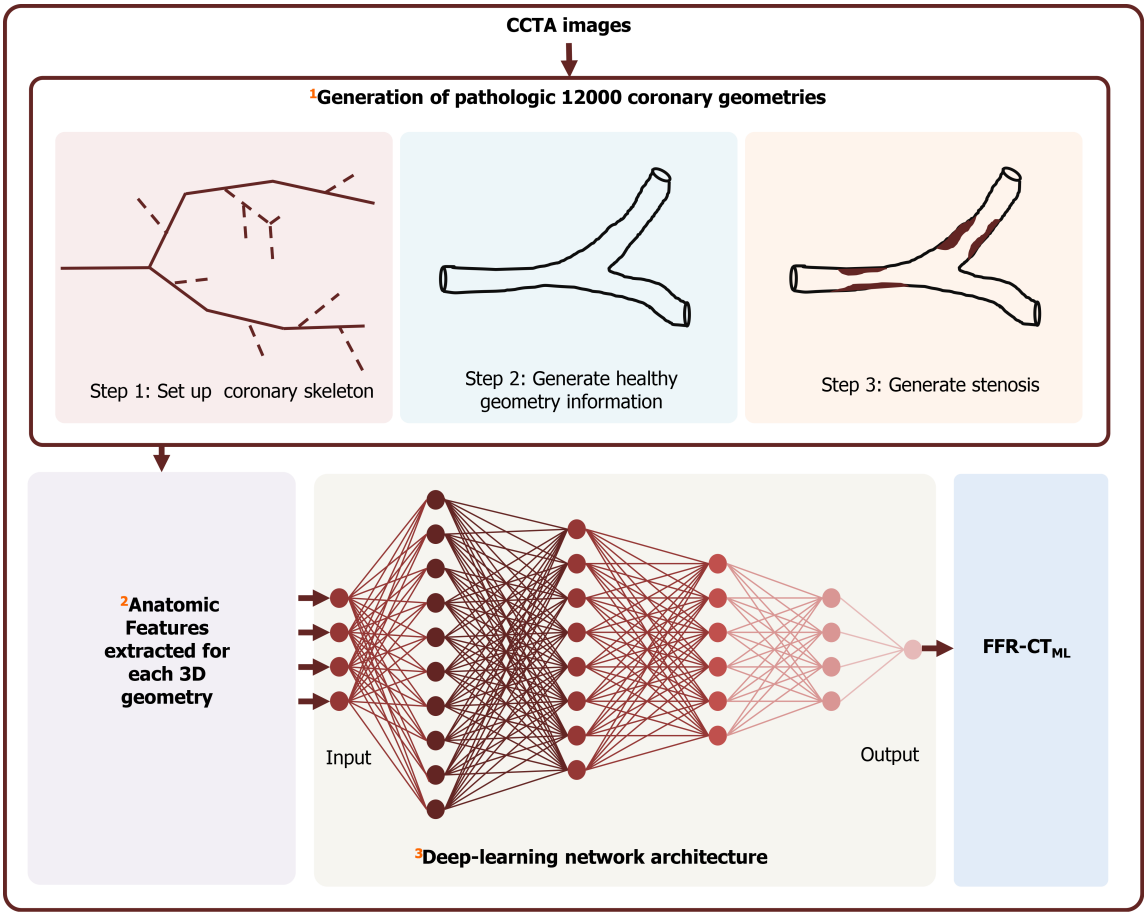

Figure 2 The workflow of the fractional flow reserve-computed tomography derivation. [1]A total of 12000 coronary anatomies were generated; [2]twenty-eight geometric features were extracted from the synthetically generated database; [3]a deep neural network with four hidden layers was used to train the machine learning-based model. FFR-CT: Fractional flow reserve-computed tomography; CCTA: Coronary computed tomography angiography.

[32] evaluated the impact of gender on the performance of FFRCTML and they found that FFRCTML performs equally in men and women (both with an AUC of 0.83). In a retrospective Chinese multicenter study, Xu *et al*[33] investigated the effect of image quality on the diagnostic performance of FFRCTML in 437 patients with 570 vessels. They found that the AUC of high-quality images [0.93 (95%CI: 0.88-0.98), n = 159] was significantly (P = 0.02) superior to that of low-quality images [0.80 (95%CI: 0.70-0.90), n = 92]. And CCTA with a score ≥ 3, intracoronary enhancement degree of 300–400 HU, and heart rate below 70 bpm at scanning could be of great benefit to more accurate FFRCTML analysis. In a retrospective single center study, Mastrodicasa *et al*[34] evaluated the influence of different CT reconstruction algorithms on the performance of CT-FFR$_{ML}$ in 40 CCTA datasets. CT-FFRML values were significantly different between iterative reconstruction in image space (IRIS) and filtered back projection algorithms, whereas no difference was observed in diagnostic accuracy (both 81.8%, P = 1.000). Additionally, they found that IRIS improved CT-FFRML post-processing speed significantly.

It should be mentioned that CT-FFR$_{ML}$ value for each location along the coronary is trained when taking the CT-FFR$_{CFD}$ as ground truth. Although the diagnostic accuracy of CT-FFR derived using deep learning (DL) methods was validated in several studies, it is still susceptible to the CCTA scanning factors. In the future, more attention should be paid to the widespread use of a local software solution that allows for image-variation and user-variation.

OTHER AI ALGORITHMS FOR PREDICTION OF MYOCARDIAL ISCHEMIA

Except for the ML based FFR-CT platforms described above, some other AI algorithms were developed recently for prediction of myocardial ischemia. These approaches are in early stage but show better interpretability, which were established *via* an

integration of qualitative or quantitative features derived from CCTA images and clinical factors.

In 2018, Dey *et al*[37] developed an integrated ML ischemia risk score (ML-IRS) from quantitative plaque measures using a supervised learning process to predict functionally significant stenosis in a prospective multicenter trial of 254 patients with 484 vessels. The ML-IRS exhibited a higher AUC (0.84) than conventional CCTA measures, including stenosis (0.76), LD-NCP volume (0.77), total plaque volume (0.74), and pre-test likelihood of CAD (0.63), for predicting lesion-specific ischemia by invasive FFR. Thereafter, the ML-IRS was integrated into coronary plaque analysis research software for generating a percent probability of pathological FFR on CCTA data.

In 2019, van Hamersvelt *et al*[38] proposed a DL method based on the LVM in resting CCTA images to identify functionally significant coronary artery stenosis using 126 patients. The DL approach achieved a higher AUC of 0.76 compared to degree of stenosis (AUC = 0.68).

In 2020, Shu *et al*[39] established a radiomics nomogram based on myocardial segments for predicting chronic myocardial ischemia using multivariate logistic regression. The accuracy of the nomogram for distinguishing chronic myocardial ischemia from normal myocardium was 0.839, 0.832, and 0.816 in the training, test, and validation cohorts, respectively.

PROGNOSTIC SIGNIFICANCE

PVAT-based radiomics for improving cardiac risk prediction

Early detection of vascular inflammation, which is a major contributor to atherogenesis and atherosclerotic plaque rupture[40,41], would enable better cardiovascular risk stratification[42]. The vascular inflammation can be detected by characterizing the phenotypic changes in PVAT using the fat attenuation index (FAI) in routine CCTA images[43,44]. FAI was defined as the average attenuation of all voxels with attenuation values between -190 HU and -30 HU located within a radial distance from the outer coronary artery wall equal to the average diameter of the respective vessel, as described previously[43,44]. However, FAI is an average of the voxel intensity values and does not account for the complex spatial relationship among voxels.

Recently, some studies investigated whether radiomics analysis could help to extract more information from the PVAT that cannot be captured by human eyes. The radiomics features surrounding PVAT mainly include two parts: (1) PVAT surrounding the standardized coronary segments, which was often investigated at a per-patient level; and (2) PVAT around the target lesion, which was at a per-lesion level.

As for the per-patient level, Oikonomou *et al*[45] developed an AI-powered radiotranscriptomic signature for predicting cardiac risk based on the radiomics features extracted from PVAT around the proximal to distal right coronary artery (RCA) and the left coronary artery in CCTA images. A fat radiomic profile (FRP) was established, using random forest model based on the features extracted from the standardized coronary segments, to distinguish the 101 patients who experienced major adverse cardiac events (MACE) within 5 years from 101 matched controls. The FRP was significantly associated with the risk of MACE [adjusted hazard ratio (HR): 1.12, 95%CI: 1.08-1.15, $P < 0.001$]. And patients with an FRP ≥ 0.63 had a 10.8-fold higher risk of MACE than those with an FRP < 0.63, after adjusted for clinical factors. The AUC of FRP in predicting MACE was 0.774 (95%CI: 0.622-0.926) in the external validation dataset (20% of the 202 samples). When added to the traditional model, FRP improved the distinguishing performance from an AUC of 0.754 to 0.880. Additionally, they found that FRP was significantly higher in 44 patients with acute MI compared with 44 controls ($P < 0.001$), but unlike FAI, FRP remained unchanged 6 mo later in 16 patients with acute MI (AMI), confirming that FRP detects persistent PVAT changes that cannot be captured by FAI.

As for the per-lesion level, in 2020, Lin *et al*[46] further explored the prognostic value of the radiomics features of PVAT around not only the standardized coronary segments but also lesions in a prospective case-control study. They found no significant difference between the PVAT radiomics features of culprit and non-culprit lesions in patients with AMI, lending further support to the pan-coronary inflammatory hypothesis. But on the other hand, as for the per-patient level, patients with AMI ($n = 60$) have a distinct PVAT radiomics phenotype surrounding the proximal RCA compared with patients with stable (matched, $n = 60$) or no CAD (matched, $n =$

60). Among the three models that they developed, the PVAT-based radiomics model (AUC: 0.87) outperforms the clinical model (AUC: 0.76) and the combined model incorporating clinical factors and PVAT attenuation (AUC: 0.77) in identifying AMI with stable CAD and controls. Additionally, after a 6-mo follow-up of patients with AMI, no significant change was observed in the radiomics features of PVAT surrounding the proximal RCA or non-culprit lesions.

QUANTITATIVE CT FEATURES-BASED ML FOR OUTCOME PREDICTION

Information extracted from CCTA images along with other clinical factors are associated with prognosis, and AI technology demonstrated great potential to enhance decision-making and improve patient outcomes. Currently, the prognostic value of ML algorithms using quantitative CCTA features together with clinical variables was investigated by researchers in several studies[47-53], in which promising results were obtained. The ML algorithms performed better than traditional predictors, not only for short-term treatment decisions but also for long-term risk predictions, as summarized in Table 2.

One of the first major studies using CCTA based ML approach for prognosis evaluation is a large prospective multi-center study conducted by Motwani *et al*[48] in 2017. They developed an ML model in CCTA to predict 5-year all-cause mortality using a dataset of 10030 patients with suspected CAD from the CONFIRM registry (Coronary CT Angiography Evaluation for Clinical Outcomes: An International Multicenter). The ML model was established after an automated feature selection procedure based on 44 CCTA-derived parameters and 25 clinical parameters. One summary score for clinical parameters (Framingham risk score, FRS) and three composite CCTA-based scores [including the segment stenosis score (SSS), the segment involvement score (SIS), and the modified Duke prognostic CAD index (DI)] were derived. The ML model exhibited a significant higher AUC compared with the conventional scores alone for predicting 5-year all-cause mortality (ML: 0.79 *vs* FRS: 0.61, SSS: 0.64, SIS: 0.64, and DI: 0.62; $P < 0.001$).

Two years later, in 2019, Johnson *et al*[49] developed another ML model using 64 vessel features derived from CCTA images, to discriminate between patients with and without subsequent death or cardiovascular events in a retrospective single-center study with 6892 patients. The performance of the ML model was compared with that of Coronary Artery Disease Reporting and Data System (CAD-RADS) score. For prediction of all-cause mortality, the AUC of the ML model was significantly higher than that of CAD-RADS (0.77 *vs* 0.72, $P < 0.001$). For prediction of coronary artery deaths, the AUC was significantly higher for the ML model than for CAD-RADS (0.85 *vs* 0.79, $P < 0.001$).

In 2020, Commandeur *et al*[52] developed an ML model integrating clinical parameters with quantitative imaging-based variables for predicting events of long-term risk of MI and cardiac death in asymptomatic subjects using the dataset with 1912 cases from the randomized EISNER trial. The ML model obtained a significantly higher AUC than atherosclerotic cardiovascular disease (ASCVD) risk and CAC score for predicting events (ML: 0.82; ASCVD: 0.77; CAC: 0.77; $P < 0.05$). Subjects with a higher ML score had a significant high hazard of suffering events (HR: 10.38, $P < 0.001$).

As for the short-term decision-making, in 2020, Kwan *et al*[53] examined whether the ML-IRS, developed by Dey *et al*[37] in 2018, as described previously (Figures 1 and 2), can predict revascularization in patients referred to ICA after CCTA in a prospective dual-center study of 352 patients with 1056 analyzable vessels. It would be beneficial to effectively identify the patients who were referred for standard clinical CCTA followed by ICA due to decision by a primary treating physician but did not receive revascularization, because those patients are a high-cost population with low yield from the invasive procedure. The results indicated that ML-IRS, when added to the traditional risk model, significantly improve the prediction of future revascularization with an increased AUC from 0.69 (95%CI: 0.65-0.72) to 0.78 (95%CI: 0.75-0.81) ($P < 0.0001$).

Overall, the application of AI in CCTA has a potential future for improving the short-term risk stratification and long-term prognostic evaluation. The ML algorithms that have been proposed should be validated and tested in real world with larger external cohorts including diversity of patients so as to make sure the models be optimized and generalized.

Table 2 summary of the current literature on the prognostic value of machine learning algorithms in coronary computed tomography angiography

Ref.	Journal	Prospective	Multi Center	No. of Patients	No. of Events	Algorithm	Endpoint	Follow-up time	Performance
Motwani *et al* [48], 2017	*European Heart Journal*	Yes	Yes	10030	745 died	LogitBoost	5-yr all-cause mortality	5.4 ± 1.4 yr	AUC = 0.79
van Rosendael *et al*[47], 2018	*Journal of Cardiovascular Computed Tomograph*	Yes	Yes	8844	350 death and 259 non-fatal MI	XGBoost	MI and death	4.6 ± 1.5 yr	AUC = 0.77
Johnson *et al* [49], 2019	*Radiology*	No	No	6892	380 died of all causes and 70 died of CAD	Logistic regression, KNN, Bagged trees, and classification neural network	Death or cardiovascular events	9.0 yr (interquartile range, 8.2–9.8 yr)	For all-cause mortality: AUC = 0.77; For CAD deaths: AUC = 0.85
van Assen *et al* [50], 2019	*European Journal of Radiology*	No	No	45	16 MACEs	Regression analysis	MACE	12 mo	AUC = 0.94
von Knebel Doeberitz *et al* [51], 2019	*The American Journal of Cardiology*	No	No	82	18 MACEs	Integration of CT-FFR, stenosis ≥ 50% and plaque markers	MACE	18.5 mo (interquartile range 11.5 to 26.6 mo)	AUC = 0.94
Commandeur *et al*[52], 2020	*Cardiovascular Research*	Yes		1912	76 MI and/or cardiac death	ML	Long-term risk of MI and cardiac death	14.5 ± 2 yr	AUC = 0.82
Kwan *et al* [53], 2021	*European Radiology*	Yes	Yes	352		ML	Future revascularization		AUC = 0.78

XGBoost: Extreme gradient boosting; KNN: K-nearest neighbors; ML: Machine learning; AUC: Area under the curve; MACE: Major adverse cardiac events; CT-FFR: Computed tomography-fractional flow reserve; CAD: Coronary artery disease; MI: Myocardial infarction.

CONCLUSION

Current AI applications in CCTA images are mostly designed in two dimensions: (1) For the radiologists, AI is applied to improve efficiency and reduce workload *via* optimizing the clinical workflow, such as improvement of image reconstruction from lower quality to high quality (*e.g.*, low-dose acquisition or motion artifacts) and structured reporting; and (2) For the patients, AI is utilized to increase benefit and improve prognostic evaluation *via* providing valuable diagnostic information more accurately, such as detection of anatomic and functional stenosis, quantification of plaques, and estimation of the vascular inflammation.

In this review, we mainly focused on the second dimension which is patient oriented. AI algorithms in CCTA images provide information in a more objective, reproducible, and rational manner compared to human perception, and exhibits its potential to outperform human in several cardiac fields. However, CCTA imaging lagged behind cancer imaging in the clinical translational of AI-based methods, especially the radiomics analysis. It has long been demonstrated in the field of cancer imaging that radiomics signatures are superior to traditional factors in predicting outcomes of patients. But only a few studies using radiomics analysis have been conducted in CCTA images. Considering that regions of interest (ROIs) segmented before the extraction of radiomics features, can be drawn along the edge of the tumor in cancer imaging generally, in CCTA images the selection of ROIs brings about challenges. Researchers hereby performed radiomics analysis around the PVAT or LVM or plaques. And recently, several groups succeeded in developing automated segmentation of PVAT and LVM, which provides probabilities to explore more novel non-invasive predictors for improvement of risk stratification and prognosis in patients with CAD.

Additionally, FFR-CT driven by AI is a hot topic in recent years. Various FFR-CT platforms are developed and adding into the clinical diagnostic workflow for not only research purpose but also commercial use. In the near future, the FFR-CT platforms

would bring major changes in the way to make decisions for patients with CAD before invasive coronary angiography.

However, before AI solutions can be truly widely implemented in daily clinical workflow or the reading room, several issues should be noted: (1) The algorithms need to be carefully validated in multi-center studies or large clinical trials to ensure the robustness and generalization; (2) The approval of clinical application is required to prove the accuracy and safety of the AI products; and (3) The legal and ethical issues should be taken into consideration.

In summary, AI offers the possibility to optimize clinical workflow and provide precise information for diagnostic and treatment, which will benefit both radiologists and patients. However, it is pertinent to note that AI will not simply substitute the cardiac radiologists, and human support or supervision is still needed. Rather, the cardiac radiologists need to be fully aware of the strengths and limitations of AI.

ACKNOWLEDGEMENTS

First, I want to show my great gratitude to my teacher Dr. Hou, a responsible and respectable scholar, offering valuable suggestions for revision. In addition, I am grateful to Guo Y for her contribution to the writing process. Also, I wish to thank those who have offered me great help and support, such as editors, reviewers, and publishers.

REFERENCES

1 **Padley SPG**, Roditi G, Nicol ED; BSCI/BSCCT. Chest pain of recent onset: assessment and diagnosis (CG95). A step change in the requirement for cardiovascular CT. *Clin Radiol* 2017; **72**: 751-753 [PMID: 28647044 DOI: 10.1016/j.crad.2017.04.020]

2 **Knuuti J**, Wijns W, Saraste A, Capodanno D, Barbato E, Funck-Brentano C, Prescott E, Storey RF, Deaton C, Cuisset T, Agewall S, Dickstein K, Edvardsen T, Escaned J, Gersh BJ, Svitil P, Gilard M, Hasdai D, Hatala R, Mahfoud F, Masip J, Muneretto C, Valgimigli M, Achenbach S, Bax JJ; ESC Scientific Document Group. 2019 ESC Guidelines for the diagnosis and management of chronic coronary syndromes. *Eur Heart J* 2020; **41**: 407-477 [PMID: 31504439 DOI: 10.1093/eurheartj/ehz425]

3 **Lamata P**. Teaching cardiovascular medicine to machines. *Cardiovasc Res* 2018; **114**: e62-e64 [PMID: 29850780 DOI: 10.1093/cvr/cvy127]

4 **Deo RC**. Machine Learning in Medicine. *Circulation* 2015; **132**: 1920-1930 [PMID: 26572668 DOI: 10.1161/CIRCULATIONAHA.115.001593]

5 **Kang D**, Dey D, Slomka PJ, Arsanjani R, Nakazato R, Ko H, Berman DS, Li D, Kuo CC. Structured learning algorithm for detection of nonobstructive and obstructive coronary plaque lesions from computed tomography angiography. *J Med Imaging (Bellingham)* 2015; **2**: 014003 [PMID: 26158081 DOI: 10.1117/1.JMI.2.1.014003]

6 **Zreik M**, van Hamersvelt RW, Wolterink JM, Leiner T, Viergever MA, Isgum I. A Recurrent CNN for Automatic Detection and Classification of Coronary Artery Plaque and Stenosis in Coronary CT Angiography. *IEEE Trans Med Imaging* 2019; **38**: 1588-1598 [PMID: 30507498 DOI: 10.1109/TMI.2018.2883807]

7 **Wei J**, Zhou C, Chan HP, Chughtai A, Agarwal P, Kuriakose J, Hadjiiski L, Patel S, Kazerooni E. Computerized detection of noncalcified plaques in coronary CT angiography: evaluation of topological soft gradient prescreening method and luminal analysis. *Med Phys* 2014; **41**: 081901 [PMID: 25086532 DOI: 10.1118/1.4885958]

8 **Jawaid MM**, Riaz A, Rajani R, Reyes-Aldasoro CC, Slabaugh G. Framework for detection and localization of coronary non-calcified plaques in cardiac CTA using mean radial profiles. *Comput Biol Med* 2017; **89**: 84-95 [PMID: 28797740 DOI: 10.1016/j.compbiomed.2017.07.021]

9 **Kolossváry M**, Karády J, Szilveszter B, Kitslaar P, Hoffmann U, Merkely B, Maurovich-Horvat P. Radiomic Features Are Superior to Conventional Quantitative Computed Tomographic Metrics to Identify Coronary Plaques With Napkin-Ring Sign. *Circ Cardiovasc Imaging* 2017; **10**: e006843 [PMID: 29233836 DOI: 10.1161/CIRCIMAGING.117.006843]

10 **Narula J**, Achenbach S. Napkin-ring necrotic cores: defining circumferential extent of necrotic cores in unstable plaques. *JACC Cardiovasc Imaging* 2009; **2**: 1436-1438 [PMID: 20083080 DOI: 10.1016/j.jcmg.2009.10.004]

11 **Maurovich-Horvat P**, Hoffmann U, Vorpahl M, Nakano M, Virmani R, Alkadhi H. The napkin-ring sign: CT signature of high-risk coronary plaques? *JACC Cardiovasc Imaging* 2010; **3**: 440-444 [PMID: 20394906 DOI: 10.1016/j.jcmg.2010.02.003]

12 **Puchner SB**, Liu T, Mayrhofer T, Truong QA, Lee H, Fleg JL, Nagurney JT, Udelson JE, Hoffmann U, Ferencik M. High-risk plaque detected on coronary CT angiography predicts acute coronary syndromes independent of significant stenosis in acute chest pain: results from the ROMICAT-II trial.

J Am Coll Cardiol 2014; **64**: 684-692 [PMID: 25125300 DOI: 10.1016/j.jacc.2014.05.039]

13 **Kolossváry M**, Karády J, Kikuchi Y, Ivanov A, Schlett CL, Lu MT, Foldyna B, Merkely B, Aerts HJ, Hoffmann U, Maurovich-Horvat P. Radiomics versus Visual and Histogram-based Assessment to Identify Atheromatous Lesions at Coronary CT Angiography: An ex Vivo Study. *Radiology* 2019; **293**: 89-96 [PMID: 31385755 DOI: 10.1148/radiol.2019190407]

14 **Voros S**, Qian Z. Agatston score tried and true: by contrast, can we quantify calcium on CTA? *J Cardiovasc Comput Tomogr* 2012; **6**: 45-47 [PMID: 22264631 DOI: 10.1016/j.jcct.2011.12.002]

15 **Ahmed W**, de Graaf MA, Broersen A, Kitslaar PH, Oost E, Dijkstra J, Bax JJ, Reiber JH, Scholte AJ. Automatic detection and quantification of the Agatston coronary artery calcium score on contrast computed tomography angiography. *Int J Cardiovasc Imaging* 2015; **31**: 151-161 [PMID: 25159031 DOI: 10.1007/s10554-014-0519-4]

16 **Eilot D**, Goldenberg R. Fully automatic model-based calcium segmentation and scoring in coronary CT angiography. *Int J Comput Assist Radiol Surg* 2014; **9**: 595-608 [PMID: 24203575 DOI: 10.1007/s11548-013-0955-y]

17 **Wolterink JM**, Leiner T, de Vos BD, Coatrieux JL, Kelm BM, Kondo S, Salgado RA, Shahzad R, Shu H, Snoeren M, Takx RA, van Vliet LJ, van Walsum T, Willems TP, Yang G, Zheng Y, Viergever MA, Išgum I. An evaluation of automatic coronary artery calcium scoring methods with cardiac CT using the orCaScore framework. *Med Phys* 2016; **43**: 2361 [PMID: 27147348 DOI: 10.1118/1.4945696]

18 **Wolterink JM**, Leiner T, de Vos BD, van Hamersvelt RW, Viergever MA, Išgum I. Automatic coronary artery calcium scoring in cardiac CT angiography using paired convolutional neural networks. *Med Image Anal* 2016; **34**: 123-136 [PMID: 27138584 DOI: 10.1016/j.media.2016.04.004]

19 **Fischer AM**, Eid M, De Cecco CN, Gulsun MA, van Assen M, Nance JW, Sahbaee P, De Santis D, Bauer MJ, Jacobs BE, Varga-Szemes A, Kabakus IM, Sharma P, Jackson LJ, Schoepf UJ. Accuracy of an Artificial Intelligence Deep Learning Algorithm Implementing a Recurrent Neural Network With Long Short-term Memory for the Automated Detection of Calcified Plaques From Coronary Computed Tomography Angiography. *J Thorac Imaging* 2020; **35** Suppl 1: S49-S57 [PMID: 32168163 DOI: 10.1097/RTI.0000000000000491]

20 **Meijboom WB**, Van Mieghem CA, van Pelt N, Weustink A, Pugliese F, Mollet NR, Boersma E, Regar E, van Geuns RJ, de Jaegere PJ, Serruys PW, Krestin GP, de Feyter PJ. Comprehensive assessment of coronary artery stenoses: computed tomography coronary angiography versus conventional coronary angiography and correlation with fractional flow reserve in patients with stable angina. *J Am Coll Cardiol* 2008; **52**: 636-643 [PMID: 18702967 DOI: 10.1016/j.jacc.2008.05.024]

21 **Conte E**, Sonck J, Mushtaq S, Collet C, Mizukami T, Barbato E, Tanzilli A, Nicoli F, De Bruyne B, Andreini D. FFR_{CT} and CT perfusion: A review on the evaluation of functional impact of coronary artery stenosis by cardiac CT. *Int J Cardiol* 2020; **300**: 289-296 [PMID: 31466886 DOI: 10.1016/j.ijcard.2019.08.018]

22 **Tonino PA**, De Bruyne B, Pijls NH, Siebert U, Ikeno F, van' t Veer M, Klauss V, Manoharan G, Engstrøm T, Oldroyd KG, Ver Lee PN, MacCarthy PA, Fearon WF; FAME Study Investigators. Fractional flow reserve versus angiography for guiding percutaneous coronary intervention. *N Engl J Med* 2009; **360**: 213-224 [PMID: 19144937 DOI: 10.1056/NEJMoa0807611]

23 **Itu L**, Rapaka S, Passerini T, Georgescu B, Schwemmer C, Schoebinger M, Flohr T, Sharma P, Comaniciu D. A machine-learning approach for computation of fractional flow reserve from coronary computed tomography. *J Appl Physiol (1985)* 2016; **121**: 42-52 [PMID: 27079692 DOI: 10.1152/japplphysiol.00752.2015]

24 **Wang ZQ**, Zhou YJ, Zhao YX, Shi DM, Liu YY, Liu W, Liu XL, Li YP. Diagnostic accuracy of a deep learning approach to calculate FFR from coronary CT angiography. *J Geriatr Cardiol* 2019; **16**: 42-48 [PMID: 30800150 DOI: 10.11909/j.issn.1671-5411.2019.01.010]

25 **Coenen A**, Kim YH, Kruk M, Tesche C, De Geer J, Kurata A, Lubbers ML, Daemen J, Itu L, Rapaka S, Sharma P, Schwemmer C, Persson A, Schoepf UJ, Kepka C, Hyun Yang D, Nieman K. Diagnostic Accuracy of a Machine-Learning Approach to Coronary Computed Tomographic Angiography-Based Fractional Flow Reserve: Result From the MACHINE Consortium. *Circ Cardiovasc Imaging* 2018; **11**: e007217 [PMID: 29914866 DOI: 10.1161/CIRCIMAGING.117.007217]

26 **Tesche C**, De Cecco CN, Baumann S, Renker M, McLaurin TW, Duguay TM, Bayer RR 2nd, Steinberg DH, Grant KL, Canstein C, Schwemmer C, Schoebinger M, Itu LM, Rapaka S, Sharma P, Schoepf UJ. Coronary CT Angiography-derived Fractional Flow Reserve: Machine Learning Algorithm versus Computational Fluid Dynamics Modeling. *Radiology* 2018; **288**: 64-72 [PMID: 29634438 DOI: 10.1148/radiol.2018171291]

27 **von Knebel Doeberitz PL**, De Cecco CN, Schoepf UJ, Duguay TM, Albrecht MH, van Assen M, Bauer MJ, Savage RH, Pannell JT, De Santis D, Johnson AA, Varga-Szemes A, Bayer RR, Schönberg SO, Nance JW, Tesche C. Coronary CT angiography-derived plaque quantification with artificial intelligence CT fractional flow reserve for the identification of lesion-specific ischemia. *Eur Radiol* 2019; **29**: 2378-2387 [PMID: 30523456 DOI: 10.1007/s00330-018-5834-z]

28 **Kumamaru KK**, Fujimoto S, Otsuka Y, Kawasaki T, Kawaguchi Y, Kato E, Takamura K, Aoshima C, Kamo Y, Kogure Y, Inage H, Daida H, Aoki S. Diagnostic accuracy of 3D deep-learning-based fully automated estimation of patient-level minimum fractional flow reserve from coronary computed tomography angiography. *Eur Heart J Cardiovasc Imaging* 2020; **21**: 437-445 [PMID: 31230076 DOI: 10.1093/ehjci/jez160]

29 **Li Y**, Qiu H, Hou Z, Zheng J, Li J, Yin Y, Gao R. Additional value of deep learning computed

tomographic angiography-based fractional flow reserve in detecting coronary stenosis and predicting outcomes. *Acta Radiol* 2021; 284185120983977 [PMID: 33423530 DOI: 10.1177/0284185120983977]

30 **Tesche C**, Otani K, De Cecco CN, Coenen A, De Geer J, Kruk M, Kim YH, Albrecht MH, Baumann S, Renker M, Bayer RR, Duguay TM, Litwin SE, Varga-Szemes A, Steinberg DH, Yang DH, Kepka C, Persson A, Nieman K, Schoepf UJ. Influence of Coronary Calcium on Diagnostic Performance of Machine Learning CT-FFR: Results From MACHINE Registry. *JACC Cardiovasc Imaging* 2020; **13**: 760-770 [PMID: 31422141 DOI: 10.1016/j.jcmg.2019.06.027]

31 **De Geer J**, Coenen A, Kim YH, Kruk M, Tesche C, Schoepf UJ, Kepka C, Yang DH, Nieman K, Persson A. Effect of Tube Voltage on Diagnostic Performance of Fractional Flow Reserve Derived From Coronary CT Angiography With Machine Learning: Results From the MACHINE Registry. *AJR Am J Roentgenol* 2019; **213**: 325-331 [PMID: 31039021 DOI: 10.2214/AJR.18.20774]

32 **Baumann S**, Renker M, Schoepf UJ, De Cecco CN, Coenen A, De Geer J, Kruk M, Kim YH, Albrecht MH, Duguay TM, Jacobs BE, Bayer RR, Litwin SE, Weiss C, Akin I, Borggrefe M, Yang DH, Kepka C, Persson A, Nieman K, Tesche C. Gender differences in the diagnostic performance of machine learning coronary CT angiography-derived fractional flow reserve -results from the MACHINE registry. *Eur J Radiol* 2019; **119**: 108657 [PMID: 31521876 DOI: 10.1016/j.ejrad.2019.108657]

33 **Xu PP**, Li JH, Zhou F, Jiang MD, Zhou CS, Lu MJ, Tang CX, Zhang XL, Yang L, Zhang YX, Wang YN, Zhang JY, Yu MM, Hou Y, Zheng MW, Zhang B, Zhang DM, Yi Y, Xu L, Hu XH, Liu H, Lu GM, Ni QQ, Zhang LJ. The influence of image quality on diagnostic performance of a machine learning-based fractional flow reserve derived from coronary CT angiography. *Eur Radiol* 2020; **30**: 2525-2534 [PMID: 32006167 DOI: 10.1007/s00330-019-06571-4]

34 **Mastrodicasa D**, Albrecht MH, Schoepf UJ, Varga-Szemes A, Jacobs BE, Gassenmaier S, De Santis D, Eid MH, van Assen M, Tesche C, Mantini C, De Cecco CN. Artificial intelligence machine learning-based coronary CT fractional flow reserve ($CT\text{-}FFR_{ML}$): Impact of iterative and filtered back projection reconstruction techniques. *J Cardiovasc Comput Tomogr* 2019; **13**: 331-335 [PMID: 30391256 DOI: 10.1016/j.jcct.2018.10.026]

35 **Di Jiang M**, Zhang XL, Liu H, Tang CX, Li JH, Wang YN, Xu PP, Zhou CS, Zhou F, Lu MJ, Zhang JY, Yu MM, Hou Y, Zheng MW, Zhang B, Zhang DM, Yi Y, Xu L, Hu XH, Yang J, Lu GM, Ni QQ, Zhang LJ. The effect of coronary calcification on diagnostic performance of machine learning-based CT-FFR: a Chinese multicenter study. *Eur Radiol* 2021; **31**: 1482-1493 [PMID: 32929641 DOI: 10.1007/s00330-020-07261-2]

36 **Gaur S**, Øvrehus KA, Dey D, Leipsic J, Bøtker HE, Jensen JM, Narula J, Ahmadi A, Achenbach S, Ko BS, Christiansen EH, Kaltoft AK, Berman DS, Bezerra H, Lassen JF, Nørgaard BL. Coronary plaque quantification and fractional flow reserve by coronary computed tomography angiography identify ischaemia-causing lesions. *Eur Heart J* 2016; **37**: 1220-1227 [PMID: 26763790 DOI: 10.1093/eurheartj/ehv690]

37 **Dey D**, Gaur S, Ovrehus KA, Slomka PJ, Betancur J, Goeller M, Hell MM, Gransar H, Berman DS, Achenbach S, Botker HE, Jensen JM, Lassen JF, Norgaard BL. Integrated prediction of lesion-specific ischaemia from quantitative coronary CT angiography using machine learning: a multicentre study. *Eur Radiol* 2018; **28**: 2655-2664 [PMID: 29352380 DOI: 10.1007/s00330-017-5223-z]

38 **van Hamersvelt RW**, Zreik M, Voskuil M, Viergever MA, Išgum I, Leiner T. Deep learning analysis of left ventricular myocardium in CT angiographic intermediate-degree coronary stenosis improves the diagnostic accuracy for identification of functionally significant stenosis. *Eur Radiol* 2019; **29**: 2350-2359 [PMID: 30421020 DOI: 10.1007/s00330-018-5822-3]

39 **Shu ZY**, Cui SJ, Zhang YQ, Xu YY, Hung SC, Fu LP, Pang PP, Gong XY, Jin QY. Predicting Chronic Myocardial Ischemia Using CCTA-Based Radiomics Machine Learning Nomogram. *J Nucl Cardiol*2020 epub ahead of print [PMID: 32557238 DOI: 10.1007/s12350-020-02204-2]

40 **Ridker PM**, Everett BM, Thuren T, MacFadyen JG, Chang WH, Ballantyne C, Fonseca F, Nicolau J, Koenig W, Anker SD, Kastelein JJP, Cornel JH, Pais P, Pella D, Genest J, Cifkova R, Lorenzatti A, Forster T, Kobalava Z, Vida-Simiti L, Flather M, Shimokawa H, Ogawa H, Dellborg M, Rossi PRF, Troquay RPT, Libby P, Glynn RJ; CANTOS Trial Group. Antiinflammatory Therapy with Canakinumab for Atherosclerotic Disease. *N Engl J Med* 2017; **377**: 1119-1131 [PMID: 28845751 DOI: 10.1056/NEJMoa1707914]

41 **Ridker PM**, Libby P, MacFadyen JG, Thuren T, Ballantyne C, Fonseca F, Koenig W, Shimokawa H, Everett BM, Glynn RJ. Modulation of the interleukin-6 signalling pathway and incidence rates of atherosclerotic events and all-cause mortality: analyses from the Canakinumab Anti-Inflammatory Thrombosis Outcomes Study (CANTOS). *Eur Heart J* 2018; **39**: 3499-3507 [PMID: 30165610 DOI: 10.1093/eurheartj/ehy310]

42 **Ross R**. Atherosclerosis--an inflammatory disease. *N Engl J Med* 1999; **340**: 115-126 [PMID: 9887164 DOI: 10.1056/NEJM199901143400207]

43 **Antonopoulos AS**, Sanna F, Sabharwal N, Thomas S, Oikonomou EK, Herdman L, Margaritis M, Shirodaria C, Kampoli AM, Akoumianakis I, Petrou M, Sayeed R, Krasopoulos G, Psarros C, Ciccone P, Brophy CM, Digby J, Kelion A, Uberoi R, Anthony S, Alexopoulos N, Tousoulis D, Achenbach S, Neubauer S, Channon KM, Antoniades C. Detecting human coronary inflammation by imaging perivascular fat. *Sci Transl Med* 2017; **9**: eaal2658 [PMID: 28701474 DOI: 10.1126/scitranslmed.aal2658]

44 **Oikonomou EK**, Marwan M, Desai MY, Mancio J, Alashi A, Hutt Centeno E, Thomas S, Herdman

L, Kotanidis CP, Thomas KE, Griffin BP, Flamm SD, Antonopoulos AS, Shirodaria C, Sabharwal N, Deanfield J, Neubauer S, Hopewell JC, Channon KM, Achenbach S, Antoniades C. Non-invasive detection of coronary inflammation using computed tomography and prediction of residual cardiovascular risk (the CRISP CT study): a post-hoc analysis of prospective outcome data. *Lancet* 2018; **392**: 929-939 [PMID: 30170852 DOI: 10.1016/S0140-6736(18)31114-0]

45 **Oikonomou EK**, Williams MC, Kotanidis CP, Desai MY, Marwan M, Antonopoulos AS, Thomas KE, Thomas S, Akoumianakis I, Fan LM, Kesavan S, Herdman L, Alashi A, Centeno EH, Lyasheva M, Griffin BP, Flamm SD, Shirodaria C, Sabharwal N, Kelion A, Dweck MR, Van Beek EJR, Deanfield J, Hopewell JC, Neubauer S, Channon KM, Achenbach S, Newby DE, Antoniades C. A novel machine learning-derived radiotranscriptomic signature of perivascular fat improves cardiac risk prediction using coronary CT angiography. *Eur Heart J* 2019; **40**: 3529-3543 [PMID: 31504423 DOI: 10.1093/eurheartj/ehz592]

46 **Lin A**, Kolossváry M, Yuvaraj J, Cadet S, McElhinney PA, Jiang C, Nerlekar N, Nicholls SJ, Slomka PJ, Maurovich-Horvat P, Wong DTL, Dey D. Myocardial Infarction Associates With a Distinct Pericoronary Adipose Tissue Radiomic Phenotype: A Prospective Case-Control Study. *JACC Cardiovasc Imaging* 2020; **13**: 2371-2383 [PMID: 32861654 DOI: 10.1016/j.jcmg.2020.06.033]

47 **van Rosendael AR**, Maliakal G, Kolli KK, Beecy A, Al'Aref SJ, Dwivedi A, Singh G, Panday M, Kumar A, Ma X, Achenbach S, Al-Mallah MH, Andreini D, Bax JJ, Berman DS, Budoff MJ, Cademartiri F, Callister TQ, Chang HJ, Chinnaiyan K, Chow BJW, Cury RC, DeLago A, Feuchtner G, Hadamitzky M, Hausleiter J, Kaufmann PA, Kim YJ, Leipsic JA, Maffei E, Marques H, Pontone G, Raff GL, Rubinshtein R, Shaw LJ, Villines TC, Gransar H, Lu Y, Jones EC, Peña JM, Lin FY, Min JK. Maximization of the usage of coronary CTA derived plaque information using a machine learning based algorithm to improve risk stratification; insights from the CONFIRM registry. *J Cardiovasc Comput Tomogr* 2018; **12**: 204-209 [PMID: 29753765 DOI: 10.1016/j.jcct.2018.04.011]

48 **Motwani M**, Dey D, Berman DS, Germano G, Achenbach S, Al-Mallah MH, Andreini D, Budoff MJ, Cademartiri F, Callister TQ, Chang HJ, Chinnaiyan K, Chow BJ, Cury RC, Delago A, Gomez M, Gransar H, Hadamitzky M, Hausleiter J, Hindoyan N, Feuchtner G, Kaufmann PA, Kim YJ, Leipsic J, Lin FY, Maffei E, Marques H, Pontone G, Raff G, Rubinshtein R, Shaw LJ, Stehli J, Villines TC, Dunning A, Min JK, Slomka PJ. Machine learning for prediction of all-cause mortality in patients with suspected coronary artery disease: a 5-year multicentre prospective registry analysis. *Eur Heart J* 2017; **38**: 500-507 [PMID: 27252451 DOI: 10.1093/eurheartj/ehw188]

49 **Johnson KM**, Johnson HE, Zhao Y, Dowe DA, Staib LH. Scoring of Coronary Artery Disease Characteristics on Coronary CT Angiograms by Using Machine Learning. *Radiology* 2019; **292**: 354-362 [PMID: 31237495 DOI: 10.1148/radiol.2019182061]

50 **van Assen M**, Varga-Szemes A, Schoepf UJ, Duguay TM, Hudson HT, Egorova S, Johnson K, St Pierre S, Zaki B, Oudkerk M, Vliegenthart R, Buckler AJ. Automated plaque analysis for the prognostication of major adverse cardiac events. *Eur J Radiol* 2019; **116**: 76-83 [PMID: 31153577 DOI: 10.1016/j.ejrad.2019.04.013]

51 **von Knebel Doeberitz PL**, De Cecco CN, Schoepf UJ, Albrecht MH, van Assen M, De Santis D, Gaskins J, Martin S, Bauer MJ, Ebersberger U, Giovagnoli DA, Varga-Szemes A, Bayer RR 2nd, , Schönberg SO, Tesche C. Impact of Coronary Computerized Tomography Angiography-Derived Plaque Quantification and Machine-Learning Computerized Tomography Fractional Flow Reserve on Adverse Cardiac Outcome. *Am J Cardiol* 2019; **124**: 1340-1348 [PMID: 31481177 DOI: 10.1016/j.amjcard.2019.07.061]

52 **Commandeur F**, Slomka PJ, Goeller M, Chen X, Cadet S, Razipour A, McElhinney P, Gransar H, Cantu S, Miller RJH, Rozanski A, Achenbach S, Tamarappoo BK, Berman DS, Dey D. Machine learning to predict the long-term risk of myocardial infarction and cardiac death based on clinical risk, coronary calcium, and epicardial adipose tissue: a prospective study. *Cardiovasc Res* 2020; **116**: 2216-2225 [PMID: 31853543 DOI: 10.1093/cvr/cvz321]

53 **Kwan AC**, McElhinney PA, Tamarappoo BK, Cadet S, Hurtado C, Miller RJH, Han D, Otaki Y, Eisenberg E, Ebinger JE, Slomka PJ, Cheng VY, Berman DS, Dey D. Prediction of revascularization by coronary CT angiography using a machine learning ischemia risk score. *Eur Radiol* 2021; **31**: 1227-1235 [PMID: 32880697 DOI: 10.1007/s00330-020-07142-8]

Published by **Baishideng Publishing Group Inc**
7041 Koll Center Parkway, Suite 160, Pleasanton, CA 94566, USA
Telephone: +1-925-3991568
E-mail: bpgoffice@wjgnet.com
Help Desk: https://www.f6publishing.com/helpdesk
https://www.wjgnet.com

ISSN 2644-3260 (online)

Artificial Intelligence in *Medical Imaging*

Artif Intell Med Imaging 2021 August 28; 2(4): 86-94

Published by Baishideng Publishing Group Inc

AIMI

Artificial Intelligence in Medical Imaging

Contents

Bimonthly Volume 2 Number 4 August 28, 2021

MINIREVIEWS

86 Current status of deep learning in abdominal image reconstruction

Li GY, Wang CY, Lv J

Artificial Intelligence in Medical Imaging

Bimonthly Volume 2 Number 4 August 28, 2021

Contents

ABOUT COVER

Editorial board member of *Artificial Intelligence in Medical Imaging*,Kwang-Sig Lee, PhD, Associate Professor, Anam Hospital AI Center, Korea University College of Medicine, Seoul 02841, South Korea

AIMS AND SCOPE

The primary aim of *Artificial Intelligence in Medical Imaging* (*AIMI*, *Artif Intell Med Imaging*) is to provide scholars and readers from various fields of artificial intelligence in medical imaging with a platform to publish high-quality basic and clinical research articles and communicate their research findings online.

AIMI mainly publishes articles reporting research results obtained in the field of artificial intelligence in medical imaging and covering a wide range of topics, including artificial intelligence in radiology, pathology image analysis, endoscopy, molecular imaging, and ultrasonography.

INDEXING/ABSTRACTING

There is currently no indexing.

RESPONSIBLE EDITORS FOR THIS ISSUE

NAME OF JOURNAL
Artificial Intelligence in Medical Imaging

ISSN
ISSN 2644-3260 (online)

LAUNCH DATE
June 28, 2020

FREQUENCY
Bimonthly

PUBLICATION DATE
August 28, 2021

Artificial Intelligence in Medical Imaging

Submit a Manuscript: https://www.f6publishing.com

Artif Intell Med Imaging 2021 August 28; 2(4): 86-94

DOI: 10.35711/aimi.v2.i4.86

ISSN 2644-3260 (online)

MINIREVIEWS

Current status of deep learning in abdominal image reconstruction

Guang-Yuan Li, Cheng-Yan Wang, Jun Lv

ORCID number: Guang-Yuan Li 0000-0002-2938-527X; Cheng-Yan Wang 0000-0002-8890-4973; Jun Lv 0000-0003-1989-1360.

Author contributions: Li GY, Wang CY and Lv J collected and analyzed the references mentioned in the review; Li GY wrote the manuscript; Wang CY and Lv J revised the manuscript; all authors have read and approved the final manuscript.

Supported by National Natural Science Foundation of China, No. 61902338 and No. 62001120; and Shanghai Sailing Program, No. 20YF1402400.

Conflict-of-interest statement: Authors have no conflict-of-interest to declare.

Guang-Yuan Li, Jun Lv, School of Computer and Control Engineering, Yantai University, Yantai 264000, Shandong Province, China

Cheng-Yan Wang, Human Phenome Institute, Fudan University, Shanghai 201203, China

Corresponding author: Cheng-Yan Wang, PhD, Associate Professor, Human Phenome Institute, Fudan University, No. 825 Zhangheng Road, Pudong New District, Shanghai 201203, China. wangcy@fudan.edu.cn

Abstract

Abdominal magnetic resonance imaging (MRI) and computed tomography (CT) are commonly used for disease screening, diagnosis, and treatment guidance. However, abdominal MRI has disadvantages including slow speed and vulnerability to motions, while CT suffers from problems of radiation. It has been reported that deep learning reconstruction can solve such problems while maintaining good image quality. Recently, deep learning-based image reconstruction has become a hot topic in the field of medical imaging. This study reviews the latest research on deep learning reconstruction in abdominal imaging, including the widely used convolutional neural network, generative adversarial network, and recurrent neural network.

Key Words: Abdominal imaging; Reconstruction; Magnetic resonance imaging; Computed tomography; Deep learning

Core Tip: We summarized the current deep learning-based abdominal image reconstruction methods in this review. The deep learning reconstruction methods can solve the issues of slow imaging speed in magnetic resonance imaging and high-dose radiation in computed tomography while maintaining high image quality. Deep learning has a wide range of clinical applications in current abdominal imaging.

Citation: Li GY, Wang CY, Lv J. Current status of deep learning in abdominal image reconstruction. *Artif Intell Med Imaging* 2021; 2(4): 86-94

URL: https://www.wjgnet.com/2644-3260/full/v2/i4/86.htm

DOI: https://dx.doi.org/10.35711/aimi.v2.i4.86

Manuscript source: Invited manuscript

Specialty type: Engineering, biomedical

Country/Territory of origin: China

Peer-review report's scientific quality classification

Grade A (Excellent): 0
Grade B (Very good): B
Grade C (Good): C
Grade D (Fair): 0
Grade E (Poor): 0

Received: May 24, 2021
Peer-review started: May 24, 2021
First decision: June 16, 2021
Revised: June 24, 2021
Accepted: August 17, 2021
Article in press: August 17, 2021
Published online: August 28, 2021

P-Reviewer: Maheshwarappa RP, Vernuccio F
S-Editor: Liu M
L-Editor: Webster JR
P-Editor: Guo X

INTRODUCTION

The emergence of deep learning has made intelligent image reconstruction a hot topic in the field of medical imaging. The applications of deep learning technology in image reconstruction have the advantages of reduced scan time and improved image quality. Magnetic resonance imaging (MRI) is a critical medical imaging technology with characteristics such as non-invasiveness, non-radiation, and high contrast. However, prolonged scanning time is the main obstacle that restrict the development of MRI technology[1]. Long acquisition time can cause discomfort to the patients and severe artifacts due to the patient's motion. In order to solve this issue, under-sampled k-space data can be acquired by reducing the measuring time during scans, and then an artifact-free image can be obtained through advanced reconstruction. Deep learning reconstruction (DLR) produces high-quality images while reducing scan time and patient discomfort. However, traditional MRI, has problems including low acceleration factor, long calculation time, and variability in parameter selection in the reconstruction algorithm[2]. Deep learning automatically captures high-level features from a large amount of data and builds non-linear mapping between the input and output. Wang *et al*[3] introduced deep learning into fast MRI reconstruction. The deep learning-based MRI reconstruction avoids the difficulty of parameter adjustment in traditional model-based reconstruction algorithms, which has the potential for a wide range of clinical applications. In addition, deep learning has also been used to solve the problem of abdominal motion. Presently, abdominal MRI reconstruction based on deep learning mainly adopts end-to-end remodeling. The current network structures for MRI reconstruction include the convolutional neural network (CNN)[4], U-net[5], generative adversarial network (GAN)[6], recurrent neural network (RNN)[7], and cascade-net[8].

On the other hand, CT imaging suffers from the problem of radiation. Low-dose CT (LDCT) is achieved by reducing the radiation dose. However, reduced radiation dose decreases the image quality, causing bias in the diagnosis. Therefore, an improved reconstruction algorithm is required for LDCT images. Traditional methods for reconstructing CT images include total variation[9], model-based iterative reconstruction (MBIR)[10], and dictionary learning[11]. However, the performance of LDCT image reconstruction could be improved further by introducing some latest techniques. The emergence of deep learning[12-15] has become the mainstream research of LDCT in recent years.

In this review, we assessed the current status of deep learning in abdominal image reconstruction. Specifically, we reviewed the latest research on deep learning methods in abdominal image reconstruction, attempted to solve the related problems, and address the challenges in this field.

DEEP LEARNING ALGORITHM

The deep learning method is obtained through a simple combination of non-linear layers. Each module can transform the initial low-level features into high-level representation. The core of deep learning is feature representation to obtain information at various levels through network layering. Compared to traditional machine learning algorithms, deep learning improves the accuracy of learning from a large amount of data. Another advantage of deep learning is that it does not require feature engineering. Typically, classic machine learning algorithms require complex feature engineering. Conversely, deep learning algorithms only need to feed data into the network and learn the representation. Finally, the deep learning network is highly adaptable and easily converted into different applications. Transfer learning makes the pre-trained deep networks suitable for similar applications.

At present, several studies have applied deep learning to different aspects of medical imaging, such as image detection[16,17], image segmentation[18,19], image denoising[20,21], super-resolution[22,23], and image reconstruction[3,24,25]. As described above, traditional model-based reconstruction algorithms require manual adjustment of the reconstruction parameters, which results in low reconstruction speed and unstable performance. With the increased acceleration factor, the image quality worsens. The reconstruction method based on deep learning avoids the difficulty of manual parameter adjustment. In the case of high acceleration, DLR can still perform well. After the network model is trained, the image can be reconstructed within seconds.

CNN FOR IMAGE RECONSTRUCTION

MRI

CNN has an excellent performance in image reconstruction[4]. In recent years, a large number of CNN-based abdominal image reconstruction methods have been proposed [26-36]. A major problem in abdominal imaging is the patient's motion, which blurs the image and produces severe artifacts. Breath holding while scanning can minimize these artifacts, but residual artifacts are persistent[37]. Self-gating techniques[38,39] can overcome this problem, but the reconstructed image at a low sampling rate causes additional streaking artifacts. In order to address the problem of free-breathing abdominal imaging under a high under-sampling rate, Lv *et al*[26] proposed a reconstruction algorithm based on a stacked convolutional autoencoder (SCAE). Experimental results showed that the SCAE method eliminates the streak artifacts caused by insufficient sampling. In order to realize high-resolution image reconstruction from radial under-sampled k-space data, Han *et al*[27] proposed a deep learning method with domain adaptation function. The network model was pre-trained with CT images, and then tuned for MRI with radial sampling. This method could be applied to limited training real-time data and multichannel reconstruction, which is in line with the clinical situation when multiple coils are used to acquire signals. Zhou *et al*[28] proposed a network combining parallel imaging (PI) and CNN for reconstruction. Real-time abdominal imaging was used to train and test the network; expected results were obtained.

In addition, CNN can also be applied to improve the quality of dynamic contrast-enhanced MRI. Tamada *et al*[29] proposed a multichannel CNN to reduce the artifacts and blur caused by the patient's motion. The detailed information on the MRI reconstruction methods mentioned above is described in Table 1.

CT imaging

In addition to the above application in abdominal MRI, CNN-based reconstruction methods show satisfactory results in CT images. Kang *et al*[30] used a deep CNN with residuals for LDCT imaging. The experimental results showed that this method reduces the noise level in the reconstructed image. Chen *et al*[31] proposed a residual encoder-decoder CNN by adding the autoencoder, deconvolution, and short jump connection to the residual encoder-decoder for LDCT imaging. This method had great advantages over the conventional method in terms of noise suppression, structure preservation, and lesion detection. Ge *et al*[32] proposed an ADAPTIVE-NET that directly reconstructs CT from sinograms. CNN can also be applied to pediatric LDCT images[33]. Zhang *et al*[34] proposed a graph attention neural network and CNN to reconstruct liver vessels.

Limited view tomographic reconstruction aimed to reconstruct images with a limited number of sinograms that could lead to high noise and artifacts. Zhou *et al*[35] proposed a novel residual dense reconstruction network architecture with spatial attention and channel attention to address this problem. The network used sinogram consistency layer interleaved to ensure that the output by the intermediate loop block was consistent with the sampled sinogram input. This method used the AAPM LDCT dataset[40] for validation and achieved the desired performance in both limited-angle and sparse-view reconstruction. In order to further improve the quality of sparse-view CT and low-dose CT reconstruction, Kazuo *et al*[36] proposed a reconstruction framework that combined CS and CNN. This method input a degraded filtered back projection image and multiplied CS reconstructed images obtained using various regularization items into a CNN. The detailed information on the abdominal CT reconstruction methods mentioned above is listed in Table 1.

GAN FOR IMAGE RECONSTRUCTION

MRI

GAN is optimized and learned through the game between generator G and discriminator D. This method is also suitable for abdominal image reconstruction. Mardani *et al*[41] used GAN for abdominal MRI reconstruction. This method also solves the problem of poor reconstruction performance of traditional CS-MRI[42,43] due to its slow iteration process and artifacts caused by noise. This method used least-squares GAN[44] and pixel-wise L1 as the cost function during training. The data showed that the reconstructed abdominal MR image was superior to that obtained using the

Table 1 Abdominal image reconstruction algorithms based on a convolutional neural network

Ref.	Task	Method	Images	Metric
Kang *et al*[30], 2017	Low-dose CT reconstruction	CNN	Abdominal CT images	PSNR: 34.55
Chen *et al*[31], 2017	Low-dose CT reconstruction	RED-CNN	Low-dose abdominal CT images	PSNR: 43.79 ± 2.01; SSIM: 0.98 ± 0.01; RMSE: 0.69 ± 0.07
Han *et al*[27], 2018	Accelerated projection-reconstruction MRI	U-netCNN	Low-dose abdominal CT images; synthetic radial abdominal MR images	PSNR: 31.55
Lv *et al*[26], 2018	Undersampled radial free-breathing 3D abdominal MRI	Auto-encoderCNN	3D golden angle-radial SOS liver MR images	$P < 0.001$
Ge *et al*[32], 2020	CT image reconstruction directly from a sinogram	Residual encoder-decoder + CNN	Low-dose abdominal CT images	PSNR: 43.15 ± 1.93; SSIM: 0.97 ± 0.01; NRMSE: 0.71 ± 0.16
MacDougall *et al*[33], 2019	Improving low-dose pediatric abdominal CT	CNN	Liver CT images;Spleen CT images	$P < 0.001$
Tamada *et al*[29], 2020	DCE MR imaging of the liver	CNN	T1-weighted liver MR images	SSIM: 0.91
Zhou *et al*[28], 2019	Applications in low-latency accelerated real-time imaging	PICNN	bSSFP cardiac MR images; bSSFP abdominal MR images	Abdominal: NRMSE: 0.08 ± 0.02; SSIM: 0.90 ± 0.02
Zhang *et al*[34], 2020	Reconstructing 3D liver vessel morphology from contrasted CT images	GNNCNN	Multi-phase contrasted liver CT images	F1 score: 0.8762 ± 0.0549
Zhou *et al*[35], 2020	Limited view tomographic reconstruction	Residual dense spatial-channel attention + CNN	Whole body CT images	LAR: PSNR: 35.82; SSIM: 0.97 SVR: PSNR: 41.98; SSIM: 0.97
Kazuo *et al*[36], 2021	Image reconstructionin low-dose and sparse-view CT	CS + CNN	Low-dose abdominal CT images; Sparse-view abdominal CT images	Low-Dose CT case: PSNR: 33.2; SSIM: 0.91 Sparse-View CT case: PSNR: 29.2; SSIM: 0.91

NRMSE ($\times 10^{-2}$); RMSE (10^{-2}). MRI: Magnetic resonance imaging; CT: Computed tomography; CNN: Convolutional neural network; PSNR: Peak signal to noise ratio; SSIM: Structural similarity; RMSE: Root mean square error; NRMSE: Normalized root mean square error; RED: Residual encoder-decoder; DCE: Dynamic contrast-enhanced; PI: Parallel imaging; CS: Compressed sensing; LAR: Limited angle reconstruction; SVR: Sparse view reconstruction; GNN: Graph neural network; RNN: Recurrent neural network; SOS: Stack-of-stars.

traditional CS method with respect to image quality and reconstruction speed. Lv *et al*[45] compared the performance of GAN-based image reconstruction with DAGAN[46], ReconGAN[25], RefineGAN[25], and KIGAN[47]. Among these, the RefineGAN method was slightly better than DAGAN and KIGAN. In addition, Lv *et al*[48] combined PI and GAN for end-to-end reconstruction. The network added data fidelity items and regularization terms to the generator to obtain the information from multiple coils.

Most supervised learning methods require a large amount of fully sampled data for training. However, it is difficult or even impossible to obtain the full sampled data, and hence, unsupervised learning is necessary under the circumstances. Cole *et al*[49] proposed an unsupervised reconstruction method based on GAN. The detailed information on the reconstruction methods is described in Table 2.

CT imaging

The usage of GAN can also improve the quality of abdominal LDCT images. Yang *et al*[50] used GAN combined with Wasserstein distance and perceptual loss for LDCT abdominal image denoising. Based on Wasserstein GAN (WGAN)[51], Kuanar *et al*[52] proposed an end-to-end RegNet-based autoencoder network model, in which GAN was used in the autoencoder. The loss function of this network was composed of RegNet perceptual loss[52] and WGAN adversarial loss[51]. The experimental results showed that this method improves the quality of the reconstructed image while reducing the noise.

Zhang *et al*[53] proposed the use of conditional GAN (CGAN) to reconstruct super-resolution CT images. The edge detection loss function was proposed in the CGAN to minimize the loss of the image edge. In addition, this study used appropriate bounding boxes to reduce the number of rays when performing 3D reconstruction. The reconstruction methods are described in Table 2.

Table 2 Abdominal image reconstruction based on generative adversarial network and recurrent neural network

Ref.	Task	Method	Images	Metric
Mardani *et al* [41], 2017	Compressed sensing automates MRI reconstruction	GANCS	Abdominal MR images	SNR: 20.48; SSIM: 0.87
Yang *et al*[50], 2018	Low dose CT image denoising	WGAN	Abdominal CT images	PSNR: 23.39; SSIM: 0.79
Kuanar *et al* [52], 2019	Low-dose abdominal CT image reconstruction	Auto-encoderWGAN	Abdominal CT images	PSNR: 37.76; SSIM: 0.94; RMSE: 0.92
Lv *et al*[45], 2021	A comparative study of GAN-based fast MRI reconstruction	DAGANKIGANReconGANRefineGAN	T2-weighted liver images; 3D FSE CUBE knee images; T1-weighted brain images	Liver: PSNR: 36.25 ± 3.39; SSIM: 0.95 ± 0.02; RMSE: 2.12 ± 1.54; VIF: 0.93 ± 0.05; FID: 31.94
Zhang *et al*[53], 2020	3D reconstruction for super-resolution CT images	Conditional GAN	3D-IRCADb-01database liver CT images	Male: PSNR: 34.51; SSIM: 0.90Female: PSNR: 34.75; SSIM: 0.90
Cole *et al*[49], 2020	Unsupervised MRI reconstruction	UnsupervisedGAN	3D FSE CUBE knee images; DCE abdominal MR images	PSNR: 31.55; NRMSE: 0.23; SSIM: 0.83
Lv *et al*[48], 2021	Accelerated multichannel MRI reconstruction	PIGAN	3D FSE CUBE knee MR images; abdominal MR images	Abdominal: PSNR: 31.76 ± 3.04; SSIM: 0.86 ± 0.02; NMSE: 1.22 ± 0.97
Zhang *et al*[54], 2019	4D abdominal and *in utero* MR imaging	Self-supervised RNN	bSSFP uterus MR images; bSSFP kidney MR images	PSNR: 36.08 ± 1.13; SSIM: 0.96 ± 0.01

RMSE ($\times 10^{-2}$); NMSE ($\times 10^{-5}$). MRI: Magnetic resonance imaging; CT: Computed tomography; SNR: Signal-to-noise ratio; PSNR: Peak signal to noise ratio; SSIM: Structural similarity; RMSE: Root mean square error; NRMSE: Normalized root mean square error; VIF: Variance inflation factor; FID: Frechet inception distance; GAN: Generative adversarial network; RNN: Recurrent neural network; PI: Parallel imaging.

RNN FOR IMAGE RECONSTRUCTION

RNN is suitable for processing data with sequence information. The dynamic abdominal images were collected from the currently collected frame and were similar to the previous and following frames. Unlike other networks, the nodes between the hidden layers of RNN are connected. Zhang *et al*[54] proposed a self-supervised RNN to estimate the breathing motion of the abdomen and *in utero* 4D MRI. The network used a self-supervised RNN to estimate breathing motion and then a 3D deconvolution network for super-resolution reconstruction. Compared to slice-to-volume registration, the experimental results of this method predicted the respiratory motion and reconstructed high-quality images accurately. The detailed information on the reconstruction method mentioned above is shown in Table 2.

APPLICATION OF DL IMAGE RECONSTRUCTION

Motion correction

Deep learning can also be applied to abdominal motion correction. Lv *et al*[55] proposed a CNN-based image registration algorithm to obtain images during the respiratory cycle. In addition, methods based on U-net and GAN can also be applied to abdominal motion correction. Jiang *et al*[56] proposed a densely connected U-net and GAN for abdominal MRI respiration correction. Küstner *et al*[57] combined non-rigid registration with 4D reconstruction networks for motion correction. The detailed information on the reconstruction methods mentioned above is summarized in Table 3.

DLR

The DLR developed by Canon Medical Systems' Advanced Intelligent Clear-IQ Engine is a commercial deep learning tool for image reconstruction. Some studies have confirmed the feasibility and effectiveness of this tool for abdominal image reconstruction. Akagi *et al*[58] used DLR for abdominal ultra-high-resolution computed tomography (U-HRCT) image reconstruction. The present study proved that DLR reconstruction has clinical applicability in U-HRCT. Compared to hybrid-IR

Table 3 Applications of deep learning in abdominal reconstruction

Ref.	Task	Method	Images	Metric
Lv *et al*[55], 2018	Respiratory motion correction for free-breathing 3D abdominal MRI	CNN	3D golden angle-radial SOS abdominal images	SNR: 207.42 ± 96.73
Jiang *et al*[56], 2019	Respiratory motion correction in abdominal MRI	U-NetGAN	T1-weighted abdominal images	FSE: 0.920; GRE: 0.910; Simulated motion: 0.928
Küstner *et al*[57], 2020	Motion-corrected image reconstruction in 4D MRI	U-netCNN	T1-weighted *in-vivo* 4D MR images	EPE: 0.17 ± 0.26; EAE: 7.9 ± 9.9; SSIM: 0.94 ± 0.04; NRMSE: 0.5 ± 0.1
Akagi *et al*[58], 2019	Improving image quality of abdominal U-HRCT using DLR method	DLR	U-HRCT abdominal CT images	$P < 0.01$
Nakamura *et al*[59], 2019	To evaluate the effect of a DLR method	DLR	Abdominal CT images	$P < 0.001$

NRMSE ($\times 10^{-2}$). MRI: Magnetic resonance imaging; CT: Computed tomography; CNN: Convolutional neural network; GAN: Generative adversarial network; SNR: Signal-to-noise ratio; SSIM: Structural similarity; NRMSE: Normalized root mean square error; EPE: End-point error; EAE: End-angulation error; U-HRCT: Ultra-high-resolution computed tomography; DLR: Deep learning reconstruction; SOS: Stack-of-stars; FSE: Fast-spin echo; GRE: Gradient echo.

and MBIR[10], DLR reduces the noise of abdominal U-HRCT and improves image quality. In addition, the DLR method is applicable to widely-used CT images. Nakamura *et al*[59] evaluated the effectiveness of the DLR method on hypovascular hepatic metastasis on abdominal CT images. The detailed information on the reconstruction methods mentioned is summarized in Table 3.

CURRENT CHALLENGES AND FUTURE DIRECTIONS

In summary, deep learning provides a powerful tool for abdominal image reconstruction. However, deep learning-based abdominal image reconstruction has several challenges. First, collecting a large amount of data for training the neural networks is rather challenging. Supervised learning means that a large amount of fully sampled data is required, which is time-consuming in clinical medicine. In addition, it is difficult or even impossible to obtain full sampling data in some specific applications[49]. Therefore, some semi-supervised learning is necessary. In addition, some researchers have proposed the use of self-supervised learning methods[54,60,61]. Self-supervised learning does not require training labels. It is suitable for image reconstruction problems when fully sampled data cannot be obtained easily. Therefore, self-supervised learning has great development potential and is one of the major research directions in the future. Second, deep learning is difficult to explain even if satisfactory reconstruction is achieved.

The current workflow of abdominal imaging starts from data acquisition to image reconstruction and then to diagnosis, deeming it possible to perform multiple tasks at the same time. For example, SegNetMRI[62] realizes image segmentation and image reconstruction simultaneously. Joint-FR-Net[63] can directly use k-space data for image segmentation. Thus, future studies could use the k-space data for lesion detection, classification, and other clinical applications directly.

CONCLUSION

We summarized the current deep learning-based abdominal image reconstruction methods in this review. The DLR methods can solve the issues of slow imaging speed in MRI and high-dose radiation in CT while maintaining high image quality. Deep learning has a wide range of clinical applications in current abdominal imaging. More advanced techniques are expected to be utilized in future studies.

REFERENCES

1 **Lustig M**, Donoho DL, Santos JM, Pauly JM. Compressed sensing MRI. *IEEE Signal Process Mag* 2008; **25**: 72-82 [DOI: 10.1109/MSP.2007.914728]

2 **Ravishankar S**, Bresler Y. MR image reconstruction from highly undersampled k-space data by dictionary learning. *IEEE Trans Med Imaging* 2011; **30**: 1028-1041 [PMID: 21047708 DOI: 10.1109/TMI.2010.2090538]

3 **Wang S**, Su Z, Ying L, Peng X, Zhu S, Liang F, Feng D, Liang D. Accelerating magnetic resonance imaging *via* deep learning. *Proc IEEE Int Symp Biomed Imaging* 2016; **2016**: 514-517 [PMID: 31709031 DOI: 10.1109/ISBI.2016.7493320]

4 **Wang SS**, Xiao TH, Liu QG, Zheng HR. Deep learning for fast MR imaging: a review for learning reconstruction from incomplete k-space data. *Biomed Signal Process Control* 2021; **68**: 102579 [DOI: 10.1016/j.bspc.2021.102579]

5 **Zbontar J**, Knoll F, Sriram A, Murrel T, Huang ZN, Muckley MJ, Defazio A, Stern R, Johnson P, Bruno M, Parente M, Geras KJ, Katsnelson J, Chandarana H, Zhang ZZ, Drozdzal M, Romero A, Rabbat M, Vincent P, Yakubova N, Pinkerton J, Wang D, Owens E, Zitnick CL, Recht MP, Sodickson DK, Lui YW. fastMRI: An open dataset and benchmarks for accelerated MRI. 2018 Preprint. Available from: arXiv: 1811.08839

6 **Wang JB**, Wang HT, Wang LS, Li LP, Xv J, Xv C, Li XH, Wu YH, Liu HY, Li BJ, Yu H, Tian X, Zhang ZY, Wang Y, Zhao R, Liu JY, Wang W, Gu Y. Epidemiological and clinical characteristics of fifty-six cases of COVID-19 in Liaoning Province, China. *World J Clin Cases* 2020; **8**: 5188-5202 [PMID: 33269255 DOI: 10.12998/wjcc.v8.i21.5188]

7 **Qin C**, Schlemper J, Caballero J, Price AN, Hajnal JV, Rueckert D. Convolutional Recurrent Neural Networks for Dynamic MR Image Reconstruction. *IEEE Trans Med Imaging* 2019; **38**: 280-290 [PMID: 30080145 DOI: 10.1109/TMI.2018.2863670]

8 **Schlemper J**, Caballero J, Hajnal JV, Price AN, Rueckert D. A Deep Cascade of Convolutional Neural Networks for Dynamic MR Image Reconstruction. *IEEE Trans Med Imaging* 2018; **37**: 491-503 [PMID: 29035212 DOI: 10.1109/TMI.2017.2760978]

9 **Olinescu A**, Hristescu S, Poliopol M, Agache F, Kerek F. The effects of Boicil on some immunocompetent cells. II. In vitro and *in vivo* modulation of the mouse cellular and humoral immune response. *Arch Roum Pathol Exp Microbiol* 1987; **46**: 147-158 [PMID: 3502686 DOI: 10.1088/0031-9155/57/23/7923]

10 **Li K**, Tang J, Chen GH. Statistical model based iterative reconstruction (MBIR) in clinical CT systems: experimental assessment of noise performance. *Med Phys* 2014; **41**: 041906 [PMID: 24694137 DOI: 10.1118/1.4867863]

11 **Xu Q**, Yu H, Mou X, Zhang L, Hsieh J, Wang G. Low-dose X-ray CT reconstruction *via* dictionary learning. *IEEE Trans Med Imaging* 2012; **31**: 1682-1697 [PMID: 22542666 DOI: 10.1109/TMI.2012.2195669]

12 **Zhu JY**, Krähenbühl P, Shechtman E, Efros AA. Generative visual manipulation on the natural image manifold. In: European conference on computer vision. Springer, 2016: 597-613 [DOI: 10.1007/978-3-319-46454-1_36]

13 **Johnson J**, Alahi A, Li FF. Perceptual losses for real-time style transfer and super-resolution. In: European conference on computer vision. Springer, 2016: 694-711 [DOI: 10.1007/978-3-319-46475-6_43]

14 **Gatys LA**, Ecker AS, Bethge M. A neural algorithm of artistic style. 2015 Preprint. Available from: arXiv: 1508.06576

15 **Simonyan K**, Zisserman A. Very deep convolutional networks for large-scale image recognition. 2014 Preprint. Available from: arXiv: 1409.1556

16 **Xu J**, Xiang L, Liu Q, Gilmore H, Wu J, Tang J, Madabhushi A. Stacked Sparse Autoencoder (SSAE) for Nuclei Detection on Breast Cancer Histopathology Images. *IEEE Trans Med Imaging* 2016; **35**: 119-130 [PMID: 26208307 DOI: 10.1109/TMI.2015.2458702]

17 **Qi Dou**, Hao Chen, Lequan Yu, Lei Zhao, Jing Qin, Defeng Wang, Mok VC, Lin Shi, Pheng-Ann Heng. Automatic Detection of Cerebral Microbleeds From MR Images *via* 3D Convolutional Neural Networks. *IEEE Trans Med Imaging* 2016; **35**: 1182-1195 [PMID: 26886975 DOI: 10.1109/TMI.2016.2528129]

18 **Guo Y**, Gao Y, Shen D. Deformable MR Prostate Segmentation *via* Deep Feature Learning and Sparse Patch Matching. *IEEE Trans Med Imaging* 2016; **35**: 1077-1089 [PMID: 26685226 DOI: 10.1109/TMI.2015.2508280]

19 **Zhang W**, Li R, Deng H, Wang L, Lin W, Ji S, Shen D. Deep convolutional neural networks for multi-modality isointense infant brain image segmentation. *Neuroimage* 2015; **108**: 214-224 [PMID: 25562829 DOI: 10.1016/j.neuroimage.2014.12.061]

20 **Burger HC**, Schuler CJ, Harmeling S. Image denoising: Can plain neural networks compete with BM3D? IEEE conference on computer vision and pattern recognition. 2012 Jun 16-21; Providence, RI, United States: IEEE, 2012: 2392-2399 [DOI: 10.1109/CVPR.2012.6247952]

21 **Solomon J**, Samei E. A generic framework to simulate realistic lung, liver and renal pathologies in CT imaging. *Phys Med Biol* 2014; **59**: 6637-6657 [PMID: 25325156 DOI: 10.1088/0031-9155/59/21/6637]

22 **Bahrami K**, Shi F, Rekik I, Shen DG. Convolutional neural network for reconstruction of 7T-like images from 3T MRI using appearance and anatomical features. In: Deep Learning and Data Labeling

for Medical Applications. Springer, 2016: 39-47 [DOI: 10.1007/978-3-319-46976-8_5]
23 **Dong C**, Loy CC, He KM, Tang X. Learning a deep convolutional network for image super-resolution. In: European conference on computer vision. Springer, 2014: 184-199 [DOI: 10.1007/978-3-319-10593-2_13]
24 **Zhu JY**, Park T, Isola P, Efros AA. Unpaired image-to-image translation using cycle-consistent adversarial networks. Proceedings of the IEEE international conference on computer vision; 2017 Oct 22-29; Venice, Italy. IEEE, 2017: 2223-2232 [DOI: 10.1109/ICCV.2017.244]
25 **Quan TM**, Nguyen-Duc T, Jeong WK. Compressed Sensing MRI Reconstruction Using a Generative Adversarial Network With a Cyclic Loss. *IEEE Trans Med Imaging* 2018; **37**: 1488-1497 [PMID: 29870376 DOI: 10.1109/TMI.2018.2820120]
26 **Lv J**, Chen K, Yang M, Zhang J, Wang X. Reconstruction of undersampled radial free-breathing 3D abdominal MRI using stacked convolutional auto-encoders. *Med Phys* 2018; **45**: 2023-2032 [PMID: 29574939 DOI: 10.1002/mp.12870]
27 **Han Y**, Yoo J, Kim HH, Shin HJ, Sung K, Ye JC. Deep learning with domain adaptation for accelerated projection-reconstruction MR. *Magn Reson Med* 2018; **80**: 1189-1205 [PMID: 29399869 DOI: 10.1002/mrm.27106]
28 **Zhou Z**, Han F, Ghodrati V, Gao Y, Yin W, Yang Y, Hu P. Parallel imaging and convolutional neural network combined fast MR image reconstruction: Applications in low-latency accelerated real-time imaging. *Med Phys* 2019; **46**: 3399-3413 [PMID: 31135966 DOI: 10.1002/mp.13628]
29 **Tamada D**, Kromrey ML, Ichikawa S, Onishi H, Motosugi U. Motion Artifact Reduction Using a Convolutional Neural Network for Dynamic Contrast Enhanced MR Imaging of the Liver. *Magn Reson Med Sci* 2020; **19**: 64-76 [PMID: 31061259 DOI: 10.2463/mrms.mp.2018-0156]
30 **Kang E**, Min J, Ye JC. A deep convolutional neural network using directional wavelets for low-dose X-ray CT reconstruction. *Med Phys* 2017; **44**: e360-e375 [PMID: 29027238 DOI: 10.1002/mp.12344]
31 **Chen H**, Zhang Y, Kalra MK, Lin F, Chen Y, Liao P, Zhou J, Wang G. Low-Dose CT With a Residual Encoder-Decoder Convolutional Neural Network. *IEEE Trans Med Imaging* 2017; **36**: 2524-2535 [PMID: 28622671 DOI: 10.1109/TMI.2017.2715284]
32 **Ge Y**, Su T, Zhu J, Deng X, Zhang Q, Chen J, Hu Z, Zheng H, Liang D. ADAPTIVE-NET: deep computed tomography reconstruction network with analytical domain transformation knowledge. *Quant Imaging Med Surg* 2020; **10**: 415-427 [PMID: 32190567 DOI: 10.21037/qims.2019.12.12]
33 **MacDougall RD**, Zhang Y, Callahan MJ, Perez-Rossello J, Breen MA, Johnston PR, Yu H. Improving Low-Dose Pediatric Abdominal CT by Using Convolutional Neural Networks. *Radiol Artif Intell* 2019; **1**: e180087 [PMID: 32090205 DOI: 10.1148/ryai.2019180087]
34 **Zhang DH**, Liu SQ, Chaganti S, Gibson E, Xu ZB, Grbic S, Cai WD, Comaniciu D. Graph Attention Network based Pruning for Reconstructing 3D Liver Vessel Morphology from Contrasted CT Images. 2020 Preprint. Available from: arXiv: 2003.07999
35 **Zhou B**, Zhou SK, Duncan JS, Liu C. Limited View Tomographic Reconstruction Using a Deep Recurrent Framework with Residual Dense Spatial-Channel Attention Network and Sinogram Consistency. 2020 Preprint. Available from: arXiv: 2009.01782
36 **Kazuo S**, Kawamata K, Kudo H. Combining compressed sensing and deep learning using multi-channel CNN for image reconstruction in low-dose and sparse-view CT. International Forum on Medical Imaging in Asia 2021; 2021 Apr 20; Taipei, Taiwan. Proc. SPIE, 2021: 117920M [DOI: 10.1117/12.2590743]
37 **Bernstein MA**, King KF, Zhou XJ. Handbook of MRI pulse sequences. Burlington, MA: Elsevier, 2004
38 **Cruz G**, Atkinson D, Buerger C, Schaeffter T, Prieto C. Accelerated motion corrected three-dimensional abdominal MRI using total variation regularized SENSE reconstruction. *Magn Reson Med* 2016; **75**: 1484-1498 [PMID: 25996443 DOI: 10.1002/mrm.25708]
39 **Stehning C**, Börnert P, Nehrke K, Eggers H, Stuber M. Free-breathing whole-heart coronary MRA with 3D radial SSFP and self-navigated image reconstruction. *Magn Reson Med* 2005; **54**: 476-480 [PMID: 16032682 DOI: 10.1002/mrm.20557]
40 **McCollough C**. TU-FG-207A-04: Overview of the Low Dose CT Grand Challenge. Fifty-eighth annual meeting of the american association of physicists in medicine; 2016. Medical physics, 2016: 3759-3760 [DOI: 10.1118/1.4957556]
41 **Mardani M**, Gong E, Cheng JY, Vasanawala S, Zaharchuk G, Alley M, Thakur N, Han S, Dally W, Pauly JM, Xing L. Deep generative adversarial networks for compressed sensing automates MRI. 2017 Preprint. Available from: arXiv: 1706.00051
42 **Donoho DL**. Compressed sensing. *IEEE Trans Inf Theory* 2006; **52**: 1289-1306 [DOI: 10.1109/TIT.2006.871582]
43 **Jaspan ON**, Fleysher R, Lipton ML. Compressed sensing MRI: a review of the clinical literature. *Br J Radiol* 2015; **88**: 20150487 [PMID: 26402216 DOI: 10.1259/bjr.20150487]
44 **Mao X**, Li Q, Xie HR, Lau RY, Wang Zhen, Smolley SP. Least squares generative adversarial networks. Proceedings of the IEEE international conference on computer vision; 2017 Oct 22-29; Venice, Italy. IEEE, 2017: 2794-2802 [DOI: 10.1109/ICCV.2017.304]
45 **Lv J**, Zhu J, Yang G. Which GAN? *Philos Trans A Math Phys Eng Sci* 2021; **379**: 20200203 [PMID: 33966462 DOI: 10.1098/rsta.2020.0203]
46 **Yang G**, Yu S, Dong H, Slabaugh G, Dragotti PL, Ye X, Liu F, Arridge S, Keegan J, Guo Y, Firmin D, Yang G. DAGAN: Deep De-Aliasing Generative Adversarial Networks for Fast Compressed Sensing MRI Reconstruction. *IEEE Trans Med Imaging* 2018; **37**: 1310-1321 [PMID: 29870361

DOI: 10.1109/TMI.2017.2785879]
47 **Shaul R**, David I, Shitrit O, Riklin Raviv T. Subsampled brain MRI reconstruction by generative adversarial neural networks. *Med Image Anal* 2020; **65**: 101747 [PMID: 32593933 DOI: 10.1016/j.media.2020.101747]
48 **Lv J**, Wang C, Yang G. PIC-GAN: A Parallel Imaging Coupled Generative Adversarial Network for Accelerated Multi-Channel MRI Reconstruction. *Diagnostics (Basel)* 2021; **11**: 61 [PMID: 33401777 DOI: 10.3390/diagnostics11010061]
49 **Cole EK**, Pauly JM, Vasanawala SS, Ong F. Unsupervised MRI Reconstruction with Generative Adversarial Networks. 2020 Preprint. Available from: arXiv: 2008.13065
50 **Yang Q**, Yan P, Zhang Y, Yu H, Shi Y, Mou X, Kalra MK, Sun L, Wang G. Low-Dose CT Image Denoising Using a Generative Adversarial Network With Wasserstein Distance and Perceptual Loss. *IEEE Trans Med Imaging* 2018; **37**: 1348-1357 [PMID: 29870364 DOI: 10.1109/TMI.2018.2827462]
51 **Arjovsky M**, Chintala S, Bottou L. Wasserstein GAN. 2017 Preprint. Available from: arXiv: 1701.07875
52 **Kuanar S**, Athitsos V, Mahapatra D, Rao KR, Akhtar Z, Dasgupta D. Low dose abdominal CT image reconstruction: An unsupervised learning based approach. IEEE International Conference on Image Processing (ICIP); 2019 Sept 22-25; Taipei, Taiwan. IEEE, 2019: 1351-1355 [DOI: 10.1109/ICIP.2019.8803037]
53 **Zhang J**, Gong LR, Yu K, Qi X, Wen Z, Hua QZ, Myint SH. 3D reconstruction for super-resolution CT images in the Internet of health things using deep learning. *IEEE Access* 2020; **8**: 121513-121525 [DOI: 10.1109/ACCESS.2020.3007024]
54 **Zhang T**, Jackson LH, Uus A, Clough JR, Story L, Rutherford MA, Hajnal JV, Deprez M. Self-supervised Recurrent Neural Network for 4D Abdominal and In-utero MR Imaging. In: International Workshop on Machine Learning for Medical Image Reconstruction. Springer, 2019: 16-24 [DOI: 10.1007/978-3-030-33843-5_2]
55 **Lv J**, Yang M, Zhang J, Wang X. Respiratory motion correction for free-breathing 3D abdominal MRI using CNN-based image registration: a feasibility study. *Br J Radiol* 2018; **91**: 20170788 [PMID: 29261334 DOI: 10.1259/bjr.20170788]
56 **Jiang WH**, Liu ZY, Lee KH, Chen SH, Ng YL, Dou Q, Chang HC, Kwok KW. Respiratory motion correction in abdominal MRI using a densely connected U-Net with GAN-guided training. 2019 Preprint. Available from: arXiv: 1906.09745
57 **Küstner T**, Pan JZ, Gilliam C, Qi HK, Cruz G, Hammernik K, Yang B, Blu T, Rueckert D, Botnar R, Prieto C, Gatidis S. Deep-learning based motion-corrected image reconstruction in 4D magnetic resonance imaging of the body trunk. 2020 Asia-Pacific Signal and Information Processing Association Annual Summit and Conference (APSIPA ASC); 2020 Dec 7-10; Auckland, New Zealand. IEEE, 2020: 976-985
58 **Akagi M**, Nakamura Y, Higaki T, Narita K, Honda Y, Zhou J, Yu Z, Akino N, Awai K. Deep learning reconstruction improves image quality of abdominal ultra-high-resolution CT. *Eur Radiol* 2019; **29**: 6163-6171 [PMID: 30976831 DOI: 10.1007/s00330-019-06170-3]
59 **Nakamura Y**, Higaki T, Tatsugami F, Zhou J, Yu Z, Akino N, Ito Y, Iida M, Awai K. Deep Learning-based CT Image Reconstruction: Initial Evaluation Targeting Hypovascular Hepatic Metastases. *Radiol Artif Intell* 2019; **1**: e180011 [PMID: 33937803 DOI: 10.1148/ryai.2019180011]
60 **Yaman B**, Hosseini SH, Moeller S, Ellermann J, Uğurbil K, Akcakaya M. Self-supervised physics-based deep learning MRI reconstruction without fully-sampled data. 2020 IEEE 17th International Symposium on Biomedical Imaging (ISBI); 2020 Apr 3-7; Iowa City, IA, United States. IEEE, 2020: 921-925 [DOI: 10.1109/ISBI45749.2020.9098514]
61 **Chen T**, Kornblith S, Norouzi M, Hinton G. A simple framework for contrastive learning of visual representations. Proceedings of the 37th International Conference on Machine Learning. 2020: 1597-1607
62 **Sun LY**, Fan ZW, Ding XH, Huang Y, Paisley J. Joint cs-mri reconstruction and segmentation with a unified deep network. In: Chung A, Gee J, Yushkevich P, Bao S. Information Processing in Medical Imaging. Springer, 2019: 492-504 [DOI: 10.1007/978-3-030-20351-1_38]
63 **Huang QY**, Yang D, Yi JR, Axel L, Metaxas D. FR-Net: Joint reconstruction and segmentation in compressed sensing cardiac MRI. In: Coudière Y, Ozenne V, Vigmond E, Zemzemi N. Functional Imaging and Modeling of the Heart. Springer, 2019: 352-360 [DOI: 10.1007/978-3-030-21949-9_38]

Published by **Baishideng Publishing Group Inc**
7041 Koll Center Parkway, Suite 160, Pleasanton, CA 94566, USA
Telephone: +1-925-3991568
E-mail: bpgoffice@wjgnet.com
Help Desk: https://www.f6publishing.com/helpdesk
https://www.wjgnet.com

ISSN 2644-3260 (online)

Artificial Intelligence in *Medical Imaging*

Artif Intell Med Imaging 2021 October 28; 2(5): 95-103

Published by Baishideng Publishing Group Inc

AIMI

Artificial Intelligence in Medical Imaging

Contents

Bimonthly Volume 2 Number 5 October 28, 2021

MINIREVIEWS

95 Artificial intelligence in ophthalmology and visual sciences: Current implications and future directions

Jahangir S, Khan HA

Artificial Intelligence in Medical Imaging

Bimonthly Volume 2 Number 5 October 28, 2021

Contents

ABOUT COVER

Editorial board member of *Artificial Intelligence in Medical Imaging*, Sarah Shafqat, MS, Academic Fellow, Research Scientist, Department of Basic and Applied Sciences, International Islamic University, Islamabad 44000, Pakistan

AIMS AND SCOPE

The primary aim of *Artificial Intelligence in Medical Imaging* (*AIMI*, *Artif Intell Med Imaging*) is to provide scholars and readers from various fields of artificial intelligence in medical imaging with a platform to publish high-quality basic and clinical research articles and communicate their research findings online.

AIMI mainly publishes articles reporting research results obtained in the field of artificial intelligence in medical imaging and covering a wide range of topics, including artificial intelligence in radiology, pathology image analysis, endoscopy, molecular imaging, and ultrasonography.

INDEXING/ABSTRACTING

There is currently no indexing.

RESPONSIBLE EDITORS FOR THIS ISSUE

NAME OF JOURNAL
Artificial Intelligence in Medical Imaging

ISSN
ISSN 2644-3260 (online)

LAUNCH DATE
June 28, 2020

FREQUENCY
Bimonthly

PUBLICATION DATE
October 28, 2021

Artificial Intelligence in Medical Imaging

Submit a Manuscript: https://www.f6publishing.com

Artif Intell Med Imaging 2021 October 28; 2(5): 95-103

DOI: 10.35711/aimi.v2.i5.95

ISSN 2644-3260 (online)

MINIREVIEWS

Artificial intelligence in ophthalmology and visual sciences: Current implications and future directions

Smaha Jahangir, Hashim Ali Khan

ORCID number: Smaha Jahangir 0000-0002-1745-766X; Hashim Ali Khan 0000-0002-6538-2033.

Author contributions: Jahangir S searched the literature and wrote the initial draft; Khan HA revised and edited the manuscript; both authors were involved in the basic idea and creating the outline of the review.

Conflict-of-interest statement: There is no conflict of interest among authors nor any source of bias towards this research.

Specialty type: Ophthalmology

Country/Territory of origin: Pakistan

Peer-review report's scientific

Smaha Jahangir, School of Optometry, The University of Faisalabad, Faisalabad, Punjab 38000, Pakistan

Hashim Ali Khan, Department of Ophthalmology, SEHHAT Foundation, Gilgit 15100, Gilgit-Baltistan, Pakistan

Corresponding author: Hashim Ali Khan, Department of Ophthalmology, SEHHAT Foundation, Main KKH, Danyore, Gilgit 15100, Gilgit-Baltistan, Pakistan. retinadr.hashimalikhan@gmail.com

Abstract

Since its inception in 1959, artificial intelligence (AI) has evolved at an unprecedented rate and has revolutionized the world of medicine. Ophthalmology, being an image-driven field of medicine, is well-suited for the implementation of AI. Machine learning (ML) and deep learning (DL) models are being utilized for screening of vision threatening ocular conditions of the eye. These models have proven to be accurate and reliable for diagnosing anterior and posterior segment diseases, screening large populations, and even predicting the natural course of various ocular morbidities. With the increase in population and global burden of managing irreversible blindness, AI offers a unique solution when implemented in clinical practice. In this review, we discuss what are AI, ML, and DL, their uses, future direction for AI, and its limitations in ophthalmology.

Key Words: Artificial intelligence; Ophthalmology; Retina; Machine learning; Eye care

Core Tip: Machine learning and artificial intelligence have evolved rapidly in recent years. Powerful machines and futuristic algorithms are bringing many possibilities towards the utilization of artificial intelligence in medical sciences. Ophthalmology is versatile in its adapting to newer and novel technologies earlier than other fields. Machine learning techniques assist clinicians and researchers in the detection and diagnosis of diseases as well as quantification of different disease biomarkers from ocular images. Interestingly, recent innovations like auto-machine learning has made it

quality classification
Grade A (Excellent): A
Grade B (Very good): 0
Grade C (Good): C
Grade D (Fair): D, D
Grade E (Poor): 0

Received: June 3, 2021
Peer-review started: June 3, 2021
First decision: June 23, 2021
Revised: June 30, 2021
Accepted: October 22, 2021
Article in press: October 27, 2021
Published online: October 28, 2021

P-Reviewer: Calabro F, Cheungpasitporn W, Saraiva MM
S-Editor: Liu M
L-Editor: Wang TQ
P-Editor: Liu M

possible for clinicians, with little knowledge in computing and mathematics, to partake in creating, modifying, and training models tailored to their area of interest.

Citation: Jahangir S, Khan HA. Artificial intelligence in ophthalmology and visual sciences: Current implications and future directions. *Artif Intell Med Imaging* 2021; 2(5): 95-103
URL: https://www.wjgnet.com/2644-3260/full/v2/i5/95.htm
DOI: https://dx.doi.org/10.35711/aimi.v2.i5.95

INTRODUCTION

Artificial intelligence (AI) refers to the ability of a machine to think independently. In 1956, it was first described by John McCarthy at his workshop in Darthmouth which is now considered as the birthplace of AI[1]. Later in 1959, Arthur Samuel defined machine learning (ML) as the ability of a machine to learn and improve with experience without being explicitly programmed[2,3].

The two major subfields of AI used in medicine are ML and deep learning (DL). ML derives information based on manually selected features and classifiers from already labeled data which is presented to the machine as a training dataset. This approach can be used with small datasets and requires comparatively shorter training time. In contrast, DL implements the use of artificial neural network (ANN) which is a complex system consisting of several layers of artificial neurons mimicking the neural network of human brain and its pattern recognition abilities. When input is provided to a DL algorithm, it is propagated through the multiple layers of the ANN and pattern recognition is performed by the DL algorithm itself without manual feature selection. Figure 1 illustrates the principle difference between ML and DL. The DL algorithms are fed large volumes of data containing both negative and positive examples (for instance, images of the healthy and diseased retina) for training. The algorithm autonomously trains itself and learns to recognize the differences between the two types of data, thus classifying it into positive and negative categories. The deep neural network (DNN) is a more efficient subtype of ANN in which the pattern recognition ability of the algorithm improves with the volume of training dataset. The larger the input data volume, the better the performance of the DNN at the given task. Another type of ANN is convolutional neural network (CNN) that has found its application in ophthalmology owing to its image recognition and classification ability. Although DL requires substantially larger training data and high computational power, the recent advances in technology and availability of graphics processing units have made its application in medicine and research more convenient[1-3].

For diagnosis and record-keeping, modern ophthalmology is dependent on imaging and large volumes of visual data are generated in the form of color fundus photographs (CFP) and scans from optical coherence tomography (OCT), OCT angiography, corneal topography, and other diagnostic procedures. The multimodal imaging approach allows the clinicians to view relevant structures in greater detail and provides them with useful information for decision-making in routine practice. The accurate processing of this large data volume can be cumbersome if efficient data processing methods are not accessible; however, its availability offers an optimal platform to bridge AI with ophthalmology as it is essential to analyze massive volumes of data for making data-driven decisions in the training of DL algorithms[4]. This review aims to summarize the applications of AI in ophthalmology, its limitations, and potential paths forward.

SCREENING FOR OCULAR DISEASES

With the increase in population, the burden of managing ocular disease has also increased. The need for regular follow-ups to timely detect and treat ocular adversities in the patients at risk can be challenging for the clinician as well as the patient. Diabetic retinopathy (DR), age-related macular degeneration (ARMD), and glaucoma are the leading causes of irreversible blindness worldwide. It has been estimated that 288 million people will suffer from ARMD while 600 million people will be affected by DR by the year 2040. The care of these disorders requires frequent follow-ups as the

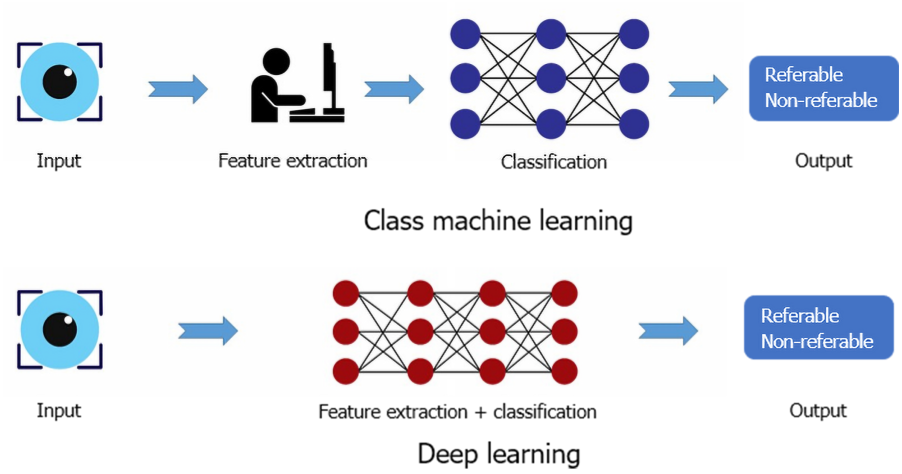

Figure 1 Outline of principle difference between machine learning and deep learning.

optimal time of treatment is at the early stage of the disease to prevent profound visual loss[5]. AI can play a huge role in the screening of ocular diseases in large populations where the care of an optometrist or ophthalmologist is not accessible to the masses. The screening of DR with the help of CFPs by utilizing AI has been well documented [6]. A summary of applications of AI in detection of various retinal diseases is given in Table 1. Moreover, studies have shown that DL can determine refractive errors from CFPs, which puts into perspective of how useful AI can be in extracting details from fundus images that are, otherwise, not discernable to human graders[7].

DIABETIC RETINOPATHY

DR is the most prevalent cause of irreversible blindness in adults. The progressive nature of the disease requires vigilant monitoring of the retina over time to initiate treatment as soon as possible. The early treatment of DR is the key to avoid visual impairment in the working-age groups which experience visual impairment or blindness by the ocular complications of diabetes mellitus (DM). Therefore, yearly follow-ups are required for the clinical examination of the eye in patients with DM, which presents a challenge to the ophthalmic community particularly in countries where medical services are not easily available to people. Moreover, about half of the patients fail to stick to their follow-up regimen[1,5]. To screen a large group of people and to keep efficient and timely follow-ups, AI can help reduce the burden by providing the convenience of quick analysis of large datasets[8].

The use of DL in ophthalmology has seen a rapid increase after its successful application for screening DR was reported in multiple papers in 2016[2]. Abràmoff *et al* [9] conducted a study in 2016 using a validation dataset of 1748 images and a DL algorithm to detect referable DR from CFPs. Their algorithm achieved an accuracy of 98% with a sensitivity of 96.8% and specificity of 87% in detecting vision threatening referable DR. In another study, Ting *et al*[6] trained an algorithm with a total of 494661 CFPs obtained from a population of ten various ethnic origin groups for detecting referable DR, ARMD, and glaucoma. In the validity dataset, the area under receiver operating curve (AUC), sensitivity, and specificity for referable DR were 0.936, 90.5%, and 91.6%; for vision-threatening DR were 0.958, 100%, and 91.1%; for possible glaucoma were 0.942, 96.4%, and 87.2%; and for ARMD were 0.931, 93.2%, and 88.7% respectively[6]. In 2018, inception V3, a DL algorithm, was trained by Li *et al*[10] with 58790 CFPs for the detection of DR. The model had an AUC of 0.989 with a sensitivity of 97% and specificity of 91.4%. It was also reported that 77.3% of false negatives were due to the undetected intraretinal microvascular abnormalities[10]. Son *et al*[11] developed a DL algorithm based on 103262 macula centered retinal photographs to detect hemorrhages, hard exudates, cotton-wool spots, macular hole, myelinated nerve fiber layer, chorioretinal atrophy, retinal nerve fiber layer (RNFL) defect, vascular abnormalities, glaucomatous disc change, and nonglaucomatous disc change. They reported that the DL accurately and reliably detected multiple abnormalities of the retina and recommended that DL could be used as a screening tool for routine clinical

Table 1 Summary of artificial intelligence applications in detection of suspected diabetic retinopathy, age related macular degeneration, and glaucoma

Ref.	Imaging modality	AI algorithm	Dataset for training	Dataset for validation	AUC	Sensitivity (%)	Specificity (%)
Diabetic retinopathy							
Abràmoff *et al*[9], 2016	CFP	AlexNet and VGGNet	10000 to 1250000 images	Messidor-2: 1748	0.980	96.8	87
Gulshan *et al*[29], 2016	CFP	Inception-V3	128175 images	EyePACS-1: 8788 Messidor-2: 1745	0.9910.990	97.596.1	93.493.9
Ting *et al*[6], 2017	CFP	VGG -19	76370 images	SiDRP: 71896 images	0.936	90.5	91.6
				Guangdong: 15798	0.949	98.7	81.6
				SIMES: 3052	0.889	97.1	82
				SINDI: 4512	0.917	99.3	73.3
				SCES: 1936	0.919	100	76.3
				BES: 1052	0.929	94.4	88.5
				AFEDS: 1968	0.98	98.8	86.5
				RVEEH: 2302	0.983	98.9	92.2
				MEXICAN: 1172	0.95	91.8	84.8
				CUHK: 1254	0.948	99.3	83.1
				HKU: 7706	0.964	100	81.3
Abràmoff *et al*[30], 2018	CFP	AlexNet and VGGNet	10000 to 1250000 images	819 patients	N/A	87.2	90.7
Li *et al*[10], 2018	CFP	Inception V3	58790 images	8000 images for referable DR	0.989	97	91.4
Ruamviboonsuk *et al*[31], 2019	CFP	Inception V4	1665151 images	25326 images	0.987	96.8	95.6
Son *et al*[11], 2020	CFP	Custom CNN	95350 images	Two data sets: IDRiD: 144 images &	0.957 to 0.980	88.9-92.6	94.0- 100
				e-ophtha: 434 images	0.947 to 0.965	89.2-93.6	91.4 - 97.1
Age related macular degeneration							
Ting *et al*[6], 2017	CFP	VGG-19	72610 images	35948 images	0.932	93.20	88.70
Lee *et al*[13], 2017	OCT scans - Spectralis	Modified VGG 16	80839 images	20163 images	0.974	92.64	93.69
Zapata *et al*[14], 2020	CFP	CNN 1 image type selection	53396	20% of training datasets	0.979	97.7	92.4
		CNN 1 CFP quality selection	150075		0.989	98.3	96.6
		CNN 1 OD/OS	30119		0.947	96.9	81.8
		AMDNET	8832		0.936	90.2	82.5
		Modified RESNET 50 (23) Referable GON	3776		0.863	76.8	83.8
Glaucoma suspect							
Ting *et al*[6], 2017	CFP	VGG-19	125189 images	71896 images	0.942	96.40	93.20
Li *et al*[18], 2018	CFP		31745 images	8000 images	0.986	95.6	92

CFP: Color fundus photographs; AUC: Area under curve; GON: Glaucomatous optic neuropathy; OCT: Optical coherence tomography; DR: Diabetic retinopathy; SiDRP: Singapore integrated diabetic retinopathy screening program; CNN: Convolutional neural network; VGG-19: Visual geometry group; CUHK: Chinese University Hong Kong; HKU: Hong Kong University; N/A: Not available; RVEEH: Royal Victorian Eye and Ear Hospital; SCES: Singapore Chinese Eye Study; SIMES: Singapore Malay Eye Study; SINDI: Singapore Indian Eye Study; BES: Beijing Eye Study; IDRiD: Indian Diabetic Retinopathy Image Dataset; AFEDS: African American Eye Disease Study.

practice[11]. The success of DL in detecting vision threatening DR shows that screening for DR can be carried out by utilizing AI in clinical practice, particularly, in the areas where direct access to an eye care provider is not available.

AGE-RELATED MACULAR DEGENERATION

ARMD is a progressive disease of the retina and is one of the major causes of irreversible blindness in developed countries. The early stage of the disease can stay quiescent for several years without causing any further visual deterioration; however, it can rapidly progress to advanced geographic atrophy (GA) or CNV. The development of CNV can cause profound visual loss if not treated at the earliest, which makes the observation of the at-risk population indispensable[1]. For the screening of ARMD, Venhuizen *et al*[12] trained an algorithm on 3256 OCT scans to identify five stages of ARMD: No ARMD, early ARMD, intermediate ARMD, advanced GA, and advanced CNV. On a test dataset of 384 OCT scans, the algorithm had a sensitivity of 98.2%, specificity of 91.2%, and AUC of 0.980, thus performing fairly well at the given task[12]. Lee *et al*[13] used 80839 OCT scans for the training of a DL model and 20163 scans as the validation dataset to detect ARMD and achieved an AUC of 0.974 with a sensitivity of 92.64% and specificity of 93.69%[13]. In 2020, Zapata *et al*[14] used 8832 CFPs as a training dataset to classify the images into three stages of ARMD as early ARMD, intermediate ARMD, and advanced ARMD. Their model achieved an AUC of 0.936 with a 90.2% sensitivity and 82.5% specificity[14].

Another potential use of AI is to predict visual acuity outcomes and disease progression. The visual acuity outcomes of patients being treated with anti-vascular endothelial growth factor treatment (Anti-VEGF) are rather erratic. If AI could help the clinician decide which patients will have good functional response post-therapy, it would reduce the burden of extra treatment. One such study was conducted by Schmidt-Erfurth *et al*[15] in which they trained a DL model over one year to predict visual acuity outcomes after Anti-VEGF therapy. The model was able to predict with a 71% accuracy[1].

As the course of ARMD progression is unpredictable in most cases, some studies have addressed this matter by applying AI in an attempt to predict the development of CNV. Schmidt-Erfurth *et al*[16] trained a model on 495 patients with intermediate ARMD in one eye and CNV in the fellow eye for 24 mo. The model was able to predict CNV development with an accuracy of 68% and development of GA with an accuracy of 80%[1]. Likewise, the progression of GA, its speed, and its course have also been investigated with the help of AI. Niu *et al*[17] reported a successful model trained for 2.25 years on 38 eyes for predicting GA progression. The model accurately projected the future direction of GA development. The major biomarkers that governed this prediction by the model were thinning of outer retinal layers and reticular pseudodrusen[17]. These studies show the benefits that implementation of AI in clinical practice can help in screening, management, and future prediction of disease progression. However, for the introduction of AI in routine practice, more research work is crucial in future by training the algorithms on larger datasets and studying their use in clinical practice.

GLAUCOMA

Glaucoma is a neurodegenerative disease that leads to irreversible loss of vision and is the second most prevalent cause of global blindness. The patient remains asymptomatic in the early stages of most types of glaucoma and only a comprehensive eye examination may detect the pathology. The diagnosis of glaucoma consists of optic nerve examination, visual field assessment (VFA), corneal thickness profile, anterior chamber assessment, and RNFL analysis. Owing to the lack of eye care professionals in developing countries and the limited availability of adjunct imaging devices, the

need of an AI model for screening the disease efficiently is inevitable[5]. Previous studies have focused on the diagnosis of glaucoma by implementation of AI with the c-d ratio of the optic disc, neuroretinal rim width, and ISNT rule; however, the diagnosis of glaucoma without VFA remains incomplete[1].

In 2018, Li *et al*[18] developed a DL system by training it on 48116 CFPs to detect referable glaucomatous optic neuropathy. Their algorithm achieved an AUC of 0.986, sensitivity of 95.6%, and specificity of 92%. The false-negative results obtained were due to high myopia, DR, and ARMD while the false positives were attributed to physiological cupping of the optic disc by the authors[18]. In another study, to diagnose glaucoma from VFA and RNFL thickness, Kim *et al*[19] trained and compared various ML approaches. They found that the random forest model gave the most accurate result with an AUC of 0.979, sensitivity of 0.983, and specificity of 0.975 while distinguishing between healthy and glaucomatous eyes[19]. A DL model was implemented on the macular RNFL thickness and ganglion cell complex layer thickness to diagnose open angle glaucoma by Asaoka *et al*[20]. The DL model had an AUC of 93.7%, whereas the AUC decreased to 82% and 67.4% with random forest and support vector model, respectively[20].

ANTERIOR SEGMENT DISORDERS

The growing use of imaging for anterior segment disease management and diagnosis has facilitated the application of AI in this area. Recent studies have shown that AI algorithms can successfully differentiate between keratoconic and normal eyes from the corneal topography scans. Reportedly, KeratoDirect, a CNN integrated algorithm, was trained on 3000 scans containing 50% healthy scans and 50% scans from keratoconic eyes. When tested on a final set of 200 eyes, it distinguished between the normal and ectatic eyes with a 99.3% success rate[2]. By using corneal SS-OCT scans of 3156 eyes, Yousefi *et al*[21] developed and trained an unsupervised algorithm that distinguished between normal and keratoconic corneas with a specificity of 97.4% and sensitivity of 96.3%. Moreover, the algorithm included a small number of normal eyes in the category of mild keratoconus which, according to the authors, represented form fruste keratoconus and needed further evaluation[21].

Owing to the development of Ocular Response Analyser and Corvis ST for the assessment of corneal biomechanics, it has become possible to evaluate the corneal ectatic disorders in greater detail. The development of Corvis, which used Scheimpflug camera with non-contact air-puff tonometer to evaluate the central 8mm horizontal cornea at a rate of 140 images per 33 ms, has yielded new parameters to study corneal ectasia. With the implementation of AI, Ambrosio *et al*[22] combined these parameters with corneal topographical data leading to the development of Tomographic and Biomechanical Index (TBI). TBI has not only detected the mild forms of corneal ectasia but it has also been suggested that TBI provided data about the susceptibility of the cornea to developing ectasia. It can play an important role in the pre-operative assessment for laser vision correction to rule out patients that might be at risk of developing postoperative complications[23,24]. AI has also been implemented in the grading of nuclear sclerosis. Recent studies have shown improvement in the grading of nuclear sclerosis from cross-sectional slit-lamp images of the lens with CNN as compared to its previous attempts[25].

FUTURE DIRECTIONS

The digital revolution has changed the pace of medicine globally. New treatments are being discovered and new investigative technologies are being introduced; meanwhile, the patients are growing older and co-morbidities are increasing. AI has been successfully integrated in the field of radiology and dermatology to make the decision-making process easier for clinicians. It has also been applied to screen people who cannot reach eye care services.

DR, ARMD, and glaucoma are the leading causes of blindness worldwide. These pathologies result in irreversible blindness which can be prevented if they are timely detected and treated. In rural areas and developing countries, there is a lack of eye care professionals and facilities. In future, the utilization of AI based screening strategies coupled with telemedicine can make it possible to screen the populations at risk in a time and cost- efficient manner. For the screening of DR, an FDA approved hybrid algorithm, IDx-DR, is currently in use to detect referable and non-referable

cases of DR[26]. Moreover, clinicians and researchers are working on training AI models by using larger datasets to enhance the already available models. Currently, an improved TBI model is in progress by training the model with bigger dataset[24].

BARRIERS

The process by which a DL algorithm learns pattern recognition from the training data remains largely unknown, which is often termed as the "black box", consequently making it harder for the researchers to understand how the algorithm reaches its final decision. Moreover, the process of troubleshooting and debugging becomes inexplicable unless the researcher becomes familiar with the ANN.

Although the multimodal approach in ophthalmology has helped in attaining large datasets of digital images, the easy access to the data of patients can pose ethical challenges. Furthermore, the digital data may also be subject to cyberattacks[1]. Despite the recent advances that AI has made in ophthalmology, most of the successful ML models have not been validated or used in actual clinical practices where the machine models, cameras, and image quality vary from each other. Therefore, further studies need to be done by testing these models in real-world settings[27]. Lastly, another limitation of AI is the use of two-dimensional images for the training of DL algorithms, which makes the detection of space-occupying and three-dimensional lesions impractical. In future, the inclusion of stereoscopic images in training and validation datasets might address this challenge[28].

CONCLUSION

AI has revolutionized the world of medicine and ophthalmology in recent years. The success of DL in detecting ophthalmic pathologies in recent years is well proven; however, its implementation in routine practice is rare. Future research is crucial to address the challenges and limitations of AI in order to make it a part of daily practice in eye clinics.

REFERENCES

1 **Schmidt-Erfurth U**, Sadeghipour A, Gerendas BS, Waldstein SM, Bogunović H. Artificial intelligence in retina. *Prog Retin Eye Res* 2018; **67**: 1-29 [PMID: 30076935 DOI: 10.1016/j.preteyeres.2018.07.004]

2 **Ting DSJ**, Foo VH, Yang LWY, Sia JT, Ang M, Lin H, Chodosh J, Mehta JS, Ting DSW. Artificial intelligence for anterior segment diseases: Emerging applications in ophthalmology. *Br J Ophthalmol* 2021; **105**: 158-168 [PMID: 32532762 DOI: 10.1136/bjophthalmol-2019-315651]

3 **Kapoor R**, Walters SP, Al-Aswad LA. The current state of artificial intelligence in ophthalmology. *Surv Ophthalmol* 2019; **64**: 233-240 [PMID: 30248307 DOI: 10.1016/j.survophthal.2018.09.002]

4 **Stagg BC**, Stein JD, Medeiros FA, Wirostko B, Crandall A, Hartnett ME, Cummins M, Morris A, Hess R, Kawamoto K. Special Commentary: Using Clinical Decision Support Systems to Bring Predictive Models to the Glaucoma Clinic. *Ophthalmol Glaucoma* 2021; **4**: 5-9 [PMID: 32810611 DOI: 10.1016/j.ogla.2020.08.006]

5 **Balyen L**, Peto T. Promising Artificial Intelligence-Machine Learning-Deep Learning Algorithms in Ophthalmology. *Asia Pac J Ophthalmol (Phila)* 2019; **8**: 264-272 [PMID: 31149787 DOI: 10.22608/APO.2018479]

6 **Ting DSW**, Cheung CY, Lim G, Tan GSW, Quang ND, Gan A, Hamzah H, Garcia-Franco R, San Yeo IY, Lee SY, Wong EYM, Sabanayagam C, Baskaran M, Ibrahim F, Tan NC, Finkelstein EA, Lamoureux EL, Wong IY, Bressler NM, Sivaprasad S, Varma R, Jonas JB, He MG, Cheng CY, Cheung GCM, Aung T, Hsu W, Lee ML, Wong TY. Development and Validation of a Deep Learning System for Diabetic Retinopathy and Related Eye Diseases Using Retinal Images From Multiethnic Populations With Diabetes. *JAMA* 2017; **318**: 2211-2223 [PMID: 29234807 DOI: 10.1001/jama.2017.18152]

7 **Varadarajan AV**, Poplin R, Blumer K, Angermueller C, Ledsam J, Chopra R, Keane PA, Corrado GS, Peng L, Webster DR. Deep Learning for Predicting Refractive Error From Retinal Fundus Images. *Invest Ophthalmol Vis Sci* 2018; **59**: 2861-2868 [PMID: 30025129 DOI: 10.1167/iovs.18-23887]

8 **Armstrong GW**, Lorch AC. A(eye): A Review of Current Applications of Artificial Intelligence and Machine Learning in Ophthalmology. *Int Ophthalmol Clin* 2020; **60**: 57-71 [PMID: 31855896 DOI: 10.1097/IIO.0000000000000298]

9 **Abràmoff MD**, Lou Y, Erginay A, Clarida W, Amelon R, Folk JC, Niemeijer M. Improved

Automated Detection of Diabetic Retinopathy on a Publicly Available Dataset Through Integration of Deep Learning. *Invest Ophthalmol Vis Sci* 2016; **57**: 5200-5206 [PMID: 27701631 DOI: 10.1167/iovs.16-19964]

10 **Li Z**, Keel S, Liu C, He Y, Meng W, Scheetz J, Lee PY, Shaw J, Ting D, Wong TY, Taylor H, Chang R, He M. An Automated Grading System for Detection of Vision-Threatening Referable Diabetic Retinopathy on the Basis of Color Fundus Photographs. *Diabetes Care* 2018; **41**: 2509-2516 [PMID: 30275284 DOI: 10.2337/dc18-0147]

11 **Son J**, Shin JY, Kim HD, Jung KH, Park KH, Park SJ. Development and Validation of Deep Learning Models for Screening Multiple Abnormal Findings in Retinal Fundus Images. *Ophthalmology* 2020; **127**: 85-94 [PMID: 31281057 DOI: 10.1016/j.ophtha.2019.05.029]

12 **Venhuizen FG**, van Ginneken B, van Asten F, van Grinsven MJJP, Fauser S, Hoyng CB, Theelen T, Sánchez CI. Automated Staging of Age-Related Macular Degeneration Using Optical Coherence Tomography. *Invest Ophthalmol Vis Sci* 2017; **58**: 2318-2328 [PMID: 28437528 DOI: 10.1167/iovs.16-20541]

13 **Lee CS**, Baughman DM, Lee AY. Deep learning is effective for the classification of OCT images of normal *vs* Age-related Macular Degeneration. *Ophthalmol Retina* 2017; **1**: 322-327 [PMID: 30693348 DOI: 10.1016/j.oret.2016.12.009]

14 **Zapata MA**, Royo-Fibla D, Font O, Vela JI, Marcantonio I, Moya-Sánchez EU, Sánchez-Pérez A, Garcia-Gasulla D, Cortés U, Ayguadé E, Labarta J. Artificial Intelligence to Identify Retinal Fundus Images, Quality Validation, Laterality Evaluation, Macular Degeneration, and Suspected Glaucoma. *Clin Ophthalmol* 2020; **14**: 419-429 [PMID: 32103888 DOI: 10.2147/OPTH.S235751]

15 **Schmidt-Erfurth U**, Bogunovic H, Sadeghipour A, Schlegl T, Langs G, Gerendas BS, Osborne A, Waldstein SM. Machine Learning to Analyze the Prognostic Value of Current Imaging Biomarkers in Neovascular Age-Related Macular Degeneration. *Ophthalmol Retina* 2018; **2**: 24-30 [PMID: 31047298 DOI: 10.1016/j.oret.2017.03.015]

16 **Schmidt-Erfurth U**, Waldstein SM, Klimscha S, Sadeghipour A, Hu X, Gerendas BS, Osborne A, Bogunovic H. Prediction of Individual Disease Conversion in Early AMD Using Artificial Intelligence. *Invest Ophthalmol Vis Sci* 2018; **59**: 3199-3208 [PMID: 29971444 DOI: 10.1167/iovs.18-24106]

17 **Niu S**, de Sisternes L, Chen Q, Rubin DL, Leng T. Fully Automated Prediction of Geographic Atrophy Growth Using Quantitative Spectral-Domain Optical Coherence Tomography Biomarkers. *Ophthalmology* 2016; **123**: 1737-1750 [PMID: 27262765 DOI: 10.1016/j.ophtha.2016.04.042]

18 **Li Z**, He Y, Keel S, Meng W, Chang RT, He M. Efficacy of a Deep Learning System for Detecting Glaucomatous Optic Neuropathy Based on Color Fundus Photographs. *Ophthalmology* 2018; **125**: 1199-1206 [PMID: 29506863 DOI: 10.1016/j.ophtha.2018.01.023]

19 **Kim SJ**, Cho KJ, Oh S. Development of machine learning models for diagnosis of glaucoma. *PLoS One* 2017; **12**: e0177726 [PMID: 28542342 DOI: 10.1371/journal.pone.0177726]

20 **Asaoka R**, Murata H, Hirasawa K, Fujino Y, Matsuura M, Miki A, Kanamoto T, Ikeda Y, Mori K, Iwase A, Shoji N, Inoue K, Yamagami J, Araie M. Using Deep Learning and Transfer Learning to Accurately Diagnose Early-Onset Glaucoma From Macular Optical Coherence Tomography Images. *Am J Ophthalmol* 2019; **198**: 136-145 [PMID: 30316669 DOI: 10.1016/j.ajo.2018.10.007]

21 **Yousefi S**, Yousefi E, Takahashi H, Hayashi T, Tampo H, Inoda S, Arai Y, Asbell P. Keratoconus severity identification using unsupervised machine learning. *PLoS One* 2018; **13**: e0205998 [PMID: 30399144 DOI: 10.1371/journal.pone.0205998]

22 **Ambrósio R Jr**, Lopes BT, Faria-Correia F, Salomão MQ, Bühren J, Roberts CJ, Elsheikh A, Vinciguerra R, Vinciguerra P. Integration of Scheimpflug-Based Corneal Tomography and Biomechanical Assessments for Enhancing Ectasia Detection. *J Refract Surg* 2017; **33**: 434-443 [PMID: 28681902 DOI: 10.3928/1081597X-20170426-02]

23 **Baptista PM**, Marta AA, Marques JH, Abreu AC, Monteiro S, Menéres P, Pinto MDC. The Role of Corneal Biomechanics in the Assessment of Ectasia Susceptibility Before Laser Vision Correction. *Clin Ophthalmol* 2021; **15**: 745-758 [PMID: 33642854 DOI: 10.2147/OPTH.S296744]

24 **Esporcatte LPG**, Salomão MQ, Lopes BT, Vinciguerra P, Vinciguerra R, Roberts C, Elsheikh A, Dawson DG, Ambrósio R Jr. Biomechanical diagnostics of the cornea. *Eye Vis (Lond)* 2020; **7**: 9 [PMID: 32042837 DOI: 10.1186/s40662-020-0174-x]

25 **Gao X**, Lin S, Wong TY. Automatic Feature Learning to Grade Nuclear Cataracts Based on Deep Learning. *IEEE Trans Biomed Eng* 2015; **62**: 2693-2701 [PMID: 26080373 DOI: 10.1109/TBME.2015.2444389]

26 **Moraru AD**, Costin D, Moraru RL, Branisteanu DC. Artificial intelligence and deep learning in ophthalmology - present and future (Review). *Exp Ther Med* 2020; **20**: 3469-3473 [PMID: 32905155 DOI: 10.3892/etm.2020.9118]

27 **Tan Z**, Scheetz J, He M. Artificial Intelligence in Ophthalmology: Accuracy, Challenges, and Clinical Application. *Asia Pac J Ophthalmol (Phila)* 2019; **8**: 197-199 [PMID: 31179666 DOI: 10.22608/APO.2019122]

28 **Ting DSW**, Pasquale LR, Peng L, Campbell JP, Lee AY, Raman R, Tan GSW, Schmetterer L, Keane PA, Wong TY. Artificial intelligence and deep learning in ophthalmology. *Br J Ophthalmol* 2019; **103**: 167-175 [PMID: 30361278 DOI: 10.1136/bjophthalmol-2018-313173]

29 **Gulshan V**, Peng L, Coram M, Stumpe MC, Wu D, Narayanaswamy A, Venugopalan S, Widner K, Madams T, Cuadros J, Kim R, Raman R, Nelson PC, Mega JL, Webster DR. Development and Validation of a Deep Learning Algorithm for Detection of Diabetic Retinopathy in Retinal Fundus

Photographs. *JAMA* 2016; **316**: 2402-2410 [PMID: 27898976 DOI: 10.1001/jama.2016.17216]

30 **Abràmoff MD**, Lavin PT, Birch M, Shah N, Folk JC. Pivotal trial of an autonomous AI-based diagnostic system for detection of diabetic retinopathy in primary care offices. *NPJ Digit Med* 2018; **1**: 39 [PMID: 31304320 DOI: 10.1038/s41746-018-0040-6]

31 **Ruamviboonsuk P**, Krause J, Chotcomwongse P, Sayres R, Raman R, Widner K, Campana BJL, Phene S, Hemarat K, Tadarati M, Silpa-Archa S, Limwattanayingyong J, Rao C, Kuruvilla O, Jung J, Tan J, Orprayoon S, Kangwanwongpaisan C, Sukumalpaiboon R, Luengchaichawang C, Fuangkaew J, Kongsap P, Chualinpha L, Saree S, Kawinpanitan S, Mitvongsa K, Lawanasakol S, Thepchatri C, Wongpichedchai L, Corrado GS, Peng L, Webster DR. Erratum: Author Correction: Deep learning *vs* human graders for classifying diabetic retinopathy severity in a nationwide screening program. *NPJ Digit Med* 2019; **2**: 68 [PMID: 31341955 DOI: 10.1038/s41746-019-0146-5]

Published by **Baishideng Publishing Group Inc**
7041 Koll Center Parkway, Suite 160, Pleasanton, CA 94566, USA
Telephone: +1-925-3991568
E-mail: bpgoffice@wjgnet.com
Help Desk: https://www.f6publishing.com/helpdesk
https://www.wjgnet.com

ISSN 2644-3260 (online)

Artificial Intelligence in *Medical Imaging*

Artif Intell Med Imaging 2021 December 28; 2(6): 104-117

Published by Baishideng Publishing Group Inc

AIMI

Artificial Intelligence in Medical Imaging

Contents

Bimonthly Volume 2 Number 6 December 28, 2021

MINIREVIEWS

104 Application of machine learning in oral and maxillofacial surgery

Yan KX, Liu L, Li H

LETTER TO THE EDITOR

115 Pictorial research of pancreas with artificial intelligence and simulacra in the works of Fellini

Tahara H

Artificial Intelligence in Medical Imaging

Bimonthly Volume 2 Number 6 December 28, 2021

Contents

ABOUT COVER

Editorial Board Member of *Artificial Intelligence in Medical Imaging*, Sarasa Cabezuelo, PhD, Professor, Department of Information Systems and Computing, Complutense University of Madrid, Calle Profesor José García Santesmases, Madrid 28040, Spain. asarasa@ucm.es

AIMS AND SCOPE

The primary aim of *Artificial Intelligence in Medical Imaging* (*AIMI*, *Artif Intell Med Imaging*) is to provide scholars and readers from various fields of artificial intelligence in medical imaging with a platform to publish high-quality basic and clinical research articles and communicate their research findings online.

AIMI mainly publishes articles reporting research results obtained in the field of artificial intelligence in medical imaging and covering a wide range of topics, including artificial intelligence in radiology, pathology image analysis, endoscopy, molecular imaging, and ultrasonography.

INDEXING/ABSTRACTING

There is currently no indexing.

RESPONSIBLE EDITORS FOR THIS ISSUE

Production Editor: *Ying-Yi Yuan*; **Production Department Director:** *Xu Guo*; **Editorial Office Director:** *Yun-Xiaojiao Wu*.

NAME OF JOURNAL
Artificial Intelligence in Medical Imaging

ISSN
ISSN 2644-3260 (online)

LAUNCH DATE
June 28, 2020

FREQUENCY
Bimonthly

EDITORS-IN-CHIEF
Xue-Li Chen, Caroline Chung, Jun Shen

EDITORIAL BOARD MEMBERS
https://www.wjgnet.com/2644-3260/editorialboard.htm

PUBLICATION DATE
December 28, 2021

INSTRUCTIONS TO AUTHORS
https://www.wjgnet.com/bpg/gerinfo/204

GUIDELINES FOR ETHICS DOCUMENTS
https://www.wjgnet.com/bpg/GerInfo/287

GUIDELINES FOR NON-NATIVE SPEAKERS OF ENGLISH
https://www.wjgnet.com/bpg/gerinfo/240

PUBLICATION ETHICS
https://www.wjgnet.com/bpg/GerInfo/288

PUBLICATION MISCONDUCT
https://www.wjgnet.com/bpg/gerinfo/208

ARTICLE PROCESSING CHARGE
https://www.wjgnet.com/bpg/gerinfo/242

STEPS FOR SUBMITTING MANUSCRIPTS
https://www.wjgnet.com/bpg/GerInfo/239

ONLINE SUBMISSION
https://www.f6publishing.com

Artificial Intelligence in Medical Imaging

Submit a Manuscript: https://www.f6publishing.com

Artif Intell Med Imaging 2021 December 28; 2(6): 104-114

DOI: 10.35711/aimi.v2.i6.104

ISSN 2644-3260 (online)

MINIREVIEWS

Application of machine learning in oral and maxillofacial surgery

Kai-Xin Yan, Lei Liu, Hui Li

ORCID number: Kai-Xin Yan 0000-0002-1041-494X; Lei Liu 0000-0001-5309-1979; Hui Li 0000-0001-6841-2229.

Author contributions: Yan KX, Liu L, and Li H contributed to drafting the paper; Yan KX and Liu L contributed to the literature review; Yan KX wrote this paper as the first author; Li H contributed to critical revision and editing of the manuscript, and gave approval to the final version as the corresponding author.

Conflict-of-interest statement: There is no conflict of interest associated with any of the senior author or other coauthors who contributed their efforts in this manuscript.

Supported by National Natural Science Foundation of China, No. 82100961.

Country/Territory of origin: China

Specialty type: Dentistry, oral surgery and medicine

Provenance and peer review: Invited article; Externally peer reviewed.

Peer-review model: Single blind

Peer-review report's scientific quality classification

Grade A (Excellent): 0

Grade B (Very good): 0

Grade C (Good): C

Kai-Xin Yan, Lei Liu, Hui Li, State Key Laboratory of Oral Diseases & National Clinical Research Center for Oral Diseases & Department of Oral and Maxillofacial Surgery, West China Hospital of Stomatology, Sichuan University, Chengdu 610041, Sichuan Province, China

Corresponding author: Hui Li, MD, PhD, Assistant Professor, State Key Laboratory of Oral Diseases & National Clinical Research Center for Oral Diseases & Department of Oral and Maxillofacial Surgery, West China Hospital of Stomatology, Sichuan University, No. 14 Section 3 Renminnan Road, Chengdu 610041, Sichuan Province, China. 475393040@qq.com

Abstract

Oral and maxillofacial anatomy is extremely complex, and medical imaging is critical in the diagnosis and treatment of soft and bone tissue lesions. Hence, there exists accumulating imaging data without being properly utilized over the last decades. As a result, problems are emerging regarding how to integrate and interpret a large amount of medical data and alleviate clinicians' workload. Recently, artificial intelligence has been developing rapidly to analyze complex medical data, and machine learning is one of the specific methods of achieving this goal, which is based on a set of algorithms and previous results. Machine learning has been considered useful in assisting early diagnosis, treatment planning, and prognostic estimation through extracting key features and building mathematical models by computers. Over the past decade, machine learning techniques have been applied to the field of oral and maxillofacial surgery and increasingly achieved expert-level performance. Thus, we hold a positive attitude towards developing machine learning for reducing the number of medical errors, improving the quality of patient care, and optimizing clinical decision-making in oral and maxillofacial surgery. In this review, we explore the clinical application of machine learning in maxillofacial cysts and tumors, maxillofacial defect reconstruction, orthognathic surgery, and dental implant and discuss its current problems and solutions.

Key Words: Radiography; Artificial intelligence; Machine learning; Deep learning; Oral surgery; Maxillofacial surgery

Core Tip: A dramatic increase in medical imaging data has exceeded the ability of clinicians to process and analyze, which calls for higher-level analytic tools. Machine

Grade D (Fair): 0
Grade E (Poor): 0

Received: December 7, 2021
Peer-review started: December 7, 2021
First decision: December 13, 2021
Revised: December 20, 2021
Accepted: December 28, 2021
Article in press: December 28, 2021
Published online: December 28, 2021

P-Reviewer: Anysz H
S-Editor: Liu M
L-Editor: Wang TQ
P-Editor: Liu M

learning-based image analysis is useful for extracting key information to improve diagnostic accuracy and treatment efficacy. In this review, we summarize the applications of machine learning in oral and maxillofacial surgery as well as its current problems and solutions.

Citation: Yan KX, Liu L, Li H. Application of machine learning in oral and maxillofacial surgery. *Artif Intell Med Imaging* 2021; 2(6): 104-114
URL: https://www.wjgnet.com/2644-3260/full/v2/i6/104.htm
DOI: https://dx.doi.org/10.35711/aimi.v2.i6.104

INTRODUCTION

The oral and maxillofacial region is extremely complex, including many critical anatomical structures such as the maxillofacial bone, parotid gland, facial nerve, and major vessels. Computed tomography (CT), magnetic resonance imaging (MRI; an imaging technique mainly used for the examination of soft tissue), and other radiological examinations are commonly applied to improve the understanding of the three-dimensional spatial positional relationships among these anatomical structures. It is unavoidable to face rapid growth in the amount and complexity of medical imaging data, leading to increased workload for clinicians[1-2].

In recent years, artificial intelligence (AI) has been implemented in medicine to explore these enormous datasets and extract key information[1,3]. AI is a field focused on completing intellectual tasks normally performed by humans, and machine learning (ML) is one of the specific methods of achieving this goal[4]. AI models based on ML algorithms have demonstrated excellent performance in imaging data extraction and analysis and have increasingly matched specialist performance in medical imaging applications[5]. The integration of ML in oral and maxillofacial surgery has been proved to improve diagnostic accuracy, treatment efficacy, and prognostic estimation and reduce health care costs[6,7]. The purpose of this review is to explore the clinical application of ML in maxillofacial cysts and tumors, maxillofacial defect reconstruction, orthognathic surgery, and dental implant and discuss the current problems and solutions.

Arthur Samuel[6-8] first described the term ML in 1952. ML is a technique to build prediction outcomes by statistical algorithms learning from experience. According to the training types of the algorithms, ML can be divided into three categories: Supervised, unsupervised, and reinforcement learning[9]. Currently, supervised learning is the most commonly used training style in medical image analysis[10].

In supervised learning, labels are inputted simultaneously with the training data and then algorithms predict the known outcome[10]. Examples of supervised learning methods include classic Naive Bayes, decision tree (DF), support vector machine (SVM), random forest (RF), logistic regression, artificial neural network (ANN), and deep learning (DL). Specifically, SVM results in data classification by setting up an imaginary high-dimensional space and then separating labeled samples by a hyperplane[4,11]. RF is an extension of DF, in which each DF is independently trained and subsequently combined with others[4,12]. ANN has one hidden layer in addition to the input and output layer. Each layer is composed of neurons and sequentially stacked one after the other *via* weighted connections. The signals are transformed among neurons from the previous layer to the next and DL is comprised of multi-layered ANN[13].

In unsupervised learning[10], the algorithm system will not be provided with labels but depends on itself for the detection of the hidden patterns in the data. Examples of algorithms of unsupervised learning include K-means, affinity propagation, and fuzzy C-means systems. Besides, reinforcement learning[14] holds a system including unlabeled data, agent, and environment. It aims to repeatedly optimize parameters based on environmental feedback through reward and punishment mechanisms. By accumulating the rewards, the models can keep adapting to the changing environment and obtaining the best return. Examples of reinforcement learning algorithms include Maja and Teaching-Box systems.

The protocol of ML comprises data procession and model construction, and the workflow of the model construction can be further divided into the training phase and

the validating/testing phase. Due to the impact of data volume and quality on the performance of machine-learning models, raw data should be standardized in advance for the following aspects: (1) Reducing noise without losing the important features [15]; (2) Splitting the image into parts and delineating the region of interest; and (3) Accumulating enough data[16]. Effective methods have been proposed for achieving the tasks, including image denoising, segment, and augment[15,17-20].

APPLICATION IN ORAL AND MAXILLOFACIAL SURGERY

Maxillofacial cystic lesions and benign tumors

Maxillofacial cysts and benign tumors are common lesions in the oral and maxillofacial region. In most cases, maxillofacial cysts and benign tumors cause facial swelling, tooth displacement, large bone cavity, and even pathological fracture when diagnosed. Surgery is the only treatment option, including enucleation, decompression, and resection. And the choice of treatment modality is based on the final diagnosis, lesion size, and age of selected patients. However, these lesions are asymptomatic at the early stage. Consequently, early detection and diagnosis of maxillofacial cysts and benign tumors are crucial for avoiding serious surgery and achieving satisfactory treatment outcomes[21,22]. Numerous studies have demonstrated the usefulness of ML in early screening, accurate diagnosis, proper treatment, and morbidity prevention in maxillofacial cysts and benign tumors.

Frydenlund *et al*[23] applied two ML classifiers (a SVM and bagging with logistic regression) to distinguish among lateral periodontal cysts, odontogenic keratocysts, and glandular odontogenic cysts in hematoxylin and eosin-stained digital micrographs. The results proved the effectiveness of the ML-based classifiers in predicting these three types of odontogenic cysts (96.2% correct classification for both classifiers). Moreover, Okada *et al*[24] demonstrated the usefulness of a semiautomatic computer-aided diagnosis framework to differentiate between periapical cysts and granulomas in cone-beam CT (CBCT) data. And the 94.1% best accuracy was yielded with the integration of graph-based random walks segmentation and ML-based boosted classification algorithms. Similarly, Endres *et al*[25] compared the performance of the DL algorithm with that of 24 oral and maxillofacial surgeons in detecting periapical radiolucencies in panoramic radiographs, demonstrating the reliable diagnoses of ML algorithms in dentistry. In addition, Kwon *et al*[26] developed a deep convolution neural network (DCNN) to automatically diagnose jaw odontogenic cysts and tumors in panoramic images, showing higher diagnostic sensitivity, specificity, and accuracy with augmented datasets. Liu *et al*[27] applied deep transfer learning to classify ameloblastoma and odontogenic keratocyst in panoramic radiographs and achieved an accuracy of 90.36%. Yang *et al*[28] also showed that the diagnostic performance of CNN You OnlyLook Once v2 was similar to that of experienced dentists in detecting odontogenic cysts and tumors on panoramic radiographs.

Maxillofacial malignant tumors

Oral cancer is the most common malignancy in the oral and maxillofacial region, which can exert a severe impact on the survival and quality of life of the patients[29]. The most effective method for reducing mortality rates is early detection. However, the optimal strategy for early screening remains debated. The advent of high-quality ML provides potential to improve early diagnosis, prognostic evaluation, and accurate prediction of treatment associated toxicity in oral cancer patients.

Aubreville *et al*[30] presented a novel automatic identification of oral squamous cell carcinoma (OSCC) in confocal laser endomicroscopy images, using a deep ANN. The accuracy of this deep ANN-based method was 88.3%, with a sensitivity of 86.6% and specificity of 90%. It outperformed textural feature-based classification. DL algorithms, including the DenseNet121 and faster R-CNN algorithm, have also been applied to automatically classify and detect oral cancer in photographic images, achieving acceptable precision[31]. Furthermore, Kar *et al*[29] and Jeyaraj and Samuel Nadar[32] developed regression-based partitioned CNN using hyperspectral image datasets for automated detecting oral cancer, obtaining improved quality of diagnosis compared to traditional image classifiers including the SVM and the deep belief network.

In addition, ML has also been applied to predict cancer outcomes using the following prognostic variables: (1) Histological grade; (2) Five-year survival; (3) Cervical lymph node metastases; and (4) Distant metastasis. Ren *et al*[33] included 80 patients finally diagnosed with OSCC and performed ML-based MRI texture analysis using a minimum-redundancy maximum-relevance algorithm, achieving the best

performance with an accuracy of 86.3%. Others also concluded that the predictive performance of DL-based survival prediction algorithms exceeded that of conventional statistical methods[34-38]. Chu *et al*[17] and Ariji *et al*[39] have achieved a DL accuracy of extranodal extension of 84% on 703 CT images. The diagnostic performance outranked that of radiologists. Others also proved the effectiveness of ML in predicting lymph node metastasis in patients with early-stage oral cancer and thus guiding proper treatment plans[32,40,41]. Keek *et al*[42] found that compared with peritumoral radiomics based prediction models, a clinical model was useful for the prediction of distant metastasis in oropharyngeal cancer patients.

ML also contributes to the evaluation of treatment complications. Chu *et al*[17] and Men *et al*[43] have introduced a 3D residual CNN for the prediction of xerostomia in patients with head and neck cancer and achieved satisfying performance with an area under the curve value of 0.84 (0.74-0.91), an index for reflecting the authenticity of the detection method (the closer the numerical value to 1.0, the higher the authenticity of the detection method).

Nasopharyngeal carcinoma is a malignancy of the head and neck, and radiotherapy is the primary treatment option for the suffered patients[44]. To avoid unnecessary toxicities derived from radiotherapy, radiation oncologists propose the concepts of precise radiotherapy and adaptive radiotherapy. Recently, advanced ML techniques have mainly been applied to auto-recognition, early diagnosis, target contouring, and complication prediction in patients with nasopharyngeal carcinoma[45].

Li *et al*[46] developed an endoscopic image-based model to detect nasopharyngeal malignancies. And this DL model outperformed experts in detecting malignancies. Du *et al*[47] investigated the diagnostic performance of seven ML classifiers cross-combined with six feature selection methods for distinguishing inflammation and recurrence based on post-treatment nasopharyngeal positron emission tomography/X-ray CT images (a high-level imaging method that can make an early diagnosis of tumors) and identified the optimal methods in the diagnosis of nasopharyngeal carcinoma.

Lin *et al*[48] constructed a 3D CNN on MRI data sets and validated the performance of automated primary gross tumor (GTV) contouring in patients with nasopharyngeal carcinoma, demonstrating improved contouring accuracy and efficacy with the assistance of a DL-based contouring tool. Men *et al*[49] proposed an end-to-end deep deconvolutional neural network for segmentation of nasopharyngeal carcinoma in planning CT images, showing a high-level performance than that of the VGG-16 model in the segmentation of the nasopharynx GTV, the metastatic lymph node GTV, and the clinical target volume. In addition, Liang *et al*[44] developed a fully automated DL-based method for the accurate detection and segmentation of organs at risk in nasopharyngeal carcinoma CT images and achieved excellent performance. The results showed a sensitivity of 0.997 to 1 and specificity of 0.983 to 0.999. For early detecting the radiotherapy complication in nasopharyngeal carcinoma patients, Zhang *et al*[50] applied the RF method to early predict radiation-induced temporal lobe injury (RTLI) based on MRI examinations. The results demonstrated that the RF models can successfully predict RTLI in advance, which can allow clinicians to take measures to stop or slow down the deterioration of RTLI.

Altogether, ML techniques have been shown well-performed in early screening and prognosis evaluation of maxillofacial malignant tumors.

Maxillofacial bone defect reconstruction

Maxillofacial bone defects after congenital deformities, trauma, and oncological resection greatly decrease patients' quality of life. The goal of reconstruction of maxillofacial bone defects is to restore optimal function and facial appearance using free tissue, vascularized autogenous bone flap transplantation, or prostheses. Maxillofacial reconstructive surgery remains challenging, especially in the cases of massive maxillofacial bone defects across the midline. Most recently, ML algorithms have achieved major success in virtual surgical planning and thus posed great potential in the reconstruction of facial defects.

Jie *et al*[51] proposed an iterative closest point (ICP) algorithm based on normal people database (a database comprised of normal and healthy adults) to predict the reference data of missing bone and performed symmetry evaluation between the postoperative skull and its mirrored model. The result showed that the ICP model achieved similar accuracy to that of navigation-guided surgery. Dalvit Carvalho da Silva *et al*[52] combined CNN with geometric moments to identify the midline symmetry plane of the facial skeleton from CT scans, which aided the surgeons in the maxillofacial reconstructive surgery.

With the development of an imaging database, ML is a promising tool to assist the maxillofacial bone defect reconstruction.

Orthognathic surgery

Orthognathic surgery is used for the treatment of dental malocclusion, facial deformities, and obstructive sleep apnea to improve facial aesthetics and function. Traditionally, surgical planning is based on clinical examination, two-dimensional cephalometric analysis, and manually made splints. However, these procedures require considerable labor efforts and lack precision[53-56]. With the rapid development of technologies and materials, 3D printers, digital software, and ML are increasingly used in orthognathic surgery and greatly improve surgical outcomes. Hence, the applications of ML are promising in orthognathic surgery.

According to the study of Shin *et al*[57], the authors extracted the features from posteroanterior and lateral cephalogram and evaluated the necessity for orthognathic surgery using DL networks. The results showed that the accuracy, sensitivity, and specificity were 0.954, 0.844, and 0.993, respectively, proving the excellent performance. Lin *et al*[58] used a CNN with a transfer learning approach on 3D CBCT images for the assessment of the facial symmetry before and after orthognathic surgery. In a retrospective cohort study, Lo *et al*[59] first applied a ML model based on the 3D contour images to automatically assess the facial symmetry before and after orthognathic surgery. According to the study by Knoops *et al*[60], a 3D morphable model, a ML-based framework involving supervised learning, was trained with 4216 3D scans of healthy volunteers and orthognathic surgery patients. The model showed high diagnostic accuracy with a sensitivity of 95.5% and specificity of 95.2%, satisfying treatment simulation. In addition, Patcas *et al*[61] demonstrated that patients' facial appearance and attractiveness improved after orthognathic surgery using a CNN model.

To sum up, ML has been considered a useful tool in orthognathic surgery for establishing a precise diagnosis, evaluating surgical necessity, and predicting treatment outcomes.

Dental implant

The dental implant has been considered a reliable treatment option for the replacement of missing teeth. Undoubtedly, an excellent bone environment and implant planning are key to the success rate of dental implants. It is crucial to have a basic understanding of the quality and quantity of bone at the planned site and site of placement[62]. In recent decades, ML is growing in the field of dental implants and its use has been applied to improve the success rate of implants and identify dental implants.

Kurt *et al*[63] applied a DL approach on three-dimensional CBCT images to perform implant planning and compared the performance of this method with manual assessment, achieving similarly acceptable results in the measurements in the maxilla molar/premolar region, as well as in the mandible premolar region. A pilot study by Ha *et al*[64] demonstrated that the mesiodistal position of the inserted implant is the most significant factor predicting implant prognosis using ML methods.

Besides, Lee *et al*[65] evaluated the performance of three different DCNN architectures for the detection and classification of a fractured dental implant using panoramic and periapical radiographic images. The results showed the best performance by the automated DCNN architecture based on only periapical images. Mameno *et al*[66] applied three ML methods for the prediction of peri-implantitis and analyzed the risk indicators. RF model achieved the highest performance in the prediction. And the results demonstrated that implant functional time influenced most on prediction.

In addition, several investigations proved the effectiveness of ML methods for implant type recognition using radiographic images[67-69]. As for the application of ML models for implant design optimization, Roy *et al*[70] used an ANN combined with genetic algorithms for the prediction of the optimum implant dimension.

ML models have demonstrated great potential in the field of dental implants for assisting implant planning, evaluating implant performance, improving implant designs, and identifying dental implants.

PROBLEMS AND SOLUTIONS

ML has shown great potential in the field of oral and maxillofacial surgery for

Table 1 Machine learning applications in oral and maxillofacial surgery

Ref.	Applications	Purpose	Method
[23]	Maxillofacial cystic lesions and benign tumors	Accurate diagnosis	A support vector machine and bagging with logistic regression
[24]			Integration of graph-based random walks segmentation and machine learning-based boosted classification algorithms
[26]			Deep convolution neural network
[27]			Deep transfer learning
[28]			Convolution neural work You OnlyLook Once v2's
[25]		Early detection	Deep learning
[30]	Maxillofacial malignant tumors	Early diagnosis	Deep artificial neural network
[31]			Deep learning (DenseNet121 and faster R-Convolution neural work)
[29, 32]			Regression-based partitioned convolution neural network
[46]			Deep learning
[47]			Machine learning
[48]		Early detection	Convolution neural network
[49]			End-to-end deep deconvolutional neural network
[44]			Deep learning
[33]		Prognosis estimation	Minimum-redundancy maximum-relevance algorithm
[34-39]			Deep learning
[40-42]			Machine learning
[43]		Treatment complication evaluation	Convolution neural network
[50]			Random forest
[51]	Maxillofacial bone defect reconstruction	Missing bone prediction and facia symmetry evaluation	Iterative closest point
[52]		Midline symmetry plane identification	Convolution neural network
[57]	Orthognathic surgery	Surgery necessity evaluation	Deep learning
[58]		Facial symmetry assessment	Convolution neural network
[59]			Machine learning
[60]		Diagnosis	Machine learning
[61]		Facial appearance and attractiveness evaluation	Convolution neural network
[63]	Dental implant	Implant planning designing	Deep learning
[70]		Implant planning optimizing	Artificial neural network
[64]		Prognosis estimation	Machine learning
[65]		Detection and classification of fractured dental implant	Deep convolution neural network
[66]		Complicationprediction	Machine learning
[67-69]		Implant type recognition	Machine learning

improving detection accuracy, optimizing treatment plans, and providing reliable prognostic prediction. Despite all the potential, there still exist some limitations.

First, the performance of ML mainly depends on the volume and quality of data and superior algorithms. The scattered distribution of dental databases across healthcare settings often leads to the problem of relatively small datasets, exerting an impact on real clinical decision-making. Efforts should be made for the development of cloud-

based image databases and large open-access databases from diverse settings and populations[71].

Second, it is quite difficult for ML to analyze a large number of different and heterogeneous datasets. A set of well-standardized, segmented, and enhanced training data will enhance the performance of the ML model. Thus, the involved data should get properly pre-processed for maximally achieving homogenization of the data sets and reducing errors[15,17,72].

Third, the performance of ML algorithms in completing various common clinical tasks is similar to or outmatches that of experts. However, when dealing with cases of rare and complicated diseases, existing algorithms may have inferior performance[73, 74]. Consequently, further improvement of ML algorithms is required for computing enormous and complex medical data.

Lastly, there exist many ethical challenges, including privacy protection, data security, and legal and regulatory issue. Patients' informed consent has to be obtained before using their clinical data for ML. Moreover, relevant guidelines should be developed for data acquisition and data sharing. Meanwhile, data should be transparent and traceable without the disclosure of personal information. Strict legal requirements should be made regarding health data privacy.

CONCLUSION

ML will have an immense impact in the field of oral and maxillofacial surgery in the following aspects. First, ML is useful in early screening, accurate diagnosis, proper treatment, morbidity prevention, and accurate prediction of treatment associated toxicity in the treatment of maxillofacial cysts, benign tumors, and malignant tumors. Second, ML algorithms have achieved major success in virtual surgical planning and thus posed great potential in the reconstruction of facial defects. Third, ML has been considered a useful tool in orthognathic surgery for establishing a precise diagnosis, evaluating surgical necessity, and predicting treatment outcomes. Lastly, ML models have demonstrated great potential in the field of dental implants for assisting implant planning, evaluating implant performance, improving implant designs, and identifying dental implants (Table 1).

Nonetheless, it remains vital to evaluate the reliability, accuracy, and repeatability of ML in medicine. Further studies should continually focus on improving the usability of algorithms for different diseases. Moreover, there exists an urgent need to develop guidelines for many ethical challenges, including privacy protection, data security, and legal and regulatory issue. Despite these issues, ML is still considered to be a powerful tool for clinicians. We believe that this review may provide detailed information regarding ML applications in oral and maxillofacial surgery and help assist clinicians to facilitate the clinical practices.

ACKNOWLEDGEMENTS

We are grateful to professor Ji-Xiang Guo, an IT specialist, for her assistance with the editing of this article.

REFERENCES

1 **Fujima N**, Andreu-Arasa VC, Meibom SK, Mercier GA, Salama AR, Truong MT, Sakai O. Prediction of the treatment outcome using machine learning with FDG-PET image-based multiparametric approach in patients with oral cavity squamous cell carcinoma. *Clin Radiol* 2021; **76**: 711.e1-711.e7 [PMID: 33934877 DOI: 10.1016/j.crad.2021.03.017]

2 **Creff G**, Devillers A, Depeursinge A, Palard-Novello X, Acosta O, Jegoux F, Castelli J. Evaluation of the prognostic value of FDG PET/CT parameters for patients with surgically treated head and neck cancer: A systematic review. *JAMA Otolaryngol Head Neck Surg* 2020; **146**: 471-479 [PMID: 32215611 DOI: 10.1001/jamaoto.2020.0014]

3 **Heo MS**, Kim JE, Hwang JJ, Han SS, Kim JS, Yi WJ, Park IW. Artificial intelligence in oral and maxillofacial radiology: What is currently possible? *Dentomaxillofac Radiol* 2021; **50**: 20200375 [PMID: 33197209 DOI: 10.1259/dmfr.20200375]

4 **Choi RY**, Coyner AS, Kalpathy-Cramer J, Chiang MF, Campbell JP. Introduction to Machine Learning, Neural Networks, and Deep Learning. *Transl Vis Sci Technol* 2020; **9**: 14 [PMID: 32704420 DOI: 10.1167/tvst.9.2.14]

5 **Seyyed-Kalantari L**, Zhang H, McDermott MBA, Chen IY, Ghassemi M. Underdiagnosis bias of artificial intelligence algorithms applied to chest radiographs in under-served patient populations. *Nat Med* 2021; **27**: 2176-2182 [PMID: 34893776 DOI: 10.1038/s41591-021-01595-0]

6 **Shan T**, Tay FR, Gu L. Application of artificial intelligence in dentistry. *J Dent Res* 2021; **100**: 232-244 [PMID: 33118431 DOI: 10.1177/0022034520969115]

7 **Bichu YM**, Hansa I, Bichu AY, Premjani P, Flores-Mir C, Vaid NR. Applications of artificial intelligence and machine learning in orthodontics: a scoping review. *Prog Orthod* 2021; **22**: 18 [PMID: 34219198 DOI: 10.1186/s40510-021-00361-9]

8 **Schwendicke F**, Samek W, Krois J. Artificial Intelligence in Dentistry: Chances and Challenges. *J Dent Res* 2020; **99**: 769-774 [PMID: 32315260 DOI: 10.1177/0022034520915714]

9 **Mak KK**, Lee K, Park C. Applications of machine learning in addiction studies: A systematic review. *Psychiatry Res* 2019; **275**: 53-60 [PMID: 30878857 DOI: 10.1016/j.psychres.2019.03.001]

10 **Erickson BJ**, Korfiatis P, Akkus Z, Kline TL. Machine learning for medical imaging. *Radiographics* 2017; **37**: 505-515 [PMID: 28212054 DOI: 10.1148/rg.2017160130]

11 **Amasya H**, Yildirim D, Aydogan T, Kemaloglu N, Orhan K. Cervical vertebral maturation assessment on lateral cephalometric radiographs using artificial intelligence: comparison of machine learning classifier models. *Dentomaxillofac Radiol* 2020; **49**: 20190441 [PMID: 32105499 DOI: 10.1259/dmfr.20190441]

12 **Krittanawong C**, Zhang H, Wang Z, Aydar M, Kitai T. Artificial intelligence in precision cardiovascular medicine. *J Am Coll Cardiol* 2017; **69**: 2657-2664 [PMID: 28545640 DOI: 10.1016/j.jacc.2017.03.571]

13 **Alhazmi A**, Alhazmi Y, Makrami A, Masmali A, Salawi N, Masmali K, Patil S. Application of artificial intelligence and machine learning for prediction of oral cancer risk. *J Oral Pathol Med* 2021; **50**: 444-450 [PMID: 33394536 DOI: 10.1111/jop.13157]

14 **Saha A**, Tso S, Rabski J, Sadeghian A, Cusimano MD. Machine learning applications in imaging analysis for patients with pituitary tumors: a review of the current literature and future directions. *Pituitary* 2020; **23**: 273-293 [PMID: 31907710 DOI: 10.1007/s11102-019-01026-x]

15 **Diwakar M**, Kumar M. A review on CT image noise and its denoising. *Biomed Signal Process Control* 2018; **42**: 73-88 [DOI: 10.1016/j.bspc.2018.01.010]

16 **Hussain Z**, Gimenez F, Yi D, Rubin D. Differential Data Augmentation Techniques for Medical Imaging Classification Tasks. *AMIA Annu Symp Proc* 2017; **2017**: 979-984 [PMID: 29854165]

17 **Chu CS**, Lee NP, Ho JWK, Choi SW, Thomson PJ. Deep learning for clinical image analyses in oral squamous cell carcinoma: A review. *JAMA Otolaryngol Head Neck Surg* 2021; **147**: 893-900 [PMID: 34410314 DOI: 10.1001/jamaoto.2021.2028]

18 **Mobadersany P**, Yousefi S, Amgad M, Gutman DA, Barnholtz-Sloan JS, Velázquez Vega JE, Brat DJ, Cooper LAD. Predicting cancer outcomes from histology and genomics using convolutional networks. *Proc Natl Acad Sci U S A* 2018; **115**: E2970-E2979 [PMID: 29531073 DOI: 10.1073/pnas.1717139115]

19 **Shi JY**, Wang X, Ding GY, Dong Z, Han J, Guan Z, Ma LJ, Zheng Y, Zhang L, Yu GZ, Wang XY, Ding ZB, Ke AW, Yang H, Wang L, Ai L, Cao Y, Zhou J, Fan J, Liu X, Gao Q. Exploring prognostic indicators in the pathological images of hepatocellular carcinoma based on deep learning. *Gut* 2021; **70**: 951-961 [PMID: 32998878 DOI: 10.1136/gutjnl-2020-320930]

20 **Akkus Z**, Galimzianova A, Hoogi A, Rubin DL, Erickson BJ. Deep learning for brain MRI segmentation: State of the art and future directions. *J Digit Imaging* 2017; **30**: 449-459 [PMID: 28577131 DOI: 10.1007/s10278-017-9983-4]

21 **Huang S**, Yang J, Fong S, Zhao Q. Artificial intelligence in cancer diagnosis and prognosis: Opportunities and challenges. *Cancer Lett* 2020; **471**: 61-71 [PMID: 31830558 DOI: 10.1016/j.canlet.2019.12.007]

22 **Simmons CPL**, McMillan DC, McWilliams K, Sande TA, Fearon KC, Tuck S, Fallon MT, Laird BJ. Prognostic Tools in Patients With Advanced Cancer: A Systematic Review. *J Pain Symptom Manage* 2017; **53**: 962-970.e10 [PMID: 28062344 DOI: 10.1016/j.jpainsymman.2016.12.330]

23 **Frydenlund A**, Eramian M, Daley T. Automated classification of four types of developmental odontogenic cysts. *Comput Med Imaging Graph* 2014; **38**: 151-162 [PMID: 24411103 DOI: 10.1016/j.compmedimag.2013.12.002]

24 **Okada K**, Rysavy S, Flores A, Linguraru MG. Noninvasive differential diagnosis of dental periapical lesions in cone-beam CT scans. *Med Phys* 2015; **42**: 1653-1665 [PMID: 25832055 DOI: 10.1118/1.4914418]

25 **Endres MG**, Hillen F, Salloumis M, Sedaghat AR, Niehues SM, Quatela O, Hanken H, Smeets R, Beck-Broichsitter B, Rendenbach C, Lakhani K, Heiland M, Gaudin RA. Development of a Deep Learning Algorithm for Periapical Disease Detection in Dental Radiographs. *Diagnostics (Basel)* 2020; **10**: 430 [PMID: 32599942 DOI: 10.3390/diagnostics10060430]

26 **Kwon O**, Yong TH, Kang SR, Kim JE, Huh KH, Heo MS, Lee SS, Choi SC, Yi WJ. Automatic diagnosis for cysts and tumors of both jaws on panoramic radiographs using a deep convolution neural network. *Dentomaxillofac Radiol* 2020; **49**: 20200185 [PMID: 32574113 DOI: 10.1259/dmfr.20200185]

27 **Liu Z**, Liu J, Zhou Z, Zhang Q, Wu H, Zhai G, Han J. Differential diagnosis of ameloblastoma and odontogenic keratocyst by machine learning of panoramic radiographs. *Int J Comput Assist Radiol Surg* 2021; **16**: 415-422 [PMID: 33547985 DOI: 10.1007/s11548-021-02309-0]

28 **Yang H**, Jo E, Kim HJ, Cha IH, Jung YS, Nam W, Kim JY, Kim JK, Kim YH, Oh TG, Han SS, Kim

H, Kim D. Deep Learning for Automated Detection of Cyst and Tumors of the Jaw in Panoramic Radiographs. *J Clin Med* 2020; **9**: 1839 [PMID: 32545602 DOI: 10.3390/jcm9061839]

29 **Kar A**, Wreesmann VB, Shwetha V, Thakur S, Rao VUS, Arakeri G, Brennan PA. Improvement of oral cancer screening quality and reach: The promise of artificial intelligence. *J Oral Pathol Med* 2020; **49**: 727-730 [PMID: 32162398 DOI: 10.1111/jop.13013]

30 **Aubreville M**, Knipfer C, Oetter N, Jaremenko C, Rodner E, Denzler J, Bohr C, Neumann H, Stelzle F, Maier A. Automatic Classification of Cancerous Tissue in Laserendomicroscopy Images of the Oral Cavity using Deep Learning. *Sci Rep* 2017; **7**: 11979 [PMID: 28931888 DOI: 10.1038/s41598-017-12320-8]

31 **Warin K**, Limprasert W, Suebnukarn S, Jinaporntham S, Jantana P. Automatic classification and detection of oral cancer in photographic images using deep learning algorithms. *J Oral Pathol Med* 2021; **50**: 911-918 [PMID: 34358372 DOI: 10.1111/jop.13227]

32 **Jeyaraj PR**, Samuel Nadar ER. Computer-assisted medical image classification for early diagnosis of oral cancer employing deep learning algorithm. *J Cancer Res Clin Oncol* 2019; **145**: 829-837 [PMID: 30603908 DOI: 10.1007/s00432-018-02834-7]

33 **Ren J**, Qi M, Yuan Y, Duan S, Tao X. Machine Learning-Based MRI Texture Analysis to Predict the Histologic Grade of Oral Squamous Cell Carcinoma. *AJR Am J Roentgenol* 2020; **215**: 1184-1190 [PMID: 32930606 DOI: 10.2214/AJR.19.22593]

34 **Alkhadar H**, Macluskey M, White S, Ellis I, Gardner A. Comparison of machine learning algorithms for the prediction of five-year survival in oral squamous cell carcinoma. *J Oral Pathol Med* 2021; **50**: 378-384 [PMID: 33220109 DOI: 10.1111/jop.13135]

35 **Karadaghy OA**, Shew M, New J, Bur AM. Development and Assessment of a Machine Learning Model to Help Predict Survival Among Patients With Oral Squamous Cell Carcinoma. *JAMA Otolaryngol Head Neck Surg* 2019; **145**: 1115-1120 [PMID: 31045212 DOI: 10.1001/jamaoto.2019.0981]

36 **Fujima N**, Andreu-Arasa VC, Meibom SK, Mercier GA, Salama AR, Truong MT, Sakai O. Deep learning analysis using FDG-PET to predict treatment outcome in patients with oral cavity squamous cell carcinoma. *Eur Radiol* 2020; **30**: 6322-6330 [PMID: 32524219 DOI: 10.1007/s00330-020-06982-8]

37 **Kim DW**, Lee S, Kwon S, Nam W, Cha IH, Kim HJ. Deep learning-based survival prediction of oral cancer patients. *Sci Rep* 2019; **9**: 6994 [PMID: 31061433 DOI: 10.1038/s41598-019-43372-7]

38 **Pan X**, Zhang T, Yang Q, Yang D, Rwigema JC, Qi XS. Survival prediction for oral tongue cancer patients *via* probabilistic genetic algorithm optimized neural network models. *Br J Radiol* 2020; **93**: 20190825 [PMID: 32520585 DOI: 10.1259/bjr.20190825]

39 **Ariji Y**, Sugita Y, Nagao T, Nakayama A, Fukuda M, Kise Y, Nozawa M, Nishiyama M, Katumata A, Ariji E. CT evaluation of extranodal extension of cervical lymph node metastases in patients with oral squamous cell carcinoma using deep learning classification. *Oral Radiol* 2020; **36**: 148-155 [PMID: 31197738 DOI: 10.1007/s11282-019-00391-4]

40 **Bur AM**, Holcomb A, Goodwin S, Woodroof J, Karadaghy O, Shnayder Y, Kakarala K, Brant J, Shew M. Machine learning to predict occult nodal metastasis in early oral squamous cell carcinoma. *Oral Oncol* 2019; **92**: 20-25 [PMID: 31010618 DOI: 10.1016/j.oraloncology.2019.03.011]

41 **Yuan Y**, Ren J, Tao X. Machine learning-based MRI texture analysis to predict occult lymph node metastasis in early-stage oral tongue squamous cell carcinoma. *Eur Radiol* 2021; **31**: 6429-6437 [PMID: 33569617 DOI: 10.1007/s00330-021-07731-1]

42 **Keek S**, Sanduleanu S, Wesseling F, de Roest R, van den Brekel M, van der Heijden M, Vens C, Giuseppina C, Licitra L, Scheckenbach K, Vergeer M, Leemans CR, Brakenhoff RH, Nauta I, Cavalieri S, Woodruff HC, Poli T, Leijenaar R, Hoebers F, Lambin P. Computed tomography-derived radiomic signature of head and neck squamous cell carcinoma (peri)tumoral tissue for the prediction of locoregional recurrence and distant metastasis after concurrent chemo-radiotherapy. *PLoS One* 2020; **15**: e0232639 [PMID: 32442178 DOI: 10.1371/journal.pone.0232639]

43 **Men K**, Geng H, Zhong H, Fan Y, Lin A, Xiao Y. A Deep Learning Model for Predicting Xerostomia Due to Radiation Therapy for Head and Neck Squamous Cell Carcinoma in the RTOG 0522 Clinical Trial. *Int J Radiat Oncol Biol Phys* 2019; **105**: 440-447 [PMID: 31201897 DOI: 10.1016/j.ijrobp.2019.06.009]

44 **Liang S**, Tang F, Huang X, Yang K, Zhong T, Hu R, Liu S, Yuan X, Zhang Y. Deep-learning-based detection and segmentation of organs at risk in nasopharyngeal carcinoma computed tomographic images for radiotherapy planning. *Eur Radiol* 2019; **29**: 1961-1967 [PMID: 30302589 DOI: 10.1007/s00330-018-5748-9]

45 **Sun XS**, Li XY, Chen QY, Tang LQ, Mai HQ. Future of Radiotherapy in Nasopharyngeal Carcinoma. *Br J Radiol* 2019; **92**: 20190209 [PMID: 31265322 DOI: 10.1259/bjr.20190209]

46 **Li C**, Jing B, Ke L, Li B, Xia W, He C, Qian C, Zhao C, Mai H, Chen M, Cao K, Mo H, Guo L, Chen Q, Tang L, Qiu W, Yu Y, Liang H, Huang X, Liu G, Li W, Wang L, Sun R, Zou X, Guo S, Huang P, Luo D, Qiu F, Wu Y, Hua Y, Liu K, Lv S, Miao J, Xiang Y, Sun Y, Guo X, Lv X. Development and validation of an endoscopic images-based deep learning model for detection with nasopharyngeal malignancies. *Cancer Commun (Lond)* 2018; **38**: 59 [PMID: 30253801 DOI: 10.1186/s40880-018-0325-9]

47 **Du D**, Feng H, Lv W, Ashrafinia S, Yuan Q, Wang Q, Yang W, Feng Q, Chen W, Rahmim A, Lu L. Machine Learning Methods for Optimal Radiomics-Based Differentiation Between Recurrence and Inflammation: Application to Nasopharyngeal Carcinoma Post-therapy PET/CT Images. *Mol Imaging*

Biol 2020; **22**: 730-738 [PMID: 31338709 DOI: 10.1007/s11307-019-01411-9]
48 **Lin L**, Dou Q, Jin YM, Zhou GQ, Tang YQ, Chen WL, Su BA, Liu F, Tao CJ, Jiang N, Li JY, Tang LL, Xie CM, Huang SM, Ma J, Heng PA, Wee JTS, Chua MLK, Chen H, Sun Y. Deep Learning for Automated Contouring of Primary Tumor Volumes by MRI for Nasopharyngeal Carcinoma. *Radiology* 2019; **291**: 677-686 [PMID: 30912722 DOI: 10.1148/radiol.2019182012]
49 **Men K**, Chen X, Zhang Y, Zhang T, Dai J, Yi J, Li Y. Deep Deconvolutional Neural Network for Target Segmentation of Nasopharyngeal Cancer in Planning Computed Tomography Images. *Front Oncol* 2017; **7**: 315 [PMID: 29376025 DOI: 10.3389/fonc.2017.00315]
50 **Zhang B**, Lian Z, Zhong L, Zhang X, Dong Y, Chen Q, Zhang L, Mo X, Huang W, Yang W, Zhang S. Machine-learning based MRI radiomics models for early detection of radiation-induced brain injury in nasopharyngeal carcinoma. *BMC Cancer* 2020; **20**: 502 [PMID: 32487085 DOI: 10.1186/s12885-020-06957-4]
51 **Jie B**, Han B, Yao B, Zhang Y, Liao H, He Y. Automatic virtual reconstruction of maxillofacial bone defects assisted by ICP (iterative closest point) algorithm and normal people database. *Clin Oral Investig* 2021; epub ahead of print [PMID: 34564760 DOI: 10.1007/s00784-021-04181-3]
52 **Dalvit Carvalho da Silva R**, Jenkyn TR, Carranza VA. Convolutional neural networks and geometric moments to identify the bilateral symmetric midplane in facial skeletons from CT scans. *Biology (Basel)* 2021; **10**: 182 [PMID: 33801432 DOI: 10.3390/biology10030182]
53 **Lee SJ**, Yoo JY, Woo SY, Yang HJ, Kim JE, Huh KH, Lee SS, Heo MS, Hwang SJ, Yi WJ. A Complete Digital Workflow for Planning, Simulation, and Evaluation in Orthognathic Surgery. *J Clin Med* 2021; **10**: 4000 [PMID: 34501449 DOI: 10.3390/jcm10174000]
54 **Shaheen E**, Sun Y, Jacobs R, Politis C. Three-dimensional printed final occlusal splint for orthognathic surgery: design and validation. *Int J Oral Maxillofac Surg* 2017; **46**: 67-71 [PMID: 27815012 DOI: 10.1016/j.ijom.2016.10.002]
55 **Fawzy HH**, Choi JW. Evaluation of virtual surgical plan applicability in 3D simulation-guided two-jaw surgery. *J Craniomaxillofac Surg* 2019; **47**: 860-866 [PMID: 30914227 DOI: 10.1016/j.jcms.2019.03.005]
56 **Lin HH**, Lonic D, Lo LJ. 3D printing in orthognathic surgery - A literature review. *J Formos Med Assoc* 2018; **117**: 547-558 [PMID: 29398097 DOI: 10.1016/j.jfma.2018.01.008]
57 **Shin W**, Yeom HG, Lee GH, Yun JP, Jeong SH, Lee JH, Kim HK, Kim BC. Deep learning based prediction of necessity for orthognathic surgery of skeletal malocclusion using cephalogram in Korean individuals. *BMC Oral Health* 2021; **21**: 130 [PMID: 33736627 DOI: 10.1186/s12903-021-01513-3]
58 **Lin HH**, Chiang WC, Yang CT, Cheng CT, Zhang T, Lo LJ. On construction of transfer learning for facial symmetry assessment before and after orthognathic surgery. *Comput Methods Programs Biomed* 2021; **200**: 105928 [PMID: 33485074 DOI: 10.1016/j.cmpb.2021.105928]
59 **Lo LJ**, Yang CT, Ho CT, Liao CH, Lin HH. Automatic Assessment of 3-Dimensional Facial Soft Tissue Symmetry Before and After Orthognathic Surgery Using a Machine Learning Model: A Preliminary Experience. *Ann Plast Surg* 2021; **86**: S224-S228 [PMID: 33443885 DOI: 10.1097/SAP.0000000000002687]
60 **Knoops PGM**, Papaioannou A, Borghi A, Breakey RWF, Wilson AT, Jeelani O, Zafeiriou S, Steinbacher D, Padwa BL, Dunaway DJ, Schievano S. A machine learning framework for automated diagnosis and computer-assisted planning in plastic and reconstructive surgery. *Sci Rep* 2019; **9**: 13597 [PMID: 31537815 DOI: 10.1038/s41598-019-49506-1]
61 **Patcas R**, Bernini DAJ, Volokitin A, Agustsson E, Rothe R, Timofte R. Applying artificial intelligence to assess the impact of orthognathic treatment on facial attractiveness and estimated age. *Int J Oral Maxillofac Surg* 2019; **48**: 77-83 [PMID: 30087062 DOI: 10.1016/j.ijom.2018.07.010]
62 **Alghamdi HS**, Jansen JA. The development and future of dental implants. *Dent Mater J* 2020; **39**: 167-172 [PMID: 31969548 DOI: 10.4012/dmj.2019-140]
63 **Kurt Bayrakdar S**, Orhan K, Bayrakdar IS, Bilgir E, Ezhov M, Gusarev M, Shumilov E. A deep learning approach for dental implant planning in cone-beam computed tomography images. *BMC Med Imaging* 2021; **21**: 86 [PMID: 34011314 DOI: 10.1186/s12880-021-00618-z]
64 **Ha SR**, Park HS, Kim EH, Kim HK, Yang JY, Heo J, Yeo IL. A pilot study using machine learning methods about factors influencing prognosis of dental implants. *J Adv Prosthodont* 2018; **10**: 395-400 [PMID: 30584467 DOI: 10.4047/jap.2018.10.6.395]
65 **Lee DW**, Kim SY, Jeong SN, Lee JH. Artificial Intelligence in Fractured Dental Implant Detection and Classification: Evaluation Using Dataset from Two Dental Hospitals. *Diagnostics (Basel)* 2021; **11**: 233 [PMID: 33546446 DOI: 10.3390/diagnostics11020233]
66 **Mameno T**, Wada M, Nozaki K, Takahashi T, Tsujioka Y, Akema S, Hasegawa D, Ikebe K. Predictive modeling for peri-implantitis by using machine learning techniques. *Sci Rep* 2021; **11**: 11090 [PMID: 34045590 DOI: 10.1038/s41598-021-90642-4]
67 **Sukegawa S**, Yoshii K, Hara T, Yamashita K, Nakano K, Yamamoto N, Nagatsuka H, Furuki Y. Deep Neural Networks for Dental Implant System Classification. *Biomolecules* 2020; **10**: 984 [PMID: 32630195 DOI: 10.3390/biom10070984]
68 **Sukegawa S**, Yoshii K, Hara T, Matsuyama T, Yamashita K, Nakano K, Takabatake K, Kawai H, Nagatsuka H, Furuki Y. Multi-Task Deep Learning Model for Classification of Dental Implant Brand and Treatment Stage Using Dental Panoramic Radiograph Images. *Biomolecules* 2021; **11**: 815 [PMID: 34070916 DOI: 10.3390/biom11060815]
69 **Hadj Saïd M**, Le Roux MK, Catherine JH, Lan R. Development of an Artificial Intelligence Model to

Identify a Dental Implant from a Radiograph. *Int J Oral Maxillofac Implants* 2020; **36**: 1077-1082 [PMID: 33270045 DOI: 10.11607/jomi.8060]

70 **Roy S**, Dey S, Khutia N, Chowdhury AR, Datta S. Design of patient specific dental implant using FE analysis and computational intelligence techniques. *Appl Soft Comput* 2018; **65**: 272-9 [DOI: 10.1016/j.asoc.2018.01.025]

71 **Mupparapu M**, Wu CW, Chen YC. Artificial intelligence, machine learning, neural networks, and deep learning: Futuristic concepts for new dental diagnosis. *Quintessence Int* 2018; **49**: 687-688 [PMID: 30202834 DOI: 10.3290/j.qi.a41107]

72 **Rizzo S**, Botta F, Raimondi S, Origgi D, Fanciullo C, Morganti AG, Bellomi M. Radiomics: the facts and the challenges of image analysis. *Eur Radiol Exp* 2018; **2**: 36 [PMID: 30426318 DOI: 10.1186/s41747-018-0068-z]

73 **Ma Q**, Kobayashi E, Fan B, Nakagawa K, Sakuma I, Masamune K, Suenaga H. Automatic 3D landmarking model using patch-based deep neural networks for CT image of oral and maxillofacial surgery. *Int J Med Robot* 2020; **16**: e2093 [PMID: 32065718 DOI: 10.1002/rcs.2093]

74 **Leite AF**, Vasconcelos KF, Willems H, Jacobs R. Radiomics and Machine Learning in Oral Healthcare. *Proteomics Clin Appl* 2020; **14**: e1900040 [PMID: 31950592 DOI: 10.1002/prca.201900040]

Artificial Intelligence in Medical Imaging

Submit a Manuscript: https://www.f6publishing.com

Artif Intell Med Imaging 2021 December 28; 2(6): 115-117

DOI: 10.35711/aimi.v2.i6.115

ISSN 2644-3260 (online)

LETTER TO THE EDITOR

Pictorial research of pancreas with artificial intelligence and simulacra in the works of Fellini

Hiroki Tahara

ORCID number: Hiroki Tahara taharahiroki2@gmail.com.

Author contributions: Tahara H contributed anything in research.

Conflict-of-interest statement: Hiroki Tahara has no conflict-of-interest.

Country/Territory of origin: Japan

Specialty type: Social Science

Provenance and peer review: Unsolicited article; Externally peer reviewed.

Peer-review model: Single blind

Peer-review report's scientific quality classification

Grade A (Excellent): 0
Grade B (Very good): 0
Grade C (Good): C, C
Grade D (Fair): 0
Grade E (Poor): E

Hiroki Tahara, Faculty of Integrated Human Studies, Kyoto University, Kyoto 606-8501, Japan

Corresponding author: Hiroki Tahara, Faculty of Integrated Human Studies, Kyoto University, Yoshida-honmachi, Sakyo-ku, Kyoto 606-8501, Japan. taharahiroki2@gmail.com

Abstract

This is the consideration recalled from my reading of *Acute pancreatitis: A pictorial review of early pancreatic fluid collections* by Xiao. This perspective related to the works of Fellini might be able to contribute the future development of the research of pancreatic diseases.

Key Words: Pancreatic diseases; Medical imaging; Artificial intelligence; Baudrillard; Simulacra; Fellini

Core Tip: This paper offers, so to speak, a new postmodernist view of medicine. Particularly in medical imaging, where phenomena are observed in pictorial ways, research engaging with art and epistemology will be essential in the future. It will also go hand in hand with the use of artificial intelligence. Although philosophical discourse has not been greatly used in clinical research, the rapid development of psychopathology and medical philosophy suggests that such research will be needed in these fields. This thought was inspired by an article in this journal; therefore, it is most appropriate that it should be published in this journal.

Citation: Tahara H. Pictorial research of pancreas with artificial intelligence and simulacra in the works of Fellini. *Artif Intell Med Imaging* 2021; 2(6): 115-117
URL: https://www.wjgnet.com/2644-3260/full/v2/i6/115.htm
DOI: https://dx.doi.org/10.35711/aimi.v2.i6.115

TO THE EDITOR

This is what I have considered since I read the article *Acute pancreatitis: A pictorial review of early pancreatic fluid collections* by Xiao[1]. This consideration is related with

Received: September 22, 2021
Peer-review started: September 22, 2021
First decision: October 13, 2021
Revised: October 26, 2021
Accepted: December 28, 2021
Article in press: December 28, 2021
Published online: December 28, 2021

P-Reviewer: Cabezuelo AS, Jheng YC
S-Editor: Liu M
L-Editor: Filipodia
P-Editor: Liu M

the works of Fellini, as follows:

REALITIES OF DEFINING CHARACTERISTIC

In the works of Fellini, a predominant concept is the concept of precapitalist consciousness. In a sense, Marx uses the term 'dialectic socialism' to denote the common ground between sexual identity and society.

"*Truth is meaningless*," says Foucault; however, according to Bailey[2], it is not so much truth that is meaningless, but rather the defining characteristic, and some would say the failure, of truth. The main theme of Parry[3]'s model of the postconceptual paradigm of reality is the role of the writer as artist. But if the deconstructivist theory holds, we have to choose between dialectic socialism and Sartreist existentialism.

The primary theme of the works of Fellini is a subcapitalist reality. In a sense, Lyotard uses the term 'semioticist narrative' to denote the difference between society and class.

Any number of deconstructions concerning dialectic socialism exist. But Sartre promotes the use of the postconceptual paradigm of reality to modify society.

The main theme of Pickett[4]'s critique of dialectic socialism is the economy, and therefore the paradigm, of pretextual class. It could be said that Foucault uses the term 'Baudrillardist simulacra' to denote a mythopoetical whole.

An abundance of narratives concerning the role of the participant as artist may be discovered. But the subject is contextualized into a dialectic socialism that includes art as a paradox.

MATERIAL RATIONALISM AND SUBCULTURAL DEAPPROPRIATION

If one examines dialectic socialism, one is faced with a choice: either reject capitalist libertarianism or conclude that sexual identity, perhaps ironically, has intrinsic meaning. Subcultural deappropriation implies that consensus is a product of the masses, but only if the premise of dialectic socialism is valid. Thus, several narratives concerning neomodern capitalist theory exist.

The primary theme of the works of Fellini is a self-sufficient totality. The main theme of Hernández[5] is an analysis of subcultural deappropriation as the common ground between narrativity and society. It could be said that Derrida uses the term 'dialectic socialism' to denote not discourse as such, but postdiscourse.

The subject is interpolated into a subcultural deappropriation that includes culture as a whole. Therefore, a number of theories concerning a subconstructive reality may be found.

The primary theme of the works of Fellini is the bridge between truth and sexual identity. However, the subject is contextualised into a dialectic rationalism that includes reality as a paradox.

Geoffrey[6] holds that we have to choose between dialectic socialism and postdialectic textual theory. In a sense, in La Dolce Vita, Fellini denies substructuralist nationalism; in Amarcord he affirms subcultural deappropriation.

CONCLUSION

Though mentioned above is my perspective recalled from Xiao's article, it pertains to research on applying pictorial ways to the research of pancreatitis and other pancreatic diseases. This perspective concerning the works of Fellini might be able to contribute to the future development of the research field.

REFERENCES

1 **Xiao B**. Acute pancreatitis: A pictorial review of early pancreatic fluid collections. *Artif Intell Med Imaging* 2020; **1**: 40-49 [DOI: 10.35711/aimi.v1.i1.40]
2 **Bailey P**. Conspiracies of meaning: music-hall and the knowingness of popular culture. *Past Present* 1994; **144**: 138-170 [DOI: 10.1093/past/144.1.138]
3 **Parry A**. Why we tell stories: The narrative construction of reality. *Trans Anal J* 1997; **2**: 118-127 [DOI: 10.1177/036215379702700207]

4 **Pickett J**. Soviet Civilization through a Persian Lens: Iranian Intellectuals, Cultural Diplomacy and Socialist Modernity 1941–55. *Iranian Studies* 2015; **48**: 805-826 [DOI: 10.1080/00210862.2015.1058639]
5 **Hernández ÁDH**. Hatsune Miku and the Double Nature of Voice Library Software: Content Consumption and Production in Japan. *Dōjin J* 2020; 37 [DOI: 10.5040/9781501325953.ch-002]
6 **Geoffrey B**. A philosophical and socio-historical defense of the secular, democratic and mixed economic state. 2020 Preprint. Available from: ResearchGate [DOI: 10.31235/osf.io/8xt9f]

Published by **Baishideng Publishing Group Inc**
7041 Koll Center Parkway, Suite 160, Pleasanton, CA 94566, USA
Telephone: +1-925-3991568
E-mail: bpgoffice@wjgnet.com
Help Desk: https://www.f6publishing.com/helpdesk
https://www.wjgnet.com